Effect of *pgi* and *edd* gene deletion in *Escherichia coli* K12 on production of poly(3-hydroxybutyrate) and copolymer poly(3-hydroxybutyrate-*co*-3-hydroxyvalerate)

Miss Jittakan Pachimsawat

A Dissertation Submitted in Partial Fulfillment of the Requirements for the Degree of Doctor of Philosophy in Biotechnology

Faculty of Science

Chulalongkorn University

Academic Year 2024

ผลของการกำจัดยีน *pgi* และ *edd* ใน *Escherichia coli* K12 ต่อการผลิตพอลิ(3-ไฮดรอกซีบิวทิเรต) และโคพอลิ(3-ไฮดรอกซีบิวทิเรต-*โค*-3-ไฮดรอกซีวาเลอเรต)

นางสาวจิตตกานต์ ปัจฉิมสวัสดิ์

วิทยานิพนธ์นี้เป็นส่วนหนึ่งของการศึกษาตามหลักสูตรปริญญาวิทยาศาสตรดุษฎีบัณฑิต
สาขาวิชาเทคโนโลยีชีวภาพ
คณะวิทยาศาสตร์ จุฬาลงกรณ์มหาวิทยาลัย
ปีการศึกษา 2567

Thesis Title	Effect of *pgi* and *edd* gene deletion in *Escherichia coli* K12 on production of poly(3-hydroxybutyrate) and copolymer poly(3-hydroxybutyrate-*co*-3-hydroxyvalerate)
By	Miss Jittakan Pachimsawat
Field of Study	Biotechnology
Thesis Advisor	Associate Professor Suchada Chanprateep Napathorn, Ph.D.

Accepted by the Faculty of Science, Chulalongkorn University in Partial Fulfillment of the Requirement for the Doctor of Philosophy

..... Dean of the Faculty of Science
(Professor Pranut Potiyaraj, Ph.D.)

DISSERTATION COMMITTEE

..... Chairman
(Assistant Professor Kobchai Pattaragulwanit, Ph.D.)

..... Thesis Advisor
(Associate Professor Suchada Chanprateep Napathorn, Ph.D.)

..... Examiner
(Associate Professor Kuakarun Krusong, Ph.D.)

..... Examiner
(Associate Professor Cheewanun Dachoupakan Sirisomboon, Ph.D.)

..... External Examiner
(Sophon Sirisattha, Ph.D.)

จิตตกานต์ ปัจฉิมสวัสดิ์ : ผลของการกำจัดยีน *pgi* และ *edd* ใน *Escherichia coli* K12 ต่อการผลิตพอลิ(3-ไฮดรอกซีบิวทิเรต) และโคพอลิ(3-ไฮดรอกซีบิวทิเรต-*โค*-3-ไฮดรอกซีวาเลอเรต). (Effect of *pgi* and *edd* gene deletion in *Escherichia coli* K12 on production of poly(3-hydroxybutyrate) and copolymer poly(3-hydroxybutyrate-*co*-3-hydroxyvalerate)) อ.ที่ปรึกษาหลัก : รศ. ดร.สุชาดา จันทร์ประทีป นภาธร

พอลิ(3-ไฮดรอกซีบิวทิเรต)เป็นวัสดุชีวภาพทางเลือกที่เป็นมิตรต่อสิ่งแวดล้อม งานวิจัยนี้นำเสนอการกำจัดยีนฟอสโฟกลูโคเนตดีไฮดราเทสและฟอสโฟกลูโคสไอโซเมอเรสใน *E. coli* เพื่อการผลิตพอลิ(3-ไฮดรอกซีบิวทิเรต)เป็นครั้งแรก ผลการทดลองพบว่าสายพันธุ์ที่ไม่มียีนฟอสโฟกลูโคเนตดีไฮดราเทสสามารถสะสมพอลิ(3-ไฮดรอกซีบิวทิเรต)ได้สูงสุดถึงร้อยละ 93 โดยน้ำหนักและได้ความเข้มข้นสูงสุด 7.55 กรัมต่อลิตรในชั่วโมงที่ 30 ในสภาวะการเลี้ยงที่มีน้ำตาลกลูโคสเป็นแหล่งคาร์บอน สายพันธุ์ที่ไม่มียีนฟอสโฟกลูโคเนตดีไฮดราเทสมีค่าอัตราการผลิตพอลิ(3-ไฮดรอกซีบิวทิเรต)จำเพาะเท่ากับ 0.21 ต่อชั่วโมงและมีประสิทธิภาพการผลิตสูงสุด 0.25 กรัมต่อลิตรต่อชั่วโมง อย่างไรก็ตามการกำจัดยีนฟอสโฟกลูโคสไอโซเมอเรสมีผลทำให้การเจริญของแบคทีเรียดีขึ้นแต่ไม่ได้เพิ่มการผลิตพอลิ(3-ไฮดรอกซีบิวทิเรต)แต่อย่างใด นอกจากนี้ยังได้ศึกษาถึงความสามารถของแบคทีเรียในการใช้แหล่งคาร์บอนที่มีราคาถูก เช่น น้ำมันดิบจากอุตสาหกรรมไบโอดีเซลพบว่า สายพันธุ์ที่ไม่มียีนฟอสโฟกลูโคเนตดีไฮดราเทสมีการสะสมพอลิ(3-ไฮดรอกซีบิวทิเรต)ได้สูงถึง 2.7 กรัมต่อลิตรและร้อยละ 74.8 โดยน้ำหนักใน 24 ชั่วโมง ซึ่งเป็นค่าที่มากกว่างานวิจัยอื่นๆที่ผลิตพอลิ(3-ไฮดรอกซีบิวทิเรต)จากน้ำมันดิบ อีกทั้งสายพันธุ์ที่ไม่มียีนฟอสโฟกลูโคเนตดีไฮดราเทสยังสามารถสะสมโคพอลิเมอร์ของ(3-ไฮดรอกซีบิวทิเรต-โค-3-ไฮดรอกซีวาริเลต)โดยมีสัดส่วนโมลร้อยละ 9-32 และร้อยละ 35.95-74.62 โดยน้ำหนัก ด้วยความสามารถในการผลิตพอลิ(3-ไฮดรอกซีบิวทิเรต)โดยใช้ระยะเวลาน้อยลงและความสามารถในการใช้แหล่งคาร์บอนที่มีราคาถูกมาเป็นอาหาร สายพันธุ์ที่ไม่มียีนฟอสโฟกลูโคเนตดีไฮดราเทสจึงมีความน่าสนใจเพื่อนำมาใช้ในการผลิตพอลิไฮดรอกซีอัลคาโนเอตในอนาคต

สาขาวิชา เทคโนโลยีชีวภาพ ลายมือชื่อนิสิต .....

ปีการศึกษา 2567 ลายมือชื่อ อ.ที่ปรึกษาหลัก .....

5872839223 : MAJOR BIOTECHNOLOGY

KEYWORD: Pentose Phosphate Pathway, Polyhydroxybutyrate, phosphogluconate dehydratase, phosphoglucose isomerase, NADPH

Jittakan Pachimsawat : Effect of *pgi* and *edd* gene deletion in *Escherichia coli* K12 on production of poly(3-hydroxybutyrate) and copolymer poly(3-hydroxybutyrate-*co*-3-hydroxyvalerate). Advisor: Assoc. Prof. Suchada Chanprateep Napathorn, Ph.D.

The biomaterial poly(3-hydroxybutyrate) (PHB) is a promising alternative renewable and green polymer. In this research, we incorporated deletion of phosphogluconate dehydratase (*edd*) and phosphoglucose isomerase (*pgi*) in *E. coli* for PHB production for the first time. As a result, the *edd* mutant harboring pBSK*CAB*$_{A-04}$ reached the highest PHB production of 93.0%wt with 7.55 g/L PHB concentration at 30 hours of cultivation. A specific production rate of 0.21 h^{-1} and maximum productivity of 0.25 g/L.h were obtained using glucose as a sole carbon source. On the other hand, deletion of *pgi* gene only recovered the cell growth but did not promote any additional PHAs production. We further observed the ability of bacteria to assimilate cheap carbon sources such as crude glycerol from biodiesel industry. Surprisingly, *edd* mutant harboring pBSK*CAB*$_{A-04}$ had the highest PHB concentration of 2.7 g/L with 74.8%wt in 24 hours, superior amount than any other reports of PHB production from crude glycerol. In addition, *edd* mutant harboring pBSK*CAB*$_{A-04}$ can also accumulate 35.9-74.6%wt poly(3-hydroxybutyrate-*co*-3-hydroxyvalyrate) [P(3HB-*co*-3HV)] with 9-32 mol% of 3HV fraction. With the ability to accumulate PHAs within a short cultivation time and ability to utilize cheap carbon source, *E. coli* strain *edd* mutant represented a promising candidate for PHAs production in future trend.

Field of Study: Biotechnology Student's Signature .....

Academic Year: 2024 Advisor's Signature .....

ACKNOWLEDGEMENTS

I would like to express my sincere gratitude to my advisor Associate Professor Dr. Suchada Chanprateep Napathorn for her invaluable advice, expert guidance and unwavering encouragement throughout my research and thesis writing.

It gives me great pleasure in acknowledging the support and help of Associate Professor Dr. Takeharu Tsuge for his expertise and insightful discussions throughout my research at School of Materials and Chemical Technology, Tokyo Institute of Technology, Japan.

It is immense gratitude to my thesis committee: Assistant Professor Kobchai Pattaragulwanit, Associate Professor Kuakarun Krusong, Associate Professor Cheewanun Dachoupakan Sirisomboon and Dr. Sophon Sirisattha for their beneficial advice.

This thesis would not have been completed without funding from the Graduate School of Chulalongkorn University Scholarship, the 100th Anniversary Chulalongkorn University Fund for Doctoral Scholarship, the 90th Anniversary of Chulalongkorn University Scholarship and Overseas Research Experience Scholarship for Graduate Students.

I am indebted to my colleagues, especially Mr. Thanawat Boontip, Mr. Natthaphat Phothong and Miss Kanokjun Jaiboon, and all my friends in laboratory room 1904/16 for their encouragement and general helps over all the time.

I could not have completed this project without my beloved family for their love and mentally support during my hard time.

Jittakan Pachimsawat

TABLE OF CONTENTS

LIST OF TABLES

Page

LIST OF FIGURES

Page

CHAPTER I
INTRODUCTION

The use of conventional plastics made from non-renewable fossil fuels benefits society in several ways due to its diverse ranges of material properties (Thompson et al., 2009). The basic characteristics of traditional plastics such as transparency, light weight, low electrical conductivity, excellent thermal and corrosion resistance property allow the variety practical applications of plastics in mankind. Unfortunately, plastics waste is a crucial part of municipal solid waste causing lethal health and tremendous environmental damage (Iroegbu et al., 2021; Thompson et al., 2009). Most of plastics wastes, especially single use plastics, end up in landfills. Since the decomposition period of plastics may take up to 500 years, it brings about microplastics contamination in both soil and marine environments. In addition, incineration of conventional plastics releases enormous amounts of greenhouse gases emissions per unit energy than any other form of energy production, which promotes climate change and contributes to respiratory disease from smog and air pollution (Pathak et al., 2023). The recycling process of plastics is likely practically unfeasible due to the variety of plastics and recycled plastics price compared to virgin plastics (Sarah Perreard, 2024). Hence, biodegradable and bio-based materials such as polylactic (PLA), polyhydroxyalkanoates (PHAs) and starch-blended plastics could be promising alternatives to petroleum-based plastics on account of their environmentally sustainability and circularity in plastics industry within the near future.

Polyhydroxyalkanoates (PHAs) are biobased polymeric materials from R-hydroxyl-alkanoic acids linked by ester bonds (Tang et al., 2014). They are naturally synthesized and stored as cytoplasmic inclusion bodies for carbon and energy storage in microorganisms including *Cupriavidus necator, Pseudomonas* species, *Alcaligenes* species, *Halomonas Haloferix* and cyanobacteria. The biosynthesis of PHAs is primarily regulated under unbalanced growth conditions whereas carbon is presented in an excess amount and other essential nutrients are limited (Silva et al., 2021). To date, over 150 different types of PHAs have been identified (Chen & Patel,

2012). Among all of them, poly(3-hydroxybutyrate) (PHB), a short-chain-length PHAs (scl-PHAs) comprising 3-5 carbon atoms, was the first one identified and most widely studied (Lemoigne, 1926). PHB is a semicrystalline thermoplastic polyester due to its linear chain structure exhibiting both amorphous and crystalline phases (Matsumoto et al., 2009). It is insoluble in water and relatively resistant to hydrolytic degradation, but it is soluble in chloroform and chlorinated hydrocarbons. The melting temperature of PHB ranges from 165-180°C and its glass transition temperature is between 5 and 9°C, like those of fossil-derived thermoplastics (Chen & Patel, 2012; Grassie et al., 1984). Due to its large elastic modulus, PHB is not only stiff and brittle, but also very rigid and exhibits good barrier properties against oxygen compared to other biopolymers. However, low degradation temperature of approximately 220-290°C limits the possibility of thermal processing to prepare PHB films (Grassie et al., 1984). To enhance thermal degradation resistance of PHB, the addition of plasticizers, such as tributyl citrate and tributyl 2-acetylcitrate, blending and copolymerization with other monomers were widely studied. PHAs can be completely degraded naturally into carbon dioxide and water with the aid of hydrolytic and depolymerase enzymes secreted by microorganisms (Hankermeyer & Tjeerdema, 1999). The expanding usage of biodegradable PHAs plays a helpful role in reducing accumulation of plastics waste in both soil and marine environments.

Although PHAs gain much attention due to safe and environmentally friendly characteristics, industrializing PHAs struggles with various challenges including high production cost, unstable thermal and unsteady mechanical properties (Tan et al., 2021). Recruiting a host with ability to uptake inexpensive and renewable carbon sources is an essential factor to improve the cost and productivity of the process. Although natural PHAs producers can synthesize PHAs easily from various monomers, the efficiency of process is limited only on laboratory scale. Most of PHAs producers need structurally related precursors to produce different types of PHAs, while these precursors are hardly available in environment (Gao et al., 2022). Understanding in metabolic engineering influences *E. coli* as a promising host in large-scale production of PHAs. Unlike natural PHAs producers, *E. coli* does not possess endogenous PHA

depolymerase enzymes causing intracellular polymer degradation and resulting in low PHAs content. The biosynthesis of PHB in *E. coli* starts from the central carbon metabolite acetyl-CoA. Briefly, acetyl-CoA is condensed, followed by reduction and polymerization of 3-hydroxybutyryl-CoA into PHB (Meng et al., 2014). The biosynthesis of PHB requires nicotinamide adenine dinucleotide phosphate (NADPH) as a cofactor. In organisms, NADPH plays an important role in cellular antioxidation systems by serving as an electron donor used in a variety of biological settings (Spaans et al., 2015). It also serves as the reducing power to drive anabolic reactions by essential enzymes in central biosynthetic pathway. Several studies have shown that the availability of NADPH is the main bottleneck limiting the productivity of such biotransformation processes (Leen Assil-Companioni et al., 2020; Li et al., 2017; C. Wang et al., 2018). The regeneration of NADPH occurs mainly in three main sources, oxidative branch of the pentose phosphate pathway (PPP), tricarboxylic acid (TCA) cycle and by trans-hydrogenase enzymes from aerobic respiration (Sauer et al., 2004).

Our attempt to explore new possibilities to engineer the PHAs production by alteration of a metabolic pathway was presented. The idea was to elevate levels of cytosolic NADPH in recombinant *E. coli* by promoting the carbon flux through pentose phosphate pathway (PPP). The central metabolic pathway for glucose catabolism in *E. coli* includes the Embden-Meyerhof-Parnas pathway (EMP), Entner-Doudoroff pathway (EDP) and PPP. The EMP is the main glucose catabolism pathway, yielding two pyruvate, two ATP and two NADPH molecules per glucose molecule (Cori, 1983). The EDP produces one pyruvate, one glyceraldehyde-3-phosphate and one NADPH molecule per glucose molecule (Sokatch, 1969). The PPP serves as an oxidation route for NADPH, yielding one ribose-5-phosphate (R5P) and two NADPH molecules per glucose molecule (Landau, 2004). Phosphoglucose isomerase (*pgi*), which converts glucose-6-phosphate (G6P) to fructose-6-phosphate (F6P), is located at the first junction between the EMP and PPP. While phosphogluconate dehydratase (*edd*), which converts 6-phosphogluconate to 2-keto-3-deoxy-6-phosphogluconate, is the first junction between the EDP and PPP. Inactivation of the *pgi* and *edd* genes redirects glucose catabolism into the PPP (Meyer et al., 2018; Shimaoka et al., 2005).

Consequently, metabolic redirection in *pgi* and *edd* mutants accumulate more NADPH compared to its utilization. By introducing PHAs biosynthesis pathway, which is NADPH-consuming pathway, can not only enhance the PHAs production but also recover cellular growth rate of these mutants as NADPH sinks. In fact, disruption of the *pgi* and *edd* genes was proven to benefit the NADPH-dependent and PPP-related products such as shikimic acid and inosine (Ahn et al., 2011; Shimaoka et al., 2005). Although deletion of EMP and EDP pathway could result in decrease of bacterial growth due to excess amount of NADPH, these mutant strains could represent suitable hosts for PHAs production. Protein expression analysis of *pgi* disruption on PHB production revealed gene patterns affected from the redirection of glucose metabolism in *E. coli* and bacterial growth improved after incorporation with PHB biosynthesis (Md Mohiuddin Kabir & Kazuyuki Shimizu, 2003). Interestingly, fermentation characteristics of these mutants on PHAs production is still unclear.

Therefore, this research aimed to study the effect of *pgi* and *edd* gene deletion on PHB production. The *phaCAB* operon from *C. necator* strain A-04 with native promoter was cloned and expressed in *E. coli* in flask and bioreactor cultivation. Next, fermentation characteristics of the mutant strains were observed compared to the parental strain. PHB was extracted and used to prepare the film for mechanical and thermal analysis.

The objectives of this research

1. To construct recombinant plasmid for PHAs production
2. To study the effect of *pgi* and *edd* gene deletion on PHAs production
3. To produce PHAs from inexpensive carbon source such as crude glycerol using the *pgi* and *edd* mutants

Expected beneficial outcomes

1. Obtaining recombinant *E. coli* mutant with improved ability to produce PHAs
2. Illustrating the use of inexpensive carbon source to produce PHAs

CHAPTER II
LITERATURE REVIEW

2.1 Plastics

Plastics, originally means soft enough to be easily shaped into different forms, is a name of a category of polymer materials. Polymers are chain-like molecules composed of many repeating subunits called monomers. The most common natural polymer is cellulose making up the plants' cell walls with thousands of carbon, hydrogen and oxygen atoms (Sengupta, 2024).

2.1.1 History of plastics

The development of plastics early started from natural materials which possessed intrinsic plastic properties such as chewing gum, shellac, gutta-percha, silk and wool. Even natural polymers have lots of advantages such as biocompatibility, non-toxicity, biodegradability and low price, they have certain drawbacks which are slow production rate, weak thermal and mechanical stability. Later, the evolution of plastics involved chemical modification of natural materials resulted in synthetic polymer. The initial prototypes of artificial polymer were made by addition of alternative materials into natural rubber, exhibiting rigid, water-resistant and capable of being colored characteristics polymers (Rasmussen, 2021). The first synthetic polymer was cellulose based invented by John Wesley Hyatt in 1869. By the addition of camphor to nitrocellulose, it created the first thermoplastic called celluloids, used to substitute for ivory in making billiard balls (White, 1999). The first polymer of polyvinyl chloride was synthesized between 1838-1872. Later in 1907, the first synthetic thermosetting polymer called Bakelite was obtained from condensation of phenol and formaldehyde. Not only Bakelite was lightweight, it had electrical and thermal insulating properties, which later intensively applied to items such as electrical sockets, telephone castings and saucepan handles (Klun et al., 2022). The discovery of Bakelite opened many doors to the series of plastic manufacturing processes improvement, introducing variety of polymers such as resins, waxes, nylons and rubbers. In the 20th century, plastics were developed from petrochemical by-products such as natural gas, crude oil and coal. Petroleum-based plastics gained

much attention and were produced on a large scale due to their attractive properties such as lightweight, easy to mold and strength. Plastics have versatile thermal properties including heat resistance or combustibility, that can withstand the operation with temperature over 150-500^{o}C making them easily to be processed (Madorsky & Straus, 1959).

2.1.2 Types of conventional plastics

Plastics are composed of repeating molecular units called monomers, which are linked primarily by covalent bonds and secondary bonds such as Van der Waals and hydrogen bonds. By getting in sight the structure of plastics, amorphous and crystalline phases are represented (Figure 1). Depending on the type of monomers, the attached branching chains may prevent the molecule from forming organized regions and result in random oriented material molecules, which are called amorphous polymer. On the contrary, crystalline polymer is a material that exhibits organized and tightly packed molecular chains. Plastics can be categorized into two groups according to their thermal properties, which are thermoplastic and thermoset plastic (Lamba et al., 2021).

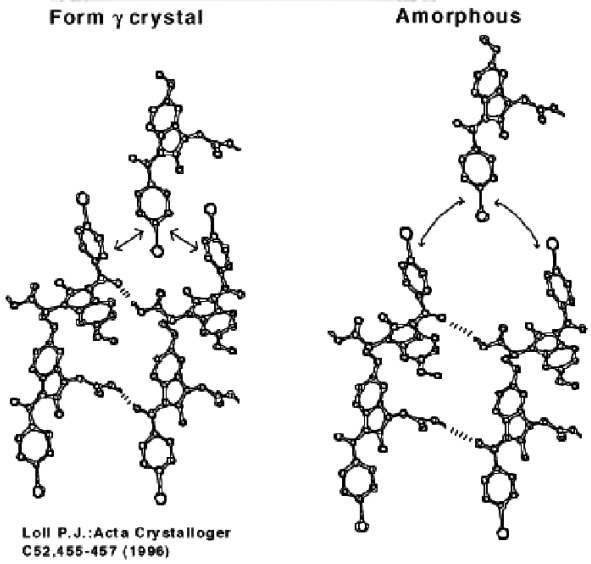

Figure 1 Molecular structure of crystalline and amorphous phase of indomethacin crystallinity by X-ray diffraction analysis (Otsuka et al., 2000)

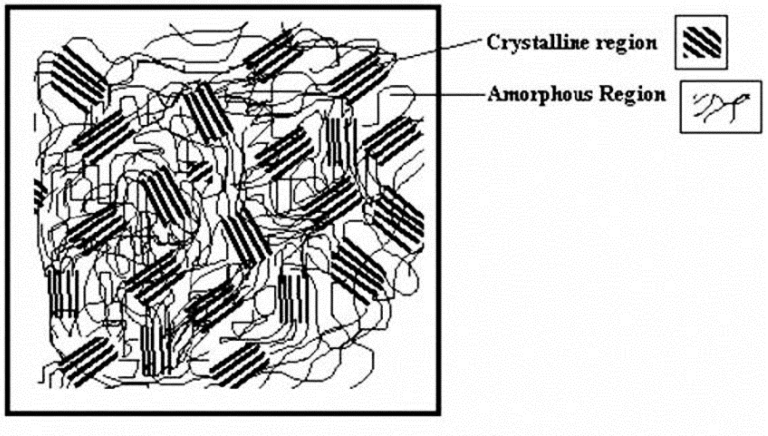

Figure 2 General mixed amorphous and crystalline phase macromolecular structure of semi-crystalline thermoplastic (Demirel et al., 2011)

2.1.2.1 Thermoplastic

Thermoplastic is a class of polymer that can be softened or moldable at a certain elevated temperature and processed by extrusion, thermoforming and blow molding. This type of polymer can be reprocessed many times without altering the chemical composition or changing the physical properties of polymer, which makes them recyclable. Generally, plastics consist of both amorphous and crystalline phase coexisting called semi-crystalline (Figure 2) (Demirel et al., 2011). Amorphous thermoplastic is re-shaped at a temperature over the glass transition temperature (T_g) whereas semi-crystalline thermoplastic is restructured at the temperature over the melting temperature (T_m).

2.1.2.2 Thermosetting plastic

Thermosetting plastic is a class of polymer made up of long chains of molecules by cross linking. Therefore, thermosetting plastic is generally stronger than thermoplastic. This polymer can be molded and pressed into shapes once heated but it is permanently stable to a solid state once set. The incredibly robustness of thermosetting plastic results in high resistance to heat with chemical and mechanical strength.

2.1.3 Properties of plastics

Plastics possess various characteristics which contribute to a wide range of applications and versatility.

2.1.3.1 Degree of polymerization and molecular weight

The degree of polymerization [(DP)-*n*] is defined as the number of monomeric units in the polymer chain (McKeen, 2023). Polymers consist of mixture monomers with different degrees of polymerization and molecular weight. Therefore, the polymer molecules are not identical. To identify the degree of polymerization of certain polymers, the number average molecular weight (M_n) and the weight average molecular weight (M_w) are represented (Figure 3). The ratio of M_w and M_n is defined as polydispersity index (PDI). PDI is used to measure heterogeneity of particles in the mixture of monomers. When molecules of the same size, mass and shape are mixed, the mixture is called monodisperse. In the other hand, molecules of the inconsistent size, mass and shaped are mixed, the mixture is called polydisperse.

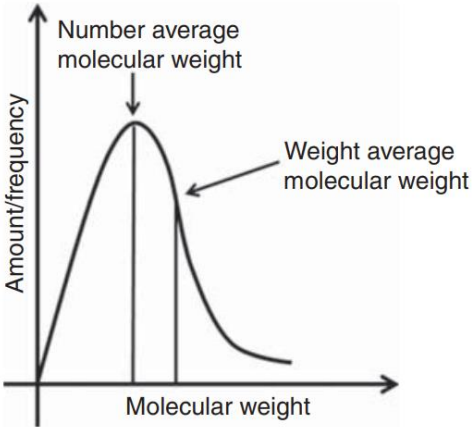

Figure 3 Average molecular weight of polymer (McKeen, 2023)

2.1.3.2 Heat capacity

The heat capacity of polymer is defined as the amount of heat needed to change the polymer temperature by one degree. This property of polymer provides perceptions to the ability of certain material to store and release thermal energy.

2.1.3.3 Crystallinity

As mentioned in 2.1.2, polymers consist of both amorphous and crystalline phases coexisting which directly affect the degree of crystallinity of polymer (Bombicz, 2022). Increase of crystallinity tends to increase polymer hardness and density. Polymers are classified by density differences into high-density and low-density polymers.

2.1.3.4 Chemical properties

Bonding between monomers greatly affects the chemical properties of polymer. The strong covalent bonds, hydrogen bonds and ionic bonds in polymers lead to more cross-linked strength while weak intramolecular bonds such as dipole-dipole result in more flexibility of the polymers. Also, polymers with Van der Waals forces tend to give low melting temperature. Generally, polymers robustness results in low reactivity to other substances.

2.1.3.5 Tensile strength

Tensile strength is defined as the maximum stress which polymer can be stretched without fracture. When stress less than the tensile strength is removed, polymer can return completely or partially to its original shape. The order of polymer arrangement as network, cross-linked, branch and linear possess polymer strength from highest to lowest, respectively.

2.1.3.6 Young's Modulus

Young's Modulus (Modulus of Elasticity) is defined as the ratio of stress to strain in the elastic region. It determines the ability of polymers to stretch and distort and is used to identify the stiffness of polymer. Polymers with weak intermolecular linkages can be stretched more than those with strong bonding.

2.1.4 Applications of plastics

Nowadays plastics play an important role in human daily life in almost every sector of the world. Plastics are synthetic materials with a wide range of applications depending on based monomer (Table 1) (Alabi et al., 2019; Chaukura et al., 2016).

Table 1 Properties and applications of commercial plastics

Plastics	T_m	Applications	Ref.
Low density polyethylene (LDPE)	105-115	Packaging films, wire and cable coatings, toys, plastic bags, electrical insulation	(Fernández & Puig, 2002)
High density polyethylene (HDPE)	120-190	Films and sheets, packaging such as shopping bags, food containers, construction builds and infrastructure endeavors	(Hamod, 2015)
Polypropylene (PP)	150-160	Packaging films, bottles, food containers, surgery tools	(Asgari & Masoomi, 2013)
Polyethylene terephthalate (PET)	235-260	Food packaging such as soft drink bottles, microwave tray, clothing and magnetic tape	(Asgari & Masoomi, 2013)
Polystyrenes (PS)	220-275	Packaging, houseware, toys, furniture construction	(Cimmino et al., 1991)
Polyvinyl chloride (PVC)	115-245	Conveyor belting, pipes, cosmetics container	(Summers, 2008)
Polycarbonate (PC)	100-110	Greenhouse walls, DVDs, sunglasses	(Balaji et al., 2018)
Acrylonitrile Butadiene Styrene (ABS)	190-250	Telecommunication applications such as keyboards, computers, luggage, housewares components	(Hamod, 2015)

2.1.5 Plastic pollution

Although the use of plastics benefits society in several ways due to their diverse properties, over 359 million tons of global annual production of plastics are generated and leads to the accumulation of plastics in the environment. Plastics has turned into a universal problem because of their strength. The durability of plastics promotes hundreds of years for plastics decomposition. Since 1950, average annual growth of global plastic production increased continuously by 8.5% (million metric tons). By the end of 2040, the global production of plastic is expected to reach 540 million metric tons with the increase of plastic pollution by triples (Sarah Perreard, 2024). Large amount of plastics contamination pointed out as the threat to wildlife and human populations (Nayanathara Thathsarani Pilapitiya & Ratnayake, 2024). Degradation of plastics into micro or nanoparticles leads to the spread of small particles plastics in air, soil and water. Microplastic exposure can cause cell death and metabolic disorders by physical harms, chemical exposure and activating inflammatory response, not only to human but also wild life and aquatic environments (Jeong et al., 2024). Several articles report the death across 80 marine species including sea turtles, sea birds, pinnipeds and cetaceans due to consumption of microplastics (Duncan et al., 2024; Hahladakis, 2024; Roman et al., 2020). Since plastics are made of petroleum-based, incineration of plastics wastes also releases heavy metals and toxic substances such as dioxin and greenhouse gases. Carbon dioxide, methane, nitrous oxide and fluorinated gases are greenhouse gases promoting climate change and contributes to respiratory disease from smog and air pollution (Verma et al., 2016). The recycling of plastics is almost practically unfeasible due to the variety of plastics. Different types of plastics combined in manufacturing processes make recycling process even much more difficult as it requires different temperatures to reprocess. In addition, huge amounts of mismanaged wastes (about 70 million tons) in the form of plastic are ended up in nature by 2024 according to the report (Sarah Perreard, 2024). These mismanaged wastes include plastics waste disposed into the sea, open waters, landfills and dumpsites. Consequently, demand for bio-degradable products is growing to substitute for conventional plastics. Polylactic acid (PLA), polyhydroxyalkanoate (PHA)

and starch-blended polymer attract much attention due to their sustainability and circularity in the plastics industry.

2.2 Polyhydroxyalkanoates

Polyhydroxyalkanoates (PHAs), a group of aliphatic polyesters, are biobased polymeric material with biocompatibility, biodegradability and non-toxic properties (Zytner et al., 2023). In nature, PHAs are synthesized continuously through a chain of chemical conversion in many types of microorganisms and accumulated as carbon and energy storage in the form of granules within cellular structure. The granules representing water-insoluble inclusions are surrounded by phospholipids membrane and proteins (Figure 4). The mechanism of PHAs granules formation represents in two models. In a membrane-budding model, hydrophobic PHAs chain are initially synthesized within the cytoplasm and granules later bud from the membrane through an unknown process (Stubbe et al., 2005). To support the theory, fluorescent tagged synthase and phasins (PhaP) with Nile Red stained PHB localized near the membrane in granule genesis were reported in various microorganisms (Hermawan & Jendrossek, 2007; Jendrossek et al., 2007; Peters et al., 2007). On the contrary, micelle model predicts that PHAs aggregate within the cytoplasm with covalently PHAs synthases attached on the surface and later form a micelle-structure due to the hydrophobicity of PHAs-synthase complex molecules (Griebel et al., 1968). In vitro PHAs polymerization by synthase monitoring revealed a formation of micelle-like and granule-like structures (Gerngross & Martin, 1995; Hiraishi et al., 2005). In addition, the majority components of PHAs granule with 97.5% of proteins and minor amounts of phospholipids encouraged the micelle model (Choy, 2012; Jendrossek, 2009). Recent research illustrated the model of an in vivo PHAs granule with only proteins on the surface layer and free of phospholipids (Bresan et al., 2016).

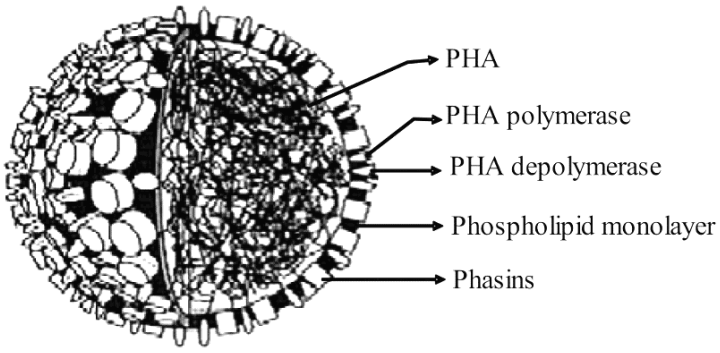

Figure 4 The ideal PHA granule surrounded by phospholipids membrane and crystalline proteins (Rehm, 2007)

Based on the nutrient stress and growth pattern, PHAs producing bacteria are classified into two groups. In *Cupriavidus necator*, *Pseudomonas oleovorans* and *Pseudomonas putida,* PHAs are primarily synthesized when excess carbon source is available and limited of growth-essential components such as nitrogen, phosphorus, oxygen or even fluctuating pH of growth media. This group of bacteria is not able to synthesize PHAs during their growth periods (Guzik et al., 2014). Under nutrient-rich conditions, high amounts of coenzyme A from TCA cycle inhibits PHAs biosynthesis to channel acetyl-CoA into TCA cycle for energy production and cell growth. During starvation and environmental stress, microorganisms accumulate PHAs for their survival. The presence of PHAs granules is also protective mechanism for bacteria in the condition of osmotic shocks, oxidative pressure, UV exposure and heavy metals exposure (Obruca et al., 2020). In the condition which nitrogen is limited, bacteria continue to assimilate carbon source without further growth as nitrogen is essential for protein and nucleic acid synthesis. Thus, carbon is used to produce storage compounds such as PHAs. On the other hand, some groups of bacteria such as *Azotobacter vinelandii* (Chou et al., 1997), *Alcaligenes latus* (Braunegg et al., 1998) and recombinant *Escherichia coli* (Wu et al., 2016) can store PHAs during its growth phase without being affected by nutrient limitations (Koller et al., 2017; Nitschke et al., 2011).

2.2.1 PHAs structure and classification

PHAs are composed of R-hydroxyl alkanoic acids linked by ester bond between the carboxyl group of the first monomer and the hydroxyl group of the second monomer (Tang et al., 2014). Up to date, there are approximately 150 different types of R-hydroxyl alkanoic acids known as the constituents of storage polyesters (Mitra et al., 2020). The general structure of PHAs and naturally PHAs monomers are shown in Figure 5 (Peregrina Lavín et al., 2021) and Figure 6 (Steinbüchel & Valentin, 1995; Yang et al., 2013). However, natural PHAs constituents can be physically and chemically modified resulted in increasing numbers of novel monomers in PHAs family (Zinn & Hany, 2005). Production of an aromatic PHA, P(3-hydroxy-5-phenylvalerate) [P(3H5PhV)] from 5-phenylvaleric acid in *P. oleovorans* was reported (Fritzsche et al., 1990). The double bonds in the side chain of poly(3-hydroxyalkanoate-*co*-3-hydroxyalkenoate) were turned into thioester bonds by radical addition reaction of 11-mercapto-1-undecanol. The terminal of hydroxyl group was reacted with cinnamic acid resulted in ester compound, followed by sulfurized with $ClSO_3H$ or combined with *tert*-butyldimethylsilyl-protected coumaric acid (Hany et al., 2004). PHAs can be categorized into three groups by the arrangement and number of carbon atoms in the chain including branching chain.

2.2.1.1 Short chain length PHAs

Short chain length (scl) PHAs are comprised of 3-5 carbon atoms. The most well studied poly(3-hydroxybutyrate) (PHB) is categorized in this group. Microorganisms produce scl-PHAs are *C. necator* (Chanprateep et al., 2008)*, Alcaligenes sp.* (Doi et al., 1992) *and Azobacter sp.* (Page, 1992).

2.2.1.2 Medium chain length PHAs

Medium chain length (mcl) PHAs are composed of 6-14 carbon atoms. The most common mcl-PHAs are poly(3-hydroxyhexanoate) (P3HHx) and poly(3-hydroxyoctanoate) (P3HO) The microorganism naturally produce mcl-PHAs is *Pseudomonas sp.* (Kellerhals et al., 2000).

2.2.1.3 Long chain length PHAs

Long chain length PHAs (lcl), less common and least studied type, are constituent of more than 14 carbon atoms. Petpheng et al. (2023) reported

newly isolated *Enterobacter sp.* from textile wastewater with ability to produce mcl-*co*-lcl PHA using waste cooking oil as carbon source (Petpheng et al., 2023).

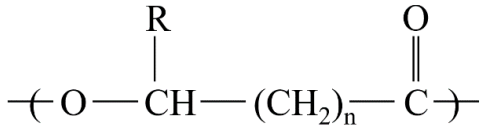

n	Type	R group	Carbon	PHA polymer
1	Scl	H	C_3	Poly(3-hydropropionate)
1	Scl	CH_3	C_4	Poly(3-hydroxybutyrate)
1	Scl	CH_2-CH_3	C_5	Poly(3-hydroxyvalerate)
1	Mcl	$(CH_2)_2$-CH_3	C_6	Poly(3-hydroxyhexanoate)
1	Mcl	$(CH_2)_3$-CH_3	C_7	Poly(3-hydroxyheptanoate)
1	Mcl	$(CH_2)_4$-CH_3	C_8	Poly(3-hydroxyoctanoate)
1	Mcl	$(CH_2)_5$-CH_3	C_9	Poly(3-hydroxynonanoate)
1	Mcl	$(CH_2)_6$-CH_3	C_{10}	Poly(3-hydroxydecanoate)
1	Mcl	$(CH_2)_7$-CH_3	C_{11}	Poly(3-hydroxyundecanoate)
1	Mcl	$(CH_2)_8$-CH_3	C_{12}	Poly(3-hydroxydodecanoate)
1	Mcl	$(CH_2)_9$-CH_3	C_{13}	Poly(3-hydroxytridecanoate)
1	Mcl	$(CH_2)_{10}$-CH_3	C_{14}	Poly(3-hydroxytetradecanoate)
1	Lcl	$(CH_2)_{11}$-CH_3	C_{15}	Poly(3-hydroxypentadecanoate)
1	Lcl	$(CH_2)_{12}$-CH_3	C_{16}	Poly(3-hydroxyhexadecanoate)
2	Scl	H	C_4	Poly(4-hydroxybutyrate)
2	Scl	CH_3	C_5	Poly(4-hydroxyvalerate)
3	Scl	H	C_5	Poly(5-hydroxyvalerate)
3	Mcl	CH_3	C_6	Poly(5-hydroxyhexanate)

Figure 5 General structure and classification of polyhydroxyalkanoates. The alkyl R group refers to the type of hydroxyl alkanoic acid monomer unit. The n refers to repeating units (Peregrina Lavín et al., 2021)

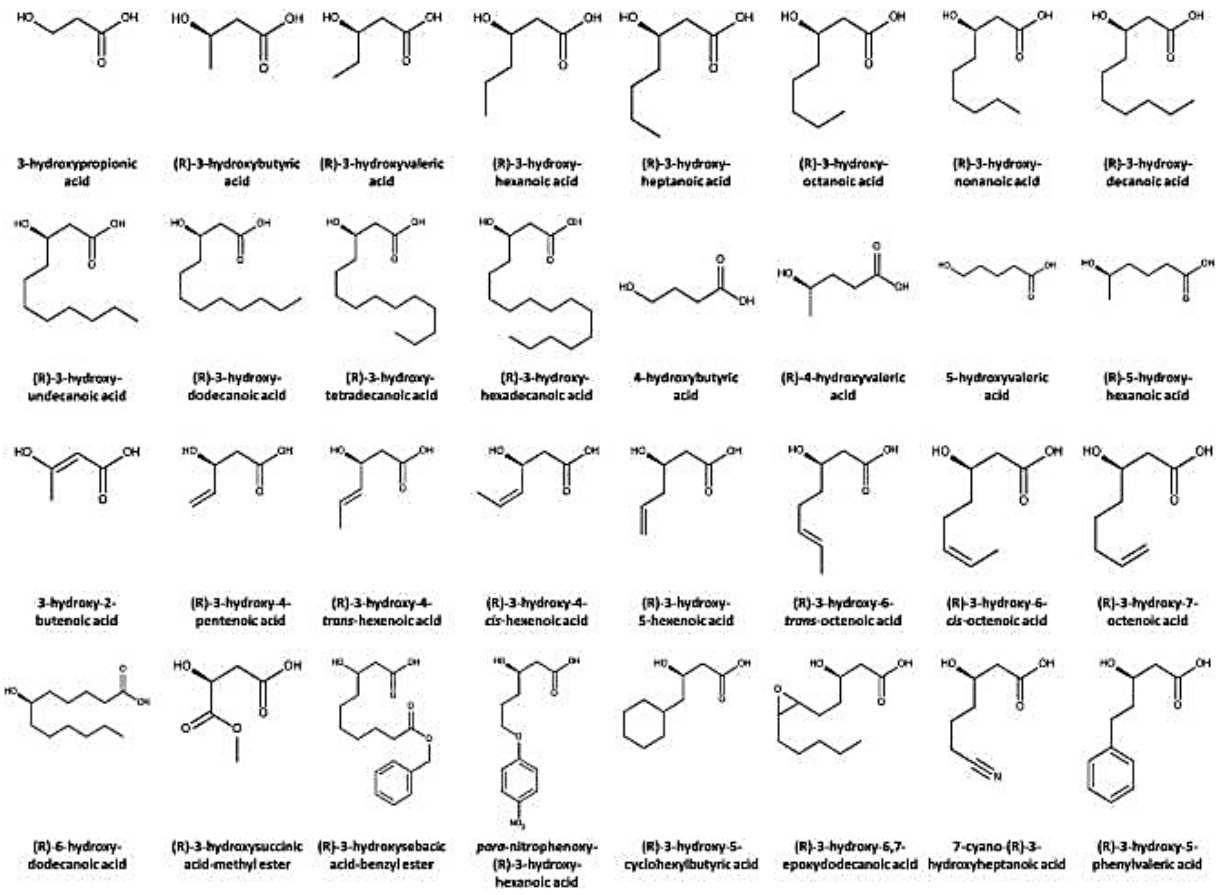

Figure 6 Molecule identified as PHA monomers in microbial synthesis. The monomer differs by the number or carbon and branching chain (Yang et al., 2013)

2.2.2 PHAs properties

The diversity of PHAs has attracted much attention due to their biodegradability, biocompatibility, low cost of feedstock, hydrophobicity and wide range of applications, especially in medical and agricultural aspects.

2.2.2.1 Biodegradability

The most remarkable property of PHAs is their biodegradability. Although synthetic polymers take hundreds to thousands of years to be decomposed, PHAs can be degraded into carbon dioxide and water in natural environments such as soil, sea and fresh water within 14-60 days as shown in Table 2.

Table 2 PHAs polymer biodegradation test in soil and marine environments

Type of PHAs	Type of environment	Degradation (%)	Length (days)	Ref.
PHA/Rice husk (60/40wt%)	Alluvial-type soil 35% soil moisture	< 90	60	(Wu, 2014)
PHB-*co*-PHV	Garden soil Room temperature	18	30	(Wang et al., 2008)
PHB – starch (75/25wt%)	Garden soil, 25°C, pH 6.8, 45% soil moisture	50-60	14-21	(Erkske et al., 2006)
PHB	Soil of temperate zone, 28°C, pH 7.1-7.8, 50% soil moisture	93	35	(Volova et al., 2017)
PHB-*co*-6.2mol%3HV	Garden soil, 23°C, pH 5.1, 35.6% soil moisture	100	30	(Gonçalves et al., 2009)
PHB-*co*-15mol%4HB	Garden soil, room temp, 20% soil moisture	93	60	(Wen & Lu, 2012)
PHB-*co*-11mol%3HV	Marine environment, 27-30°C, pH 7-7.5, salinity of water 32-35%	60	42	(Volova et al., 2010)

2.2.2.2 Thermal and mechanical properties

Thermal properties are commonly examined for PHAs material to determine the temperature conditions at which the polymer can be processed and utilized. Generally, properties of PHAs are described according to the classification of PHAs, which are scl-PHAs and mcl-PHAs. Nevertheless, PHAs in the same classification can be distinct depending on host strains, feedstocks and fermentation conditions.

Scl-PHAs are thermoplastics, similar to PP, with high melting temperature, high crystallinity and relatively high tensile strength where mcl-PHAs are elastomeric polymer with low melting temperature and low crystallinity (Bugnicourt et al., 2015). The limitation of scl-PHAs is their intrinsic brittleness, resulting in very poor mechanical properties and limiting their range of applications. Indeed, the elongation at break is very different between scl-PHAs (5%) to PP (500%) and mcl-PHAs (450%) (Silva et al., 2021). The comparison of properties of PHAs is represented in Table 3.

Table 3 Comparison of thermal and mechanical properties of PHAs (Mozejko-Ciesielska et al., 2019; Silva et al., 2021)

Properties	Scl-PHAs	Mcl-PHAs
Melting temperature (°C)	130 to 170	40 to 60
Glass transition temperature (°C)	-5 to 5	-50 to -25
Crystallinity (%)	60-80	< 40
Molecular weight (kDa)	Up to 1500	45-300
Young's modulus (GPa)	3.5 to 4000	Up to 15
Elongation to break (%)	3 to 8	Up to 450
Tensile strength (MPa)	Up to 40	Up to 10
Resistance to UV light	Good	Good
Resistance to solvents	Weak	Weak

The brittleness of scl-PHAs such as PHB and PHBV may result from the secondary crystallization of amorphous phase in these polymers (Bugnicourt et al., 2015; Seggiani et al., 2015). Since secondary crystallization takes place at room

temperature, close to the glass transition temperature (T_g), the nucleation density of these polymers is low with large spherulitic sizes (Figure 7). The large spherulites and orientation can exhibit inter-spherulitic cracks, leading to brittle PHAs (Hsieh et al., 2011). By addition of a nucleating agent or copolymerization with other monomers, the number of nucleation rate increases and the size of spherulites decreases, making the polymer more transparent and elastic (Caputo et al., 2023).

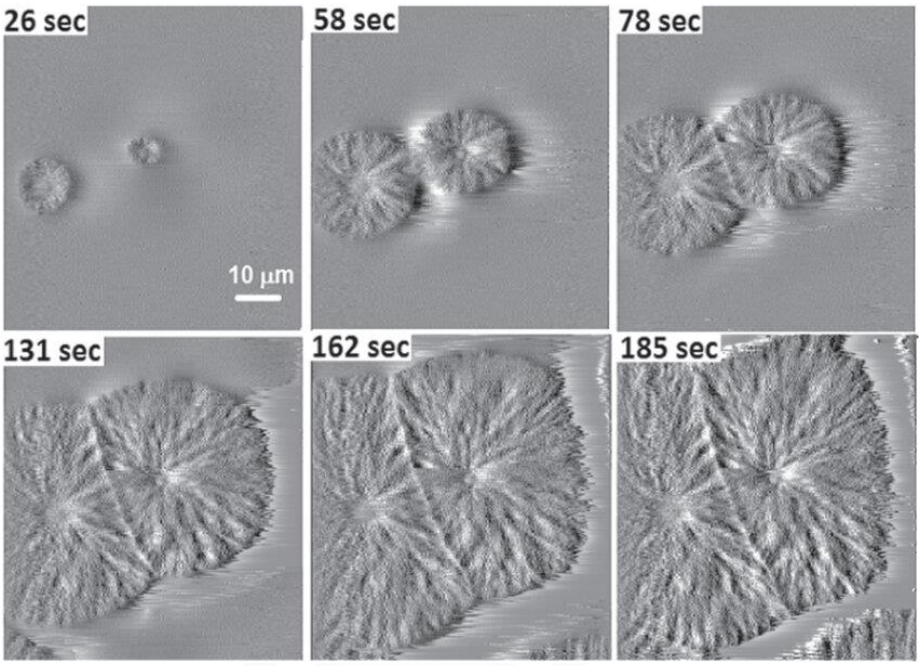

Figure 7 A series of high-speed atomic force microscopy (AFM) images from the crystallization process of polyhydroxybutyrate (PHB) polymer at room temperature where the growth of two spherulites was captured on the surface. Images were acquired in one second each with a line rate of 830 Hz. The image size is 57 × 62 μm² and the image resolution is 256 × 256 pixels. The gray scale represents the deflection signal in arbitrary units. (J.-Y. Wang et al., 2018)

2.2.2.3 Biocompatibility

PHAs display high compatibility property, which leads PHAs to be intensively used in therapeutic applications. Natural occurrence of PHAs building blocks can be degraded into D-3-hydroxybutyric acid, a normal constituent of human blood (Pachence et al., 2007). Up to date, PHB, PHBV, PHBHHx and P(3HB-*co*-4HB) had been

widely used as heart valve tissue engineering, bone tissue engineering, cartilage engineering, 3D printing and drug delivery carrier (Table 4) (Sodian et al., 2000). So far, only poly(4-hydroxybutyrate) (P4HB) has been approved as a suture material in clinical trial applications.

Table 4 Application of different types of PHAs in tissue engineering

Type of PHAs	Combination with	Key findings	Reference
PHB	PLA	The blending of PHB and PLA produced stable tubular substitute for urethra replacement.	(Findrik Balogová et al., 2018)
PHB	Chitosan	The implant supported osteochondral regeneration.	(Petrovova et al., 2021)
PHBV	Cerium oxide nanoparticles	The cerium oxide nanoparticles loaded PHBV membrane enhanced cell proliferation and promoted healing of wounds.	(Augustine et al., 2020)
P(3HB-*co*-4HB)	-	Fiber scaffolds induced cell adhesion and proliferation without cytotoxicity.	(Fu et al., 2019)
P(3HB-*co*-4HB)	Bacterial cellulose	Bacterial cellulose with P(3HB-*co*-4HB) are more effective than commercial wound dressing.	(Z. Wang et al., 2019)
PHBHHx	-	PHBHHx used as scaffold in blood vessels and promoted bone regeneration.	(Liu et al., 2020)
PHBHHx	-	PHBHHx was used in transplanted stem cells in a rat with brain injured model.	(L. Wang et al., 2019)

2.2.3 PHAs biosynthesis pathway

The PHAs biosynthesis pathway in microorganisms principally involves the cellular central metabolism. Series of catabolism and anabolism pathways including glycolysis, tricarboxylic acid (TCA) cycle, pentose phosphate pathway, serine pathway, fatty acid and amino acid synthesis and degradation, play an important role in the synthesis of PHAs precursors both directly and indirectly (G.-Y. A. Tan et al., 2014). Many common intermediates are shared between these pathways and PHAs biosynthesis pathway. Hence, PHAs biosynthesis regulation is complex. The accessibility of PHAs precursors, their molecular weight and their length of branching chains depend on many factors. Feedstock with related and unrelated structure and enzymes in PHAs biosynthesis have crucial impact on the types of produced PHAs.

PHA synthase is a key enzyme in PHAs polymerization, which can be categorized into four classes based on the substrate specificity and subunit compositions (Rehm, 2003). Class I synthase is found in mainly *C. necator* (formerly known as *Ralstonia eutropha* and *Alcaligenes eutrophus*), capable of using the CoA-thioester of hydroxyalkanoates having 3-5 carbon atoms as its substrate (Mezzolla et al., 2018). Class II synthase originated in *Pseudomonas* sp. such as *Pseudomonas aeruginosa* and *Pseudomonas putida*, polymerizing the CoA-thioesters of hydroxyalkanoates from 6-14 carbon atoms as its substrate (Mezzolla et al., 2018). Both class I and II PHA synthase are composed of homodimers of phaC subunits. Class III synthase consists of two heterosubunits (phaC and phaE), represented in *Synechocystis* sp. and *Allochromatium vinosum.* Finally, class IV synthase consists of two hetero subunits (phaC and phaR), instituted in *Bacillus megaterium* and *Bacillus cereus* (Sivashankari et al., 2023). Molecular organization of PHA synthases are displayed in Figure 8.

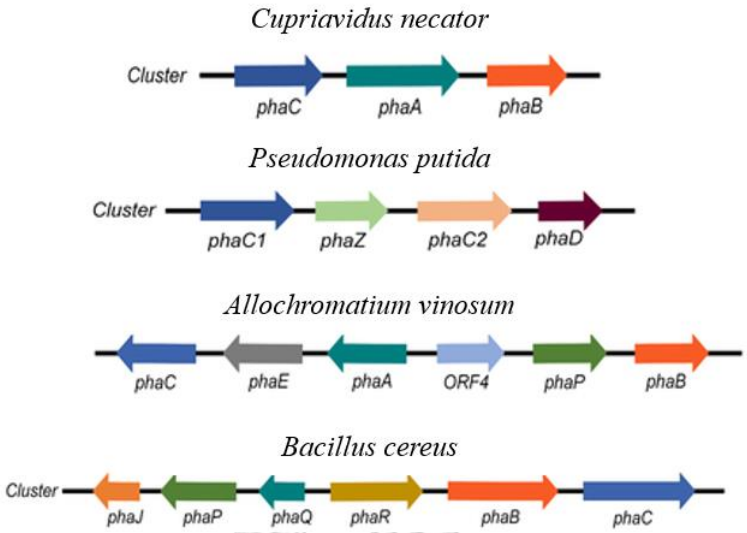

Figure 8 PHA cluster of genes organization in PHAs synthesis (Acuña & Poblete-Castro, 2022)

2.2.3.1 Poly(3-hydroxybutyrate) biosynthesis pathway

PHB is the most well-studied member of PHAs family. Therefore, PHB biosynthesis is a model for better understanding of other PHAs biosynthesis pathway. This PHB biosynthesis pathway consists of three essential enzymes, beta-ketothiolase (EC 2.3.1.9) encoded by *phaA* gene, acetoacetyl-CoA reductase (EC 1.1.1.36) encoded by *phaB* gene and PHA synthase encoded by *phaC* gene (Figure 9) (Silva et al., 2021). The reaction starts with the condensation of acetyl-CoA, an intermediate derived from the glycolytic pathway, catalyzed by beta-ketothiolase. In this head-to-tail condensation, the first acetyl-CoA serves as an electrophile at C-1 and the other acetyl-CoA serves as the equivalent of a C-2 carbanion. The powerful nucleophile carbanion attacks the carbon of a second molecule, followed by the release of coenzyme A, resulting in acetoacetyl-CoA. Next, acetoacetyl-CoA is stereoselectively reduced by NADPH-dependent acetoacetyl-CoA reductase at the 3-ketone group, resulting in the synthesis of (R)-3-hydroxybutyryl-CoA. NADPH, a universal electron donor, serves as coenzyme incorporating with acetoacetyl-CoA reductase (Matsumoto et al., 2013). Acetoacetyl-CoA reductase is generally known as NADPH-preferring enzyme although this enzyme has been reported to have activity with NADH as well in some microorganisms (Fukui et al., 1987; Olavarria et al., 2022;

Ritchie et al., 1971; Shuto et al., 1981; Yabutani et al., 1995). Finally, (R)-3-hydroxybutyryl-CoA monomers are polymerized into PHB with the aid of PHA synthase.

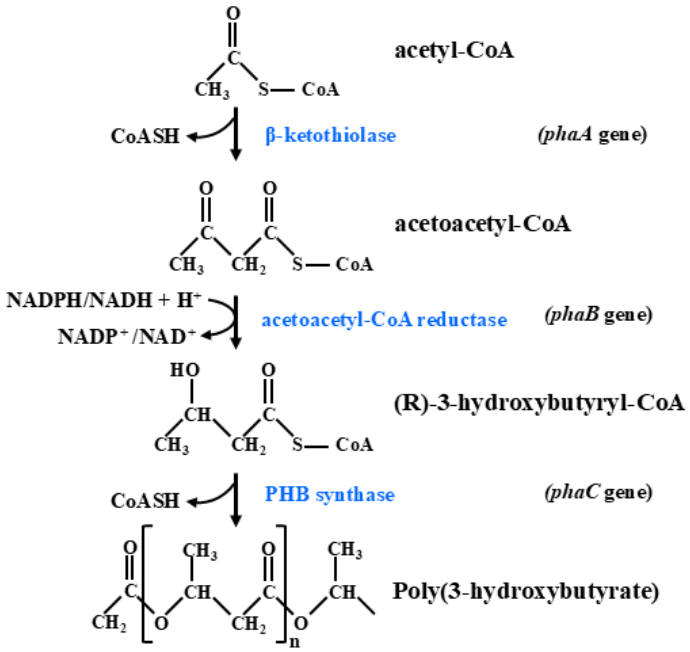

Figure 9 Polyhydroxybutyrate biosynthesis pathway.Modified from (El-Nahrawy, 2009)

2.2.3.2 Poly(3-hydroxyvalerate) biosynthesis pathway

Poly(3-hydroxyvalerate) (P3HV) is a member of scl-PHAs with 5 carbon atoms. The biosynthesis of P3HV in nature requires structural related carbon source such as propionate for 3-hydroxyvaleyrl-CoA synthesis. The biosynthesis of P3HV starts with the transfer of coenzyme A molecule by propionate CoA-transferase (*pct*) from acetyl-CoA to propionate, resulting in propionate-CoA. The propionate-CoA molecules are condensed by *phaA* (also known as *BktB*), resulting in 3-ketovaleryl CoA. After that, 3-ketovaleryl CoA is reduced by *phaB* to 3-hydroxyvaleryl CoA, followed by polymerization into poly(3-hydroxyvalerate) by *phaC* (Figure 10) (Chen et al., 2011). The mechanism of P3HV biosynthesis is similar to that found in PHB biosynthetic pathway. With the board range of substrate specificity of PHA synthase class I, many kinds of PHAs precursors such as 3-hydroxypropionyl-CoA and 4-hydroxybutyryl-CoA can be polymerized together with

PHB and P3HV. Sivashankari et al. (2023) reported site-directed mutagenesis of PHA synthase class I by error prone PCR with ability to polymerize 3-hydroxyhexanoate, 3-hydroxy-4-methylvalerate, 3-hydroxy-2-methylbutyrate and 3-hydroxypivalate monomers into PHB-based polymers (Sivashankari et al., 2023).

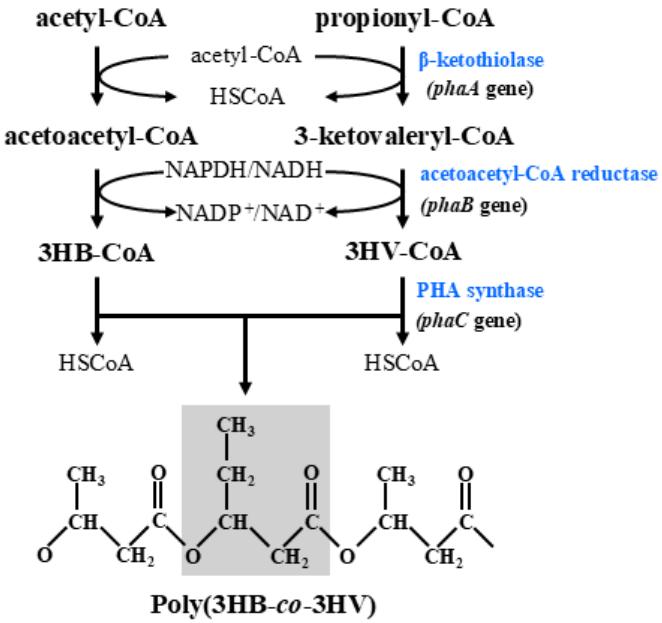

Figure 10 Poly(3-hydroxybutyrate-*co*-3-hydroxyvalyrate) biosynthesis pathway. Modified from (Chen et al., 2011)

2.2.3.3 Mcl-PHA biosynthesis pathway

Mcl-PHA biosynthesis associates with two main pathways responsible for producing mcl-PHA precursors, which are beta-oxidation of fatty acid and fatty acid de novo biosynthesis (Figure 11) (G.-Y. Tan et al., 2014).

In beta-oxidation, fatty acids are metabolized into 3-hydroxyacyl-CoA through a chain of reactions. Starting with, acyl-CoA synthase catalyzes the synthesis of acyl-CoA from fatty acid. Acyl-CoA is then oxidized to 2-*trans*-enoyl-CoA, (S)-3-hydroxyacyl-CoA and 3-ketoacyl-CoA by acyl-CoA dehydrogenase, enoyl-CoA hydratase and 3-ketoacryl-CoA thiolase enzyme (Kim et al., 2007). The intermediates, such as (S)-3-hydroxyacyl-CoA and 3-ketoacyl-CoA molecules, are subsequently converted to (R)-3-hydroxyacyl-CoA by 3-hydroxyl-CoA epimerase and 3-ketoacyl-ACP reductase, respectively. Finally, (R)-3-hydroxyacyl-CoA is polymerized by

PHA synthase class II. Apart from this, a specific enoyl-CoA hydratase (phaJ) converting 2-*trans*-enoyl-CoA to (R)-3-hydroxyacyl-CoA plays a critical role in supplying monomer units from beta-oxidation to mcl-PHA biosynthesis.

The fatty acid de novo is mainly a process of producing (R)-3-hydroxyacyl-CoA from non-related carbon sources such as glucose and gluconate (Silva et al., 2021). To begin with, non-related carbon sources are metabolized into acetyl-CoA via glycolytic pathway. Then acetyl-CoA is converted to malonyl-CoA by acetyl-CoA carboxylase (ACC). Later, malonyl-CoA is catalyzed into malonyl-ACP units by an irreversible catalytic reaction of malonyl-CoA-ACP transacrylase (FabD). In this reaction, the malonyl group is transferred to an acyl carrier protein (ACP). Then malonyl-CoA-ACP undergoes a condensation reaction with acetyl-CoA to yield acyl-ACP unit, which is two carbon unit. After that, beta-ketoacyl-ACP synthase (FabB) catalyzes the elongation of acyl-ACP unit into 3-ketoacyl-ACP, followed by the reaction which beta-ketoacyl reductase (FabG) reduces the 3-ketoacyl-ACP to (R)-3-hydroxyacyl-ACP molecule. Subsequently, the 3-hydroxyacyl group of (R)-3-hydroxyacyl-ACP is transferred from ACP to CoA by 3HA-ACP thioesterase (phaG), resulting in (R)-3-hydroxyacyl-CoA. Finally, (R)-3-hydroxyacyl-CoA monomers are polymerized by PHA synthase class II.

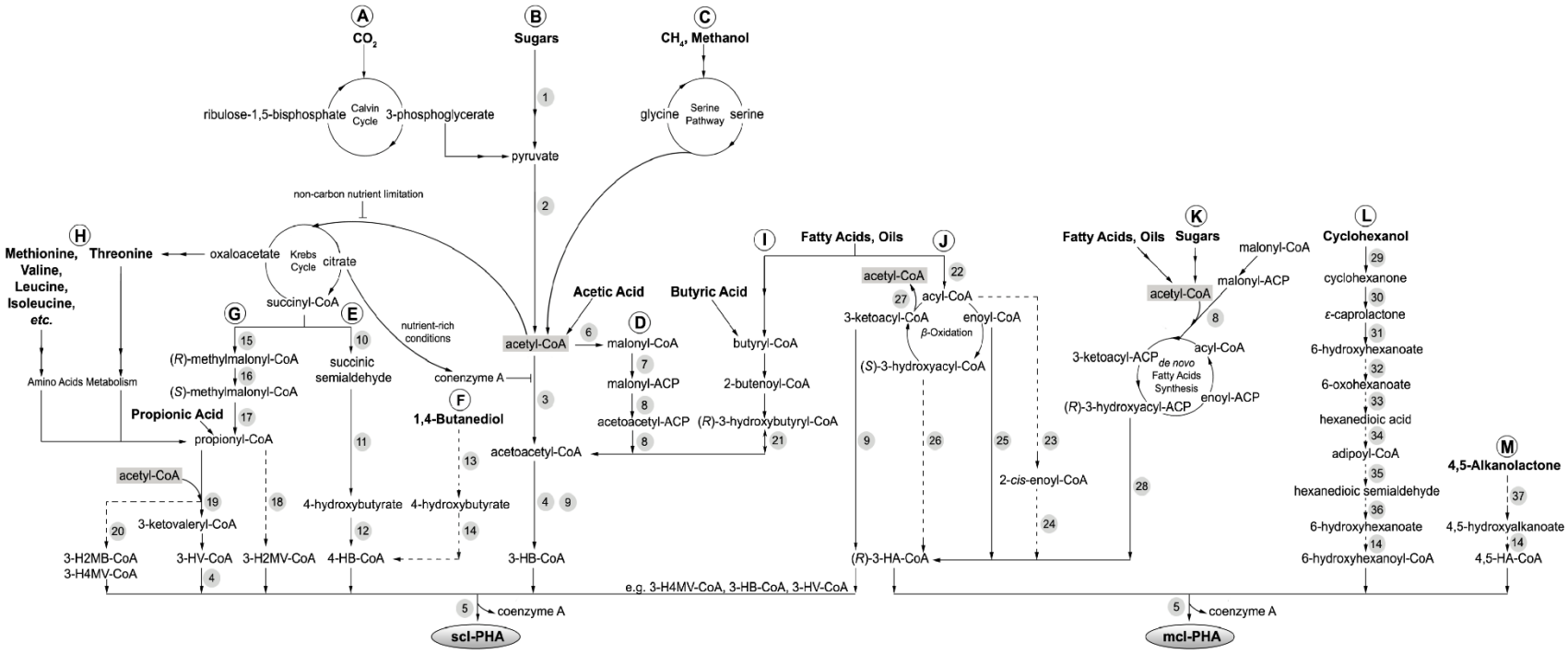

Figure 11 PHA biosynthesis pathway. Dotted lines represent putative pathways. Numbers represent enzymes involved in the chemical reactions that are summarized in table 5. (3-H2MB-CoA, 3-hydroxy-2-methylbutyryl-CoA; 3-H4MV-CoA, 3-hydroxy-4-methylvaleryl-CoA; 3-HV-CoA, 3-hydroxyvaleryl-CoA; 3-H2MV-CoA, 3-hydroxy-2-methylvaleryl-CoA; 4-HB-CoA, 4-hydroxybutyryl-CoA; 3-HB-CoA, 3-hydroxybutyryl-CoA; (R)-3-HA-CoA, (R)-3-hydroxyacyl-CoA; 4,5-HA-CoA, 4,5-hydroxyacyl-CoA (G.-Y. Tan et al., 2014)

Table 5 Enzymes involved in PHA biosynthesis pathways

No.	Enzyme	Abbreviation	Host	Reference
1	Gleceraldehyde-3-phosphate dehydrogenase	-	*Cupriavidus necator*	(Raberg et al., 2011)
2	Pyruvate dehydrogenase complex	-	*Cupriavidus necator*	(Raberg et al., 2011)
3	3-Ketothiolase	PhaA	*Cupriavidus necator*	(Peoples & Sinskey, 1989)
4	NADPH-dependent acetyl-CoA reductase	PhaB	*Cupriavidus necator*	(Peoples & Sinskey, 1989)
5	PHA synthase	PhaC	*Cupriavidus necator*	(Peoples & Sinskey, 1989)
6	Acetyl-CoA carboxylase	ACC	*Escherichia coli*	(Lee et al., 2011)
7	Malonyl-CoA:ACP transacrylase	FabD	*Escherichia coli*	(Lee et al., 2011)
8	3-Ketoacyl carrier protein synthase	FabH	*Escherichia coli*	(Lee et al., 2011)
9	NADPH-dependent 3-Ketoacyl reductase	FabG	*Pseudomonas aeruginosa*	(Ren et al., 2000)
10	Succinic semialdehyde dehydrogenase	SucD	*Clostridium kluyveri*	(Hein et al., 1997)
11	4-Hydroxybutyrate dehydrogenase	4hbD	*Clostridium kluyveri*	(Hein et al., 1997)
12	4-Hydroxybutyrate-CoA:CoA transferase	orfZ	*Clostridium kluyveri*	(Hein et al., 1997)

Table 5. Enzymes involved in PHA biosynthesis pathways (*Cont.)*

13	Alcohol dehydrogenase	-	*Aeromonas hydrophila* 4AK4	(Xie & Chen, 2008)
14	Hydroxyacyl-CoA synthase	-	*Cupriavidus necator*	(Steinbüchel & Valentin, 1995)
15	Methylmalonyl-CoA mutase	Sbm	*Escherichia coli*	(Aldor et al., 2002)
16	Methylmalonyl-CoA racemase	-	*Nocardia corallina*	(Valentin & Dennis, 1996)
17	Methylmalonyl-CoA decarboxylase	YgfG	*Escherichia coli*	(Aldor et al., 2002)
18	Ketothiolase	-	-	(Satoh et al., 1999)
19	3-Ketothiolase	BktB	*Cupriavidus necator*	(Slater et al., 1998)
20	Ketothiolase	-	-	(Satoh et al., 1999)
21	NADPH-dependent acetyl-CoA reductase	-	*Rhizobium sp.*	(Chohan & Copeland, 1998)
22	Acyl-CoA synthetase	FadD	*Escherichia coli*	(Yuan et al., 2008)
23	Acyl-CoA oxidase	-	-	(Mittendorf et al., 1998)
24	Enoyl-CoA hydratase	-	-	(Mittendorf et al., 1998)

Table 5. Enzymes involved in PHA biosynthesis pathways *(Cont.)*

25	(R)-enoyl-CoA hydratase	PhaJ	*Pseudomonas putida*	(Sato et al., 2011)
26	Epidermase	-	-	(Mittendorf et al., 1998)
27	3-Ketoacyl-CoA thiolase	FadA	*Pseudomonas putida*	(Ouyang et al., 2007)
28	3-Hydroxyacyl-ACP:CoA transacylase	PhaG	*Pseudomonas mendocina*	(Zheng et al., 2005)
29	Cyclohexanol dehydrogenase	ChnA	*Acinetobacter sp.*	(Brzostowicz et al., 2002)
30	Cyclohexanone monooxygenase	ChnB	*Acinetobacter sp.*	(Brzostowicz et al., 2002)
31	Caprolactone hydrolase	ChnC	*Acinetobacter sp.*	(Brzostowicz et al., 2002)
32	6-Hydroxyhexanoate dehydrogenase	ChnD	*Acinetobacter sp.*	(Brzostowicz et al., 2002)
33	6-Ocohexanoate dehydrogenase	ChnE	*Acinetobacter sp.*	(Brzostowicz et al., 2002)
34	Semialdehyde dehydrogenase	-	-	(Chen, 2009)
35	6-hydroxyhexanoate dehydrogenase	-	-	(Chen, 2009)
36	Hydroxyacyl-CoA synthase	-	-	(Chen, 2009)
37	Lactonase	-	*Cupriavidus necator*	(Valentin & Steinbüchel, 1995)

2.2.3.4 Other PHAs biosynthesis pathway

Poly(4-hydroxybutyrate) (P4HB) exhibits biocompatible property to human tissues in vivo and represents adequate polymer for medical and therapeutic applications. Wild type strains and recombinant strains are unable to utilize 4-hydroxybutyric acid as a carbon source, thus P4HB accumulation is likely impracticable. Hein et al. (1997) reported the first homopolymer of P4HB from recombinant *E. coli* expressing 4-hydroxybutyric acid-coenzyme A transferase (*orfZ*) from *Clostridium kluyveri* (Hein et al., 1997). With the aid of this transferase, 4-hydroxybutyryl-CoA could be supplied for P(3HB-*co*-4HB) production. The *orfZ* was reported involving in succinate degradation pathway, along with the identification of 4-hydroxybutyrate dehydrogenase (*4hbD*), succinic semialdehyde dehydrogenase (*sucD*) and succinyl-CoA:CoA transferase (*cat1*) (Söhling & Gottschalk, 1996). Valentin and Dennis (1997) successfully reported the P(3HB-*co*-4HB) production in *E. coli* expressing *orfZ, 4hbD* and *sucD* from glucose which was unrelated structural precursor (Valentin & Dennis, 1997). Brzostowicz et al. (2002) reported cyclohexanone oxidation by *Brevibacterium epidermidis* including several intermediates, cyclohexanol, cyclohexanone, caprolactone, 6-hydroxyhexanoate, 6-oxohexanoate and adipic acid (Brzostowicz et al., 2002). Structural related precursors such as adipic acid, 4,5-hydroxybutyrate and 4,5-alkanolactone can undergo the dehydrogenase enzymes (Mo**ż**ejko-Ciesielska & Kiewisz, 2016), followed by specific CoA synthetase and polymerized by PHA synthase as shown in Figure 10. Chia et al. (2010) also reported the production of novel PHAs containing 3-hydroxy-4-methylvalerate (3H4MV) monomers by feeding isocaproic acid as a substrate (Chia et al., 2010). Although PHA synthase has a wide range of substrate specificity, the supply of the R enantiomer precursors to the enzyme is a critical factor to be considered. Tajima et al. (2009) reported the decrease of molecular weight of the polymer when both enantiomers were supplied (Tajima et al., 2009). The S monomers possibly bind to the catalytic site of PHA synthase but are unable to further promote the addition of R enantiomers. The supply of only R monomers was reported to significantly improve the production of 3-hydroxytetradecanoic acid from (R)-oxirane acetic acid ethyl ester (Huang & Hollingsworth, 1998).

2.2.4 Host for PHAs production

PHAs producers such as gram-negative, gram positive bacteria and cyanobacteria can assimilate various carbon sources. These carbon sources include saccharides (e.g., glucose, fructose, xylose, arabinose, etc.), *n*-alkanes (e.g., hexane, octane, dodecane, etc.), *n*-alkanoic acids (e.g., acetic acid, propionic acid, butyric acid, oleic acid, etc.), *n*-alcohols (e.g., methanol, ethanol, octanol, glycerol, etc.) and gases (e.g., carbon dioxide, methane, etc.) (Anderson & Dawes, 1990; G.-Y. A. Tan et al., 2014). Moreover, several types of waste providing free sources of carbon include frying oil, food waste, biodiesel production waste, plastics waste and domestic waste were also used for PHAs production (Koller et al., 2009). Bacterial strains used for PHAs production are represented in Table 6.

Table 6 Bacterial strains used to produce PHAs

Bacterial strain	Carbon source	PHAs	Reference
Aeromonas hydrophila	Lauric acid, oleic acid	mcl-PHAs	(Lee et al., 2000)
Alcaligenes latus	Sucrose, malt waste, soy waste, milk waste, vinegar waste, sesame oil	PHB	(A. L. Wong et al., 2004)
Bacillus cereus	Glucose and epsilon-caprolactone	PHB and P[3HB-*co*-3HV-*co*-HHx]	(Labuzek & Radecka, 2001)
Bacillus sp.	Glucose, alkanoates, epsilon-caprolactone, soy molasses	PHB, PHBV	(Katrcolu et al., 2003; Shamala et al., 2003)
Burkholderia sacchari	Adonitol, lactose, arabinose, arabitol, cellobiose, fructose, maltose, rhamnose	PHB, PHBV	(Brämer et al., 2001)
Burkholderia cepacian	Palm olein, palm stearin, crude palm oil, palm kernel oil, oleic acid, xylose	PHB, PHBV	(Alias & Tan, 2005; Keenan et al., 2004)

Table 6 Bacterial strains used to produce PHAs *(Cont.)*

Bacterial strain	Carbon source	PHAs	Reference
Caulobacter crescentus	Glucose	PHB	(Qi & Rehm, 2001)
Cupriavidus necator	Glucose, fructose, sucrose, lactic acid, soybean oil, valerate, octanoate	PHB, copolymers	(Kichise et al., 1999; Kim & Shin, 1995; Taguchi et al., 2003)
Cupriavidus necator H16	Hydrogen, carbon dioxide	PHB	(Pohlmann et al., 2006)
Recombinant *Cupriavidus necator*	Sucrose	PHB	(Park et al., 2015)
Recombinant *Escherichia coli*	Glucose, glycerol, palm oil, ethanol, sucrose, molasses	Ultra-high-molecular-weight PHB	(Kahar et al., 2005; Mahishi et al., 2003; Sujatha & Shenbagarathai, 2006)
Haloferax mediterranei	Vinasse, hydrolyzed whey, crude glycerol	P(3HB-*co*-3HV)	(Bhattacharyya et al., 2012; Hermann-Krauss et al., 2013; Koller et al., 2008)
Halomonas boliviensis	Starch hydrolysate, maltose, maltotetraose	PHB	(Quillaguamán et al., 2006; Quillaguamán et al., 2005)
Methylocystis sp.	Methane	PHB	(Wendlandt et al., 2005)

Table 6 Bacterial strains used to produce PHAs *(Cont.)*

Bacterial strain	Carbon source	PHAs	Reference
Paracoccus denitrificans	*n*-pentanol	P(3HV)	(Yamane, Chen, et al., 1996)
Pseudomonas aeruginosa	Glucose, waste free fatty acids	mcl-PHAs	(Hoffmann & Rehm, 2004)
Pseudomonas entomophila mutant	Dodecanoic acid	P(3HDD), mcl-PHAs	(Chung et al., 2011; Wang et al., 2017)
Recombinant *Pseudomonas oleovorans*	Octanoic acid	mcl-PHAs	(Durner et al., 2000; Preusting et al., 1993)
Recombinant *Pseudomonas putida*	Sodium butyrate, sodium hexanoate	mcl-PHAs	(Tripathi et al., 2013)
Rhodococcus sp.	Acetate, fructose, glucose, valerate, succinate, hexanoate, 4-hydroxybutyrate	P(3HB-*co*-3HV)	(Haywood et al., 1991)
Recombinant *Saccharomyces cerevisiae*	Oleic acid, heptadecenoic acid	mcl-PHAs	(Poirier et al., 2001)
Thermus thermophilus	Whey	Scl-*co*-mcl PHAs	(Pantazaki et al., 2009)

Among all natural PHAs producers, *C. necator* (formerly known as *Ralstonia eutropha* or *Alcaligenes eutrophus*) has been widely employed for research and commercial use in PHAs production. Soil isolated *C. necator* strain A-04 was a negative gram stain and rod shape bacteria with 16S rRNA similarity of 99.78% to the *C. necator* strain H16 (Chanprateep et al., 2008). Genes involved in the PHB biosynthesis operon rearranged as *phaC* (1770 bp), *phaA* (1182 bp) and *phaB* (741 bp), respectively (Visetkoop, 2009). The sequence analysis of *phaC* sequence in *C. necator* strain A-04 and H16 by Expasy (bioinformatic tool for protein translation) and EMBOSS needle revealed the substitution of proline for leucine at position 122 amino acid (Figure 11). The *phaA* and *phaB* sequences were similar in both strains (Boontip et al., 2020). Chanprateep et al. (2008) displayed various carbon sources such as fructose, butyric acid, valeric acid, gamma-hydroxybutyric acid, gamma-hydroxybutyric acid lactone and 1,4-butanediol, could be utilized and produced copolymer of P(3HB-*co*-3HV) and P(3HB-*co*-4HB) with 78wt% content by *C. necator* strain A-04 under nitrogen deficient condition. The terpolymer of P(3HB-*co*-3HV-*co*-4HB) was produced with PHA content of 68wt% in 60 h (Chanprateep & Kulpreecha, 2006). Since a highly biocompatible P(3HB-*co*-4HB) can be used as healthcare materials and medical scaffolding materials, P(3HB-*co*-4HB) became valuable member of PHAs family (Huong et al., 2021). In addition, Sukruansuwan et al. (2018) reported the ability of *C. necator* strain A-04 to feed on pineapple wastes with the PHB content of 60wt% and 13.6 g/L CDM (Sukruansuwan & Napathorn, 2018). Recently, the expression of *phaCAB* operon from *C. necator* strain A-04 was studied in recombinant *E. coli* under arabinose-inducible promoter (Napathorn et al., 2021) and cold-shock promoter (Boontip et al., 2020). More than 90%(wt) of PHB was obtained from recombinant *E. coli* in flask scale production. Fed batch cultivation of this recombinant *E. coli* in 5-L bioreactor gave the highest yield of PHB with the value 0.39 g PHB/g glucose (Napathorn et al., 2021).

```
A-04     1 MATGKGAAASTQEGKSQPFKVTPGPFDPATWLEWSRQWQGTEGNGHAAAS     50
           ||||||||||||||||||||||||||||||||||||||||||||||||||||
H16      1 MATGKGAAASTQEGKSQPFKVTPGPFDPATWLEWSRQWQGTEGNGHAAAS     50

A-04    51 GIPGLDALAGVKIAPAQLGDIQQRYMKDFSALWQAMAEGKAEATGPLHDR    100
           ||||||||||||||||||||||||||||||||||||||||||||||||||||
H16     51 GIPGLDALAGVKIAPAQLGDIQQRYMKDFSALWQAMAEGKAEATGPLHDR    100

A-04   101 RFAGDAWRTNLPYRFAAAFYLPNARALTELADAVEADAKTRQRIRFAISQ    150
           ||||||||||||||||||||.||||||||||||||||||||||||||||||
H16    101 RFAGDAWRTNLPYRFAAAFYLLNARALTELADAVEADAKTRQRIRFAISQ    150

A-04   151 WVDAMSPANFLATNPEAQRLLIESGGESLRAGVRNMMEDLTRGKISQTDE    200
           ||||||||||||||||||||||||||||||||||||||||||||||||||||
H16    151 WVDAMSPANFLATNPEAQRLLIESGGESLRAGVRNMMEDLTRGKISQTDE    200

A-04   201 SAFEVGRNVAVTEGAVVFENEYFQLLQYKPLTDKVHARPLLMVPPCINKY    250
           ||||||||||||||||||||||||||||||||||||||||||||||||||||
H16    201 SAFEVGRNVAVTEGAVVFENEYFQLLQYKPLTDKVHARPLLMVPPCINKY    250

A-04   251 YILDLQPESSLVRHVVEQGHTVFLVSWRNPDASMAGSTWDDYIEHAAIRA    300
           ||||||||||||||||||||||||||||||||||||||||||||||||||||
H16    251 YILDLQPESSLVRHVVEQGHTVFLVSWRNPDASMAGSTWDDYIEHAAIRA    300

A-04   301 IEVARDISGQDKINVLGFCVGGTIVSTALAVLAARGEHPAASVTLLTTLL    350
           ||||||||||||||||||||||||||||||||||||||||||||||||||||
H16    301 IEVARDISGQDKINVLGFCVGGTIVSTALAVLAARGEHPAASVTLLTTLL    350

A-04   351 DFADTGILDVFVDEGHVQLREATLGGGAGAPCALLRGLELANTFSFLRPN    400
           ||||||||||||||||||||||||||||||||||||||||||||||||||||
H16    351 DFADTGILDVFVDEGHVQLREATLGGGAGAPCALLRGLELANTFSFLRPN    400

A-04   401 DLVWNYVVDNYLKGNTPVPFDLLFWNGDATNLPGPWYCWYLRHTYLQNEL    450
           ||||||||||||||||||||||||||||||||||||||||||||||||||||
H16    401 DLVWNYVVDNYLKGNTPVPFDLLFWNGDATNLPGPWYCWYLRHTYLQNEL    450

A-04   451 KVPGKLTVCGVPVDLASIDVPTYIYGSREDHIVPWTAAYASTALLANKLR    500
           ||||||||||||||||||||||||||||||||||||||||||||||||||||
H16    451 KVPGKLTVCGVPVDLASIDVPTYIYGSREDHIVPWTAAYASTALLANKLR    500

A-04   501 FVLGASGHIAGVINPPAKNKRSHWTNDALPESPQQWLAGAIEHHGSWWPD    550
           ||||||||||||||||||||||||||||||||||||||||||||||||||||
H16    501 FVLGASGHIAGVINPPAKNKRSHWTNDALPESPQQWLAGAIEHHGSWWPD    550

A-04   551 WTAWLAGQAGAKRAAPANYGNARYRAIEPAPGRYVKAKA    589
           |||||||||||||||||||||||||||||||||||||||
H16    551 WTAWLAGQAGAKRAAPANYGNARYRAIEPAPGRYVKAKA    589
```

Figure 12 PhaC protein alignment of *C. necator* strain A-04 and H16 (Boontip et al., 2020)

2.2.5 Challenge in industrializing PHAs

Industrial production and commercialization of PHAs is still struggling due to high production costs, 3-4 times more expensive than petroleum-based plastics (Tsang et al., 2019). Approximately 45% of the total production cost comes from source of carbon for bacteria (Kourmentza et al., 2017). Since PHAs have a functional role in bacterial survival under stress conditions with poor nutrient availability, several attempts have been made for bioremediation of waste products to produce high value-added PHAs. The use of frying oil, food waste, biodiesel production waste, plastics waste and domestic waste as carbon sources for PHAs production were reported (Favaro et al., 2019; Guzik et al., 2014; Koller et al., 2009; Petpheng et al., 2023; Sukruansuwan & Napathorn, 2018). Since PHAs are stored inside cells, extraction and purification in downstream process are essential to recover PHAs with the highest recovery yield and purity. More than 50% of PHAs production cost have been attributed to the downstream process (López-Abelairas et al., 2015). The use of large amounts of solvents, complicated extraction and recovery not only increases the cost, but also leads to polymer degradation. In addition, toxicity of solvents to human and environments is crucial because most solvents are toxic (Liang et al., 2024). Engineering of strains improvement to overexpress genes involved in PHAs biosynthesis, reduce by-product formation, change of strain morphology and enhance efficient downstream process were reported (Chae et al., 2015; Durner et al., 2000; Preusting et al., 1993; Wu et al., 2016). Finally, modification of PHAs by blending with other polymers improves mechanical and thermal properties of PHAs. With better properties, PHAs can be efficiently processed and utilized in a wide range of applications with high value-added aspects.

2.3 PHAs production in *E. coli*

Although natural PHAs producers can synthesize PHAs easily from various types of monomers, the efficiency of process is limited only on laboratory scale and from structurally related precursors (Favaro et al., 2019). Unlike natural PHAs producers, *E. coli* does not possess endogenous PHA depolymerases, causing intracellular polymer degradation and low PHAs content (Gebauer & Jendrossek, 2006). As a result, up to 90wt% of the dry cell weight of PHB could be produced by genetic engineering of the PHA synthase genes (Fidler & Dennis, 1992; Olavarria et al., 2021; Shi et al., 1999). The discovery of a linked pathway between fatty acid metabolism and PHAs biosynthesis enabled mcl-PHAs biosynthesis in recombinant *E. coli* (Langenbach et al., 1997). Copolyesters can also be synthesized in recombinant *E. coli* by adding structure related precursors and engineering corresponding metabolic pathways.

2.3.1 Strain improvement of PHAs production in recombinant *E. coli*

By focusing on the strain improvement of *E. coli* for PHAs production, several approaches were successfully achieved to enhance PHAs productivity (Table 7).

Table 7 Metabolic engineering approaches to enhance PHAs production in *E. coli*

Technique	Key findings	Reference
Deletion of carbon storage regulator A	Deletion of CsrA, serving as RNA binding protein in cell proliferation, led to high cell density of *E. coli* producing PHB.	(Wu et al., 2020)
Inactivation of transcriptional regulators	Inactivation of transcriptional regulators, ArcA and OmpR, in beta-oxidation resulted in boosting up PHAs yield from fatty acids.	(Scheel et al., 2016).
Improvement of sugar utilization	Deletion of the *cscR* can improve PHB production from sucrose in fed-batch cultivation.	(Arifin et al., 2011)

Table 7 Metabolic engineering approaches to enhance PHAs production in *E. coli (Cont.)*

Technique	Key findings	Reference
Decrease the acetyl-CoA pool to other by products	Disruption of *pflb*, *ldhA*, *adhE* and *fnr*, essential genes in the formation of formate, lactate, ethanol and transcriptional regulator proved to dramatically elevate the PHB accumulation.	(H. R. Jung et al., 2019)
Secretion of PHB for downstream process improvement	The use of PHB-bounded protein phasin (PhaP1) guided PHB secretion into medium instead of forming as granules in cytoplasm. PHB extraction and purification are no longer essential.	(Rahman et al., 2013)
Enabling the threonine bypass	Threonine bypass increased the theoretical yield of PHB by making use of the ATP and reducing power generated in the classical PHB production pathway.	(Lin et al., 2015)
Deletion of cell fission genes	Engineering cell growth and morphology by deletion of *minC* and *minD,* coupled with the overexpression of cell division inhibitor (SulA) represented the formation of multiple fission rings in elongated shape of *E. coli.*	(Wu et al., 2016).
Overexpression of *phaP*	Phasin is a surface-binding protein of PHAs granules. Increase of *phaP* expression led to smaller and densely packed PHAs granules, resulting in higher PHAs content.	(Lee et al., 2023)
Overexpression of *ftsZ*	*ftsZ* is a protein involved in cell division. Overexpression of *ftsZ* resulted in high cell density with larger internal space.	(Wang et al., 2014)

Table 7 Metabolic engineering approaches to enhance PHAs production in *E. coli (Cont.)*

Technique	Key findings	Reference
Repression of *ftsZ* or/and *mreB*	The stronger the repression on genes *ftsZ* or/and *mreB,* the larger *E. coli* cells, leading to increase of PHB accumulation and promote simple downstream process.	(Elhadi et al., 2016)
Deletion of *sad* and *gabD*	Elimination of native succinate semialdehyde dehydrogenase genes, *sad* and *gabD*, enhanced the carbon flux to 4-hydroxybutyrate synthesis.	(Li et al., 2010)
Deletion of the major thioesterases	After deletion of the major thioesterases and expression of a low-substrate-specificity phaC, 78.82 mol% of mcl-PHAs was produced from *E. coli*	(Zhuang et al., 2014)

2.3.2 Related metabolic pathways in *E. coli*

Both types of PHAs, scl-PHAs and mcl-PHAs are synthesized from precursors that are produced from sugars through metabolic pathways such as central carbon metabolism and fatty acids through beta-oxidation or de novo synthesis (Figure 13) (Nomura et al., 2004; Tsuge et al., 2000). Metabolism of glucose in *E. coli* relies on three essential pathways including Embden-Meyerhof-Parmas (EMP) pathway, Entner-Doudoroff (EDP) pathway and pentose phosphate (PPP) pathway. All three pathways are central biochemical pathways providing energy and essential intermediates for cellular mechanisms and have different roles in an individual type of microorganisms. However, some other metabolic pathways such as TCA cycle, redox balance, phosphotransacetylase/acetate kinase pathway and homeostasis also affect the switching on and off of PHAs biosynthesis.

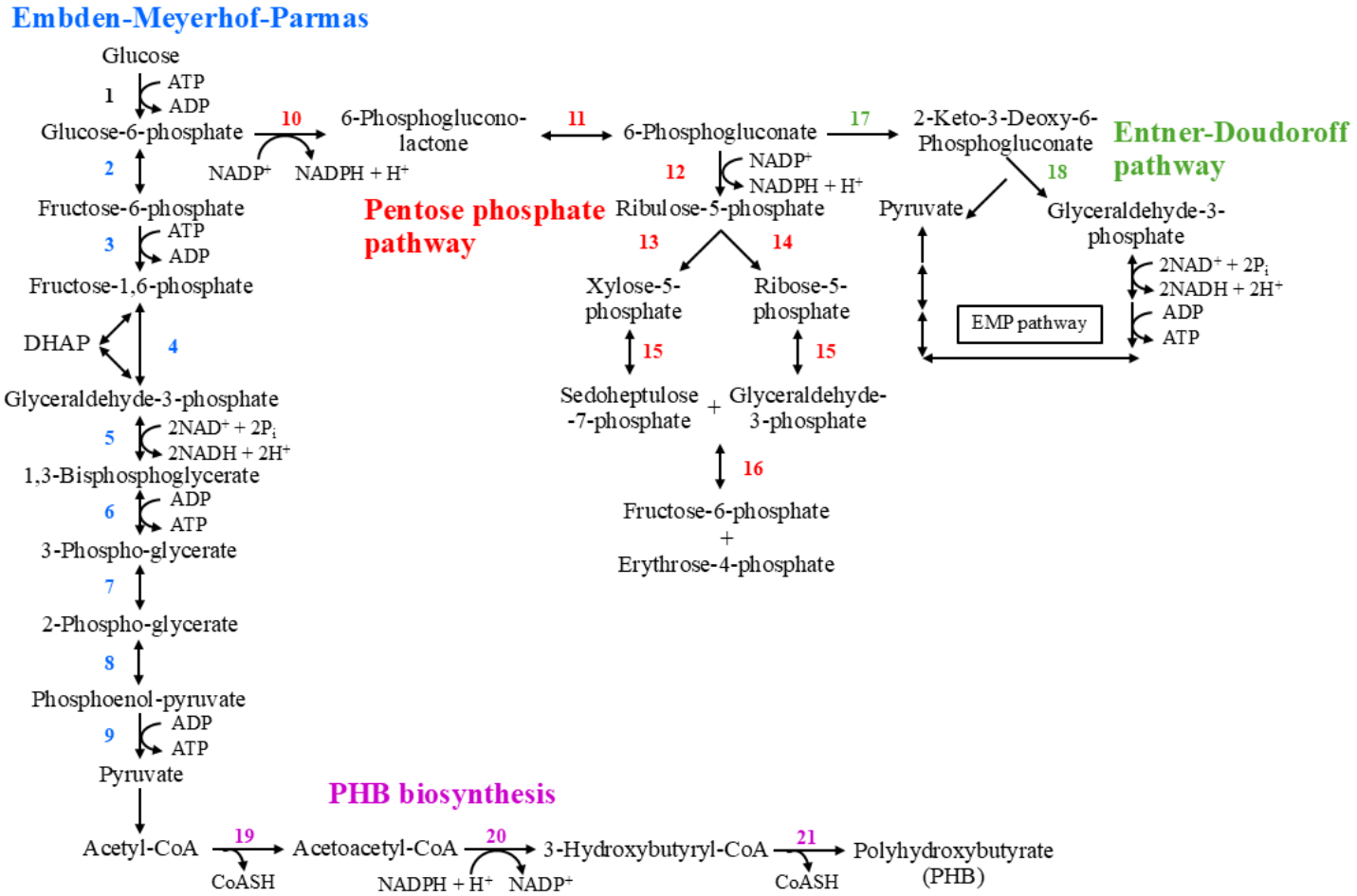

Figure 13 Schematic diagram of glucose central metabolism, Embden-Meyerhof, Entner Doudoroff and pentose phosphate pathway, and poly(3-hydroxybutyrate) biosysthesis. Numbers represent enzymes involved in the chemical reactions that are summarized in Table 8.

Table 8 Enzymes involved in central metabolism and PHB biosynthesis pathways Modified from (Spector, 2009).

No.	Enzyme	Abbreviation
1	Hexokinase	HK
2	Phosphoglucose isomerase	PGI
3	Phosphofructokinase	PKF
4	Aldolase	ALS
5	Glyceraldehyde-3-phosphate dehydrogenase	GAPDH
6	Phosphoglycerokinase	PGK
7	Phosphoglecerate mutase	PGM
8	Enolase	ENO
9	Pyruvate kinase	PYK
10	Glucose-6-phosphate dehydrogenase	G6PDH
11	6-phosphogluconolactonase	6PGL
12	6-phosphogluconate dehydrogenase	6PGDH
13	ribulose-5-phosphate epimerase	RPE
14	ribulose-5-phosphate isomerase	RPI
15	transketolase	TKT
16	transaldolase	TAL
17	6-phosphogluconate dehydratase	EDD
18	2-keto-3-deoxy-6-phosphogluconate aldolase	-
19	Beta-ketothiolase	PhaA
20	NADPH-dependent acetoacetyl-CoA reductase	PhaB
21	PHA synthase	PhaC

Embden-Meyerhof-Parnas (EMP) pathway is considered a universal pathway and fundamental cellular respiration converting glucose into pyruvate along with the formation of cellular energy in the form of ATP and reducing equivalents in the form of NADH. Pyruvate is a key intermediate which can be further catabolized through several reactions to a variety of products. EMP pathway involves a series of 10 enzymatic reactions yielding net products of two molecules of ATP (Cori, 1983; Spector, 2009). In the absence of oxygen, pyruvate molecules are converted into lactate or ethanol by fermentation. In the presence of oxygen, pyruvate molecules are broken down into acetyl-CoA which later enter the TCA cycle to produce more cellular energy and carbon dioxide. The EMP pathway is a critical metabolic process in cellular biology for many reasons. It is the source of energy production in the form of ATP and reducing equivalents in the form of NADH molecules. In addition, the EMP pathway is found in nearly all organisms and plays a fundamental role in cellular metabolism. Finally, the EMP pathway is the source of intermediates required in the synthesis of nucleotides, lipids and amino acids.

Entner-Doudoroff pathway (EDP) is another glycolytic pathway commonly found in *Pseudomonas*, *Azotobacter*, *Neisseria* and *Rhizobium* as they do not possess phosphofructokinase to navigate the carbon metabolism to the EMP pathway (Sokatch, 1969). It is widely reported that the EDP in *E. coli* is activated specifically when gluconate is supplemented and remains inactive in the presence of glucose (Egan et al., 1992). Although the EMP is recognized as preferable pathway for glucose metabolism, there are much evidence proves the existence and activity of the EDP in *E. coli* glucose catabolism (Fliege et al., 1992; Hollinshead et al., 2016; Peekhaus & Conway, 1998). The net products of the EDP pathway are one pyruvate, one G3P and one NADPH per molecule of glucose.

The pentose phosphate pathway (PPP), also known as hexose monophosphate pathway, is a fundamental component of cellular metabolism and a major source of NADPH as reducing equivalent and ribose-5-phosphate as nucleic acid precursors (Landau, 2004). The PPP is divided into two parts, oxidative phase and non-oxidative phase. Oxidative phase involves the reduction of $2NADP^+$ to form 2NADPH. Briefly, Glc-6P is converted into 6-phosphate-gluconolactone by Glc-6PDH

(*zwf*). Next, 6-phosphate-gluconolactone is converted to 6-phosphogluconate by 6-phosphogluconolactonase using one molecule of H_2O. Finally, 6-phosphogluconate is oxidatively decarboxylated to ribulose-5-phosphate (Ru5P) by 6-phosphogluconate dehydrogenase. In the non-oxidative phase, all reactions are reversible reactions allowing different molecules to metabolize in different areas of the non-oxidative branch and transform up to the first precursor, ribulose-5-phosphate.

2.3.3 Rerouting of glucose metabolism in *E. coli*

Understanding of glucose metabolic flux in *E. coli* provides essential information for strain improvement to increase product yields in fermentation process. Considering gene deletion to alter the metabolic flux in favorable pathway is an important key for successful mutant generation.

To disrupt EMP, hexokinase, phosphoglucose isomerase (*pgi*) and phosphofructokinase (Pfk) are considered as effective targets as they locate in the early stage of the pathway (Figure 13). Hexokinase catalyzes the reaction of producing G6P which is a pivotal metabolite in glycolysis, glycogen synthesis and the pentose monophosphate shunt, necessary for lipid and nucleic acid formation (Ge et al., 2020; Villar-Palasí & Guinovart, 1997). It also regulates the production of ATP and cell survival in mitochondria (Wilson, 2003). In addition, hexokinase has its function related to immune response, DNA damage response, homeostasis, autophagy and other cellular activities through noncanonical functions (Guo et al., 2023). Therefore, inactivation of hexokinase might have a wide impact on bacterial cellular network.

Although there are two isozymes of Pfk, phosphofructokinase A (*pfkA*) is responsible for 90% of the Pfk activity in *E. coli* (Kotlarz et al., 1975). Deletion of *pfkA* showed an enhancement of lycopene (Wang et al., 2013), hydrogen and ethanol (Sundara Sekar et al., 2016), 1,3-diaminopropane (Chae et al., 2015) and (R)-methyl-3-hydroxybutyrate (Siedler et al., 2014) with very low specific growth rate. In addition, mutation which result in the loss of major activity of phosphofructokinase A showed a great impact on carbon source assimilation, especially glucose and hexitols (Guitart Font & Sprenger, 2020).

Disruption of *pgi,* aiming to switch off the EMP shunt, was genuinely proposed with better growth compared to *pfkA* mutant. The *pgi* mutant exhibited consistent growth on either fructose as a sole carbon source or mixture of fructose and glucose (Ahn et al., 2011). On the contrary, a significant decrease in growth rate and sugar consumption rate was observed when *pgi* mutant grew on glucose (Ahn et al., 2011; Fraenkel & Levisohn, 1967; Shimaoka et al., 2005). The result indicated the physiological and metabolic change of *pgi* mutant depending on the carbon source. Metabolic flux ratio (METAFoR) analysis revealed that the PPP pathway was developed as the primarily route of glucose catabolism in *pgi* mutants (Canonaco et al., 2001; Hua et al., 2003) while the EDP pathway was also active with a lesser degree (Loomis & Magasanik, 1966). The increased flux through the PPP resulted in an excess amount of intracellular NADPH as the production rate was much higher than its utilization (Hua et al., 2003). Canonaco et al. (2001) reported that overexpression of soluble transhydrogenase *UdhA* significantly improved the growth of *pgi* mutant (Canonaco et al., 2001). This study suggested the *E. coli* responded to the excess amount of NADPH by reduction of growth rate and resumed when NADPH sank. Similar result was reported that *pgi* mutant had an adaptive evolution to the loss of an essential gene in the main glucose metabolism by evolving NADH/NADPH transhydrogenases *udhA* and *pntAB* (Charusanti et al., 2010). It was concluded that *E. coli* can adapt to the loss of a major metabolic gene with only handful mutations. In addition, the glyoxylate shunt, a branch of TCA cycle, is active in *pgi* mutant (Hua et al., 2003). Up to date, several studies on the benefits of *pgi* mutant have been illustrated as shown in Table 9.

Table 9 The application of *pgi* gene deletion as a strategy to improve products formation in previous reports.

Scope of the study	Key findings	Reference
Shikimic acid production	Shikimic acid production in *pgi* mutant was increased due to preferable availability of the cofactor D-erythrose-4-phosphate (E4P), an intermediate in PPP.	(Ahn et al., 2011)
D-glucose production	The use of *pgi* mutant improved the production yield of D-glucose by inhibition of catabolite repression.	(Shiue et al., 2015)
Inosine production	Inosine production in *pgi* mutant accelerated, which was the consequence of ribose-5-phosphate accumulation from PPP.	(Shimaoka et al., 2005)
Xylitol production	Large amount of NADPH produced in *pgi* mutant enhanced xylitol production from glucose.	(Chin & Cirino, 2011)
Production of 7-O-xylosyl naringenin	7-O-xylosyl naringenin, a group of flavonoids, production depended on the enhanced availability of D-glucose in *pgi* mutant.	(Simkhada et al., 2009)
Increase of furfural and 5-hydroxymethyl furfural tolerance	NADPH accumulation in *pgi* mutant increased furfural and 5-hydroxymethyl furfural tolerance as most of furfural degradation enzymes are NADPH-dependent enzymes.	(Syed Bilal Jilani et al., 2020).
Production of 3-O-xylosyl quercetin and quercetin glucoside	The *pgi* mutant was used as a strategy to block the entry of G6P into EMP, leading to increase of quercetin.	(Pandey et al., 2013; Xia & Eiteman, 2017)

The EDP pathway in *E. coli* remains inactive in glucose metabolism, while it is mainly operative in gluconate catabolism (Kim et al., 2022). Egan et al. (1992) reported the role of gluconate 6-phosphate dehydratase (*edd*) and 2-keto-3-deoxy-6-phosphogluconate aldolase (*eda*) operon in co-transcription as key mediated response to activate EDP pathway (Figure 13) (Egan et al., 1992). Inactivation of the *eda* gene resulted in great amounts of intracellular 2-keto-3-deoxy-6-phosphogluconate (KDPG) accumulation, inhibiting bacterial growth (Faik et al., 1971; Fradkin & Fraenkel, 1971; Fuhrman et al., 1998). Interestingly, metabolic flux response of *edd* deficiency strain exhibited similar glucose uptake rate and biomass yield to the parental strain even carbon flux into the EMP and PPP (Long & Antoniewicz, 2019). Disruption of the *edd* gene was proven to benefit the NADPH-dependent and PPP-related products as shown in Table 10.

Table 10 The application of *edd* gene deletion as a strategy to improve products formation in previous reports.

Scope of the study	Key findings	Reference
Inosine production	Inosine production in *edd* mutant accelerated, which was the consequence of ribose-5-phosphate accumulation from PPP.	(Shimaoka et al., 2005)
Production of riboflavin (vitamin B2)	Riboflavin, metabolized from ribulose-5-phosphate, an intermediate in PPP. from *edd* mutant increased as availability of precursor and reduction of acetate as by-products.	(Lin et al., 2014)
Methanol-growth dependent in *E. coli*	The *edd* mutant accumulated high amount of ribulose-5-phosphate, which later used in condensation with formaldehyde for bacterial growth in the presence of methanol.	(Meyer et al., 2018)

These studies provided strong evidence that inactivation of either EMP or EDP pathway redirected carbon flow through the PPP pathway, the main source of NADPH. Reduced nicotinamide adenine dinucleotide phosphate (NADPH) serves as an essential electron donor which plays an important role in the generation of reactive oxygen species (ROS) (Bylund et al., 2010; Foreman et al., 2003) and also responsible as the reducing power to drive anabolic reactions in organisms (Chandel, 2021; Ju et al., 2020). NADPH is a crucial bottle neck in many products biosynthesis such as mevalonate (Wang et al., 2022), xylitol (Yuan et al., 2021), leucocyanidin (Chemler et al., 2010) and PHAs (Lee et al., 2005). In PHAs production, NADPH plays an important role as cofactor for acetoactyl-CoA reductase (Figure 8). There are three main sources of intracellular NADPH (Figure 15). First, transhydrogenases such as the membrane-bounded PntAB transhydrogenase providing 30-45% of the total NADPH from aerobic respiration (Ling et al., 2018). Engineering transhydrogenase significantly increased the PHB yield of 0.23 g PHB/g glucose, compared to 0.16 g PHB/g glucose in native strain (Lin et al., 2015). Next, NADPH can be generated in the tricarboxylic (TCA) cycle by NADPH-dependent isocitrate dehydrogenase (IDH), providing 20-25% of the total NADPH from aerobic respiration (Ling et al., 2018). Since TCA cycle provides hydroxyacyl-CoA monomers used in PHAs production, higher activity of TCA cycle leads to increase PHAs accumulation (Higuchi-Takeuchi & Numata, 2019). As TCA cycle activity is high, large quantities of citrate are synthesized and inhibit citrate synthase activity. As a result, acetyl-CoA molecules are condensed into acetoacetyl-CoA, switching on the PHAs biosynthesis (M. Martínez et al., 2023). Finally, the main source of NADPH is oxidative branch of the PPP pathway, providing 35-45% of the total NADPH during aerobic growth on glucose (Ling et al., 2018; Shi et al., 1999). The hydrogen atoms on glucose carbons at the 1st and 3rd positions are transferred to NADPH in the conversion of G6P to 6-phosphoglucono-δ-lactone by Glc-6PDH (EC 1.1.1.49) and the conversion of 6-phosphogluconate to Ru5P by *edd* gene (EC 1.1.1.44) (Lewis et al., 2014; Zhang et al., 2017). The oxidative phase of PPP starts with metabolizing Glc-6P into Glc-6PDH

by *zwf* gene (Figure 14). The study of *zwf* overexpression to improve PHB accumulation was reported (Lim et al., 2002).

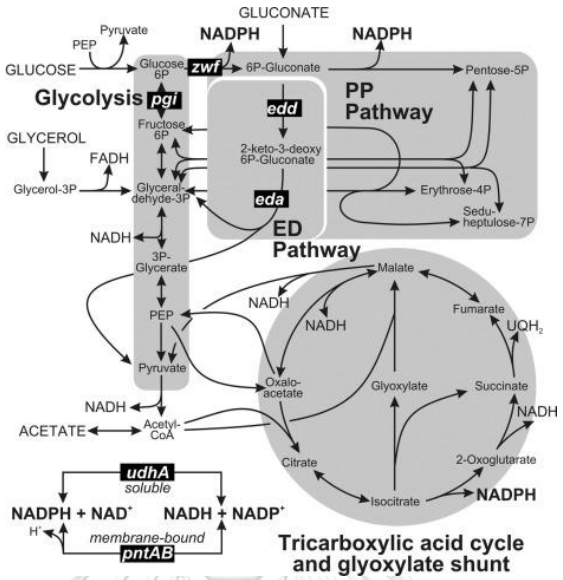

Figure 14 Biological network for NADPH production in *E. coli* (Sauer et al., 2004)

NADPH availability is a vital key as driving force in PHAs production (Alsiyabi et al., 2021; L. Assil-Companioni et al., 2020). With the excess NADPH level, the *pgi* and *edd* mutants could represent suitable hosts for PHAs biosynthesis (Figure 14), although very few studies reported on the use of the *pgi* and *edd* mutants on PHAs production. Protein expression analysis of *pgi* disruption on PHB production revealed gene pattern affected from the redirection of glucose metabolism in *E. coli* (M. M. Kabir & K. Shimizu, 2003b). Most genes in the PPP and some glycolytic genes were significantly affected by the overexpression of PHB biosynthesis genes while genes in the TCA cycle were down regulated. In addition, bacterial growth of *pgi* mutant improved after incorporation with PHB biosynthesis (M. Kabir & K. Shimizu, 2003). Unfortunately, the fermentation characteristics of these mutants on the PHAs production is still unclear.

2.3.4 Factors affecting PHAs biosynthesis

Apart from NADPH availability, there are other factors affecting PHAs biosynthesis. Regulation of PHAs biosynthesis is complex as various pathways involved. Availability of acetyl-CoA, acetoacetyl-CoA and hydroxybutyryl-CoA serving as precursors are crucial factors to enhance PHAs biosynthesis. PHAs flux was highly sensitive to the acetyl-CoA/CoA ratio with response coefficient of 0.8, the total acetyl-CoA plus CoA concentration with response coefficient of 0.7 and pH with response coefficient of -1.25 (van Wegen et al., 2001). Increase of acetyl-CoA availability via central carbon metabolism and fatty acid metabolism proved to enhance PHAs production (Kocharin et al., 2012; Park et al., 2024). Overexpression of acetyl-CoA acetyltransferase, catalyzing the breakdown of volatile fatty acids into acetyl-CoA, increased PHB yield and PHB production significantly in *Halomonas sp.* (Park et al., 2024). Engineered branched pathway by deletion of *aahE*, *ldhA*, *pflb* and *fnr*, contributing the formation of ethanol, lactate, formate and transcriptional regulator was demonstrated to increase the PHAs production (H.-R. Jung et al., 2019).

In addition, PHAs homeostasis regulates the PHAs metabolism. PHA synthase, catalyzing the polymerization of PHAs, greatly affected the rate of PHAs accumulation and PHAs properties such as molecular weight and thermal property (Stubbe & Tian, 2003). PHAs metabolism involves regulatory proteins known as PHA granule-associated proteins (PGAPs) (Maestro & Sanz, 2017; Mitra et al., 2022). These PGAPs including PhaR, PhaM, PhaF and PhaQ bind to their promoter or the promoters of other PHAs biosynthesis genes to regulate their transcription to ensure well-organized PHAs granule formation (Galán et al., 2011; Lee et al., 2004). The regulator protein, phaR, binds to the promoter of *phaR* and *phaP* when there is no PHAs chain, leading to the inhibition of gene transcription. When PHA synthase starts the polymerization and PHAs chain presences, PhaR binds to PHAs granules and release the inhibition of gene transcription (Maehara et al., 2002).

CHAPTER III

RESEARCH METHODOLOGY

3.1 Instruments

Table 11 Instruments used in this research

Instruments	Model, Manufacturer, Country
Mechanical pipette	- Eppendorf Research Plus, Germany
Autoclave	- ES-215, TOMY Digital Biology, Japan
	- SS-325, TOMY Digital Biology, Japan
Hot air oven	- UE600, Mermert, Germany
Incubator	- ULE800, Mermert, Germany
Rotary incubator shaker	- Innova 4300, New Brunswick Scientific Co., Inc., USA
Analytical balance	- AG204, Mettler Toledo Co., Ltd., Switzerland
Electronic balance	- PG 2002-S, Mettler Toledo Co., Ltd., USA
Laboratory glassware	- Pyrex, USA
Spectrophotometer	- Spectronic 20 Genesys, PerkinElmer, Inc., USA
Nanodrop spectrophotometer	- 200 UV-vis, Thermo Scientific, USA
Vortex	- G-560E, Science Industries, USA
Refrigerated microcentrifuge	- 1920 Kubota, Japan
Refrigerated centrifuge	- 5810R, Eppendorf, Germany
Refrigerator	- Mitsubishi electric, Japan
Deep freezer (-80°C)	- Sanyo Electric, Japan
Deep freezer (-20°C)	- Sanyo Electric, Japan
Thermal cycler	- T100™, Bio-rad Laboratories, USA
Gel electrophoresis	- Mini-Sub Cell GT Cell, Bio-rad Laboratories, USA
Gel imaging	- BluPAD Dual LED Blue/White Light Transilluminator, BIO-HELIX Co., LTD., Taiwan
Power supply	- PowerPac™ HC, Bio-rad Laboratories, USA
Stirring hot plate	- DS 201HS, DMC, Japan

Table 11 Instruments used in this research *(Cont.)*

Instruments	Model, Manufacturer, Country
Magnetic stirrer	- 502P-2, PMC, USA
Light microscope	- CH30RF200, Olympus, Japan
Gas chromatography	- CP3800, Varian Inc., USA
Carbowax-PEG capillary column	- Varian Inc., USA
HPLC	- Agilent 1200 Infinity Series, Agilent technology, USA
Bioreactor 5-L	- MDL500, B.E. Marubishi Co., Ltd., Japan
pH meter	- Mettler Toledo Co., Ltd., Switzerland
Laminar flow hood	- Biobase group, China

3.2 Chemicals

Table 12 Chemicals used in this research

Chemicals	Manufacturer, Country
Agarose gel	Vivantis Technologies, Malaysia
Ampicillin sodium	T.P. Drug Laboratories, Thailand
Benzoic acid	Nacalai tesque, Japan
Chloroform	Labscan Asia Co., Ltd., Ireland
Disodium hydrogen phosphate (Na_2HPO_4)	Merck, Germany
Ethanol	Labscan Asia Co., Ltd., Ireland
Ethylene-dinitrilotetraacetic acid (EDTA)	Merck, Germany
Glacial Acetic acid	Merck, Germany
Glycerol	Sigma, Germany
Hexane	Merck, Germany
Hydrochloric acid	Merck, Germany
Isoamyl alcohol	Merck, Germany
Isopropyl β-D-1-thiogalactopyranoside (IPTG)	Bio Basic, USA

Table 12 Chemicals used in this research *(Cont.)*

Chemicals	Manufacturer, Country
2-Mercaptoethanol	Bio Basic, USA
Methanol	Merck, Germany
Propionic acid sodium salt	Fluka analytical, Germany
Sodium acetate	Sigma, Germany
Sodium chloride	Merck, Germany
Sodium hydroxide	Merck, Germany
Sulfuric acid	Merck, Germany
Tetramethylethylenediamine (TEMED)	HiMedia, India
Tris-HCL	Sigma, Germany
Trizma (2-amino-2-(hydroxymethyl)-1,3-propanediol)	Sigma, Germany
Tryptone Type-I (Casitose Type-I)	HiMedia, India
5-bromo-4-chloro-3-indolyl-β-D-galactopyranoside (X-gal)	Vivantis Technologies, Malaysia
Yeast extract	HiMedia, India

3.3 Kits and enzymes

Table 13 Kits and enzymes used in this research

Kits and enzymes	Manufacturer, Country
KOD OneTM PCR master mix	Toyobo, Japan
FavorPrep™ Plasmid DNA Extraction kit	Favorgen Biotech Corp., Taiwan
HiYield™ Gel/PCR DNA Fragments Extraction kit	RBC Bioscience, Taiwan
Novel juice 6x loading buffer	BIO-HELIX Co., LTD., Taiwan
TIANquick Midi Purification kit	Tiangen, China
Taq DNA Polymerase	Apsalagen, Thailand
T4 DNA Ligase	Thermo Fisher Scientific, UK
1 kb DNA ladder	Vivantis Technologies, Malaysia
OneMark B 1 kb DNA ladder	BIO-HELIX Co., LTD., Taiwan
*Bam*HI	Vivantis Technologies, Malaysia
*Eco*RV	Vivantis Technologies, Malaysia
*Eco*RI	Vivantis Technologies, Malaysia

3.4 Bacterial strains and plasmid

Table 14 Bacterial strains and plasmids used in this research

Strains and plasmids	Characteristics	Source or reference
C. necator strain A-04	Wild type	Chanchaichaowiwat, 1993
E. coli strain JM109	F-, *traD36, proA^{+}B^{+}, lacIq, Δ(lacZ)M15/ Δ(lac-proAB), glnV44, e14-, gyrA96, recA1, relA1, endA1, thi, hsdR17*	Promega, USA
E. coli K12 strain BW25113	F-, *Δ(araD-araB)567*, *ΔlacZ4787*(::rrnB-3), λ^{-}, *rph-1*, *Δ(rhaD-rhaB)568, hsdR514*	This study
E. coli strain JW18401	F-, *Δ(araD-araB)567*, *ΔlacZ4787*(::rrnB-3), λ^{-}, *Δedd-776::kan*, *rph-1*, *Δ(rhaD-rhaB)568, hsdR514*	Keio collection
E. coli strain JW39851	F-, *Δ(araD-araB)567*, *ΔlacZ4787*(::rrnB-3), λ^{-}, *Δpgi-721::kan*, *rph-1*, *Δ(rhaD-rhaB)568, hsdR514*	Keio collection
pBluescript II (SK+)	A high copy number plasmid, Amp^{R}	Toyobo, Japan
pBSK$CAB_{A\text{-}04}$	A pBluescript II (SK+) derivative containing *phaCAB* operon from *C. necator* A-04 with native promoter, Amp^{R}	This study
pCP20	FLP recombinase helper plasmid, ts-rep, Amp^{R}, Cm^{R}	Datsenko and Wanner, 2000

3.5 Oligonucleotides

All the oligonucleotides used in this study were synthesized by U2Bio., Co., Ltd. (Bangkok, Thailand).

Table 15 Primers used in this research

Primers	Sequence (5' → 3')	Base pairs
F_BamHI_phaCAB	CTCGGATCCTCACTCGTCCTTTGCC	25
R_BamHI_phaCAB	CTCGGATCCTATGCCCAACAAGGC	24
F_XhoI_BamHI_phaCAB	ATGGATCCCTCGAGATGGCGACCGGCAAAG	30
R_HindIII_EcoRI_phaCAB	GTGAATTCAAGCTTTCAGCCCATATGCAGGCC	32
F_M13_pUC40	GTTTTCCCAGTCACGAC	17
R_M13_pUC40	CAGGAAACAGCTATGACC	18
F_Semi_phaA	AAGTCATCATGGGCCA	16
R_Semi_phaA	ACTCGTCGGTCTTGAA	16
F_pgi_verify	CGATGATGAACGTGG	15
R_pgi_berify	ACGGTATGATTTCCG	15
F_edd_verify	ACAAATTTGTCGTC	14
R_edd_verify	CGGCAACTTTGCGC	14

3.6 Bacterial culture conditions and storage

3.6.1 *Cupriavidus necator* strain A-04

Soil isolated *Cupriavidus necator* strain A-04 (Boontip et al., 2020) was used as a host for PHB biosynthesis operon (*phaC*, *phaA* and *phaB* gene) amplification and isolation. *C. necator* strain A-04 was cultivated in nutrient agar (Appendix 1) at 30°C for 24 hours. A single colony of bacteria was then inoculated into freshly prepared nutrient broth (NB) and cultivated at 30°C, 200 rpm for 24 hours. Cell culture was harvested by centrifugation at 4000 rpm at 4°C for 30 minutes. Cell pellet was washed twice with sterilized 0.85% w/v sodium chloride solution, followed by resuspended in 15% (v/v) glycerol solution. The turbidity of cell suspension was adjusted to 0.8-1.0 (equivalent to approximately 10^9 CFU/mL). Cell culture in glycerol solution was stored and maintained at -80°C for further use.

3.6.2 *Escherichia coli*

Escherichia coli strain JM109 was used as a host for the construction of plasmid. *Escherichia coli* strain K12, JW18401 and JW39851 were used as a host for gene expression and PHAs production. *E. coli* strain JW18401 and JW39851 obtained from Keio collection, represented phosphoglucose isomerase (*pgi*) and gluconate 6-phosphate dehydratase (*edd*) deletion strain, respectively. Both *E. coli* strain JW18401 and JW39851 originated from *E. coli* strain K12. All strains of *E. coli* were grown on Luria-Bertani (LB) agar (Appendix 1) at 37°C for 18 hours. A single colony of bacteria was inoculated into freshly prepared LB medium and cultivated at 37°C, 200 rpm for 18 hours. An equivalent volume of 50% (v/v) glycerol solution was added to overnight culture. The cell suspension in glycerol solution was stored and maintained at -80°C for further use. When antibiotic selection pressure was needed, the medium was supplemented with 100 µg/mL ampicillin or 50 µg/mL kanamycin. For further use, a single colony of bacteria was inoculated into freshly prepared LB medium and cultivated at 37°C, 200 rpm for 18 hours. The growth of *E. coli* was determined by measuring the optical density at 600 nm using a spectrophotometer.

3.7 Verification of single gene deletion in *E. coli* strain JW39851 and JW18401

E. coli strain JW39851 and JW18401 had kanamycin resistance gene replacing it original gene (Figure 15) (Baba et al., 2006). To eliminate kanamycin resistance cassette, both *E. coli* strain JW39851 and JW18401 were made chemically competent cells. Briefly, *E. coli* strains were inoculated into fresh LB medium and cultivated overnight at 37°C. Next, 1% (v/v) preculture was transferred into 50 mL SOB medium (Appendix 2) in 250 mL Erlenmeyer flask and grew for 3-4 hours until the optical density at 600 nm reached 0.4-0.6. Cell suspensions were chilled on ice 10 minutes prior cell collection by centrifugation at 4000 rpm for 20 minutes at 4°C. After that, cell pellets were resuspended with ice-cold TSS buffer (Appendix 2). Chemically competent *E. coli* strain JW39851 and JW18401 were introduced with pCP20 vector by heat shock method at 42°C for 30 seconds, followed by cell recover using SOC medium (Appendix 2) according to Chung et al. (1989) (Chung et al., 1989). The pCP20 vector is temperature-sensitive replication and thermal induction of FLP

recombinase synthesis. Transformants harboring pCP20 were sub-cultivated in LB plate containing ampicillin at 30°C. After confirming the successful transformants, *E. coli* strain JW39851 and JW18401 harboring pCP20 were cultivated at 43°C for 18 hours. Finally, cell cultures were randomly picked up and streaked on LB, LB containing ampicillin and LB containing kanamycin plate to verify the kanamycin resistance gene elimination and the loss of pCP20 vector. To prevent human error occurring, it was recommended to use single colony of bacteria streak on LB with antibiotic plate prior LB without antibiotic supplementation. The positive clones were bacteria capable of growing on LB plate, but not LB containing ampicillin and LB containing kanamycin plate. The successful strains were confirmed by PCR verification. The kanamycin resistant gene removal from *E. coli* strain JW39851 and JW18401 allowed these strains to further use for gene expression with kanamycin selection vector.

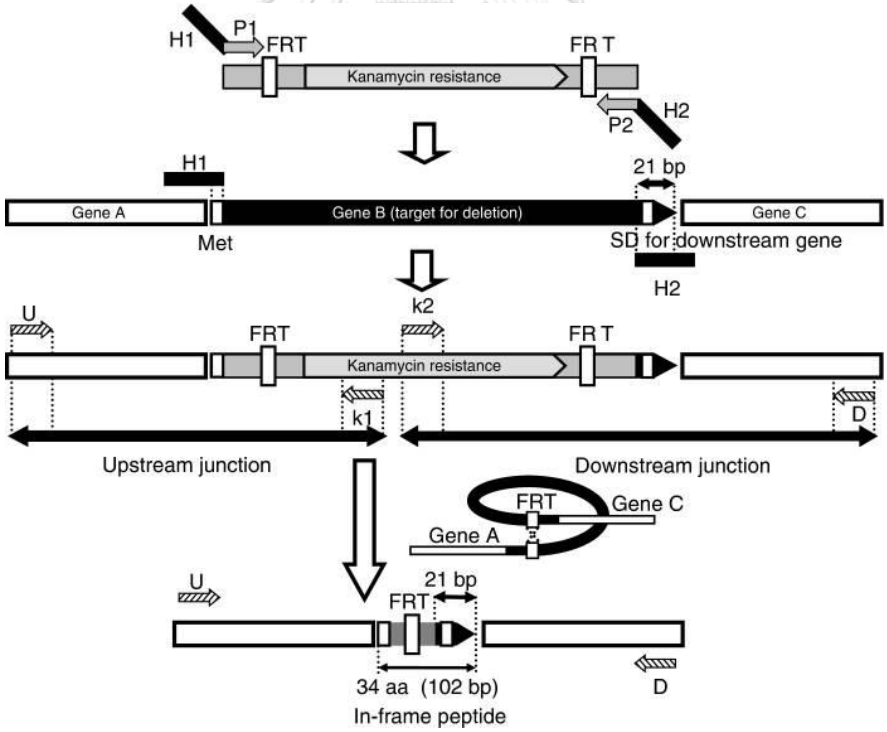

Figure 15 Design of in-frame single gene deletion in Keio collection (Baba et al., 2006)

KOD OneTM PCR master mix (Toyobo, Japan) was used in all PCR experiments. Components of the reaction were prepared according to manufacturer instruction. Related primers were designed based on *E. coli* K12 strain MG1655 chromosomal DNA deposited in GenBank (Accession number: CP027060.1). Two sets of primers for *pgi* and *edd* gene verification were shown in Table 10, F and R_pgi_verify (T_m 50°C) was used for *pgi* gene deletion verification while F and R_edd_verify (T_m 48°C) was used for *edd* gene deletion verification in *E. coli*. The PCR condition was performed as follows: pre-denaturing at 98°C for 10 seconds, 35 cycles of denaturation at 98°C for 10 seconds, annealing for 5 seconds and elongation at 68°C for 15 seconds. The annealing temperature used for *pgi* and *edd* gene primers were 48 and 46°C, respectively. The final elongation was performed at 68°C for 15 seconds. PCR product was then analyzed on 1% agarose electrophoresis (Appendix 3).

3.8 Bacterial growth profile

Microbial growth profile is the essential tool to identify the physiological characteristics of gene deletion strains. *E. coli* strain JW18401 and JW39851 had its gene-related to glucose metabolism disruption. To observe the physiological change of gene disruption, growth profile of *E. coli* strain K12, JW18401 and JW39851 were generated in the absence and presence of glucose. *E. coli* strain K12, JW18401 and JW39851 were cultivated on LB medium for 16-18 hours at 37°C. Then, a single colony of *E. coli* was inoculated into fresh LB medium supplemented with various concentrations of glucose including 0, 2.5, 5, 10, 15 and 20 g/L. Bacteria was later cultivated at 37°C, 200 rpm for 24 hours. Samples were collected for each condition at 2 hours interval. Finally, the optical density at 600 nm was measured using a spectrophotometer. Kinetics parameters including generation time (h) and specific growth rate (h^{-1}) were calculated accordingly. Generation time is described as the time required to double the initial bacterial population during the log phase, calculated by the multiplicative inverse of specific growth rate. Specific growth rate is defined as the rate of increase of biomass of a cell population per unit of biomass concentration, calculated with equation [1].

$$\mu = \frac{\ln OD_2 - \ln OD_1}{(t_2 - t_2)} \qquad [1]$$

where OD_1 is OD_{600nm} at initial time, OD_2 is OD_{600nm} at final time, t_1 is time at initial state and t_2 is time at final state.

3.9 Construction of expression vector for PHB biosynthesis

C. necator strain A-04 was used for a source of PHB biosynthesis genes. First, *C. necator* strain A-04 was cultivated according to section 3.6.2. The genomic DNA of *C. necator* strain A-04 was isolated using phenol – chloroform method (Liu et al., 2022) with some modifications. Briefly, cell pellets of *C. necator* strain A-04 were harvested by centrifugation at 10000 rpm, 4°C for 2 minutes. The 200 µL mixture solution of phenol, chloroform and isoamyl alcohol (25:24:1) was then added to the cell pellets, followed by thoroughly mix for 30 seconds. Next, sample was centrifuged at 10000 rpm for 5-10 minutes to stratify the solution. Later, the upper aqueous phase was carefully removed and transferred to a fresh tube. To prevent phenol contamination in extracted DNA, 200 µL of chloroform was added to the sample, followed by mixing, centrifugation and removal of the upper aqueous phase. The mentioned step was repeated 2-3 times. Finally, extracted DNA was purified and concentrated using ethanol precipitation (Green & Sambrook, 2016). Purification of extracted DNA started with the addition of 3M sodium acetate, pH 5.2, 1:10(v/v) and 95%(v/v) ethanol. The sample was then centrifuged at 10000 rpm for 30 minutes at 4°C. DNA pellet was washed twice with ice-cold 70%(v/v) ethanol and air-dried. Finally, 10 mM Tris-HCL pH 8.0 was added to the DNA pellet. The quality of extracted genomic DNA of *C. necator* strain A-04 was analyzed onto 1% agarose gel (Appendix 3).

Genomic DNA of *C. necator* strain A-04 was later used as the template for PHB biosynthesis gene amplification. Two sets of primers were used to construct the expression vector. The first set of primers (Table 15), F_BamHI_phaCAB and R_BamHI_phaCAB, were designed based on the chromosomal DNA sequence of *C. necator* strain H16 in GenBank (Accession number: AM260479.1) together with the

sequences of β-ketothiolase (phaA), acetoacetyl-CoA reductase (phaB) and PHA synthase (phaC) (Accession number: FJ897461, FJ897462 and FJ897463) from *C. necator* strain A-04. The first set of primers were designed to include the native promoter of *C. necator* strain A-04, 340 bp upstream of start codon of *phaC*. The second set of primers, F_XhoI_BamHI_phaCAB and R_HindIII_EcoRI_phaCAB, were designed based on literature review (Boontip et al., 2021), starting at the start codon of *phaC*. PCR was performed using KOD OneTM PCR master mix (Toyobo, Japan). This master mix generates blunt-end PCR products because of 3'→ 5' exonuclease (proof-reading). Components of the reaction were prepared according to manufacturer instruction. The PCR condition was performed as follows: pre-denaturing at 98°C for 10 seconds, 35 cycles of denaturation at 98°C for 10 seconds, annealing at 49°C for 5 seconds (decreased by 0.4°C per cycle) and elongation at 68°C for 25 seconds. The final elongation was performed at 68°C for 30 seconds. PCR product was then analyzed on 1% agarose electrophoresis (Appendix 3) and further purified by TIANquick Midi Purification kit (Tiangen, China).

Linear pBluescript II SK (+) digested with *Eco*RV (Vivantis Technologies, Malaysia) was prepared according to manufacturer instructions. Briefly, 1 µg of circular pBluescript II SK (+), 5 µL of 10X reaction buffer and 40U of *Eco*RV were mixed in a 50 µL reaction tube, followed by incubation at 37°C for 16 hours. The linear plasmid was verified on 1% agarose electrophoresis (Appendix 3) and further purified by TIANquick Midi Purification kit (Tiangen, China). The PCR product of $phaCAB_{A\text{-}04}$ was ligated to *Eco*RV digested pBluescript II SK (+) using T4 DNA Ligase (Thermo Fisher Scientific, UK) according to manufacturer instructions and later transformed into *E. coli* JM109 by chemical method (Chung et al., 1989). Successful transformants were selected by Blue-White selection on LB containing X-Gal and IPTG plate. The transformants were re-streaked on LB plate containing ampicillin.

Transformants were analyzed with colony PCR using F_M13_pUC40 and R_semi_phaA primers to demonstrate the correct orientation of inserted DNA fragment. *Taq* DNA polymerase was used according to the manufacturer's instructions with the annealing temperature of 49°C. Constructed pBSK*CAB*$_{A-04}$ was isolated from *E. coli* JM109 by using FavorPrep^{TM} Plasmid DNA Extraction kit according to manufacturer's instructions and later analyzed by agarose gel electrophoresis. The verification of the plasmid DNA was achieved by restriction enzyme, *Bam*HI and *Eco*RI, digestion. Sequence analysis showed *Bam*HI restriction site in forward and reverse primer, yielding two DNA fragments of pBluescript II SK (+) backbone and phaCAB$_{A-04}$. The digestion of pBSK*CAB*$_{A-04}$ by *Eco*RI exhibited a single DNA fragment of both pBluescript II SK (+) backbone and phaCAB$_{A-04}$. The constructed pBSK*CAB*$_{A-04}$ was submitted for sequencing (U2Bio., Co., Ltd., Bangkok, Thailand) and further used for PHAs production in recombinant *E. coli.*

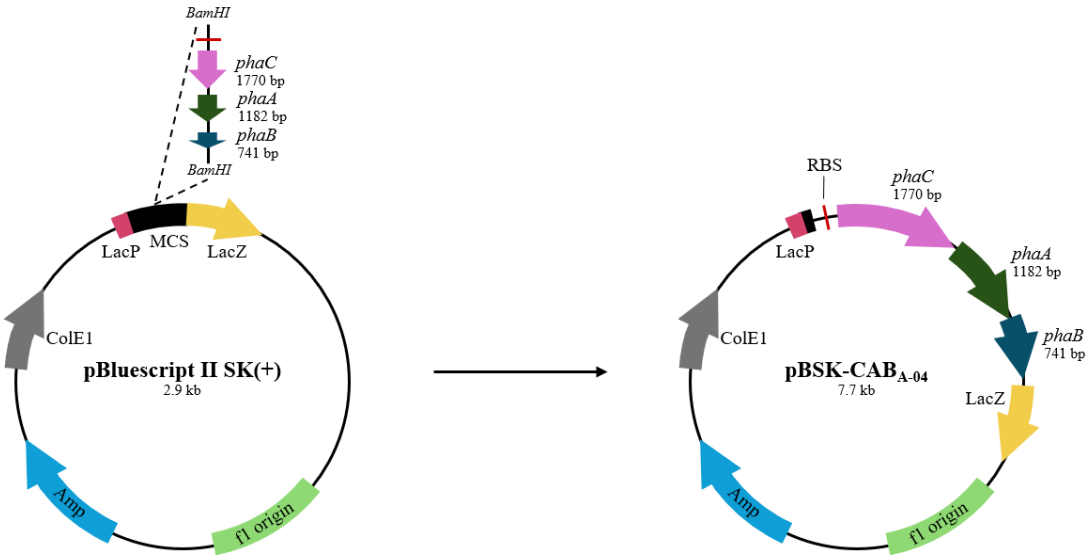

Figure 16 Construction of the pBSK*CAB*$_{A-04}$ expression plasmid containing *phaC1*$_{A-04}$, *phaA*, *phaB* and native promoter from *Cupriavidus necator* strain A-04

3.10 PHB biosynthesis in recombinant *E. coli* harboring pBSK*CAB*$_{A-04}$ using glucose as a sole carbon source

Chemically competent *E. coli* strain K12, JW39851 and JW18401 were introduced with constructed pBSK*CAB*$_{A-04}$ by heat shock method at 42°C for 30 seconds, followed by cell recovering using SOC medium (Appendix 2) (Chung et al., 1989). The resulting strains named *E. coli* strain K12-pBSK*CAB*$_{A-04}$, JW39851-pBSK*CAB*$_{A-04}$ and JW18401-pBSK*CAB*$_{A-04}$. All transformants were later re-streaked on LB plate containing ampicillin at 37°C for 18 hours.

Preliminary experiment on PHB production in recombinant *E. coli* harboring pBSK*CAB*$_{A-04}$ was performed to examine the functional plasmid. Condition settings such as inoculum concentration, cultivation temperature, inoculum age and glucose concentration were based on literature reviews (Boontip et al., 2021). Briefly, a single colony of *E. coli* strain K12-pBSK*CAB*$_{A-04}$, JW39851-pBSK*CAB*$_{A-04}$ and JW18401-pBSK*CAB*$_{A-04}$ were cultivated in 250 mL Erlenmeyer flask containing 50 mL LB medium at 37°C for 18 hours. Preculture concentration in each experiment was controlled by the number of colony forming units calculated with equation [2] (Bhuyan et al., 2023).

$$\text{CFU/ml} = \frac{\text{No. of colonies x Dilution factor}}{\text{Volume of culture plated}} \qquad [2]$$

Then, 1% (v/v) precultures were transferred into a 250 mL Erlenmeyer flask containing 47 mL LB medium supplemented 20 g/L glucose and 100 µg/ml ampicillin. The 500 g/L glucose solution was separated prepared and autoclaved, prior subjected into the flask to prevent chemical changes of media components. The volume of media was adjusted to 50 mL after addition of glucose, preculture and ampicillin with sterilized water. The recombinant cells were cultured in the shaking incubator at 200 rpm, 37°C for 24 hours without adding any inducer. Samples were collected for further PHAs quantification by gas chromatography as described in 3.13.

To confirm the PHAs production by expression of pBSK*CAB*$_{A-04}$, recombinant *E. coli* strain K12-pBSK*CAB*$_{A-04}$ was also analyzed using Nile red staining as a selective fluorescent for intracellular lipid formation (Cao et al., 2022). Briefly,

E. coli strain K12-pBSK*CAB*$_{A-04}$ was cultured on LB with 0.1% Nile red and 2% glucose at 37°C for 24 hours. The fluorescence of PHB granule was observed by BluPad Dual LED Blue/White Light Transilluminator, BIO-HELIX Co., Ltd., Taiwan.

3.11 Optimization of culture condition for PHB biosynthesis in recombinant *E. coli* harboring pBSK*CAB*$_{A-04}$

E. coli strain K12-pBSK*CAB*$_{A-04}$, JW39851-pBSK*CAB*$_{A-04}$ and JW18401-pBSK*CAB*$_{A-04}$ for PHB production were first cultivated on LB plate. After that, these strains were inoculated into a 250 mL Erlenmeyer flask containing 50 mL LB medium and cultured for 18 hours at 37°C, 200 rpm. Next, the optical density of precultures were measured by spectrophotometer at 600 nm., compared to the standard curve of CFU/ml and OD_{600}. Preculture concentrations were calculated to control the equivalent number of starting cells in each experiment. After that, precultures were transferred into 500 mL Erlenmeyer flask of LB medium supplemented with 100 µg/ml ampicillin, glucose and preculture. The final volume of each flask was 100 mL. Different parameters such as temperature, inoculum concentration and glucose concentration affecting PHB production in this study were considered and varied one factor at a time. The cultivation temperatures used in this experiment were 30 and 37°C. Various amounts of preculture inoculum (1, 3, 5 and 10% v/v) and different concentrations of glucose (10, 20, 30 and 40 g/L) were examined. Cell cultivation was performed for 48 hours, followed by sample collection. Culture samples were collected at 6 hours interval, followed by centrifugation at 8,000 rpm for 20 minutes and dried at 60°C for 2 days for further analysis as mentioned in 3.13, 3.14 and 3.15.

After all parameters were studied to optimize PHB production, *E. coli* strain K12-pBSK*CAB*$_{A-04}$, JW39851-pBSK*CAB*$_{A-04}$ and JW18401-pBSK*CAB*$_{A-04}$ were cultivated at the optimum condition. Briefly, precultures were prepared in 250 mL Erlenmeyer flask containing 50 mL LB medium supplemented with 100 µg/ml ampicillin for 18 hours at 37°C. Later, 5%(v/v) inoculum with the range of 5×10^6 - 9×10^6 CFU/mL was transferred into a 500 mL Erlenmeyer flask of LB medium containing 100 µg/ml ampicillin and 20 g/L glucose. For PHB production, recombinant strains were cultivated at 30°C for 48 hours. Culture samples were collected at 6 hours interval,

followed by centrifugation at 8,000 rpm for 20 minutes and dried at 60°C for 2 days for further analysis as mentioned in 3.13, 3.14 and 3.15.

3.12 Cultivation of PHB production in *E. coli* strain JW18401 harboring pBSK*CAB*$_{A-04}$ combined with pH-stat in fermenter

A cultivation of PHB production was scaled up in a 10-L bioreactor (MDL500, B.E. Marubishi Co., Ltd., Tokyo, Japan). A preculture was prepared in 500-mL Erlenmeyer flask containing 100 mL of LB medium and 100 µg/ml ampicillin. Cells were cultivated on a rotary shaker at 37°C at 200 rpm for 18 hours. The resulting overnight culture with the OD_{600} of 1.1 then served as a 5% (v/v) inoculum for batch cultivation. The bioreactor was equipped with a dissolved oxygen sensor thermometer, air-flow meter, pH probe and thermometer. The preculture was then transferred into a 10-L bioreactor with operation volume of 5 L LB medium supplemented with 100 µg/ml ampicillin, 20 g/L glucose at 30°C. The agitation speed controlled by electromagnetic impulse was 200 rpm. The air flow rate was 1 vvm. Samples were collected at 6 hours intervals for 48 hours. The pH was automatically controlled through the addition of ammonia water. Fed-batch fermentation with a pH-stat feeding strategy based on the upper limit as mentioned by Kim et al. (2004) (Kim et al., 2004). It operated on the principle that pH increased due to ammonium ion excretion when glucose was depleted. When the pH exceeded 7.1, the feeding solution containing 500 g/L glucose, 60 g/L tryptone, 60 g/L yeast extract and 20 g/L magnesium sulfate was automatically added to maintain the pH of the fermentation broth. Cells were cultivated for 54 hours. Samples were collected at 3-6 h intervals for further analysis as mentioned in 3.13, 3.14 and 3.15.

3.13 PHAs content analysis

The analysis of intracellular PHB was conducted after 48 hours of bacterial cultivation following method by Braunegg et al. (1978) (Braunegg et al., 1978). In brief, cell suspensions at each time intervals were harvested by centrifugation (5804 R, Eppendorf SE, Hamburg, Germany) at 4000 rpm for 15 minutes, followed by washing with distilled water repeatedly. The cell pellet was dried at 65°C for 48 hours.

Subsequently, approximately 20 mg dried cell was subjected to the treatment of methanolysis in a PTFE-lined screw-cap test tube. The PHB concentration was determined by the methyl esterification method using a mixture of 2 mL chloroform and 2 mL 15% (v/v) methanol-sulfuric acid (1:1 v/v) containing 0.5 g/L benzoic acid. Then the mixture substance was followed by incubation for 3 hours at 80°C. After cooling to room temperature, the mixture was vortexed for 2 minutes, followed by addition of distilled water for stratification. The mixture was separate into organic and aqueous layers. The organic phase containing PHAs was filtered and transferred into GC vial. The resulting monomeric methyl esters were quantified by a gas chromatograph (model CP3800, Varian Inc., Walnut Creek, CA, United States) using a Carbowax-PEG capillary column and flame ionization detector (FID), with benzoic acid and PHB (Sigma-Aldrich Corp., St. Louis, MO, United States) used as internal and external standards, respectively. The setting for operating the gas chromatography was described as follows.

Column: Carbowax-PEG capillary column (0.25-μm df, 0.25-mm ID, 60-m length, Varian Inc.)
Injection temperature: 250°C
Column temperature: 140°C
Detector temperature: 250°C
Split ratio: 50 to 1
Carrier gas: N_2 with a flow rate of 2 mL per minute
Injection volume: 1 μL

For copolymer of P3HB and P3HV analysis, P(3HB-*co*-3HV) (Tianan Industry, China) having a 3 mol% according to the supplier was used as external standard. PHB productivity (g/L.h) was calculated and PHB yield (g/g) was defined as PHB (g) produced per gram of glucose consumed.

3.14 Biomass analysis

Cell growth was monitored in terms of cell dry mass (CDM), determined by filtering 2 mL of the culture broth through pre-weighed cellulose nitrate membrane filters (pore size = 0.22 mm; Sartorius, Goettingen, Germany). The filters were dried at 80°C for 2 days and stored in desiccators. The residual biomass (RCM) was calculated by subtracting PHB concentration from the CDM and indicated the net biomass of bacteria. When needed, cell growth was also investigated by measuring the optical density at 600 nm or the turbidity of cell culture using spectrophotometer.

3.15 Glucose and glycerol concentrations determination

To investigate glucose and glycerol concentrations, medium was first filtered through 0.22 μm nylon membrane syringe filter and determined using high-performance liquid chromatography (HPLC, Agilent 1200 Infinity Series, Agilent technologies, United States) equipped with a 1260 RID and X-bridge-BEH amide column (4.6 x 250 nm x 5 mm) (Water, United States) under an isocratic mobile phase of acetonitrile to water (60:40, v/v) for glucose concentration determination and acetonitrile to water (70:30, v/v) for glycerol concentration determination at a flow rate of 1.0 mL/min and a temperature of 30°C (Simonzadeh & Ronsen, 2012).

3.16 PHB extraction, purification and preparation of PHB film

The PHB accumulated in cells was extracted in hot chloroform in a Soxhlet extractor, followed by precipitation three times with n-hexane. The purified PHB polymers were dried by evaporation and stored at room temperature. The PHB films used for the mechanical property tests were prepared according to the ASTM: D882-91 by conventional solvent-casting techniques in chloroform solutions. Briefly, 1%(w/v) PHB pellets were mixed with 5 mL chloroform to regulate the thickness of the polyester films. After that, the mixture solution was poured onto a glass tray (Pyrex, Corning Incorporated, Corning NY, USA) served as a casting surface, followed by complete evaporation of the solvent. The films were cut to 50 x 150 mm for at least ten samples and aged for four weeks to reach equilibrium crystallization prior to analysis.

3.17 PHB film molecular weight analysis

The weight average molecular weight (M_w), the number average molecular weight (M_n) and the polydispersity index (PDI) were determined by gel permeation chromatography (GPC; Shimadzu LC20AD and CTO-20A system, Shimadzu Co., Ltd., Kyoto, Japan) equipped with a Shimadzu RID-10A refractive index detector and four Shodex columns GPC K-802.5, 803, 804 and 805 columns connected in series. The PHB polymer was first dissolved in 0.1% (w/v) chloroform and filtered through a 0.45 μm Durapore® (PVDF) membrane filter with low protein binging capacity (Millex® - HV, Merck Millipore Ltd., Tullagreen, Carrigwohill Co., Cork, Ireland). Styrene standards were used to prepare standard curve. The measurement was operated under the temperature at 40°C using chloroform as an eluent with the flow rate of 1 mL/min. The measurements were carried out with an injection volume of 20 μL. The M_w was defined as the emphasis on the molecular weight of each molecule in the fraction while the M_n was calculated with the emphasis on the number of molecules of a given molecular weight in the fraction. The PDI was expressed by the ratio of M_w/M_n.

3.18 PHB film thermal properties analysis

Thermal analysis was performed by Differential Scanning Calorimetry (DSC) using a calorimetry DSC apparatus (DSC7, PerkinElmer, Inc., Waltham, MA, USA) at the Petroleum and Petrochemical College, Chulalongkorn University under nitrogen atmosphere. PHB sample (10-20 mg) was first encapsulated in an aluminum sample vessel and placed in the sample holding chamber of the DSC apparatus. STAR^e software (version SW 10.00; Mettler-Toledo International Inc., Columbus, OH, USA) was used to operate the DSC apparatus. The sample was heated from ambient temperature to 230°C at a rate of 20°C/min. Later, the sample was maintained at 230°C for 5 mins before being cooled to -50°C at a rate of 20°C/min. Afterward, the sample was thermally cycled to 230°C under a nitrogen atmosphere at a rate of 20°C/min. DSC curves were recorded and from those thermograms the following parameters were obtained. The melting temperature (T_m) was given by the intersection of the tangent with the furthest point of an endothermic peak and the extrapolated sample baseline. The enthalpy of melting (ΔH_m) was defined by the

area between the melting peak and the baseline when plotted with respect to the time. The glass transition temperature (T_g) was estimated by extrapolating the midpoint of the heat capacity difference between glassy and viscous states after heating of the quenched sample. Degree of crystallinity of PHB ($X_{C\text{-}DSC}$) was determined using equation [3] as described by Wellen et al. (R. et al., 2015).

$$X_{C\text{-}DSC}(\%) = \frac{\Delta H_m}{\Delta H_m^0 \times w_{PHB}} \times 100 \qquad [3]$$

where ΔH_m is the melting enthalpy of the sample, ΔH^0_m is the melting enthalpy of a 100% crystalline PHB (146 J/g) (Barham et al., 1984) and w_{PHB} is the weight fraction of PHB in the sample.

3.19 Cell morphology and PHA granules investigation

Cell morphology and PHA granules were observed by transmission electron microscopy (TEM) at Scientific and Technological Research Equipment Centre Chulalongkorn University, Bangkok, Thailand. Briefly, cell cultures were collected at the end of the 48-h fermentation. Cells were cooled on ice, harvested at 4000 rpm and resuspended in 2.5%(v/v) glutaraldehyde in 0.1 M phosphate buffer (pH 7.4). Later, the cells were postfixed in 1%(v/v) osmium tetroxide in 0.1 M phosphate buffer. The cells were dehydrated in 35, 70, 95 and 100%(v/v) ethanol and subsequently infiltrated in Spurr's resin (EMS, PA, United States). Sections were prepared using LKB 2088 Ultratome V (Surrey, United Kingdom), stained with 2%(w/v) uranyl acetate and 2%(w/v) lead citrate and investigated with TEM (JEM 2100, JEOL Ltd., Tokyo, Japan) at an accelerating voltage of 80 kV.

3.20 PHB biosynthesis in recombinant *E. coli* harboring pBSK*CAB*$_{A\text{-}04}$ using crude glycerol waste as a sole carbon source

With the purpose of reducing production cost of PHB, low-cost feedstock such as crude glycerol waste was introduced as a sole carbon source, substituting glucose. The crude glycerol used in this study was obtained from BBGI Biodiesel Company Limited (BBGI-BI), Bangchak Corporation Public Company Limited, Thailand.

The components of crude glycerol used in this study consisted of 81.05%wt glycerol, 13.5%wt moisture, 3.31%wt salts content as sodium chloride, 0.004%wt methanol, 1.13%wt ash and 0.99%wt calculated matter (organic) nonglycerol (MONG) content (Natthaphat Phothong et al., 2024). The condition used in PHB biosynthesis was the optimized condition of PHB production by recombinant *E. coli* harboring pBSK*CAB*$_{A-04}$ from glucose as mentioned in 3.11. Briefly, *E. coli* strain K12-pBSK*CAB*$_{A-04}$, JW39851-pBSK*CAB*$_{A-04}$ and JW18401-pBSK*CAB*$_{A-04}$ were cultured in 250 mL Erlenmeyer flask containing 50 mL LB medium for 18 hours at 37°C, 200 rpm. Later, 5%(v/v) inoculum with the range of 5 x 10^6 - 9 x 10^6 CFU/mL was transferred into a 500 mL Erlenmeyer flask of LB medium containing 100 µg/ml ampicillin and 20 g/L crude glycerol. For PHB production, recombinant strains were cultivated at 30°C for 48 hours. Culture samples were collected at 6 hours interval, followed by centrifugation at 8,000 rpm for 20 minutes and dried at 60°C for 2 days for further analysis as mentioned in 3.13, 3.14 and 3.15.

3.21 Copolymer poly(3HB-*co*-3HV) production in *E. coli* strain JW18401 harboring pBSK*CAB*$_{A-04}$

To produce value-added PHB products, we aimed to produce the copolymer of PHB and 3-hydroxyvalerate from glucose and sodium propionate salt, which is structural related carbon source to 3-hydroxyvalerate (Figure 10). *E. coli* strain JW18401 was selected as a host to produce copolymer poly(3HB-*co*-3HV) due to its ability to produce good amounts of PHB within 24 hours. The cultivation of poly(3HB-*co*-3HV) was performed at the optimized condition of PHB production by recombinant *E. coli* harboring pBSK*CAB*$_{A-04}$ from glucose as mentioned in 3.11. First, *E. coli* strain JW18401-pBSK*CAB*$_{A-04}$ were cultured in 250 mL Erlenmeyer flask containing 50 mL LB medium for 18 hours at 37°C, 200 rpm. The 5%(v/v) overnight cell culture with the range of 5 x 10^6 - 9 x 10^6 CFU/mL was inoculated into LB medium supplemented with 0, 0.5, 1 and 2 g/L propionic acid sodium salt. The total carbon concentration was controlled at 20 g/L. Cells were cultured at 30°C, 200 rpm for 30 hours. Copolymer P(3HB-*co*-3HV) concentration and biomass were analyzed as mentioned methods in 3.13, 3.14 and 3.15.

3.22 Statistical analysis

Statistical significance was evaluated using the unpaired Student's *t*-test (single comparisons) or one-way ANOVA followed by Bonferroni (multiple comparisons) testing. Data obtained from three independent repeats were expressed as the mean value ± standard deviation (SD). The analysis was carried out using SPSS version 22 (IBM Corp., Armonk, NY, USA). Differences were considered significant at $P \leq 0.05$.

CHAPTER IV
RESULT AND DISCUSSION

4.1 Single gene deletion in *E. coli* strain JW18401 and JW39851

The technique required for gene deletion was the use of homologous recombination via lambda red recombineering plasmid. The principle of homologous recombination was about pairing DNA with similar sequences that can cross over and exchange to one another (Figure 15). Hence, up and down homologous regions of target gene played an important role in gene deletion. In this case, kanamycin deletion cassette was amplified with homologous region to the target gene. Lambda red recombineering plasmid containing gam, exo and beta was used to generate the modification (Figure 17). The role of three components of lambda red recombineering plasmid was previously described by Leung et al. (2021) (Leung et al., 2021). Gam prevents endogenous nucleases such as RecBCD and SbcCD from digesting the kanamycin deletion cassette introduced to *E. coli*. Exo, serving as 5' to 3' dsDNA-dependent exonuclease, degrades dsDNA to generate a partial dsDNA duplex with a single strand overhang. Finally, Beta binds to the ssDNA overhang and promotes its annealing to a complementary ssDNA target in the cell. *E. coli* strain JW18401 and JW39851 were *E. coli* K12 derivatives with phosphogluconate dehydratase (*edd*) and phosphoglucose isomerase (*pgi*) deletion, respectively. Both *E. coli* strain JW18401 and JW39851, obtained from Keio collection (Baba et al., 2006), contained the kanamycin deletion cassette resulting from gene replacement. With the purpose of using these mutant strains to produce homopolymer and copolymer of PHB and other monomers, we planned to use two expression plasmids, pBluescript II SK (ampicillin resistance) for PHB biosynthesis and pBBR1-mcs2 (kanamycin resistance) for co-expression of related genes in copolymer biosynthesis. Therefore, in-frame deletion of kanamycin resistance gene in chromosomal DNA of *E. coli* mutants was necessary.

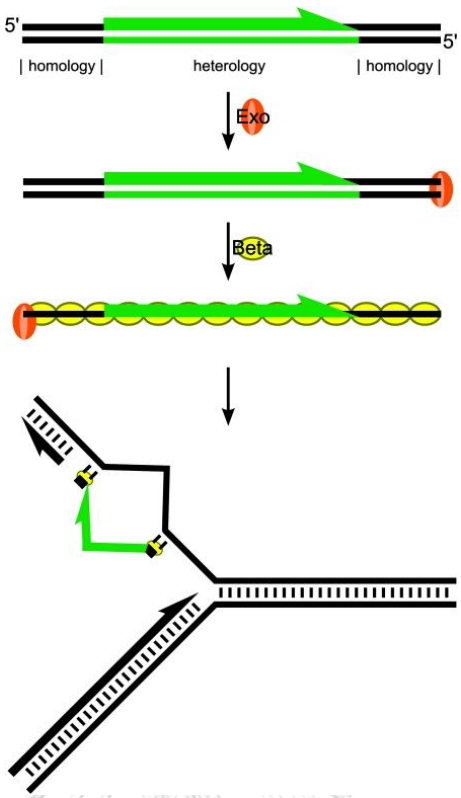

Figure 17 Components of the lambda red recombineering system (Mosberg et al., 2010)

To eliminate kanamycin resistance gene in chromosomal DNA of *E. coli* mutants, *E. coli* strain JW18401 and JW39851 were introduced with pCP20 (Figure 18) to perform an in-frame deletion (Jensen et al., 2015). The pCP20 showed temperature-sensitive replication and thermal induction of FLP synthesis (Datsenko & Wanner, 2000). After cultivation of recombinant *E. coli* strain JW18401-pCP20 and JW39851-pCP20 at 43°C as thermal induction, expression of *flp* created an in-frame deletion by flipping out the resistance marker at FRT recognition sites (Figure 15). Furthermore, pCP20 had temperature-sensitive replication. Growing recombinant *E. coli* at 43°C resulted in the loss of pCP20. Therefore, resulting *E. coli* strain JW18401 and JW39851 lost their ability to grow on LB medium supplemented with kanamycin or ampicillin.

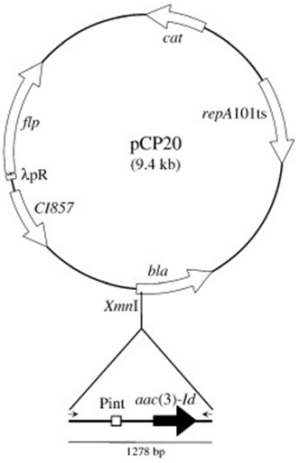

Figure 18 Plasmid map of pCP20, helper plasmid in red recombination, containing *flp* encoding flippase recombinase (Doublet et al., 2008)

The successful mutants were investigated the inability of *E. coli* to grow on LB supplemented with kanamycin and ampicillin, but able to grow on LB plate. The inability of *E. coli* to grow on LB supplemented with kanamycin confirmed the loss of kanamycin resistance gene in genomic DNA sequence while the inability of *E. coli* to grow on LB supplemented with ampicillin ensured the loss of pCP20 vector used in the in-frame deletion. As a result, a total of 3 successful mutants of *E. coli* strain JW39851 from 20 samples was obtained from the first round of in-frame deletion verification, including mutant number 10, 15 and 20 (Figure 19). Three mutants were subsequently subjected to the second round of verification. As a result, only mutant number 20 was confirmed as a completely successful mutant of *E. coli* strain JW39851 and further used for all other experiments in this research. For in-frame deletion of *E. coli* strain JW18401, the same procedure was repeated and a successful mutant strain of *E. coli* strain JW18401 was obtained (data not shown). To ensure enough cells for the ensuing plates in each experiment, it was suggested to streak the cultures on LB supplemented with antibiotics prior LB without antibiotics. By using the same loop or needle, growth of *E. coli* on LB, which was the last plate in the process of streaking, assured there were adequate amounts of cells in previous LB plate with antibiotic supplementation. Therefore, the inability to grow on LB plate

with antibiotic supplementation resulted from the loss of potential resistance gene, not insufficient amounts of cells.

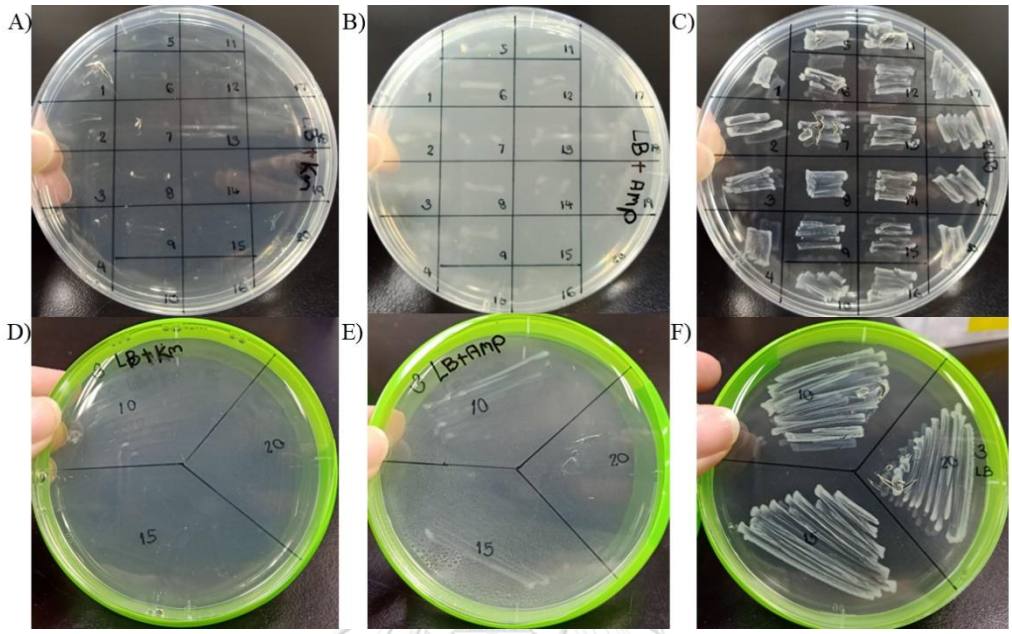

Figure 19 Verification of single gene deletion in *Escherichia coli* JW39851. First round of verification by streaking culture on (A) LB + kanamycin, (B) LB + ampicillin and (C) LB. Second round of verification by streaking culture on (D) LB + kanamycin, (E) LB + ampicillin and (F) LB.

Successful in-frame mutants of *E. coli* strain JW18401 and JW39851 were further investigated in PCR verification. Sequence analysis of *E. coli* K12 strain MG1655 chromosomal DNA (Accession number: CP027060.1) showed the size of *edd* and *pgi* gene were 1812 and 1650 bp, respectively. By using F and R_edd_verify (Table 15) to confirm the *edd* gene, PCR product size in parental strain K12 and JW18401 were 3940 and 2128 bp, respectively. By using F and R_pgi_verify (Table 15) to verify *pgi* gene, PCR product size in parental strain K12 and JW39851 were 2235 and 585 bp, respectively. Agarose gel electrophoresis result illustrated the *edd* and *pgi* gene in *E. coli* strain K12, JW18401 and JW39851 (Figure 20).

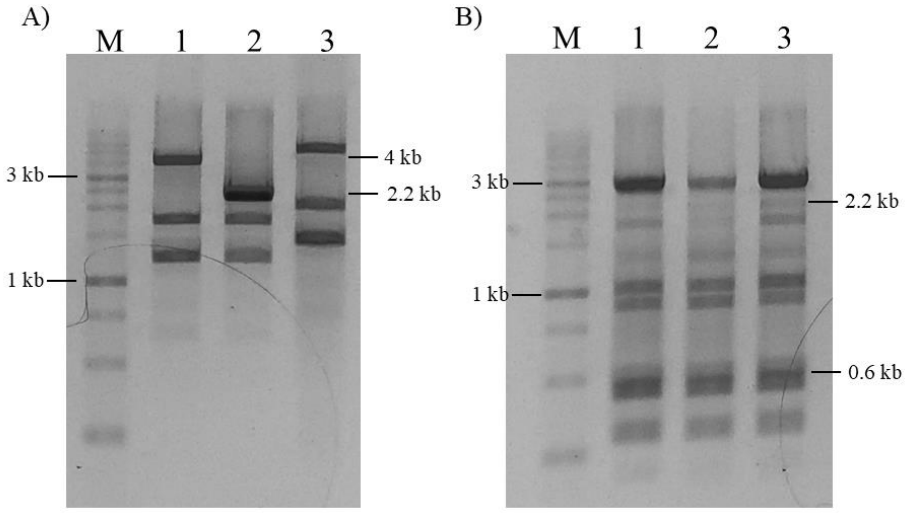

Figure 20 Amplification of *edd* gene (A) Lane M, 1kb marker, Lane 1, *edd* gene in *E. coli* K12, Lane 2, *edd* gene in *E. coli* JW18401 and Lane 3, *edd* gene in *E. coli* JW39851 and *pgi* gene (B) Lane M, 1kb marker, Lane 1, *pgi* gene in *E. coli* K12, Lane 2, *pgi* gene in *E. coli* JW39851 and Lane 3, *pgi* gene in *E. coli* JW18401

As a result of agarose gel electrophoresis, the 4-kb PCR product of *edd* gene in *E. coli* strain K12 and JW39851 was visible (Figure 20), showing the presence of native *edd* gene in both strains. For *E. coli* strain JW18401, the shift of 4-kb to 2.2-kb PCR product of *edd* gene in-flame deletion was detected. It also illustrated the size of *edd* gene deletion of 1.8 bp, which was the same size as sequence analysis by using *E. coli* K12 strain MG1655 chromosomal DNA. Likewise, the 2.2-kb PCR product of *pgi* gene in *E. coli* strain K12 and JW18401 was illustrated, showing the presence of native *pgi* gene in both strains, while the 2.2-kb band was not shown in *E. coli* strain JW39851. The result indicated the successful gene of interest deletion and complete removal of kanamycin deletion cassette from chromosomal DNA of *E. coli* mutants to create in-frame deletion. These resulting strains were later sub-cultured and stored as aliquot of cell culture for further use.

4.2 Bacterial growth profile

The growth of bacteria and the interpretation of growth kinetics are essential information to understand the fundamental physiology or microorganisms under a specified condition. *E. coli* strain K12 represented as wild-type strain whereas *E. coli* strain JW18401 and JW39851 defined the *edd* and *pgi* deletion strain, respectively. The *E. coli* strain JW18401 had its Entner-Doudoroff pathway inactivation while *E. coli* strain JW39851 had its Embden-Meyerhof pathway disruption (Figure 13). Since both *edd* and *pgi* are essential genes in glucose metabolism of *E. coli*, the effect of glucose on the growth of *E. coli* strain JW18401 and JW39851 were studied. In this experiment, *E. coli* strain K12, JW18401 and JW39851 were cultivated at 37°C for 24 hours in LB medium supplemented with various concentrations of glucose (0, 2.5, 5, 10, 15 and 20 g/L). The bacterial growth was determined by measuring the turbidity of cell suspensions at 600 nm using a spectrophotometer. Forward scattering signal intensity is proportional to the concentration of bacterial cells in suspension. Growth profiles of *E. coli* strain K12, JW18401 and JW39851 were represented in Figure 21.

The *E. coli* strain K12, parental strain, cultivated in LB medium without glucose supplementation was a control experiment. The maximum OD_{600} of *E. coli* strain K12 without glucose supplementation reached the value of 3.1 with the specific growth rate of 0.25 h^{-1} (Appendix 4). After that, the effect of glucose on the growth of *E. coli* strain K12 was investigated. As a result, *E. coli* strain K12 exhibited a similar pattern of growth profile in both absence and presence of glucose in LB medium. The maximum OD_{600} of *E. coli* strain K12 in LB supplemented with 2.5-20 g/L glucose ranged between 2.9±0.1 to 3.2±0.0. Addition of glucose in the medium tended to slightly decrease the growth of *E. coli* strain K12, compared to the condition without glucose supplementation. Interestingly, the decrease in the growth of *E. coli* strain K12 had no direct change to the glucose concentrations. The specific growth rate of *E. coli* strain K12 in various concentrations of glucose had a very tight range of 0.24-0.25 h^{-1} with the doubling time of 0.07 hours in all conditions (Table 16). Hence, statistical analysis by two-way ANOVA suggested that addition of glucose had no significant effect on the growth of *E. coli* strain K12 ($P > 0.05$).

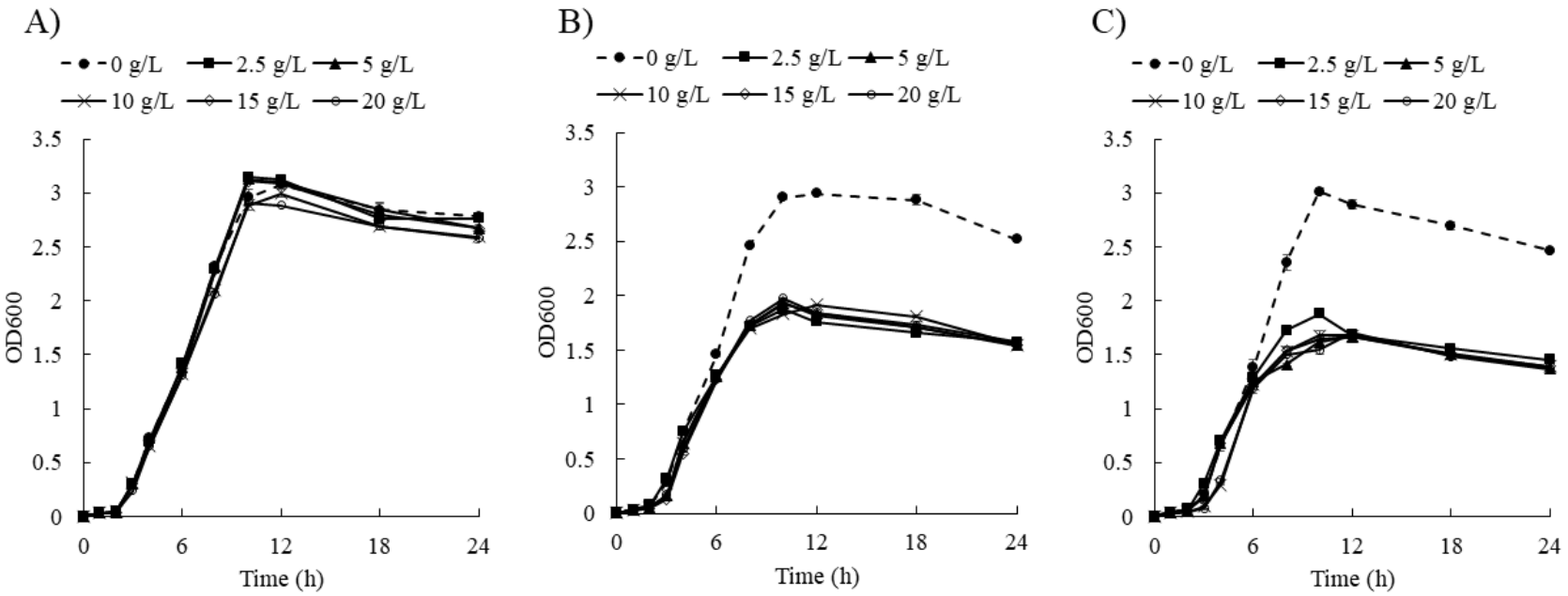

Figure 21 Growth curve of *Escherichia coli* strain (A) K12, (B) JW39851 and (C) JW18401 culturing at 37°C in LB medium supplemented with 0, 2.5, 5, 10, 15 and 20 g/L glucose.

Table 16 Growth measurement and kinetics of *E. coli* strain K12, JW39851 and JW18401 varied by glucose concentrations in LB medium

E. coli strain	Maximum OD_{600}	Specific growth rate (h^{-1})	Doubling time (h)
0 g/L glucose			
K12	3.1 ± 0.0[a]	0.25	0.07
JW39851	2.9 ± 0.0[a]	0.23	0.07
JW18401	3.0 ± 0.0[a]	0.24	0.07
2.5 g/L glucose			
K12	3.2 ± 0.0[a]	0.24	0.07
JW39851	1.9 ± 0.0[b]	0.21	0.08
JW18401	1.9 ± 0.0[b]	0.20	0.08
5 g/L glucose			
K12	3.1 ± 0.0[a]	0.24	0.07
JW39851	1.9 ± 0.0[b]	0.22	0.08
JW18401	1.7 ± 0.0[b]	0.21	0.08
10 g/L glucose			
K12	3.0 ± 0.0[a]	0.24	0.07
JW39851	1.9 ± 0.0[b]	0.22	0.08
JW18401	1.7 ± 0.0[b]	0.22	0.08
15 g/L glucose			
K12	3.1 ± 0.1[a]	0.25	0.07
JW39851	1.9 ± 0.0[b]	0.22	0.08
JW18401	1.7 ± 0.0[b]	0.22	0.08
20 g/L glucose			
K12	2.9 ± 0.1[a]	0.24	0.07
JW39851	2.0 ± 0.0[b]	0.22	0.08
JW18401	1.7 ± 0.0[b]	0.22	0.07

Results are expressed as mean ± SD (n = 3)

The different superscript letters within the same column are significantly different at $P < 0.05$

The result of this study showed that addition of glucose had no significant effect on the growth of *E. coli* strain K12. In contrast, several previous articles reported that glucose concentrations promoted the growth rate of *E. coli*. Zhang et al. (2005) reported addition of glucose in the medium increased the growth rate of *E. coli* in functional interactions study between carbon and iron regulator system (Zhang et al., 2005). Similar evidence was found according to Suresh et al. (2023), the rise of *P. aeruginosa* growth varied proportionally to the amount of glucose supplied (Suresh et al., 2023). This information displayed the importance of media type on bacterial growth assimilating glucose as a carbon source. The main reason for this is probably glucose could promote extra growth of bacteria particularly in nutrient depleted media which was used by Zhang et al. (2005) and Suresh et al. (2023) (Suresh et al., 2023; Zhang et al., 2005). Vasiljevs et al. (2023) clearly demonstrated the difference of glucose effect on bacterial growth in nutrient-rich and nutrient-limited media (Vasiljevs et al., 2023). Two strains of bacteria, *S. aureus* and *P. aeruginosa*, were cultivated in two types of media, Mueller-Hinton (MH) and artificial sputum medium (ASM) with and without supplementation of 4 mM glucose. The results illustrated that glucose promoted the growth of *S. aureus* and *P. aeruginosa* in ASM, but not MH. It can be concluded that supplementation of glucose to nutrient-rich media such as Luria-Bertani (LB), Mueller-Hinton (MH) and nutrient broth (NB) rarely promoted additional growth of bacteria. On the other hand, glucose supplementation in nutrient-limited media such as minimal medium (MM) and artificial sputum medium (ASM) greatly boosted up the bacterial growth rate.

We later observed the physiological change of *E. coli* strain JW39851 and JW18401 in LB medium. In the condition of glucose absence, *E. coli* strain JW39851 and JW18401 showed a similar pattern of growth to *E. coli* strain K12. The maximum OD_{600} of *E. coli* strain JW39851 and JW18401 was 2.9±0.0 and 3.0±0.0, respectively. A slight decrease of bacterial growth was observed in both mutant strains when compared to the parental strain. In addition, the specific growth rate for *E. coli* strain JW39851 and JW18401 implied the change of bacterial growth rate with the value of 0.23 and 0.24 h^{-1}, lower than *E. coli* stain K12 which was 0.25 h^{-1} (Appendix 4). The result indicated the effect of *pgi* and *edd* gene deletion on the decrease of

E. coli growth. Previous studies on the physiological change of *pgi* mutants reported that the disruption of *pgi* gene led to significant decrease of bacterial growth and glucose consumption rate (Canonaco et al., 2001; Charusanti et al., 2010; Hua et al., 2003). Over 80% reduction in cell growth of *pgi* mutant was observed (Charusanti et al., 2010). Not only *pgi* gene disruption, disruption of other genes in EMP also resulted in the slow growth of *E. coli* (Chae et al., 2015; Guitart Font & Sprenger, 2020; Sundara Sekar et al., 2016). On the contrary, *pgi* mutant grew better on media supplemented with fructose or mixture of fructose and glucose (Ahn et al., 2011). Although deletion of *pgi* gene may cause cell growth reduction significantly, the decrease of cell growth of *E. coli* strain JW39851 observed from this experiment was not affected as much as expected (Figure 21). This incident might be related to adaptive evolution to the loss of *pgi* gene described by Charusanti et al. (2010) (Charusanti et al., 2010). The *pgi* mutant exhibited adaptation in an increase of growth rate and carbon consumption rate by 3.6- and 2.6-fold, respectively, after 50 days of adaptive evolution. Mutations in the NADH/NADPH transhydrogenases *udhA* and *pntAB* and in the stress associated sigma factor *rpoS* arose during the adaptation in *pgi* mutant. The result demonstrated that *E. coli* can adapt to the loss of a major metabolic gene (Charusanti et al., 2010).

Interestingly, the result from this experiment displayed a slight decrease in *E. coli* strain JW18401 growth (Figure 21). Since EDP is known as an inactive pathway in *E. coli*, the growth of *E. coli* strain JW18401 was expected to be similar to that found in *E. coli* strain K12. Similar results were displayed in the research by Shimaoka et al. (2005). The *edd* mutant was reported to grow slower and reach lower OD_{600} value compared to native strain (Shimaoka et al., 2005). On the contrary, metabolic flux response of *edd* mutant showed no change of growth rate, biomass yield, glucose uptake rate and acetate yield compared to native strain (Long & Antoniewicz, 2019). It was hypothesized that *edd* mutant may also have adaptative evolution to the loss of this essential gene. Therefore, *edd* mutant showed no difference of growth to parental strain in the research by Long and Antoniewicz (2019), while some *edd* mutant had its growth decrease as mentioned in the research by Shimaoka et al. (2005) and this study.

In the presence of various concentrations (2.5-20 g/L) of glucose in LB medium, more effects on the decline of *E. coli* mutants' growth were noticeably spotted. Instead of boosting bacterial growth, glucose concentrations had a negative effect on the growth of *E. coli* strain JW18401 and JW39851. The maximum OD_{600} drastically dropped approximately to 1.7 in both *E. coli* strain JW18401 and JW39851 (Figure 21). Their specific growth rate dropped to 0.20-0.22 h^{-1} while the doubling time inversely increased to 0.08 h in the mutant strains, compared to the specific growth rate of 0.23-0.24 h^{-1} and the doubling time of 0.07-0.08 h in the condition where glucose was absent. It was worth noting that the differentiation in bacterial growth had no direct variation to the amount of glucose, meaning that the maximum OD_{600} of *E. coli* strain JW18401 and JW39851 peaked at similar value in all concentrations of glucose. It was hypothesized that there was a metabolic perturbation caused in cell proliferation process and decreased cell growth in *E. coli* strain JW18401 and JW39851 specifically when glucose was supplied as a carbon source. Unlike *E. coli* strain K12, glucose concentrations had significant effect on the growth of *E. coli* strain JW18401 and JW39851 ($P < 0.05$).

The influence of glucose on the growth of *E. coli* strain JW18401 and JW39851 could be explained by understanding of central glucose metabolic pathway (Figure 13). The EMP pathway is well known as the primarily and preferred pathway for glucose catabolism, rather than the EDP and PPP pathway (Sánchez-Pascuala et al., 2017). Phosphoglucose isomerase (*pgi*) plays an important role in providing intermediates to the EMP pathway. According to Canonaco et al. (2001), the metabolic flux ratio (METAFoR) analysis revealed that the PPP pathway was developed as a primary route for glucose metabolism in *pgi* mutant (Canonaco et al., 2001). Although the *pgi* mutant remained survival, excess NADPH production from the re-routing through the PPP was found to disturb the metabolic network, leading to over 80% reduction in cell growth (Charusanti et al., 2010). In addition, quantification of intracellular NADPH supported the idea that growth of *pgi* mutant decreased due to the excess amount of intracellular NADPH (Ahn et al., 2011; Hua et al., 2003). Ahn et al. (2011) reported flux analysis of NADPH regeneration per consumption in *pgi* mutant in three types of carbon source in medium, glucose,

fructose and a mixture of glucose and fructose (Figure 22). It was found that the ratio of NADPH formation to consumption in *pgi* mutant feeding on glucose climbed up to over 1.5 mol NADPH per mol glucose while the ratio of NADPH formation to consumption in parental strain and in *pgi* mutant feeding on fructose and mixture carbon remained below 1.0 mol NADPH per mol glucose (Ahn et al., 2011).

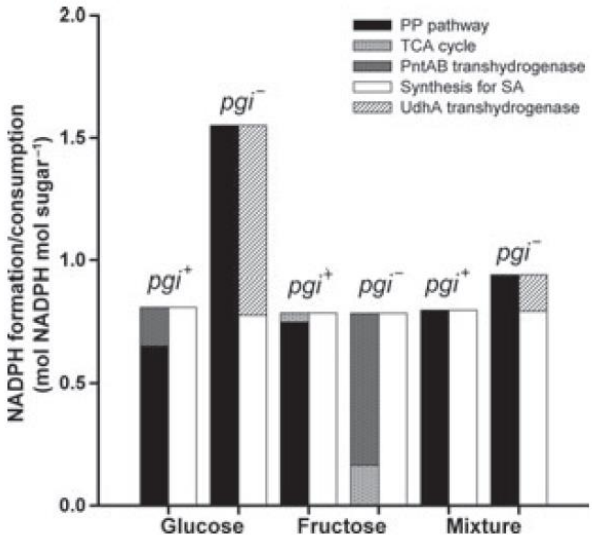

Figure 22 NADPH regeneration while minimization of total sum of reaction flux under the shikimic acid production fixed at maximum theoretical yields using the genome-scale *in silico* model of *Escherichia coli* (Ahn et al., 2011)

Moreover, gluconate-6-phosphate dehydratase (*edd*) is crucial for EDP pathway. Although there was no clear evidence on effect of *edd* mutant in *E. coli*, Meyer et al. (2018) provided the evidence proving that disruption of EDP pathway resulted in accumulation of ribulose 5-phosphate (Ru5P) via PPP pathway by 6-phosphogluconate dehydrogenase (*gnd*) (Meyer et al., 2018). According to Shimaoka et al. (2004), the *edd* mutant promoted inosine production compared to parental strain due to the availability of Ru5P produced via PPP (Shimaoka et al., 2005).

Therefore, it can be concluded that the inactivation of *edd* gene in *E. coli* strain JW18401 and *pgi* gene in *E. coli* strain JW39851 resulted in metabolic redirection and triggering the pentose phosphate pathway, a main source of intracellular NADPH. By supplying glucose as a precursor, reducing power imbalance was created due to large amount of accumulated NADPH leading to decline of *E. coli* mutants' growth rate. Remarkably, the growth of *E. coli* strain JW39851 was recorded greater than *E. coli* strain JW18401. Even though the EDP pathway is acclaimed as an inactive pathway in *E. coli* feeding on glucose, this data designated the involvement of EDP pathway in glucose metabolism. It was inferred that the fall of mutant strains in the presence of glucose affected due to metabolic perturbation from gene deletion.

4.3 Construction of expression vector for PHB biosynthesis

Genomic DNA used as the template in amplification of *phaCAB* operon was extracted from *C. necator* strain A-04. The extracted genomic DNA exhibited high quality DNA as the band showed intense color without degrading DNA. Extracted genomic DNA was further used in PCR reaction described in 3.9. Since contamination of phenol used in the extraction process could inhibit the DNA polymerase (Unger et al., 2019) and phenol contamination was undetectable on agarose gel electrophoresis, it was recommended to repeat the stratification during the genomic DNA extraction with chloroform at least 3 times. Another PCR trouble shooting could be occurred due to excess concentration of the template. Therefore, PCR optimization was recommended. As a result, an approximately 4.7-kb PCR product was achieved from PCR reaction (Figure 23). PCR product was later purified using TIANquick Midi Purification kit according to manufacturer instructions. The purified PCR product showed similar size to the unpurified PCR product with lower concentration when loaded in agarose gel at the equivalent amount. The purified PCR product was later ligated to linear pBluescript II SK digested with *Eco*RV. The ligation reaction was next transformed into a chemical competent *E. coli* and selected by blue-white screening method. The positive clone was confirmed by colony PCR and verification by PCR.

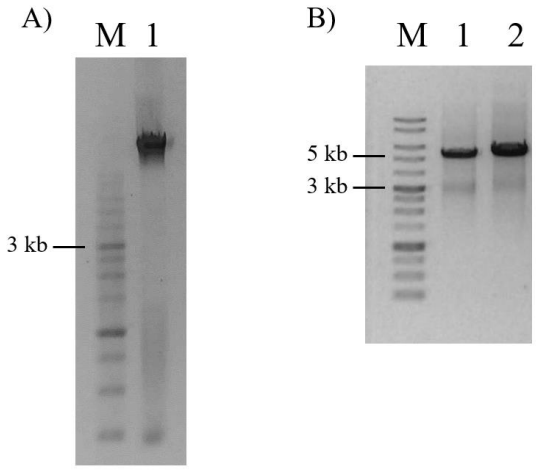

Figure 23 Gel electrophoresis displaying (A) Lane M, 1 kb marker, Lane 1, extracted and purified genomic DNA of *C. necator* strain A-04 (B) Lane M, 1kb marker, Lane 1, purified PCR product of pha*CAB*$_{A-04}$ and Lane 2, unpurified PCR product of pha*CAB*$_{A-04}$

The successful plasmid was isolated using FavorPrep^{TM} Plasmid DNA Extraction kit. Later, the isolated plasmid was confirmed by restriction enzyme digestion with *Bam*HI and *Eco*RI (Figure 24). Digestion of the recombinant plasmid with *Eco*RI yielded the linear 7.7-kb DNA. Since there was a *Bam*HI site on each site of the PCR product, digestion of the recombinant plasmid with *Bam*HI resulted in two bands with the length of 4.7 and 3 kb, responding to the size of phaCAB$_{A-04}$ and pBluescript II SK respectively. The result of restriction enzyme digestion with *Bam*HI and *Eco*RI supported the correct cloning and ligation procedure. Finally, pBSK*CAB*$_{A-04}$ was successfully constructed and sequencing. The sequence of *phaCAB* operon in pBSK*CAB*$_{A-04}$ (Appendix 5) was aligned with sequences of β-ketothiolase (phaA), acetoacetyl-CoA reductase (phaB) and PHA synthase (phaC) (Accession number: FJ897461, FJ897462 and FJ897463) from *C. necator* strain A-04 (Visetkoop, 2009). Pairwise alignment showed 100% similarity of amplified *phaCAB* operon from *C. necator* strain A-04 to mentioned sequences in database. The constructed pBSK*CAB*$_{A-04}$ was further used for PHAs biosynthesis in recombinant *E. coli.*

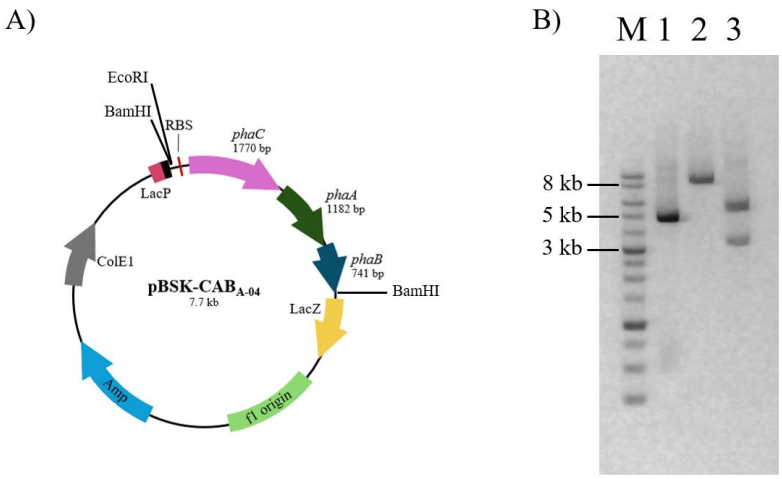

Figure 24 Plasmid map of pBSK*CAB*$_{A\text{-}04}$ (A) Restriction enzyme analysis of pBSK*CAB*$_{A\text{-}04}$ by *Bam*HI and *Eco*RI (B) Gel electrophoresis displaying restriction enzyme digestion, Lane M, 1 kb marker, Lane 1, undigested pBSK*CAB*$_{A\text{-}04}$, Lane 2, *Eco*RI-digested pBSK*CAB*$_{A\text{-}04}$, Lane 3, *Bam*HI-digested pBSK*CAB*$_{A\text{-}04}$,

A previous study suggested that PHAs yield was markedly higher in *E. coli* harboring high-copy-number plasmid, indicating that the level of PHA synthase gene expression is crucial for PHAs production (Wu et al., 2016). Lu et al. (2005) also reported that the use of high copy number plasmid for *phaJ* expression significantly increased the PHAs production to over 20% of biomass (Lu et al., 2005). The number of copies of a plasmid determines the gene dosage accessible for expression, which also leads generally to a high productivity (Friehs, 2004). In addition, the number of copies of a plasmid also affects DNA segregation in cell division (Hsu & Chang, 2019; Ilhan et al., 2018). High copy number plasmid (more than 15 copies per cell) tends to segregate randomly, therefore each daughter cell receives at least one plasmid through random diffusion (Million-Weaver & Camps, 2014). In this work, pBluescript II (SK+), with ColE1 as origin of replication and a copy number of 500-700 per chromosome (Mayer, 1995), was chosen as an expression vector. We aimed to construct *E. coli* with the ability to effectively produce PHAs and utilize cheap carbon sources such as agricultural and biodiesel waste to reduce the production cost of PHAs. Since industrial wastes as carbon sources may contain numerous kinds of impurities and physical properties such as dynamic viscosity and density may reduce

the homogeneity of the media, expression of the PHAs biosynthesis operon of *C. necator* strain A-04 using its native promoter was introduced. With this profound purpose, PHAs biosynthesis operon was expressed in *E. coli* without using additional inducer.

To compare the difference of amino acid sequence of pha*CAB* operon amplified from *C. necator* strain A-04 and H16, predicted amino acid sequence of *phaC*, *phaA* and *phaB* were first translated into amino acid sequence using EXPASY bioinformatics tool. After that, amino acid sequences were used for pairwise alignment between *C. necator* strain A-04 and H16. The result showed that $phaC_{A\text{-}04}$ was 99% similar to $phaC_{H16}$. The difference was the amino acid at position 122 of $phaC_{A\text{-}04}$ was proline where in $phaC_{H16}$ was leucine (Napathorn et al., 2021; Visetkoop, 2009) (Figure 12).

4.4 PHB biosynthesis in recombinant *Escherichia coli* harboring pBSK$CAB_{A\text{-}04}$ using glucose as a sole carbon source

E. coli strain K12, JW18401 and JW39851 were first introduced with pBSK$CAB_{A\text{-}04}$ by chemical transformation to yield *E. coli* strain K12-pBSK$CAB_{A\text{-}04}$, JW18401-pBSK$CAB_{A\text{-}04}$ and JW39851-pBSK$CAB_{A\text{-}04}$. Primary experiment was performed thoroughly to verify the expression of *phaCAB* operon from *C. necator* strain A-04 following procedure from literature reviews. After 24 hours of cultivation, *E. coli* strain K12-pBSK$CAB_{A\text{-}04}$, JW18401-pBSK$CAB_{A\text{-}04}$ and JW39851-pBSK$CAB_{A\text{-}04}$ with PHAs were harvested by centrifugation and analyzed for PHAs accumulation by gas chromatography (GC). The chromatograms of standard PHB and PHB extracted from *E. coli* strain K12-pBSK$CAB_{A\text{-}04}$, JW18401-pBSK$CAB_{A\text{-}04}$ and JW39851-pBSK$CAB_{A\text{-}04}$ were represented in Figure 25.

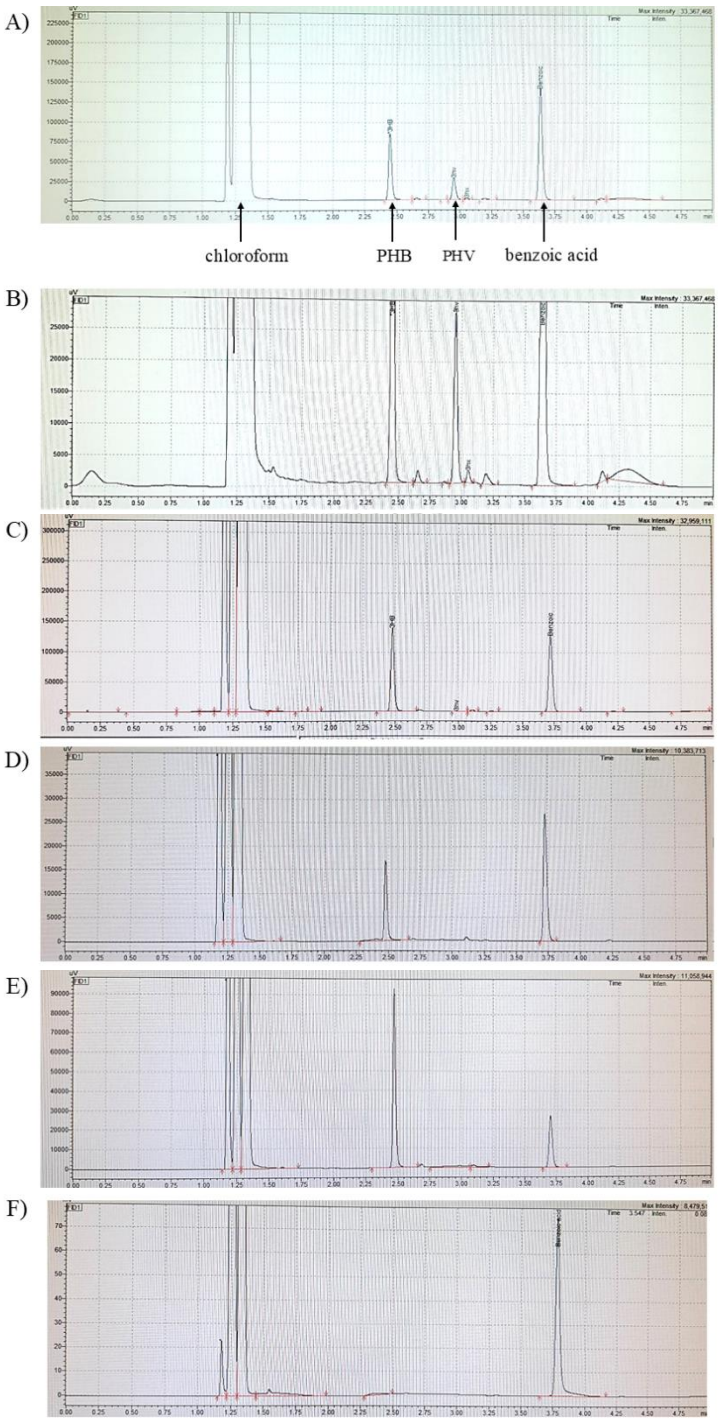

Figure 25 Chromatogram obtained from gas chromatography (GC) of (A) 1 g/L P(3HB-co-3mol%HV) standard, (B) 3 g/L P(3HB-co-3mol%HV) standard, PHB accumulation from *E. coli* strain (C) K12-pBSK*CAB*$_{A-04}$, (D) JW39851-pBSK*CAB*$_{A-04}$, (E) JW18401-pBSK*CAB*$_{A-04}$ and (F) K12-pBSK cultivated at 37^{o}C, 200 rpm in LB medium supplemented with 20 g/L glucose for 24 hours. Benzoic acid was used as an internal standard.

To determine PHAs composition, PHAs are converted into fatty acid methyl esters (FAMEs) derivatives before subjected to GC analysis. Saponification followed by methylation is a classical method of FAMEs preparation from glycerolipids and sterol esters (Ichihara & Fukubayashi, 2010). The conversion of fatty acids into FAMEs allows PHAs more volatile and convenient to be analyzed due to many reasons including polarity and thermal stability of PHAs, peak symmetry in GC chromatogram and sample activity. PHAs, made up of hydroxyl fatty acids, are non-polar, making them difficult to analyze in GC. By converting hydroxyl fatty acids into FAMEs, the molecules become polar and can be easily detected by flame ionization detector (FID) (Salamonsen & Cole, 1977). Polarity of substances affects the FID as a result of the greater mobility of electrons compared with the positive ions in the carrier stream. In an FID electric filed, positive ions move to the upper part of the flame to the collector electrode, while negative ions remain in the flame (Salamonsen & Cole, 1977). In addition, FAMEs are thermally stable and can be eluted at a reasonable temperature without thermal decompostion (Fisk et al., 2014). It was also reported that FAMEs improve peak symmetry and decrease sample activity, which provides more accurate data analysis (Quero-Jiménez et al., 2020).

To quantify PHAs in bacterial samples, cell pellets were used to perform methyl esterification to produce FAMEs, followed by subjected to GC analysis. A commercial standard P(3HB-*co*-3mol%3HV) (ENMAT Y1000, Tianan, China) was used as an external standard in GC to determine amounts of PHAs in bacterial cells. Benzoic acid at the concentration of 0.5 g/L was used as an internal standard to improve the precision of results and minimize the effects of random and systematic errors during analysis in all experiments. Standard curves of PHB and PHV were illustrated to determine PHAs concentration (Appendix 6). As a result, representative chromatogram of the standard PHB and PHV exhibited a retention time for a reference standard at 2.50 and 2.90 minutes, respectively, while benzoic acid serving as an internal standard illustrated a retention time at 3.60 minutes (Figure 25). Since methanolysis of extracted samples from cultivation of *E. coli* strain K12-pBSK*CAB*$_{A\text{-}04}$, JW39851-pBSK*CAB*$_{A\text{-}04}$ and JW18401-pBSK*CAB*$_{A\text{-}04}$ feeding on glucose also shown the retention time at 2.50 minutes, it was concluded that PHB was produced due to

successful expression of *phaCAB* operon from *C. necator* strain A-04 in pBSK*CAB*$_{A-04}$ without any addition of inducer. Chromatogram of recombinant *E. coli* strain K12-pBSK did not illustrate the PHB production at retention time of 2.50 minutes, indicating that PHB accumulation of recombinant *E. coli* occurred due to the *phaCAB* operon in pBSK*CAB*$_{A-04}$. The chromatograms displayed in this study were similar to those illustrated by Flores-Sanchez et al. (2017) with small shift in retention time (Flores-Sanchez et al., 2017). The retention time in GC changes for a number of reasons including temperature, carrier gas flow rate, column, inlet pressure and variation in the sample matrix (Rood, 1997).

Samples taken from cultivation of *E. coli* strain K12-pBSK*CAB*$_{A-04}$, JW18401-pBSK*CAB*$_{A-04}$ and JW39851-pBSK*CAB*$_{A-04}$ at early stage of cultivation (2-6 hours) were also analyzed by GC and provided evidence that PHB accumulation of *E. coli* in this research was stored during its growth phase. In addition, medium used in cultivation of *E. coli* strain K12-pBSK*CAB*$_{A-04}$, JW18401-pBSK*CAB*$_{A-04}$ and JW39851-pBSK*CAB*$_{A-04}$ was LB, nutritionally rich medium. It was concluded that there was not necessary to restrict the nutrient limitation condition in cultivation of PHB producing recombinant *E. coli* used in this study. Even though nutrient depletion or stress is a common practice for PHAs production, recombinant *E. coli* is not affected by nutrient limitation and can store PHAs during its growth phase (Nitschke et al., 2011). Compare to *C. necator* strain A-04, the gene source of *phaCAB* operon, this strain requires nutrient-limited condition to switch on the PHAs biosynthesis pathway (Zhang et al., 2022). In fact, nutrient limiting condition restricts cellular growth by suppressing macromolecules biosynthesis pathway such as protein and nucleic acid to promote carbon flux to PHAs biosynthesis. Therefore, two steps cultivation for PHAs production was required in *C. necator* strain A-04 (Costa et al., 2023). Biomass production is maximized in the first phase, and PHAs production starts after setting the suitable condition in the second phase.

Even though PHAs quantification by traditional GC analysis is useful, it is also a time-consuming process. Fluorescence staining of intracellular PHAs is promising for rapid PHAs quantification because of their sensitive signals, high accuracy and time-saving procedure (Cánovas et al., 2021; Cao et al., 2022). In this experiment,

recombinant *E. coli* strain K12 was used as host strain harboring different types of plasmid including pBSK and pBSK*CAB*$_{A-04}$ with and without native promoter of *C. necator* strain A-04. Recombinant *E. coli* strain K12 harboring mentioned vectors were cultivated on LB medium supplemented with 2% glucose and 0.1% Nile red exhibited a fluorescence light. This fluorescence staining was detected as Nile red is a selective fluorescent stain for intracellular lipid. Therefore, Nile red was able to detect PHAs accumulation in bacterial cells. Moreover, the fluorescence intensity of PHAs granules in microbial cells and PHAs concentration presented high correlations (R^2 > 0.950), showing fluorescence capability for *in situ* PHAs quantification (Cao et al., 2022). As a result, *E. coli* strain K12-pBSK*CAB*$_{A-04}$ with native promoter of *C. necator* strain A-04 (number 1 and 2) showed light yellow fluorescent light after 24 hours of cultivation. While *E. coli* strain K12-pBSK*CAB*$_{A-04}$ without native promoter of *C. necator* strain A-04 (number 3-7) and *E. coli* strain K12-pBSK (number 8) illustrated some fluorescent light with lower intensity than *E. coli* strain K12-pBSK*CAB*$_{A-04}$ with native promoter of *C. necator* strain A-04 (number 1 and 2). Due to its lipophilic nature, Nile red can migrate into cell membrane and bind unspecifically to other cell structures which also visible with fluorescence dye. This result illustrated that expression of pBSK*CAB*$_{A-04}$ with native promoter of *C. necator* strain A-04 in *E. coli* led to PHAs accumulation while expression of pBSK*CAB*$_{A-04}$ without native promoter of *C. necator* strain A-04 did not result in PHAs accumulation. The result correlated with PHAs quantification by GC, in which only *E. coli* harboring pBSK*CAB*$_{A-04}$ with native promoter of *C. necator* strain A-04 can accumulate PHB and quantify by GC analysis. Moreover, the excitation and emission wavelength of Nile red have a wide range of 60 nm according to the relative hydrophobicity of the environment (H.-Y. Wu et al., 2003). The emission range of Nile red is 570-630 nm, while the excitation range is 520-560 nm. This wide emission range of Nile red allows the distinguish of scl-PHAs and mcl-PHAs in intact cells based on varying emission maxima. Wu et al. (2003) reported rapid differentiation between scl-PHAs and mcl-PHAs bacteria with Nile red emission wavelengths (H.-A. Wu et al., 2003). At fixed excitation wavelength of 488 nm, scl-PHAs accumulating bacteria had a maximum emission wavelength of 590 nm while mcl-PHAs accumulating bacteria were seen at a wavelength of 575 nm.

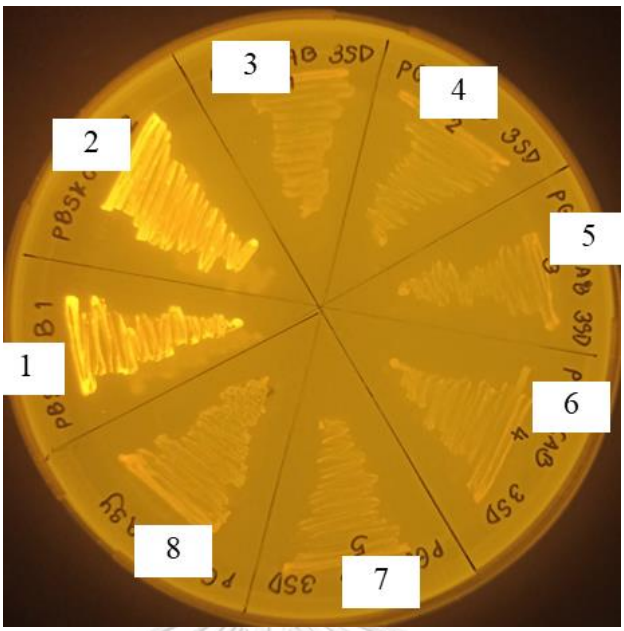

Figure 26 Nile red fluorescence staining of recombinant *E. coli* K12 (1, 2) harboring pBSK*CAB*$_{A-04}$ with native promoter of *C. necator* strain A-04, (3-7) pBSK*CAB*$_{A-04}$ without native promoter of *C. necator* strain A-04 and (8) pBSK after 24 hours of cultivation in LB medium supplemented with 2% glucose and 0.1% Nile red at 37°C

Up to date, several analytical methods for PHAs have been reported. Staining with lipophilic dyes is promising rapid PHAs quatification and visualization (Ostle & Holt, 1982; Wei et al., 2011). Due to the lipophilic nature, Sudan Black B, Nile Blue A and Nile Red can bind to the PHAs granules surrounded by lipid membranes, appearing bright granules of PHAs. Spectrophotometric methods for PHAs quantification such as fluorescence spectrometry, fourier-transform infareded spectroscopy (FTIR), high-performance liquid chromatography (HPLC), matrix-assisted laser desorption/ionization time of flight mass spectrometry (MALDI-TOF) and nuclear magnetic resonance (NMR) were established (Arcos-Hernandez et al., 2010; Korotkova et al., 1997; Meng et al., 2012). Unfortunately, those techniques can provide only quantitative information of PHAs. GC coupled with flamed ionization detector (GC-FID) is one of the most commonly-used method to identify and quantify individual PHAs components (Furrer et al., 2007). Braunegg et al. (1998) reported the first derivatization of PHB for analysis (Braunegg et al., 1998). Sulphuric acid in methanol

and hydrochloric acid in propanol were used for one-step transesterification and extraction of intracellular PHAs (Furrer et al., 2007). Identification of PHAs is done by comparing the retention times of the putative PHAs against those of analytical standards (Lee & Choi, 1995). Characterization of PHAs monomer structure can be later identified by gas chromatography-mass spectroscopy (GC-MS) analysis.

4.5 Optimization of PHB biosynthesis in recombinant *Escherichia coli* harboring pBSK*CAB*$_{A-04}$

Several parameters, such as inoculum concentrations, cultivation temperature and glucose concentrations, effecting the PHB production by recombinant *E. coli* harboring pBSK*CAB*$_{A-04}$ were investigated for optimization.

4.5.1 Cultivation temperature

Preliminary experiment on PHB production in recombinant *E. coli* JW18401-pBSK*CAB*$_{A-04}$, JW39851-pBSK*CAB*$_{A-04}$ and K12-pBSK*CAB*$_{A-04}$ in 4.4 was achieved using the condition based on literature review (Boontip et al., 2021). This result illustrated the overexpression of pBSK*CAB*$_{A-04}$ led to PHB accumulation in recombinant *E. coli*. In nature, *E. coli* JW18401, JW39851 and K12 are unable to produce PHB as these strains do not possess PHAs biosynthetic genes. When *E. coli* JW18401, JW39851 and K12 grew in LB medium supplemented with 20 g/L glucose, PHB was undetected by GC. In this experiment, the effect of temperature on PHB production was investigated. Briefly, 1%(v/v) inoculum was transferred into 50 ml LB medium supplemented with 20 g/L glucose and cultured at 30 or 37°C for 24 hours.

According to Sheu et al. (2012), PHAs synthase, a key enzyme in PHAs polymerization, from mesophile *C. necator* H16 had its specific activity of approximately 25 U/ml at 25°C. The specific activity of enzyme increased according to the rise of temperature. At 30°C, the specific activity of PhaC$_{H16}$ was 50 ± 5.2 U/ml. The specific activity of PhaC$_{H16}$ continued to increase and reached its maximum value of 70 ± 8.8 U/ml at 37°C (Sheu et al., 2012). Therefore, two different temperatures, 30 and 37 °C, were selected to use in optimization of PHAs production in *E. coli* strain JW18401, JW39851 and K12 harboring pBSK*CAB*$_{A-04}$. We observed the effect of bacterial growth in both presence and absence of glucose. As in the

condition when glucose was absent, the overall biomass of bacteria depended only on the growth of bacteria which was required for inoculum preparation. The cell dry mass (CDM), residual cell mass (RCM), consumed glucose concentration, PHB concentration and PHB content were calculated and represented in Figure 27.

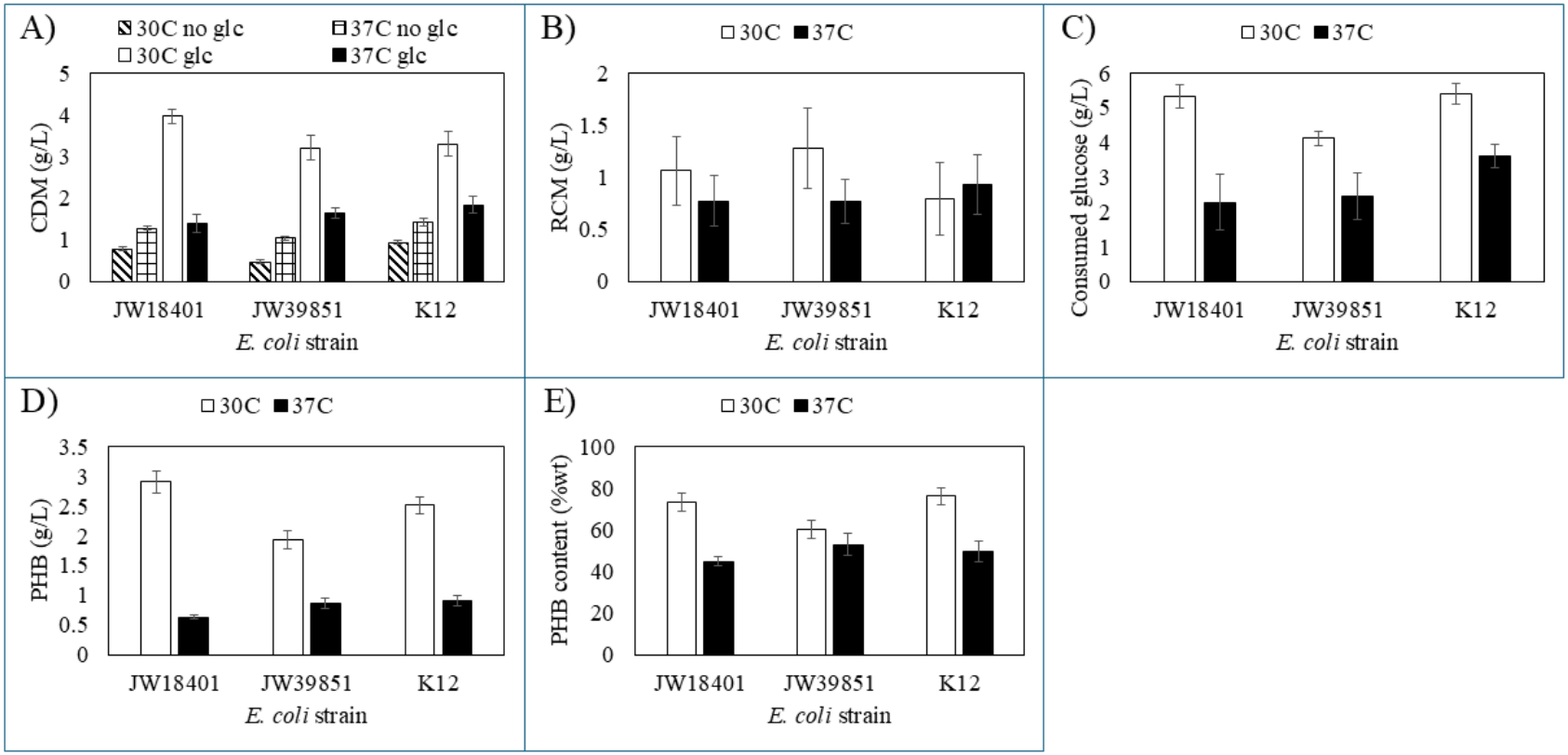

Figure 27 Effect of temperature (30 and 37℃) on (A) biomass, (B) residual cell mass, (C) consumed glucose concentration, (D) PHB concentration and (E) PHB content of *E. coli* strain JW18401, JW39851 and K12 using 1% inoculum concentration in LB medium supplemented with 20 g/L glucose and without glucose cultivated for 24 hours

In the absence of glucose in LB medium, recombinant *E. coli* JW18401-pBSK*CAB*$_{A-04}$, JW39851-pBSK*CAB*$_{A-04}$ and K12-pBSK*CAB*$_{A-04}$ did not accumulate PHB in both cultivation temperature at 30 and 37°C. As expected, the growth of *E. coli* JW18401-pBSK*CAB*$_{A-04}$, JW39851-pBSK*CAB*$_{A-04}$ and K12-pBSK*CAB*$_{A-04}$ at 37°C was better than 30°C, with the value of 1.27 ± 0.05, 1.03 ± 0.05 and 1.43 ± 0.09 g/L compared to 0.77 ± 0.05, 0.47 ± 0.05 and 0.93 ± 0.05 g/L, respectively (Appendix 7). This result was correlated with other research as 37°C is widely known as an optimum temperature for *E. coli* growth (Doyle & Schoeni, 1984; Noor et al., 2013). Nevertheless, the result illustrated that changing the cultivation temperature to 30°C had greatly affected the bacterial growth especially *E. coli* strain JW18401 and JW39851 in the medium without glucose. Therefore, temperature of 37°C was later used to prepare inoculum in all other experiments in this research.

In the presence of 20 g/L glucose, it was illustrated that cultivation of recombinant *E. coli* JW18401-pBSK*CAB*$_{A-04}$, JW39851-pBSK*CAB*$_{A-04}$ and K12-pBSK*CAB*$_{A-04}$ at 30°C significantly increased the overall biomass and PHB accumulation, compared to 37°C ($p < 0.05$). The result displayed the highest CDM of *E. coli* JW18401-pBSK*CAB*$_{A-04}$, JW39851-pBSK*CAB*$_{A-04}$ and K12-pBSK*CAB*$_{A-04}$ in the medium supplemented with glucose were noted at cultivation temperature of 30°C with the value of 3.97 ± 0.17, 3.20 ± 0.29 and 3.30 ± 0.29 g/L, respectively. On the contrary, a reduction in CDM of all strains approximately 52% was noticed at 37°C. The RCM of *E. coli* JW18401-pBSK*CAB*$_{A-04}$ and JW39851-pBSK*CAB*$_{A-04}$ cultivated in LB medium with 20 g/L glucose at 37°C reached the same value of 0.77 g/L, lower than K12 with 0.93 g/L. This result could be used to compare with the result described in 4.2, which *E. coli* strain JW18401 and JW39851 without pBSK*CAB*$_{A-04}$ exhibited extraordinarily slow growth at 37°C when glucose was supplemented in the LB medium. After incorporating the PHB biosynthesis pathway into recombinant *E. coli* strain JW18401 and JW39851, the growth of these mutants improved significantly, reaching almost the same value as the growth of *E. coli* strain K12. The dramatic increase in bacterial growth of *E. coli* strain JW18401 and JW39851 was clearly illustrated when recombinant *E. coli* JW18401-pBSK*CAB*$_{A-04}$ and JW39851-pBSK*CAB*$_{A-04}$ were cultivated at 30°C in LB medium supplemented with glucose. Interestingly, the RCM of *E. coli*

strain JW39851 was the highest, compared to other two strains. However, the RCM difference was very small with a value of less than 0.4 g/L difference.

For PHB biosynthesis, it was clearly demonstrated that *E. coli* JW18401-pBSK*CAB*$_{A-04}$, JW39851-pBSK*CAB*$_{A-04}$ and K12-pBSK*CAB*$_{A-04}$ had the maximum PHB at 30°C with PHB concentration of 2.90 ± 0.18, 1.93 ± 0.15 and 2.51 ± 0.13 g/L. respectively. More than 55% decrease of PHB concentration in all three strains was observed when *E. coli* JW18401-pBSK*CAB*$_{A-04}$, JW39851-pBSK*CAB*$_{A-04}$ and K12-pBSK*CAB*$_{A-04}$ were cultivated at 37°C. Interestingly, PHB concentration of *E. coli* JW39851-pBSK*CAB*$_{A-04}$ was lower than its parental strain K12-pBSK*CAB*$_{A-04}$. The result roughly indicated *pgi* deletion had no effect on PHB production. PHB content, the amount of PHB measured as percentage of CDM, also represented that *E. coli* JW18401-pBSK*CAB*$_{A-04}$, JW39851-pBSK*CAB*$_{A-04}$ and K12-pBSK*CAB*$_{A-04}$ could accumulate and store higher amounts of PHB at 30°C with the value of 73.2 ± 4.5, 60.2 ± 4.6 and 76.0 ± 4.0 %wt, respectively, than PHB accumulation at 37°C with the value of 44.8 ± 2.2, 52.9 ± 5.3 and 49.3 ± 4.9 %wt, respectively. The result of this study indicated that temperature had a great effect on PHB production, which may affect from enzyme activity of PHB biosynthesis. According to Sheu et al. (2012), PHA synthase of *C. necator* strain H16 (PhaC$_{H16}$) had its maximum specific activity at 37°C with the value of 70 ± 8.8 U/ml, higher than its specific activity at 30°C with the value of 50 ± 5.2 U/ml (Sheu et al., 2012). Thermal stability of PHA synthase was analyzed by incubation of PhaC$_{H16}$ in various temperatures (from 4-60°C) for 5 minutes, prior to measuring the specific activity of enzyme. Consequently, the thermal stability of PhaC$_{H16}$ declined as the temperature rose. The residual activity of PhaC$_{H16}$ remained 100% at 30°C. On the contrary, the residual activity of PhaC$_{H16}$ dropped to approximately 90% after incubation of PhaC$_{H16}$ at 37°C for 5 minutes (Sheu et al., 2012). It was concluded that the specific activity of PhaC$_{H16}$ decreased by 10% within 5 minutes of incubation under the change of temperature. Even though the specific activity of PhaC$_{H16}$ reached its maximum at 37°C, PhaC$_{H16}$ started to break down and denature. This information supported the findings in this experiment that PHB accumulation in *E. coli* JW18401-pBSK*CAB*$_{A-04}$, JW39851-pBSK*CAB*$_{A-04}$ and K12-pBSK*CAB*$_{A-04}$ were higher at 30°C due to the thermal stability of

$PhaC_{A-04}$. This is in good agreement with the correlation between the specific activity of PHA synthase and the PHB accumulation (Figure 27). Both PHB concentrations and PHB content of all three strains were peaked using 30°C as incubation temperature. Therefore, 30°C was selected as an optimum temperature for PHAs production and used in all other experiments in this research.

The starting glucose concentration used in LB medium for PHB production by *E. coli* JW18401-pBSK*CAB*$_{A-04}$, JW39851-pBSK*CAB*$_{A-04}$ and K12-pBSK*CAB*$_{A-04}$ was 20 g/L. After 24 hours of cultivation, more than 15 g/L glucose was left. It was observed that glucose concentration in *E. coli* JW18401-pBSK*CAB*$_{A-04}$, JW39851-pBSK*CAB*$_{A-04}$ and K12-pBSK*CAB*$_{A-04}$ cultivated at 30°C was higher than 37°C. The range of 4.11-5.40 g/L glucose was consumed by recombinant *E. coli* at 30°C, while 2.27-3.60 g/L glucose was assimilated by recombinant *E. coli* at 37°C. Among all three strains, *E. coli* K12-pBSK*CAB*$_{A-04}$ had the highest glucose consumption rate in both cultivation temperatures of 30°C and 37°C. As expected, *E. coli* JW39851-pBSK*CAB*$_{A-04}$, defected in EMP, had the lowest glucose consumption rate at both 30°C and 37°C conditions. As EMP is the main glucose metabolic pathway in *E. coli*, disruption of EMP causes slower glucose consumption rate in the mutant strain (Ahn et al., 2011; Charusanti et al., 2010; Guitart Font & Sprenger, 2020; Kotlarz et al., 1975). The glucose consumption rate in *E. coli* JW18401-pBSK*CAB*$_{A-04}$ was likely to K12-pBSK*CAB*$_{A-04}$ cultivated at 30°C, with the value of 5.32 ± 0.35 and 5.40 ± 0.31 g/L, respectively. However, the glucose consumption rate of *E. coli* JW18401-pBSK*CAB*$_{A-04}$ at 37°C was lower compared to K12-pBSK*CAB*$_{A-04}$. This result correlated to another research. According to Long and Antoniewicz (2019), metabolic flux response of *edd* deficiency strain exhibited no change in glucose uptake rate to the parental strain (Long & Antoniewicz, 2019).

4.5.2 Inoculum concentrations

Inoculum concentration is widely known as a crucial factor affecting cultivation time and product formation (Liu et al., 2021; Yamane, Fukunaga, et al., 1996). According to the research, low inoculum levels can lead to longer fermentation cycles and low productivity (Sood et al., 2011). While high inoculum levels can increase the production to a certain point (Sumardee et al., 2020). However, excess inoculum can lead to competition between bacteria for nutrients which can disturb the growth of bacteria. Recombinant *E. coli* strain K12-pBSK*CAB*$_{A\text{-}04}$, parental strain of JW18401 and JW39851, was selected to use as representative strain in the experiment.

To study the effect of inoculum concentrations on PHB accumulation, different amounts of inoculum (1, 3, 5 and 10%(v/v)) with $5 \times 10^6 - 9 \times 10^6$ CFU/ml were inoculated into fresh LB medium supplemented with 20 g/L glucose and cultivated at 30°C. The inoculum used in each experiment was measured by the colony forming unit (CFU) to control the amount of cell variation. The physiology of *E. coli* in LB medium was previously described by Sezonov et al. (2007) (Sezonov et al., 2007). It was suggested that *E. coli* reached the maximum OD_{600} at a certain value in LB medium and only continued to grow with the addition of glucose. Even though LB medium contains large amounts of essential inorganic nutrients, growth of *E. coli* was arrested due to insufficient amounts of carbon sources. Time course of recombinant *E. coli* strain K12-pBSK*CAB*$_{A\text{-}04}$ biomass, residual cell mass, consumed glucose concentration, PHB concentration and PHB content of each inoculum concentrations were presented in Figure 28.

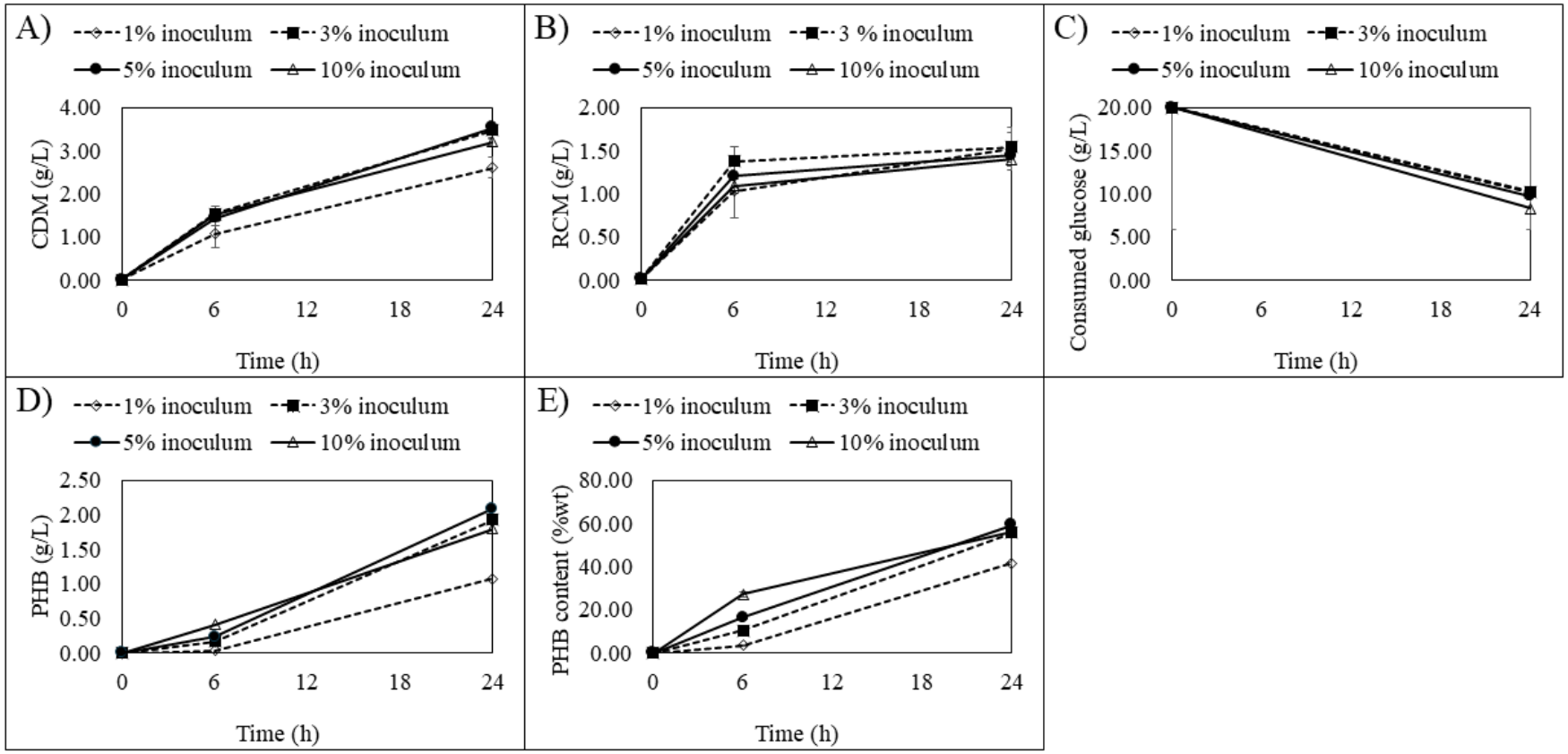

Figure 28 Effect of inoculum concentration on (A) biomass, (B) residual biomass, (C) consumed glucose concentration, (D) PHB concentration and (E) PHB content of *E. coli* strain K12-pBSK*CAB*$_{A\text{-}04}$ cultivated at 30°C in LB medium supplemented with 20 g/L glucose for 24 hours

At 6 hours of cultivation, the biomass of *E. coli* strain K12-pBSK*CAB*$_{A-04}$ using 3-10%(v/v) inoculum ranged between 1.43-1.53 g/L while using 1%(v/v) inoculum obviously represented slower growth with the value of 1.07 ± 0.31 g/L CDM (Appendix 8). Cells at early stages of cultivation were collected and analyzed for PHB accumulation. The range of 3-30%wt PHB content was obtained at 6 hours of cultivation from *E. coli* strain K12-pBSK*CAB*$_{A-04}$ using 1-10%(v/v) inoculum. Interestingly, PHB concentrations and PHB content increased accordingly to higher inoculum concentration. The highest PHB concentration was 0.41 g/L with 27.1%wt PHB content obtained at 6 hours using 10%(v/v) inoculum. This result implied that the PHB accumulation of *E. coli* strain K12-pBSK*CAB*$_{A-04}$ was growth-associated.

At 24 hours of cultivation, the biomass obtained from 3 and 5%(v/v) inoculum concentration were 3.47 ± 0.17 and 3.53 ± 0.13 g/L, respectively. Among all four concentrations of inoculum, 1% (v/v) inoculum concentration had the lowest CDM of 2.60 ± 0.25 g/L. While using 10% (v/v) inoculum resulted in lower CDM compared to 3 and 5%(v/v) inoculum, the CDM displayed was higher than 1%(v/v) inoculum, with the value of 3.20 ± 0.08 g/L. The RCM of 1-10%(v/v) inoculum concentrations had a very tight range of 1.4-1.5 g/L, indicating no change in overall biomass accumulation of bacteria. Hence, the change of CDM in all conditions depended on only PHB concentration. For PHB accumulation, using 1%(v/v) inoculum gave the lowest PHB concentration with the value of 1.08 ± 0.02 g/L and 41.5%wt PHB content at 24 hours of cultivation. The highest PHB concentration was observed by using 5%(v/v) inoculum with the value of 2.09 ± 0.03 g/L and maximum PHB content of 59.2%wt. Using 5%(v/v) inoculum concentration represented the best condition with the highest CDM and PHB concentration among all at 24 hours. Statistical analysis by two ways ANOVA revealed that inoculum size had significant differences to CDM and PHB accumulation ($P < 0.05$).

Total consumed glucose by *E. coli* strain K12-pBSK*CAB*$_{A-04}$ in this experiment ranged 9.73-11.75 g/L. The consumption of glucose increased accordingly to the increase of inoculum concentration, indicating the increase of overall production process affected by inoculum concentration (Sumardee et al., 2020).

Fermentation kinetics parameters were calculated to distinguish each condition and evaluated the best condition for PHB production (Table 17). In terms of cell production, using 1 and 3%(v/v) inoculum led to maximum CDM yield of 0.16 g CDM per g glucose with the maximum RCM yield of 0.2 g RCM per g glucose. The decrease in CDM and RCM was observed in conditions using 5 and 10%(v/v) inoculum. Using 5%(v/v) inoculum resulted in the maximum CDM yield of 0.14 g CDM per g glucose, while using 10%(v/v) inoculum illustrated the lowest CDM yield of 0.12 g CDM per g glucose. In addition, the maximum RCM of 5 and 10%(v/v) inoculum reached 0.1 g RCM per g glucose, lower than using 1 and 3%(v/v) inoculum. For PHB production, volumetric PHB productivity of 3, 5 and 10%(v/v) were equivalent with the value ranged 0.07-0.09 g/L·h while using 1%(v/v) inoculum had 0.05 g/L·h PHB productivity. The maximum PHB yield between 3 and 5%(v/v) inoculum were very close with the value of 0.19 and 0.20 g PHB per g glucose, respectively. Even the volumetric PHB productivity of the condition using 10%(v/v) inoculum was almost similar to 3 and 5%(v/v) inoculum, the PHB yield was as low as 0.15 g PHB per g glucose. The lowest PHB yield was displayed by using 1%(v/v) inoculum with 0.11 g PHB per g glucose.

This result could be explained that lower concentration of inoculum might inhibit the growth of suspension cultures as bacteria requires a certain initial density of cells at an optimum concentration for further growth in the medium (Gay et al., 1996; Gorret et al., 2004; Jeff Sumardee et al., 2020). Also, previously studies displayed higher inoculum led to competition between bacteria for nutrients, resulting in lower biomass of bacteria (Bidlas et al., 2008; M. E. Martínez et al., 2023). Higher inoculum size could also lead to nutrient depletion within short period of time (Liu et al., 2021; Saad & Abd Karim, 2016). Inoculum concentrations only affected the PHB biosynthesis rate and the length of adaptative phase of bacteria. According to Robinson et al. (2001), the increase of inoculum size shortens the cultivation period as it decreases the length of lag phase of microorganisms (Robinson et al., 2001). Nevertheless, inoculum size had no effect on the overall biomass production of bacteria (Ferran et al., 2007; Morrissey & George, 1999). By considering the maximum PHB concentration, PHB content, volumetric PHB

productivity and PHB yield, the inoculum concentration of 5%(v/v) was selected and used in further experiments (0.5-5%).

Table 17 Fermentation kinetics of PHB accumulation by *E. coli* strain K12 cultivated at 30°C using 20 g/L glucose as a sole carbon source at 24 hours of cultivation varying inoculum concentraion

Inoculum concentration	1%	3%	5%	10%
Cell production				
Maximum CDM (g/L)	2.60 ± 0.25^{a}	3.47 ± 0.17^{b}	3.53 ± 0.13^{b}	3.20 ± 0.08^{b}
Maximum CDM yield (g CDM/ g glucose)	0.16	0.16	0.14	0.12
Maximum RCM (g/L)	1.52 ± 0.25	1.54 ± 0.17	1.44 ± 0.12	1.40 ± 0.08
Maximum RCM yield (g RCM/ g glucose)	0.2	0.2	0.1	0.1
PHB production				
Maximum PHB concentration (g/L)	1.08 ± 0.02^{c}	1.93 ± 0.04^{d}	2.09 ± 0.03^{e}	1.80 ± 0.02^{f}
Volumetric productivity (g/L·h)	0.05	0.08	0.09	0.07
Maximum PHB yield (g PHB/g glucose)	0.11	0.19	0.20	0.15
Maximum PHB content (%wt)	41.5 ± 0.8	55.5 ± 1.2	59.2 ± 0.7	56.2 ± 0.6

Results are expressed as mean ± SD (n = 3)

The different superscript letters within the same column are significantly different at $P < 0.05$

4.5.3 Glucose concentrations

Glucose is a common raw material for the industrial production of PHAs, along with other saccharides, alkanes, alkanoic acids and alcohols (Anderson & Dawes, 1990; G.-Y. A. Tan et al., 2014). Glucose is an easy-to-use carbon which promotes great growth of bacteria and encourages higher PHAs production. However, there is an important advantage in using glucose as a carbon source in PHAs production. The conversion yield of glucose to PHAs is ranging between 0.3-0.5 g PHAs per g glucose (Jiang et al., 2016; Kim et al., 1994). Several types of carbon sources have been proposed with greater conversion yield for PHAs production. Using volatile fatty acids led to over 0.72 g PHB per g substrate of co-fermentation (Li et al., 2020). Production of PHB from *C. necator* from bean oil with the yield of 0.76 g/g was also reported (Zou et al., 2018). However, we aimed to study the effect of two main glucose metabolism disruption in *E. coli* on PHB production. Since glucose had a great effect of carbon assimilation activity and growth rate on mutants, we chose glucose as a sole carbon source in this experiment.

The effect of different concentrations of glucose (10, 20, 30 and 40 g/L) on PHB production was examined in *E. coli* strain K12 (Figure 29). By using 10 g/L glucose, maximum CDM of 2.87 ± 0.05 g/L with PHB content of 26.5%wt was obtained in 24 hours of cultivation (Appendix 9). The PHB concentration from 10 g/L glucose by *E. coli* strain K12-pBSK*CAB*$_{A\text{-}04}$ was as low as 0.76 g/L. Addition of glucose concentration from 10 to 20 and 30 g/L resulted in significant increase of PHB concentration at 24 hours to 1.20 and 1.33 g/L, respectively. This increase of PHB concentration by addition of glucose reflected insufficient amounts of glucose for PHB production at 10 g/L. CDM, PHB concentration and PHB content of *E. coli* strain K12-pBSK*CAB*$_{A\text{-}04}$ cultivated in 20 and 30 g/L glucose had similar value. The RCM of both conditions was 1.47 g/L with 45 and 47.6%wt PHB content. As expected, CDM at 40 g/L glucose was the lowest with the value of 2.07 ± 0.13 g/L at 24 hours. The PHB concentration and PHB content were 0.44 ± 0.03 g/L and 21.4%wt when 40 g/L glucose was supplemented.

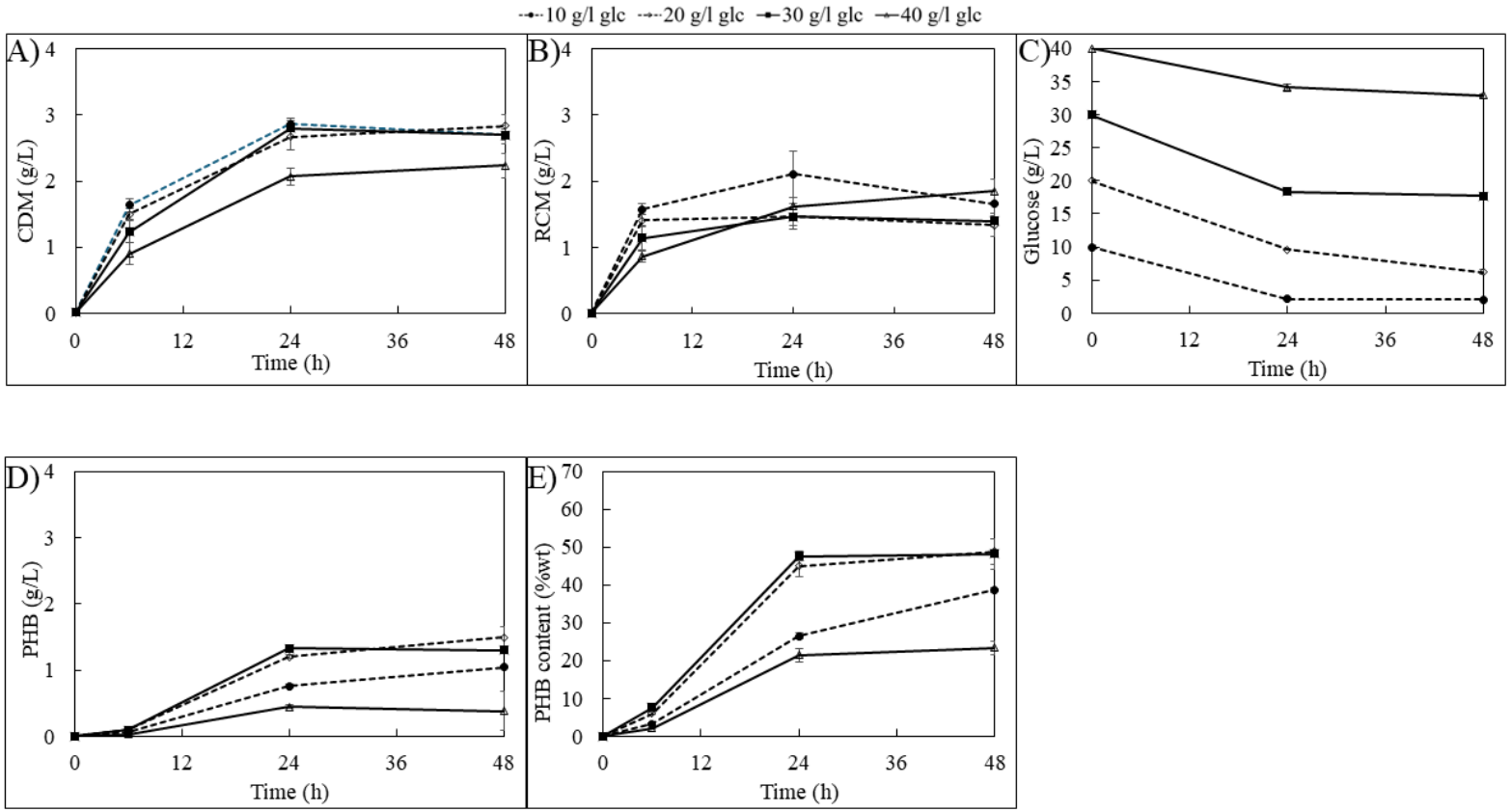

Figure 29 Effect of glucose concentrations on the (A) CDM, (B) RCM, (C) consumed glucose concentration, (D) PHB concentration and (E) PHB content of *E. coli* strain K12-pBSK*CAB*$_{A\text{-}04}$ cultivated using 5%(v/v) inoculum at 30°C in LB medium supplemented for 48 hours

After 48 hours of cultivation, the maximum CDM and PHB concentration were observed when *E. coli* strain K12-pBSK*CAB*$_{A\text{-}04}$ was cultivated using 20 g/L with the value of 2.83 ± 0.17 and 1.50 ± 0.17 g/L, respectively. The PHB content reached its peak at 48.9%wt from condition using 20 g/L glucose, which was comparable to the PHB content using 30 g/L glucose.

Fermentation kinetics parameters were calculated to observe the efficiency of PHB production in each condition (Table 18). In terms of biomass production, 10 and 40 g/L glucose gave the highest RCM with the maximum RCM yield of 0.3 g RCM per g glucose. The RCM yield of PHB production from 20 and 30 g/L glucose was 0.1 g RCM per g glucose. Although RCM yield in 20 and 30 g/L glucose was low, the maximum PHB yield in these conditions were 0.12 and 0.11, respectively, with the maximum volumetric productivity of 0.05 and 0.06 g/L·h. The PHB yield obtained from the condition in which 40 g/L glucose was used was only 0.08 g PHB/g glucose. The result indicated a biological phenomenon of catabolite repression by glucose in which high concentration of glucose downregulates gene expression and influences nutrient uptake and product formation of bacteria (Nair & Sarma, 2021). Although at 20 and 30 g/L glucose gave similar results, approximately 18 g/L glucose was left in the medium starting from 30 g/L glucose at the end of fermentation. To consider cost-effective system, glucose concentration of 20 g/L was selected to use in further experiments. The result demonstrated that different glucose concentrations had affected both CDM and PHB concentration significantly ($P < 0.05$).

Table ***18*** Fermentation kinetics of PHB accumulation by *E. coli* strain K12 cultivated at 30°C using different concentrations of glucose as a sole carbon source at 48 hours of cultivation

Glucose concentration	10 g/L	20 g/L	30 g/L	40 g/L
Maximum CDM (g/L)	2.87 ± 0.05[a]	2.83 ± 0.17[a]	2.80 ± 0.14[a]	2.23 ± 0.19[b]
Maximum RCM (g/L)	2.11 ± 0.36	1.47 ± 0.19	1.47 ± 0.14	1.85 ± 0.17
Maximum RCM yield (g RCM/ g glucose)	0.3	0.1	0.1	0.3
Maximum PHB concentration (g/L)	1.04 ± 0.02[c]	1.50 ± 0.17[d]	1.33 ± 0.02[d]	0.44 ± 0.03[e]
Volumetric productivity (g/L·h)	0.03	0.05	0.06	0.02
Maximum PHB yield (g PHB/g glucose)	0.10	0.12	0.11	0.08
Maximum PHB content (%wt)	38.7 ± 0.6	48.9 ± 3.5	48.2 ± 3.9	23.3 ± 1.8

Results are expressed as mean ± SD (n = 3)

The different superscript letters within the same column are significantly different at $P < 0.05$

4.6 Effect of *pgi* and *edd* gene deletion on PHB production in recombinant *E. coli* harboring pBSK*CAB*$_{A-04}$

In the previous experiments, we illustrated the expression of *phaCAB* operon from *C. necator* strain A-04 to produce PHB in recombinant *E. coli*. When *E. coli* JW39851, JW18401 and K12 were cultivated in LB medium supplemented with glucose, there was no PHB accumulation in *E. coli* (Figure 21). Supplementation of glucose to *E. coli* strain K12 proved no significant change of bacterial growth in LB medium. On the contrary, supplementation of glucose to *E. coli* strain JW39851 and JW18401 illustrated negative effect on the growth of both strains. *E. coli* strain JW39851 and JW18401 growth decreased significantly in the presence of glucose in the LB medium. We hypothesized that the decrease in the growth of *E. coli* strain JW39851 and JW18401 resulted from the increase of intracellular NADPH via the activation of pentose phosphate pathway (Ahn et al., 2011; Hua et al., 2003) (Figure 22). Metabolic flux analysis revealed excess amount of NADPH was produced via PPP. In addition, *pntAB* transhydrogenase, responsible for NADPH production, activity decreased significantly in the mutant strain. This finding indicated the switching off of *pntAB* transhydrogenase activity as the enzyme was not essential in the time. Moreover, *udhA* transhydrogenase, responsible for NADPH utilization and maintenance the balance of NADPH pool, activity was activated (Ahn et al., 2011; Charusanti et al., 2010; Hua et al., 2003). It indicated the high amount of NADPH in bacterial cells, so *E. coli* activated the NADPH utilizing genes to reduce the excess amount of NADPH.

The excess amounts of intracellular NADPH can be harmful to cells as it induces reductive stress and leads to reactive oxygen species (ROS) generation in an inefficient respiration (Ray et al., 2012). Bernet et al. (2014) reported the increase of NADPH by deletion of hydrogenases in the hypoxic condition resulted in cell death in mycobacteria (Berney et al., 2014). Direct and indirect of reductive and oxidative stress produced ROS-mediated damaging of nucleic acids, proteins and lipids, leading to slow growth rate of bacteria or cell death (Berridge et al., 2023). Interestingly, bacteria capable of producing large amounts of NADPH could represent as an effective host for PHAs production. As EMP and EDP was disrupted in *E. coli* strain

JW39851 and JW18401, respectively, several evidence proved more carbon flow through the PPP in EMP- or EDP-disrupted mutant (Canonaco et al., 2001; Meyer et al., 2018). We employed the use of *E. coli* strain JW39851 and JW18401 as a host for PHAs production to increase productivity and yield of PHAs due to availability of NADPH of these mutants.

The optimization condition of PHB production in recombinant *E. coli* harboring pBSK*CAB*$_{A\text{-}04}$ was investigated in 4.5. To settle the optimized condition, preculture was prepared by cultivating *E. coli* strain JW39851-pBSK*CAB*$_{A\text{-}04}$, JW18401-pBSK*CAB*$_{A\text{-}04}$ and K12-pBSK*CAB*$_{A\text{-}04}$ in LB medium at 37°C for 18 hours. Then 5%(v/v) inoculum with $5 \times 10^6 - 9 \times 10^6$ CFU/ml of *E. coli* strain JW39851-pBSK*CAB*$_{A\text{-}04}$, JW18401-pBSK*CAB*$_{A\text{-}04}$ and K12-pBSK*CAB*$_{A\text{-}04}$ were transferred into LB medium supplemented with 20 g/L glucose and cultivated at 30°C for 48 hours. Time courses of PHB production by *E. coli* strain JW39851-pBSK*CAB*$_{A\text{-}04}$, JW18401-pBSK*CAB*$_{A\text{-}04}$ and K12-pBSK*CAB*$_{A\text{-}04}$ were represented in Figure 30.

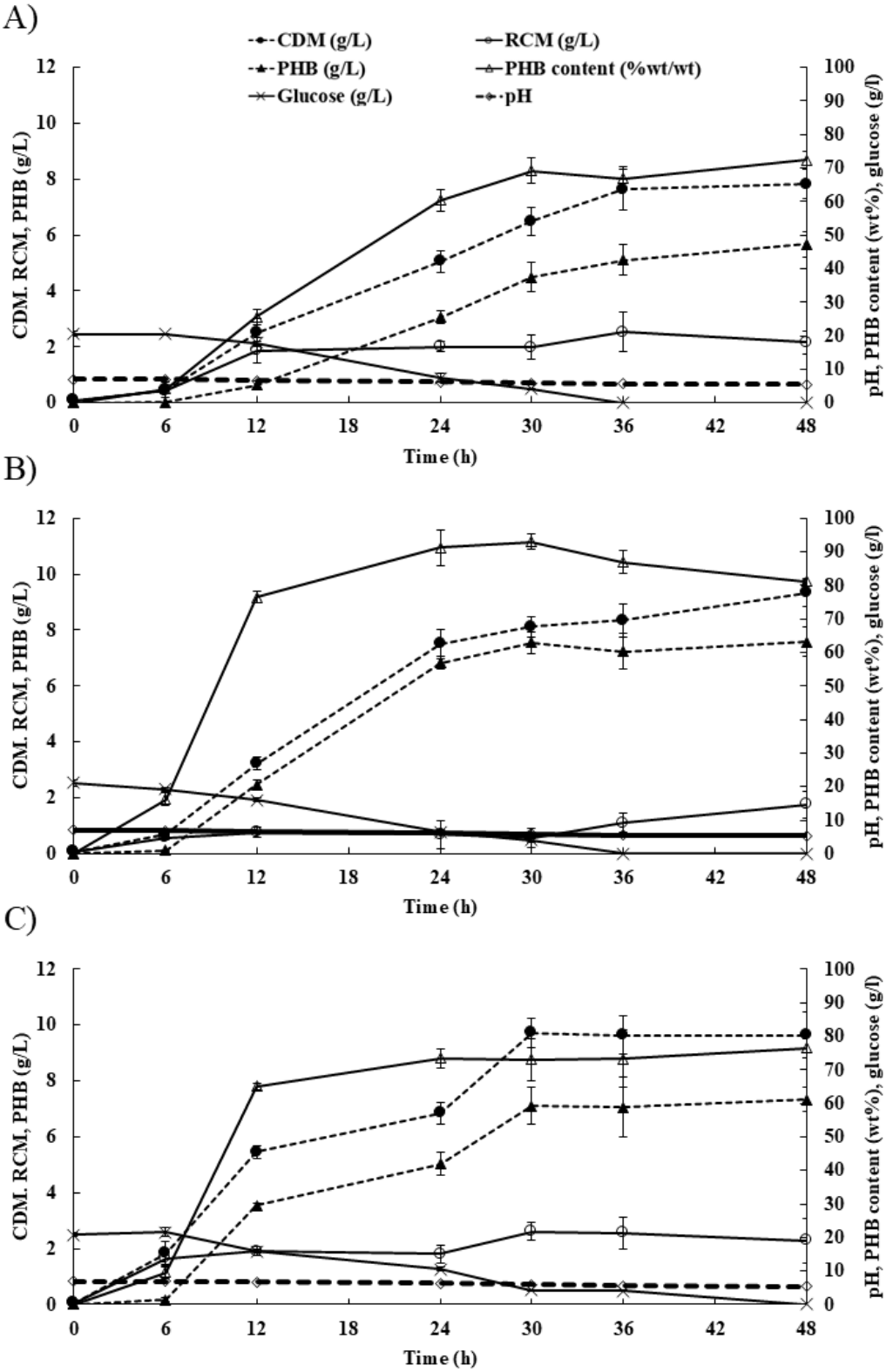

Figure 30 Time course of PHB production from recombinant *E. coli* strain (A) JW39851-pBSK*CAB*$_{A\text{-}04}$, (B) JW18401-pBSK*CAB*$_{A\text{-}04}$ and (C) K12-pBSK*CAB*$_{A\text{-}04}$ cultivated at 200 rpm, 30°C for 48 hours in LB medium supplemented with 20 g/L glucose as a sole carbon source in flask scale production.

The parental *E. coli* strain K12-pBSK*CAB*$_{A-04}$ cultivated in LB medium supplemented with 20 g/L glucose at 30°C had its CDM and RCM of 6.85 ± 0.38 and 1.81 ± 0.33 g/L at 24 hours. The PHB production by *E. coli* strain K12-pBSK*CAB*$_{A-04}$ increased up to 5.04 ± 0.42 g/L with the PHB content of 73.5%wt at 24 hours. The biomass and PHB accumulation of *E. coli* strain K12-pBSK*CAB*$_{A-04}$ peaked at 48 hours with the value of 9.64 ± 0.83 and 7.34 ± 0.44 g/L, respectively. Interestingly, PHB content of *E. coli* strain K12-pBSK*CAB*$_{A-04}$ did not change much after 24 hours and remained constant with the range of 73.5-76.5%wt, indicating stationary phase of the PHB production in the bacteria. The volumetric PHB productivity of *E. coli* strain K12-pBSK*CAB*$_{A-04}$ supported the allusion with the value of 0.21 g/L·h at 24 hours and remained in the range of 0.20-0.24 g/L·h until 36 hours, followed by the drop of volumetric PHB productivity to 0.15 g/L·h. The PHB production by *E. coli* strain K12-pBSK*CAB*$_{A-04}$ in this study was comparable amount to many reports. Napathorn et al. (2021) reported PHB accumulation by recombinant *E. coli* expressing *phaCAB* operon under arabinose-inducible promoter and cold shock inducible promoter with over 93%wt PHB content and 5.6 g/L PHB concentration within 24 hours (Napathorn et al., 2021). In addition, Hiroe et al. (2012), reported the effect of rearrangement of *phaC*, *phaA* and *phaB* in *phaCAB* operon in recombinant *E. coli* with the highest PHB of 11.2 g/L in 72 hours of cultivation (Hiroe et al., 2012). The type of promoter in gene regulation used in these mentioned research are categorized as strong promoter while *phaC* promoter in pBSK*CAB*$_{A-04}$ in this study is well categorized as constitutive weak promoter (Delamarre & Batt, 2006; Salinas et al., 2022). Therefore, pBSK*CAB*$_{A-04}$ represented an effective PHB expression vector with numerous advantages. No additional inducers were needed, which made the industrial operation of PHB even easier. Moreover, choices of carbon sources in PHB production would be flexible as no barrier of viscosity and property of those carbon sources need to be concerned in addition of inducer to start gene expression. Most importantly, a good amount of PHB was obtained within a short cultivation time of 24 hours.

E. coli strain JW39851-pBSK*CAB*$_{A-04}$ cultivated in LB medium supplemented with 20 g/L glucose at 30°C reached the CDM of 5.06 ± 0.40 g/L with the RCM of 2.00 ± 0.18 g/L in 24 hours. PHB production by *E. coli* strain JW39851-pBSK*CAB*$_{A-04}$ displayed the PHB concentration of 3.06 ± 0.24 g/L with 60.3%wt PHB content in 24 hours. The calculated volumetric PHB productivity was 0.13 g/L·h at 24 hours. Both biomass and PHB production increased continuously and reached the maximum value at 48 hours. The maximum CDM of *E. coli* strain JW39851-pBSK*CAB*$_{A-04}$ was 7.83 ± 0.53 g/L with the RCM of 2.16 ± 0.40 g/L. At the end of the cultivation, the maximum PHB accumulated in *E. coli* strain JW39851-pBSK*CAB*$_{A-04}$ was 5.67 ± 0.46 g/L with 72.3%wt PHB content. The volumetric PHB productivity at 48 hours was 0.12 g/L·h. Although it was examined and observed that glucose had a negative effect on the growth of *E. coli* JW39851 (Figure 21), there was no notable change in residual cell mass of *E. coli* JW39851 and K12 after PHB biosynthesis pathway was incorporated (Figure 30). Hence, it was assumed that incorporation of PHB biosynthesis pathway to *pgi* mutant could recover the slow growth rate of the strain.

Compared to *E. coli* strain K12-pBSK*CAB*$_{A-04}$, the RCM of *E. coli* strain JW39851-pBSK*CAB*$_{A-04}$ was lower than its parental strain with a small margin. However, the overall CDM of *E. coli* strain JW39851-pBSK*CAB*$_{A-04}$ was much lower than K12. Since the RCM between the two strains were not very different, the distinction of CDM might depend on the PHB concentration between both strains. The PHB concentration and PHB content of *E. coli* strain JW39851-pBSK*CAB*$_{A-04}$ was substantially lower than K12, specifically at 0-30 hours of cultivation. Since PHB production in recombinant *E. coli* is growth-associated, PHB can be accumulated from the beginning of the cultivation. At 12 hours, *E. coli* strain JW39851-pBSK*CAB*$_{A-04}$ had its PHB content of 25.6%wt, while PHB content of *E. coli* strain K12-pBSK*CAB*$_{A-04}$ reached 65.0%wt, indicating long adaptation phase of *E. coli* strain JW39851. A dramatic decrease in volumetric productivity was displayed at 24 hours of cultivation, which represented the peak of PHB production. *E. coli* strain JW39851 had the PHB productivity of 0.13 g/L·h while K12 reached the maximum productivity of 0.21 g/L·h. There was a change in the consumption rate of the *E. coli* strain

JW39851-pBSK*CAB*$_{A\text{-}04}$ observed compared to *E. coli* strain K12-pBSK*CAB*$_{A\text{-}04}$, describing the physiological and metabolic change in *E. coli* JW39851. Both biomass and PHB yield of *E. coli* strain JW39851 displayed the negative effect of *pgi* deletion on the growth of bacteria and PHB accumulation.

Deletion of *pgi* gene in *E. coli* was widely studied and found a significant decrease of growth rate and sugar consumption rate feeding from glucose (Ahn et al., 2011; Fraenkel & Levisohn, 1967; Shimaoka et al., 2005). According to Charusanti et. al. (2010), *pgi* mutant had ability to evolve the growth rate and glucose uptake rate after 50 days by 3.6 and 2.6 fold, respectively (Charusanti et al., 2010). Mutations in the NADH/NADPH transhydrogenases *udhA* and *pntAB* and in the stress associated sigma factor *rpoS* arose during the adaptation in *pgi* mutant. The consequence of adaptive growth of *pgi* mutant showed changes related in NADPH production and utilization of cells. In this work, we incorporated PHAs biosynthesis pathway as an utilization of NADPH pathway to *E. coli* JW39851, in order to study the effect on PHAs and growth of the mutant. Metabolic flux ratio (METAFoR) analysis revealed that the PPP pathway was developed as the primarily route of glucose catabolism in *pgi* mutants (Canonaco et al., 2001; Hua et al., 2003) resulted in the accumulation of intracellular NADPH (Canonaco et al., 2001; Charusanti et al., 2010). The excess NADPH itself acted as an inhibitor and led to growth arrest of *pgi* mutant strain (S. B. Jilani et al., 2020). Growth only resumes once NADPH level sinks. The result suggested that PPP and EDP pathway were not sufficiently activated to moderate the metabolic defect. According to Kabir and Shimizu (2003), genes involved in pentose phosphate pathway and some part of glycolytic pathway were upregulated significantly by expression of *phaCAB* operon in *pgi* mutant strain (Md Mohiuddin Kabir & Kazuyuki Shimizu, 2003). On the contrary, genes involved in TCA cycles except isocitrate dehydrogenase (*icdA*) were downregulated. The downregulation of TCA cycles genes might be the main factor for the decrease of PHB production in the *E. coli* strain JW39851-pBSK*CAB*$_{A\text{-}04}$. PHB accumulation is highly dependent on the concentration of acetyl-CoA, acetoacetyl-CoA and 3-hydroxybutyryl-CoA (Janasch et al., 2022). The downregulation of TCA cycle genes led to limitation of acetyl-CoA availability. As a result, PHB production was limited due to substrate inavailability.

In addition, semi-quantitative RT-PCR analysis showed the upregulation of *phaC*, *phaA* and *phaB* in *pgi* mutant, which lead to the assumption that EMP-disrupted strain such as *pgi* mutant may improve the PHB production. The results from this research (Figure 21 and 30) provided strong evidence that deletion of *pgi* gene in *E. coli* only recovered cell growth from unbalanced redox power, but did not enhance the PHB production. The incorporation of PHB production served as a bypass for utilization of excess NADPH. This result correlated to the experiment achieved by Kabir and Shimizu (2003), which briefly represented the PHB production by *pgi* mutant strain (M. M. Kabir & K. Shimizu, 2003a). Kabir and Shimizu (2003) reported the improvement of *pgi* mutant growth after incorporating with PHB biosynthesis genes. Unfortunately, fermentation characteristics of PHB production by *pgi* mutant compared to the parental strain was not provided.

Embden-Meyerhof pathway disruption proved no positive effect on PHB production in *E. coli*. Hence, we focused on another essential glucose metabolic pathway, Entner-Doudoroff pathway. Even though EDP was claimed to remain inactive on bacteria feeding on glucose, deletion of EDP by inactivation of *edd* gene proved to benefit products involved in the pentose phosphate pathway.

Recombinant *E. coli* strain JW18401 harboring pBSK$CAB_{A\text{-}04}$ cultivated at 30°C for 48 hours in LB medium supplemented with 20 g/L glucose reached CDM of 7.50 ± 0.54 g/L in 24 hours and 9.33 ± 0.51 g/L in 48 hours, with 91.2 and 81.1%wt PHB content. Compared to *E. coli* strain K12-pBSK$CAB_{A\text{-}04}$, a discrimination of PHB content of *E. coli* strain JW18401-pBSK$CAB_{A\text{-}04}$ was observed. At 12 hours of cultivation, *E. coli* strain JW18401-pBSK$CAB_{A\text{-}04}$ accumulated 76.5 ± 1.8%wt PHB content, which was 17.6% increase compared to the parental strain. The PHB concentration produced by *E. coli* strain JW18401-pBSK$CAB_{A\text{-}04}$ was higher compared to K12, with the value of 6.82 ± 0.23 and 7.58 ± 0.52 g/L at 24 and 48 hours, respectively. For biomass production, RCM of *E. coli* strain JW18401-pBSK$CAB_{A\text{-}04}$ ranged between 0.6-1.8 g/L, indicating low biomass production. The PHB accumulation in *E. coli* strain JW18401-pBSK$CAB_{A\text{-}04}$ overcome the parental strain from 24 hours of cultivation. The *edd* mutant strain could accumulate as high as 91.2 ± 5.2%wt PHB content, while K12 had only 73.5 ± 2.8%wt PHB content at 24

hours. At 30 hours of cultivation, PHB concentration from *E. coli* strain JW18401-pBSK*CAB*$_{A\text{-}04}$ reached its peak with 7.55 ± 0.39 g/L and 93.0 ± 2.3 %wt. The productivity of PHB from *E. coli* strain JW18401-pBSK*CAB*$_{A\text{-}04}$ at 24 and 30 hours were 0.28 and 0.25 g/L·h, respectively. After 30 hours of cultivation, the *edd* mutant strain accumulated PHB with slower rate of 0.16-0.19 g/L·h. The result indicated faster PHB production of *E. coli* strain JW18401-pBSK*CAB*$_{A\text{-}04}$ within 24 hours of cultivation. The PHB yield obtained from *E. coli* strain JW18401-pBSK*CAB*$_{A\text{-}04}$ was 0.37 g PHB/g glucose.

The EDP pathway is widely known as an inactive pathway in *E. coli* unless gluconate is used as the source of carbon (Egan et al., 1992; Kim et al., 2022). However, many studies proved that EDP is active and plays a role in metabolizing glucose metabolism and used as a strategy to modulate the carbon flux (Lin et al., 2014; Shimaoka et al., 2005). The disruption of EDP pathway resulted in accumulation of ribulose 5-phosphate via PPP pathway by 6-phosphogluconate dehydrogenase (*gnd*) (Meyer et al., 2018). Although there was no report on metabolic flux of EDP pathway disruption in *E. coli*, metabolic flux on *E. coli* parental strain growth on glucose may use to illustrate a rough idea (Figure 31). To describe, the flux of glucose into bacterial is 10.57. The 1.86 of the amount fluxes to monomers including β-D-glucose-6-phosphate, α-D-glucose and mainly pentose phosphate pathway by conversion into 6-phosphogluconolactone. Deletion of *edd* gene shunts the conversion of 6-phosphogluconate to 2-keto-3-deoxy-6-phosphogluconate (EDP pathway) into the conversion of 6-phosphogluconate to ribulose-5-phosphate (PPP pathway), by using the 1.86 flux of total 10.57 mol / kg / h. More carbon flow through the PPP led to accumulation of NADPH. Even the flux of 1.86 is a small margin of 10.57, it is an adequate amount to have impact on PPP as described by Meyer et al. (2018) and Lin et al. (2014) (Lin et al., 2014; Meyer et al., 2018). The other 8.71 of 10.57 fluxes to glycolysis which result in normal levels of acetyl-CoA and other intermediate for bacterial growth. This information supported the result in this study, which the EDP-disrupted strain JW18401 could accumulate higher amount of PHB compared to the EMP-disrupted strain JW39851. The higher accumulation of PHB in *E. coli* strain JW18401-pBSK*CAB*$_{A\text{-}04}$ affected from the availability of acetyl-CoA as the EMP existence together with auxiliary NADPH level from PPP upregulation.

Interestingly, there was no report of PHB production in *E. coli* with EDP pathway disruption before. Hence, this is the first reported on the effect of EDP pathway disruption on PHB production in *E. coli*.

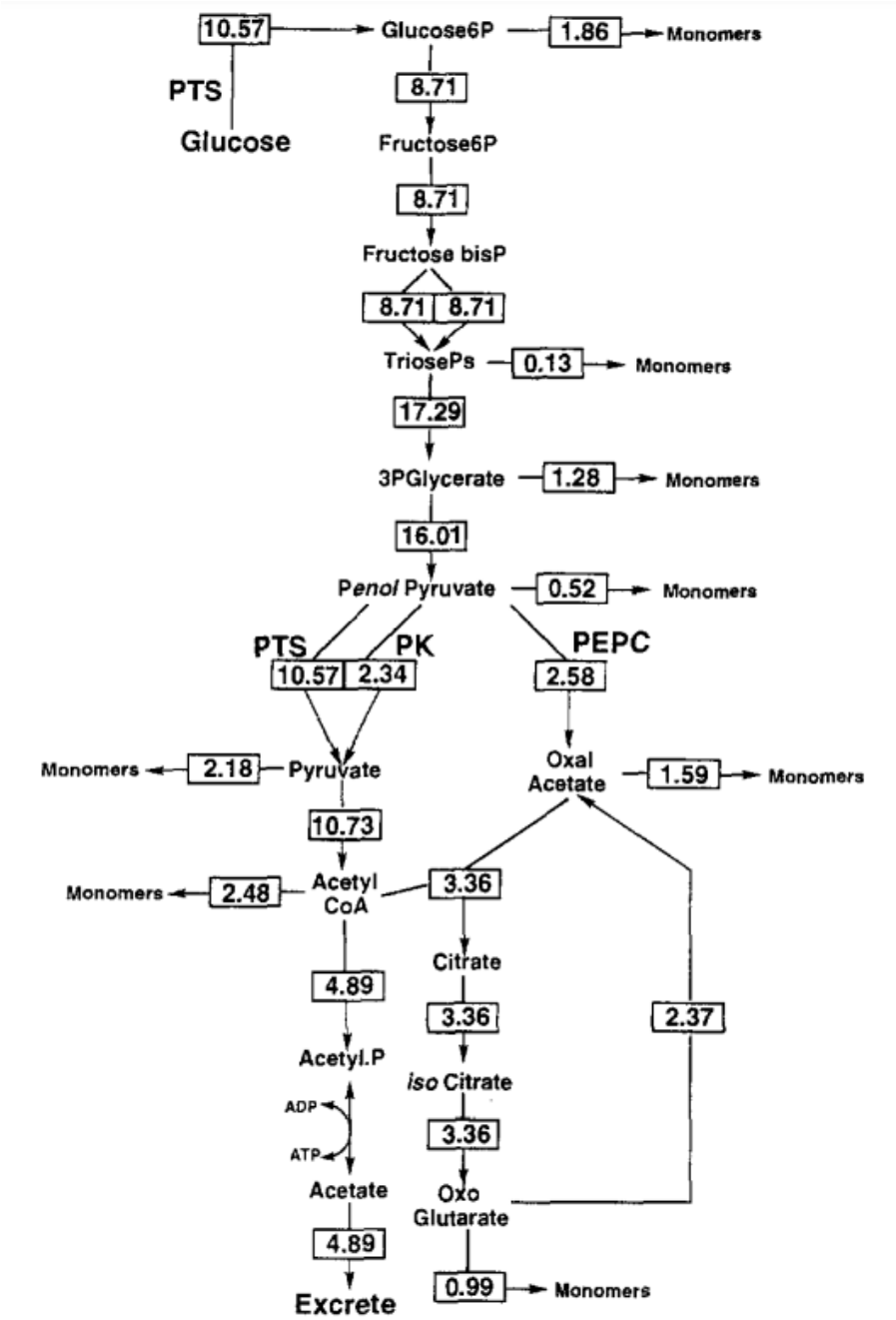

Figure 31 Flux analysis of *E. coli* growth on glucose. Fluxes are mol per kg dry weight per hour (Holms, 1996)

Table 19 Comparison of kinetic parameter, mechanical and thermal properties of PHB produced by recombinant *E. coli* strain JW39851, JW18401 and K12 harboring pBSK*CAB*$_{A\text{-}04}$ cultivated at 30oC, 200 rpm in LB medium supplemented with 20 g/L glucose as a sole carbon source

	Recombinant *E. coli* strain		
	JW39851	JW18401	K12
Maximum CDM (g/L)	7.8 ± 0.5	9.3 ± 0.5	9.7 ± 0.5
Maximum PHB concentration (g/L)	5.7 ± 0.5	7.6 ± 0.5	7.3 ± 0.4
Maximum PHB content (%wt)	72.4	93.0	76.5
Specific growth rate (h^{-1})	0.06	0.05	0.05
Specific production rate (h^{-1})	0.08	0.21	0.08
Specific consumption rate (h^{-1})	0.28	0.59	0.24
Productivity (g/(L.h)	0.15	0.25	0.24
$\gamma_{x/s}$ (g CDM/ g carbon source)	0.08	0.04	0.10
$\gamma_{p/s}$ (g PHB/ g carbon source)	0.26	0.37	0.36

4.7 Cultivation of PHB production in *E. coli* strain JW18401 harboring pBSK*CAB*$_{A-04}$ combined with pH-stat in 10L fermenter

Flask scale production of *E. coli* strain JW18401-pBSK*CAB*$_{A-04}$ displayed the maximum PHB concentration and CDM of 7.58 ± 0.52 and 9.33 ± 0.51 g/L, respectively. The PHB content of *E. coli* strain JW18401-pBSK*CAB*$_{A-04}$ reached its peak with the value of 93.0%wt within 30 hours of cultivation, representing the best strain for PHAs production among all. Batch cultivation in flask scale associates with numerous limitations such as nutrient depletion, low aeration and lack of pH control, result in limiting biomass and product formation. *E. coli* strain JW18401-pBSK*CAB*$_{A-04}$ was used for PHB production in a 10-L fermenter with the same condition as describes the optimal condition for flask scale production. Inoculum was prepared in LB medium without glucose cultivated at 37°C for 18 hours. The 5%(v/v) inoculum was transferred into a 10-L fermenter with the working volume of 5 L. The initial glucose concentration was 20 g/L. Time course of CDM, RCM, PHB concentration, PHB content and glucose concentration was represented in Figure 32.

Upscaling of PHB production from recombinant *E. coli* strain JW18401-pBSK*CAB*$_{A-04}$ into 10L fermenter was investigated. The CDM and RCM of *E. coli* strain JW18401-pBSK*CAB*$_{A-04}$ after 24 hours were 5.60 and 3.40 g/L. At 54 hours of cultivation, CDM and RCM of *E. coli* strain JW18401-pBSK*CAB*$_{A-04}$ were 5.63 and 1.63 g/L. Although the CDM of the bacteria at 24 and 54 hours were the same, RCM indicated that there was a decrease in overall biomass. The maximum PHB concentration and PHB content was observed at 54 hours with the value of 3.90 g/L and 70.5%wt, respectively. Compared to PHB production from recombinant *E. coli* strain JW18401-pBSK*CAB*$_{A-04}$ in flask scale (Figure 30), there was a dramatic decrease of biomass production and PHB accumulation of *E. coli* strain JW18401-pBSK*CAB*$_{A-04}$ in fermenter. We aimed to improve the PHB production in the fermenter using pH-stat technique to obtain high cell density. The pH-stat uses indirect feedback control of nutrient feeding with the measurement of pH to operate the fed-batch cultivation (Kim et al., 2004). The principle bases on the fact in which pH rises due to excretion of ammonium ions when carbon source is depleted (Suzuki et al., 1990). However,

E. coli strain JW18401-pBSK*CAB*$_{A-04}$ exhibited extraordinarily slow consumption rate of glucose. By 42 hours, 20 g/L glucose was depleted.

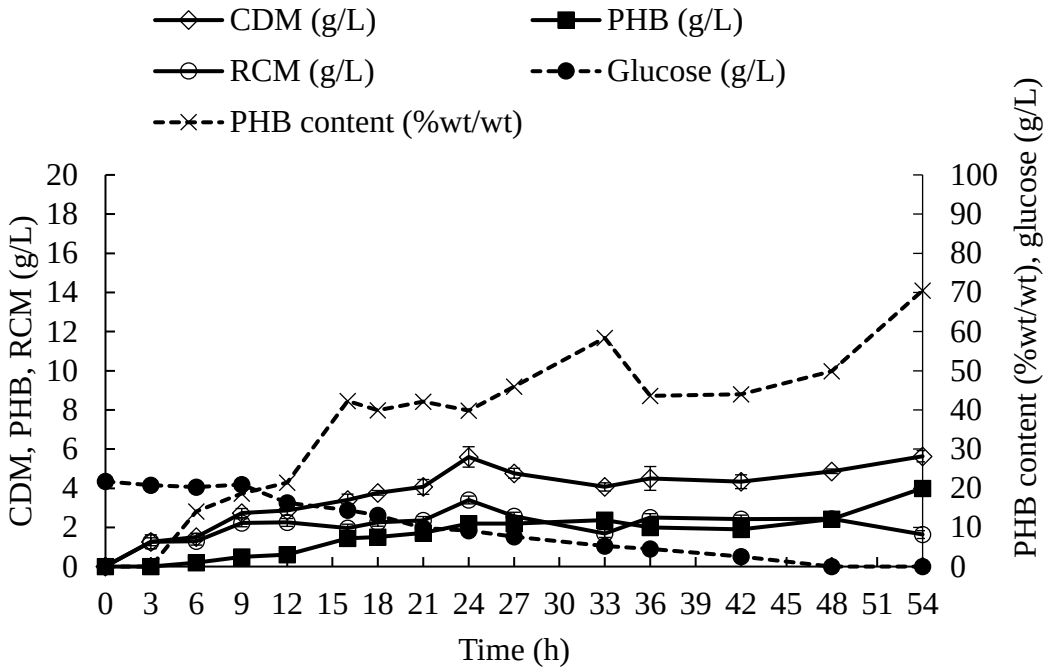

Figure 32 Time course of PHB production from recombinant *E. coli* strain JW18401 harboring pBSK*CAB*$_{A-04}$ cultivated at 30°C in LB medium supplemented with 20 g/L glucose as a sole carbon source in a 10-L bioreactor

In detail, the PHB content of *E. coli* strain JW18401-pBSK*CAB*$_{A-04}$ increased in a linear manner and peaked at 70.5%wt in 54 hours. At 12 hours PHB content from *E. coli* strain JW18401-pBSK*CAB*$_{A-04}$ in fermenter was 21.4%wt, while *E. coli* strain JW18401-pBSK*CAB*$_{A-04}$ could accumulate PHB up to 76.5%wt in flask cultivation. Moreover, the PHB concentration of *E. coli* strain JW18401-pBSK*CAB*$_{A-04}$ in fermenter reached only 2.20 g/L, while about 6.82 g/L PHB was obtained in flask cultivation at 24 hours. There were many possible reasons for the low PHB production by *E. coli* strain JW18401-pBSK*CAB*$_{A-04}$ in fermenter discussed as follows.

First, the stability of pBSK*CAB*$_{A-04}$ plasmid in *E. coli* strain JW18401 could affect the PHB production in fermenter. A high-copy number plasmid ensures the distribution of plasmids between daughter cells after cell division (Liu et al., 2020). To maintain the segregation stability of the plasmids is often a major problem during the fermentation process (Škulj et al., 2008). The accumulation of larger population without plasmids due to segregation instability can result in low productivity, which was represented in Figure 32. Even though, pBSK is a high-copy number plasmid with 500-700 copies, the problem of instability plasmid in bacteria was still observed (Mayer, 1995). Troubleshooting techniques regarding plasmid segregation and stability were reported. The addition of cer fragment, target for the XerCD system, enabled plasmids segregation improvement by recombining across the duplicated cer sites in a plasmid dimer (Allen et al., 2022; French & Ward, 1995). The addition of antibiotics during the fermentation could be the most broadly used technique to maintain a high-copy number of plasmids in bacteria (Škulj et al., 2008).

Second, aeration and dissolved oxygen might have an influence on PHB production of *E. coli* strain JW18401. The shaking flask size and ratio between the surface area to volume had a great impact on oxygen transfer rate. Dissolved oxygen and oxygen transfer are low in shake flask cultivation, while supplying of dissolved oxygen is better in fermenter (Hill, 2006). Some researchers reported that the limitation of oxygen can lead to higher PHB production by inducing an oxygen stress environment and increase nitrogen removal through nitrification (Blunt et al., 2018; X. Wang et al., 2019). Kshirsagar et al. (2012) reported the control of dissolved oxygen in the range of 1-5% level facilitated increase in PHAs production of facultative anaerobes *Halomonas campisalis* in fermenter (Kshirsagar, 2013). Since *E. coli* is also facultative anaerobes, we hypothesized that limitation of dissolved oxygen may lead to PHAs production of *E. coli* in fermenter also. However, some studies showed supplying of dissolved oxygen can promote PHB production also (Kim et al., 2004). Therefore, to improve PHB production by *E. coli* strain JW18401-pBSK*CAB*$_{A-04}$ in fermenter, varying oxygen levels to optimize the condition might be necessary.

4.8 PHB film extraction, molecular weight and thermal properties analysis

PHB films were prepared from *E. coli* strain JW39851-pBSK*CAB*$_{A-04}$, JW18401-pBSK*CAB*$_{A-04}$ and K12-pBSK*CAB*$_{A-04}$ cultivated at 200 rpm, 30°C for 48 hours in LB medium supplemented with 20 g/L glucose as a sole carbon source in flask scale production. Intracellular PHB was extracted using hot chloroform for 4 hours, followed by precipitation with *n*-hexane. The extraction and purification of PHB is based on the solubility of PHB. PHB is highly soluble in chloroform, dichloromethane, acetic anhydride, sodium hydroxide and acetic acid, while it is practically insoluble in water, methanol, ethanol, hexane and benzene (Jirage et al., 2013) (Figure 33). The solvents such as chloroform, methyl chloride or 1,2-dichloroethane were evaluated for PHB extraction (G.-Y. Tan et al., 2014). After that, the addition of 4 times volume of *n*-hexane resulted in the solution becoming less soluble, which allows separation of polymers. To purify the extracted polymer from contamination and cell debris, PHB solution was filtered by a nitrocellulose membrane filter. PHB pellet appeared white in color, showing less contamination and free of cell debris. The purified PHB was later used to make PHB film by solvent casting method (Figure 34). Briefly, 2%(w/v) PHB pellet was dissolved in chloroform and heated. The PHB solution was then poured into a glass tray allowing chloroform to evaporate slowly at room temperature for 2 weeks.

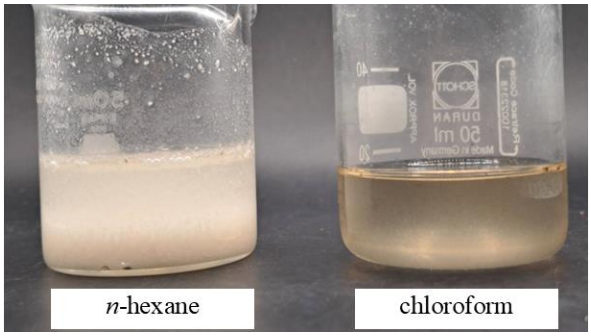

Figure 33 Solubility test of 0.5 g PHB extracted from *E. coli* strain JW18401-pBSK*CAB*$_{A-04}$ dissolved in 20 ml n-hexane and chloroform

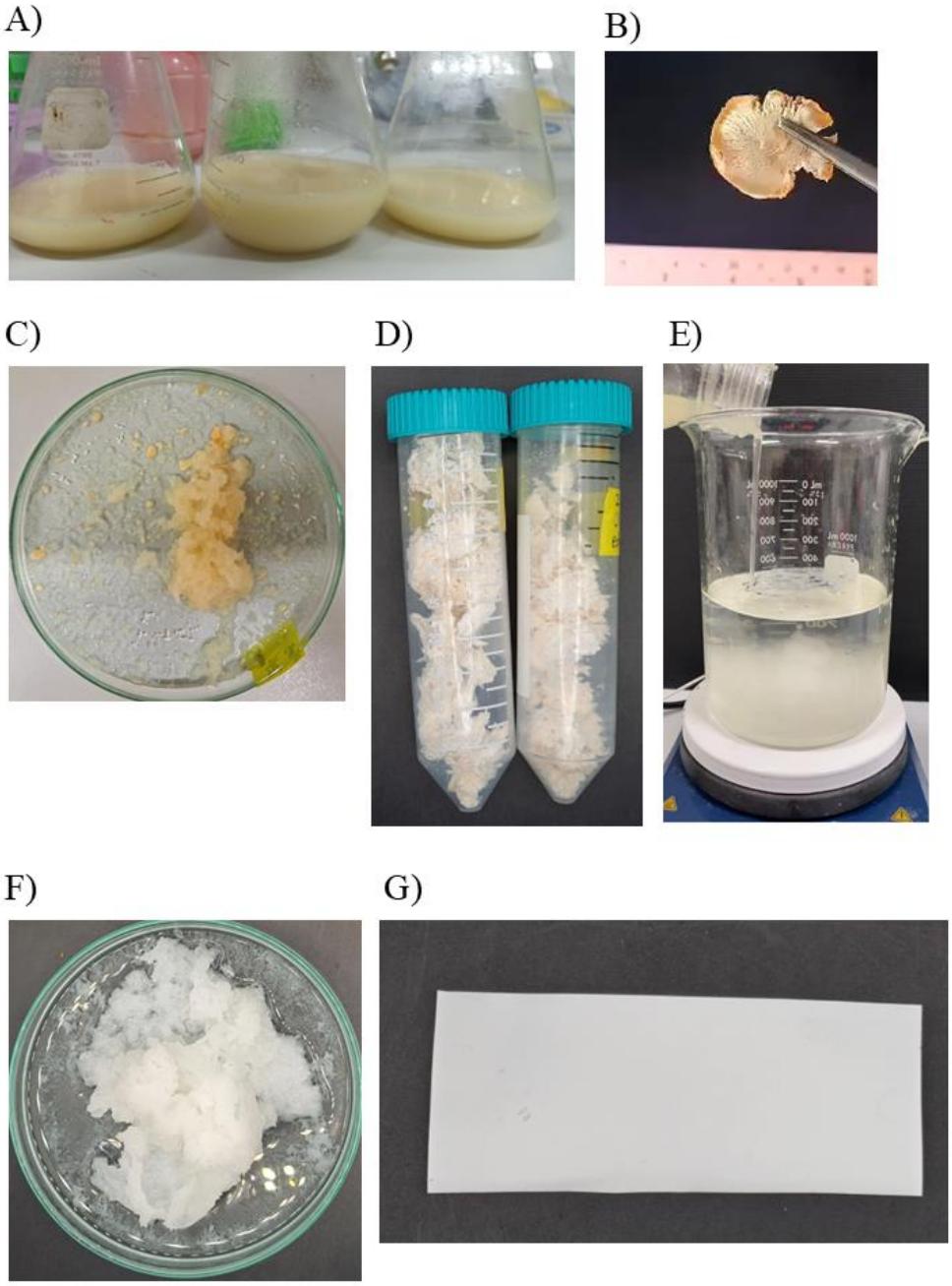

Figure 34 Preparation of PHB film extraction from recombinant *E. coli* JW18401-pBSK*CAB*$_{A\text{-}04}$ cultivated at 200 rpm, 30°C for 48 hours in LB medium supplemented with 20 g/L glucose as a sole carbon source in flask scale production: (A) sample collection, (B) dry cell after incubation at 65°C for 2 days, (C) extraction of PHB from cell pellet, (D) dry PHB pellet after extraction, (E) precipitation with *n*-hexane, (F) purified PHB pellet and (G) PHB film preparation using solvent casting method

Molecular weight of PHB polymers extracted from *E. coli* strain JW18401-pBSK*CAB*$_{A-04}$, JW39851-pBSK*CAB*$_{A-04}$ and K12-pBSK*CAB*$_{A-04}$ were analyzed by gel permeation chromatography (GPC). Number average molecular weight (M_n), weight average molecular weight (M_w) and polydispersity index of these PHB films were represented in Figure 35. The result showed that PHB film produced by *E. coli* strain K12-pBSK*CAB*$_{A-04}$ gave the highest M_w and M_n of 7.7 x 10^5 and 5.1 x 10^5 Da, respectively. On the contrary, PHB film produced by *E. coli* strain JW18401-pBSK*CAB*$_{A-04}$ had its M_w and M_n of 2.9 x 10^5 and 1.8 x 10^5 Da, respectively. PHB film produced by *E. coli* strain JW39851-pBSK*CAB*$_{A-04}$ illustrated the lowest M_w and M_n of 1.5 x 10^5 and 7.9 x 10^4 Da, respectively. These results indicated JW18401 and JW39851 produced lower molecular weight PHB than K12. Molecular weight of PHB was reported in the range of 0.1 x 10^6 to 2 x 10^6 Da (Tsuge, 2016).

Up to date, the precise mechanism of PHA monomers elongation is still unclear. The decrease of molecular weight of PHB produced from *E. coli* strain JW18401-pBSK*CAB*$_{A-04}$ and JW39851-pBSK*CAB*$_{A-04}$ when compared to K12-pBSK*CAB*$_{A-04}$ could be explained as follows. To begin with, molecular weight changed due to PHA synthase (phaC) activity. The *E. coli* strain JW18401 and JW39851 had its EDP and EMP disruption to flux carbon through PPP with the aim to produce higher amount of NADPH, incorporating and enhancing PHAs production. NADPH is known as the main bottleneck in PHAs production to generate 3-hydroxybutyryl-CoA, the main precursor for PhaC. Providing NADPH availability may lead to an increase of phaC activity. PHB biosynthesis is highly dependent on the concentration of acetyl-CoA, acetoacetyl-CoA and 3-hydroxybutyryl-CoA (Janasch et al., 2022). Thus, *E. coli* strain JW18401 and JW39851 might have higher activity of phaC, compared to K12. Many researchers reported that molecular weight of PHA decreases with an increasing of PHA synthase activity (Sim et al., 2001; Sim et al., 1997; Tsuge, 2016).

A)

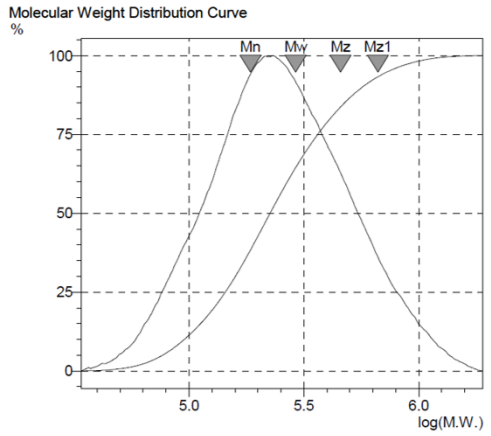

[Average Molecular Weight]	
Number Average Molecular Weight(Mn)	184762
Weight Average Molecular Weight(Mw)	290669
Z Average Molecular Weight(Mz)	456486
Z+1 Average Molecular Weight(Mz1)	664189
Mw/Mn	1.57321
Mv/Mn	0.00000
Mz/Mw	1.57046

B)

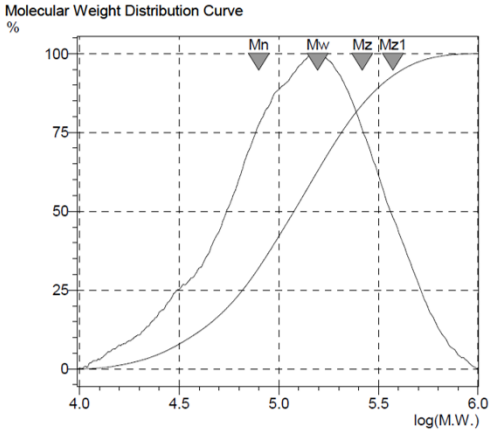

[Average Molecular Weight]	
Number Average Molecular Weight(Mn)	79265
Weight Average Molecular Weight(Mw)	156320
Z Average Molecular Weight(Mz)	261840
Z+1 Average Molecular Weight(Mz1)	373912
Mw/Mn	1.97210
Mv/Mn	0.00000
Mz/Mw	1.67503

C)

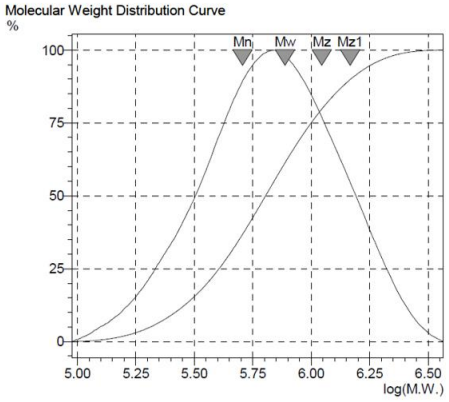

[Average Molecular Weight]	
Number Average Molecular Weight(Mn)	508972
Weight Average Molecular Weight(Mw)	773455
Z Average Molecular Weight(Mz)	1110516
Z+1 Average Molecular Weight(Mz1)	1466506
Mw/Mn	1.51964
Mv/Mn	0.00000
Mz/Mw	1.43579

Figure 35 Molecular weight analysis by gel permeation chromatography (GPC) of PHB polymer extracted from *E. coli* strain (A) JW18401-pBSK*CAB*$_{A\text{-}04}$, (B) JW39851-pBSK*CAB*$_{A\text{-}04}$, and (C) K12-pBSK*CAB*$_{A\text{-}04}$, cultivated at 30°C for 48 hours in LB medium supplemented with 20 g/L glucose as a sole carbon source

Another possible explanation for molecular weight decreases of PHB produced from *E. coli* strain JW18401-pBSK*CAB*$_{A\text{-}04}$ and JW39851-pBSK*CAB*$_{A\text{-}04}$ was ethanol formation inhibited the polymerization of PHAs chain (Rangel et al., 2023). By using glucose as a substrate, the theoretical yield of ethanol production in central glucose metabolism was described as follows (Seol et al., 2014).

EMP: Glucose → 2 H_2 + 1 Ethanol + 2 ATP

PPP: Glucose → 1.67 H_2 + 1.67 Ethanol + 1.67 ATP

EDP: Glucose → 2 H_2 + 1 Ethanol + 1 ATP

E. coli strain JW18401 and JW39851 had ability to flux carbon into PPP, resulted in the maximum theoretical yield of ethanol obtained via PPP with 1.67 mol per mol glucose. With this evidence, we can conclude that ethanol production by *E. coli* strain JW18401 and JW39851 was higher than K12. In fact, Seol et al. (2014) displayed the ethanol yield of EMP-disrupted strain with the value of 0.95 mol ethanol per mol glucose, compared to 0.84 mol ethanol per mol glucose in parental strain (Seol et al., 2014). Ethanol, a potential chain transfer agent, has ability to covalently bind to the carboxyl terminus of the PHAs chain and stop the chain polymerization (Tsuge, 2016). Hiroe et al. (2015) reported the decline of PHB molecular weight in the condition with ethanol supplementation (Hiroe et al., 2015). In conclusion, higher amount of ethanol production in *E. coli* strain JW18401 and JW39851 might terminate the PHB polymerization and result in lower molecular weight of PHB extracted from these two strains than its parental strain.

Thermal properties of PHB extracted from *E. coli* JW18401-pBSK*CAB*$_{A\text{-}04}$, JW39851-pBSK*CAB*$_{A\text{-}04}$ and K12-pBSK*CAB*$_{A\text{-}04}$ were analyzed by differential scanning calorimetry (DSC) (Figure 36). A single melting point was observed in the first heating cycle of all PHB pellets. The T_m of PHB from three strains of *E. coli* varied between 178-183^{o}C in the first heating and shifted to between 172-177^{o}C in the second heating. T_g and T_c ranged between 4-5 and 42-53^{o}C, respectively. The percent crystallinity of PHB from *E. coli* strain JW39851-pBSK*CAB*$_{A\text{-}04}$ was comparable to those found in K12-pBSK*CAB*$_{A\text{-}04}$ at 67.8%. Interestingly, the percent crystallinity of PHB from *E. coli* JW18401-pBSK*CAB*$_{A\text{-}04}$ increased up to 72.3%.

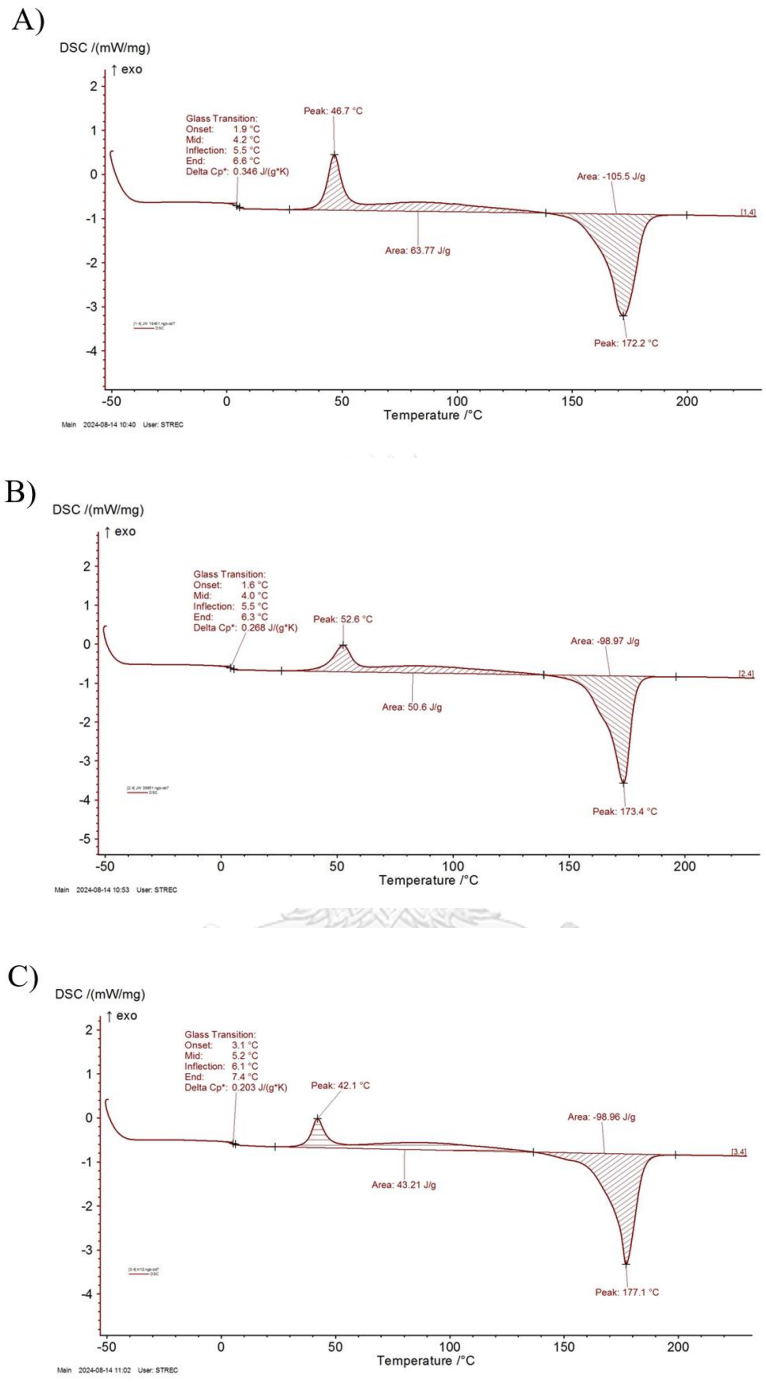

Figure 36 Differential Scanning Calorimetry thermogram of PHB polymer extracted from *Escherichia coli* strain (A) JW18401, (B) JW39851 and (C) K12 harboring pBSK*CAB*$_{A\text{-}04}$ cultivated at 30°C for 48 hours in LB medium supplemented with 20 g/L glucose as a sole carbon source

Table 20 Mechanical and thermal properties of PHB produced by recombinant *E. coli* strain JW18401, JW39851 and K12 harboring pBSK*CAB*$_{A-04}$

PHB property	Recombinant *E. coli* strain harboring pBSK*CAB*$_{A-04}$		
	JW18401	JW39851	K12
M_w (Da)	2.9×10^5	1.5×10^5	7.7×10^5
M_n (Da)	1.8×10^5	7.9×10^4	5.0×10^5
PDI	1.6	2.0	1.5
T_g (°C)	4.2	4.0	5.2
T_c (°C)	46.7	52.6	42.1
T_m (°C)	172.2	173.4	177.1
ΔH_f (J/g)	105.5	99.0	99.0
%Xc	72.3	67.8	67.8

T_g = glass transition temperature, T_c = crystallization temperature, T_m = melting temperature, ΔH_f = Heat of fusion, $\%X_c$= percent crystallinity, M_w = weight average molecular weight, M_n = number average molecular weight, PDI = polydispersity index

4.9 Cell morphology and PHA granules

E. coli strain JW18401-pBSK*CAB*$_{A-04}$ cultivated for 48 h and its PHB granules were analyzed by TEM (Figure 37). Since *E. coli* strain JW18401-pBSK*CAB*$_{A-04}$ was cultivated for 48 h, several types of histograms were represented in the images. The TEM images represented PHB granules showed in white with different sizes of histograms and *E. coli* strain JW18401-pBSK*CAB*$_{A-04}$ in gray. Each bacterium consisted of one or more PHB vesicles with the maximum size distribution at the center around 1.5-2.0 μm diameter in the cytoplasm. In addition, autolysis of cells and secretion of PHB were observed in some histograms. Also, it was observed that some of bacterial cells did not accumulate PHB even the PHB analysis by GC showed 81.1%wt PHB content. This incident might occur due to the segregation instability of plasmid during cell division (Škulj et al., 2008). This result supported the information in 4.7, PHB concentration and PHB content of *E. coli* strain JW18401-pBSK*CAB*$_{A-04}$ cultivated in

10L fermenter were low due to the plasmid instability. Moreover, numerous small vesicles clustered around the periphery of bacteria were displayed from TEM images.

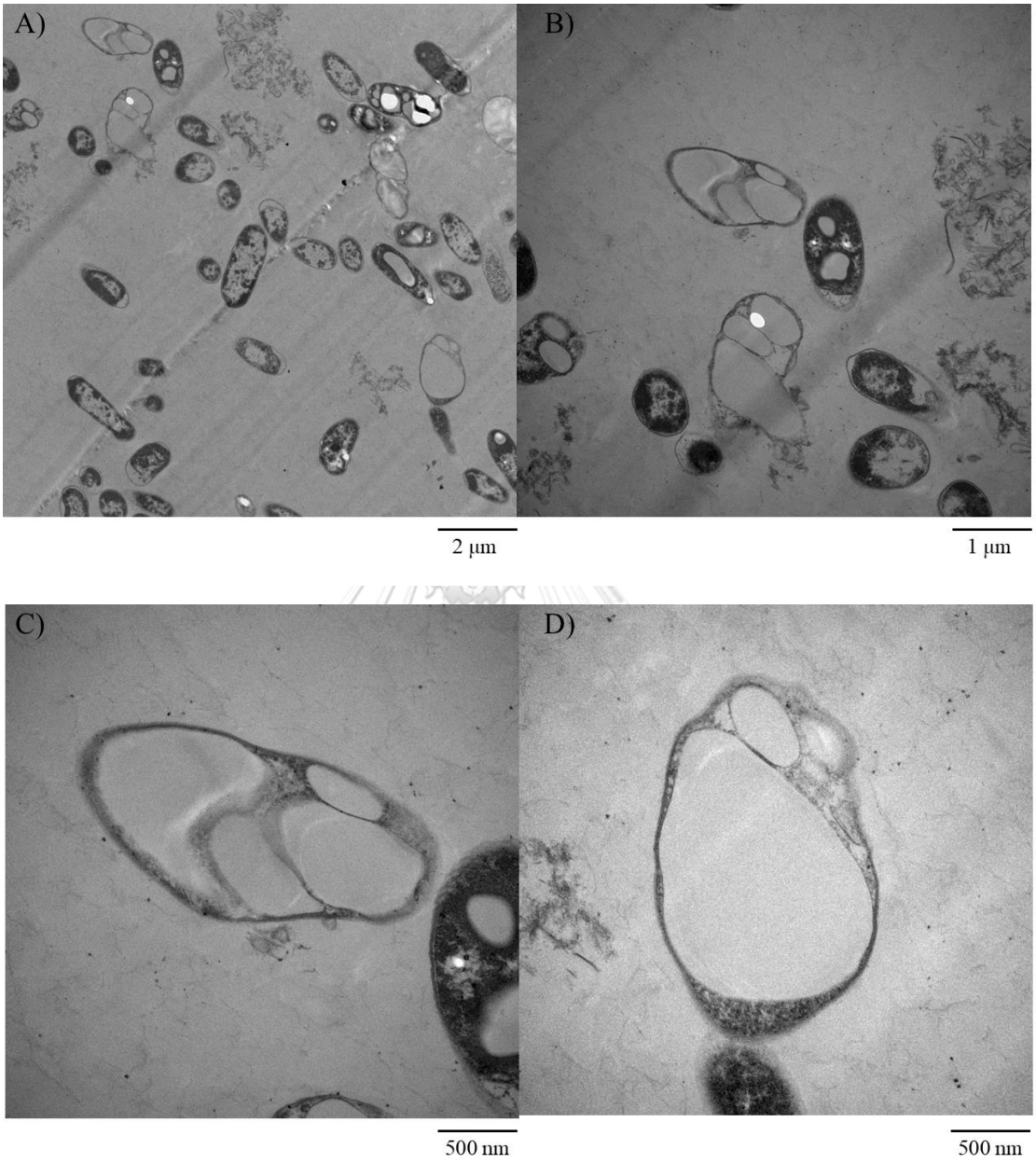

Figure 37 TEM images with magnification (A) 10000X, (B) 20000X, (C) 50000X and (D) 50000X of *E. coli* JW18401-pBSK*CAB*$_{A\text{-}04}$ morphology and PHB granules cultivated at 30°C for 48 hours in LB medium supplemented with 20 g/L glucose

4.10 PHB biosynthesis in recombinant *E. coli* harboring pBSK*CAB*$_{A-04}$ using crude glycerol waste as a sole carbon source

We further investigated the ability of *E. coli* harboring pBSK*CAB*$_{A-04}$ to assimilate inexpensive carbon source such as crude glycerol waste from biodiesel industry, provided from BBGI Biodiesel Company Limited (BBGI-BI), Bangchak Corporation Public Limited (Thailand). The crude glycerol composition was analyzed and reported containing 81.05%wt glycerol, 0.004%wt methanol, 13.5%wt moisture, 3.31%wt salt as sodium chloride, 1.13%wt ash and 0.99%wt calculated matter nonglycerol (MONG) (N. Phothong et al., 2024). Recombinant *E. coli* strain JW18401-pBSK*CAB*$_{A-04}$, JW39851-pBSK*CAB*$_{A-04}$ and K12-pBSK*CAB*$_{A-04}$ were cultivated at 30°C for 48 hours in LB medium supplemented with 20 g/L crude glycerol as a sole carbon source. The CDM, PHB concentration, RCM, glycerol concentration and PHB content were represented in Figure 38.

Recombinant *E. coli* K12-pBSK*CAB*$_{A-04}$ can accumulate PHB of 1.1 and 1.9 g/L at 24 and 48 hours, respectively, with the PHB content of 48.6 and 55.8%wt. The biomass of *E. coli* K12-pBSK*CAB*$_{A-04}$ were 2.2 and 3.4 g/L with the RCM of 1.1 and 1.5 g/L at 24 and 48 hours. Interestingly, both mutant strains JW18401-pBSK*CAB*$_{A-04}$ and JW39851-pBSK*CAB*$_{A-04}$ had greater biomass concentration and PHB concentration, compared to its parental strain K12. Recombinant *E. coli* JW18401-pBSK*CAB*$_{A-04}$ accumulated 2.7 and 3.8 g/L PHB with 74.8 and 76.9%wt in 24 and 48 hours. The biomass of this strain were 3.7 and 4.9 g/L with the RCM 3.7 and 3.5 g/L. *E. coli* strain JW18401 exhibited an outstanding ability to produce PHB from crude glycerol prior to native strain K12 with over 70%wt PHB content within 24 hours. Surprisingly, *E. coli* JW39851-pBSK*CAB*$_{A-04}$ represented the highest CDM among all strains with the value of 3.53 g/L at 24 hours and 5.47 g/L at 48 hours. The PHB content of *E. coli* JW39851-pBSK*CAB*$_{A-04}$ was larger than K12, with the value of 62%wt PHB content.

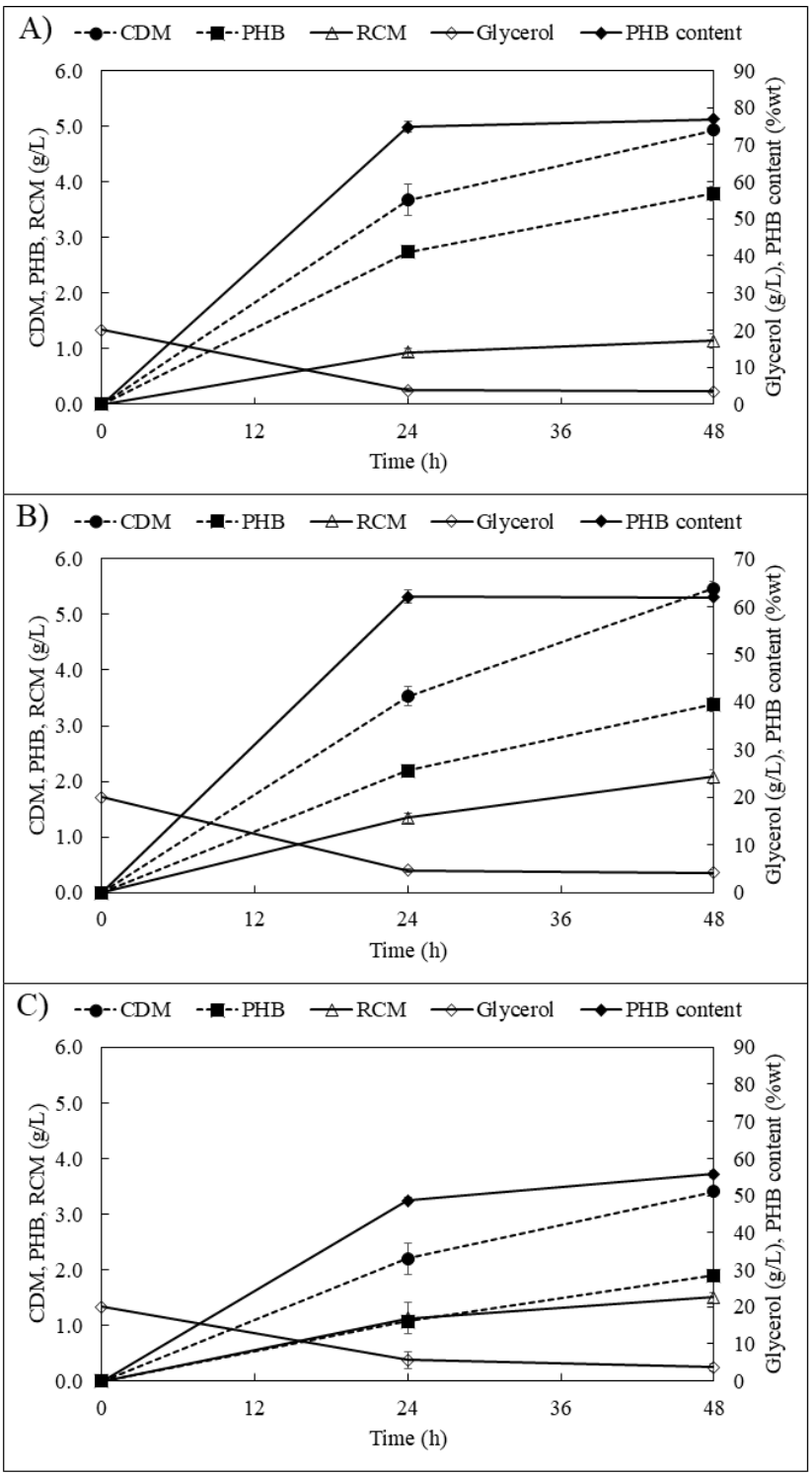

Figure 38 Time course of PHB production by recombinant *E. coli* strain (A) JW18401, (B) JW39851 and (C) K12 harboring pBSK*CAB*$_{A\text{-}04}$ cultivated at 30°C from 20 g/L crude glycerol

The PHB production by recombinant *E. coli* K12-pBSK*CAB*$_{A\text{-}04}$ had its maximum PHB content of 55.8%wt, which was equivalent amount to previous report by Photong et al. (2024) (Natthaphat Phothong et al., 2024). The relatively low productivity of PHB from crude glycerol may result from the impurities associated with methanol, hydroxide residues and by products of transesterification process. We set two hypotheses to illustrate higher production of PHB using crude glycerol as carbon source in *E. coli* JW18401-pBSK*CAB*$_{A\text{-}04}$ and JW39851-pBSK*CAB*$_{A\text{-}04}$. First, the increase of PHB production by *edd* and *pgi* mutant might be affected by the ability to tolerate toxic methanol in crude glycerol components. Several studies reported that the generation of *E. coli* strain growing on methanol required ribulose-5-phosphate (Ru-5P) availability (Keller et al., 2022; Meyer et al., 2018). As Ru-5P is a co-substrate in metabolizing methanol by hexulose phosphate synthase (Hps) into hexulose (H6P). *E. coli* JW18401-pBSK*CAB*$_{A\text{-}04}$ and JW39851-pBSK*CAB*$_{A\text{-}04}$ had its carbon flux into PPP, the main source of NADPH and Ru-5P, therefore *E. coli* JW18401 and JW39851 might be more tolerant to methanol than K12. Another reason might be the metabolism of glycerol in *E. coli*. Flux analysis of *E. coli* growth on glycerol illustrated that by using glycerol as a substrate, carbon flux into EMP yielding acetyl-CoA and small proportion fluxes to glucose-6-phosphate, which is the main precursor for oxidative phase of PPP. Unfortunately, there was no evidence regarding NADPH amount in *E. coli* feeding on glycerol.

In conclusion, both *E. coli* JW18401 and JW39851 with its carbon metabolism disrupted had ability to accumulate PHB with superior amount than any other reports of PHB production from crude glycerol (Aristya et al., 2022; Natthaphat Phothong et al., 2024; N. Phothong et al., 2024).

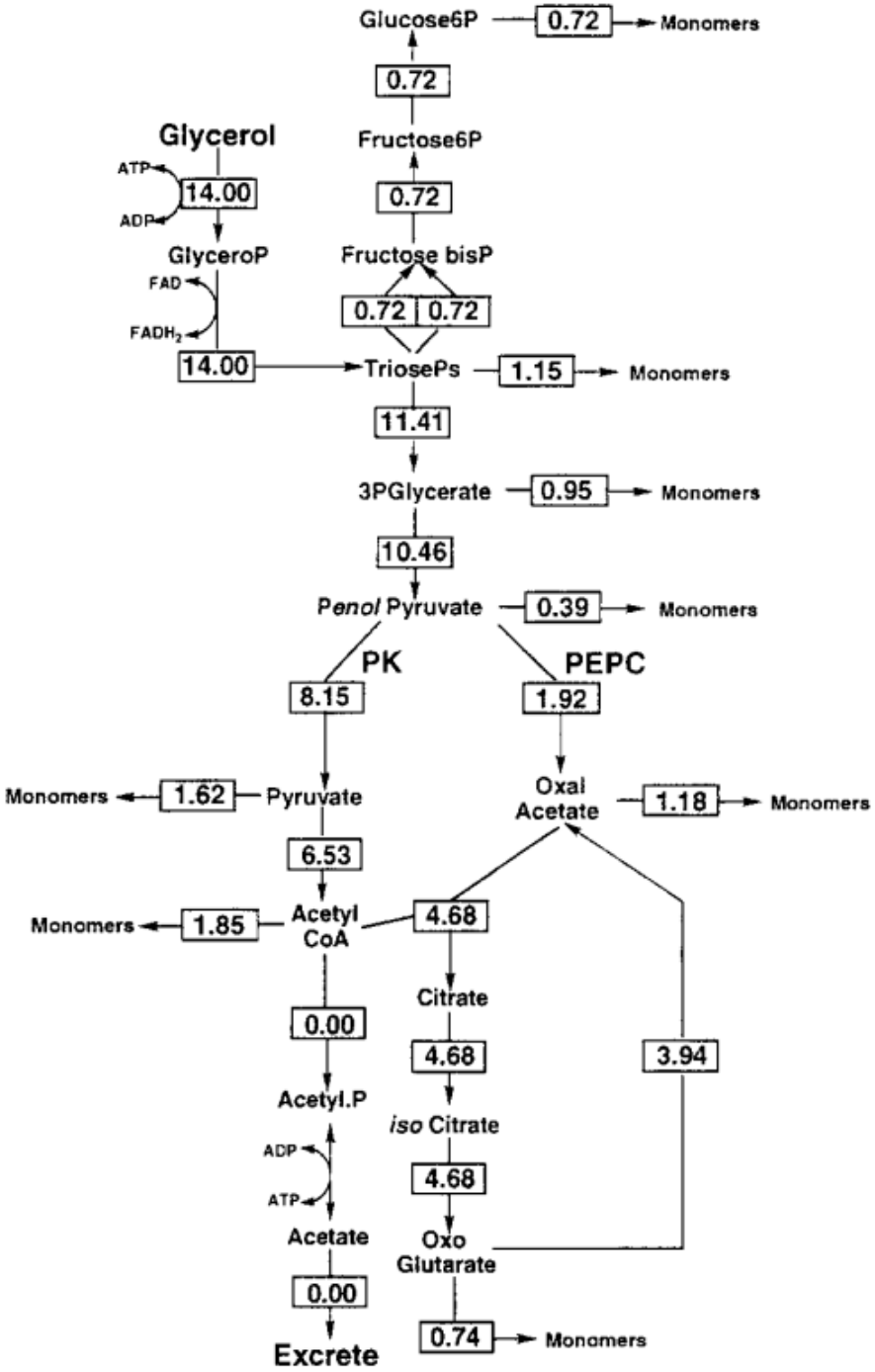

Figure 39 Flux analysis of growth of *E. coli* on glycerol (Holms, 1996)

4.11 Copolymer poly(3HB-*co*-3HV) production in *E. coli* strain JW18401 harboring pBSK*CAB*$_{A-04}$ from glucose and sodium propionate

Even PHB is the most available type of PHAs, there are some negative properties of PHB. Homopolymer of PHB is stiff and brittle. The melting temperature of PHB ranges from 165-180°C and its glass transition temperature is between 5 and 9°C, similar to those of fossil-derived thermoplastics. However, its very low degradation temperature of approximately 220-290°C limits the possibility of thermal processing to prepare PHB films (Anbukarasu et al., 2015; De et al., 2023). Copolymerization of PHB and other types of monomers can improve PHB properties.

E. coli strain JW18401-pBSK*CAB*$_{A-04}$ was cultivated at 30°C for 48 hours in LB medium supplemented with total carbon (glucose and sodium propionate) of 20 g/L. By supplementing different concentrations of sodium propionate salt, various mole fractions of poly(3-hydroxybutyrate-co-3-hydroxyvalyrate) [P(3HB-co-3HV)] were obtained (Figure 38). The maximum total PHAs was obtained in the condition which there was no sodium propionate salt. The highest total PHAs concentration was 4.68 g/L homopolymer of PHB with the content of 74.6 %wt. In the condition without sodium propionate salt, the yield of PHAs was 0.287 g PHAs per g glucose, representing the highest yield of P(3HB-co-3HV). Mole fractions of 3-hydroxyvalyrate increased along with the increase of sodium propionate salt concentration linearly. By supplementation of 0.5 g/L sodium propionate salt, PHAs concentration and PHAs content decreased compared to the condition with absence of sodium propionate salt. Total PHAs concentration of 3.51 g/L, consisting of 3.13 g/L 3HB and 0.39 g/L 3HV, was obtained with the PHAs content of 63.9%wt at 0.5 g/L sodium propionate salt. The result illustrated the increase of mole fraction of 3HV monomer resulted in lower PHAs concentration and PHB content. The range of 18-32 mol% PHV fraction was obtained from 1-2 g/L propionate salt. At 2 g/L sodium propionate salt, 32.35 mol% of 3HV was achieved with only 35.95 %wt PHAs content.

The result displayed the ability of *E. coli* strain JW18401-pBSK*CAB*$_{A-04}$ to produce poly(3-hydroxybutyrate-co-3-hydroxyvalyrate) from structural related carbon source, sodium propionate.

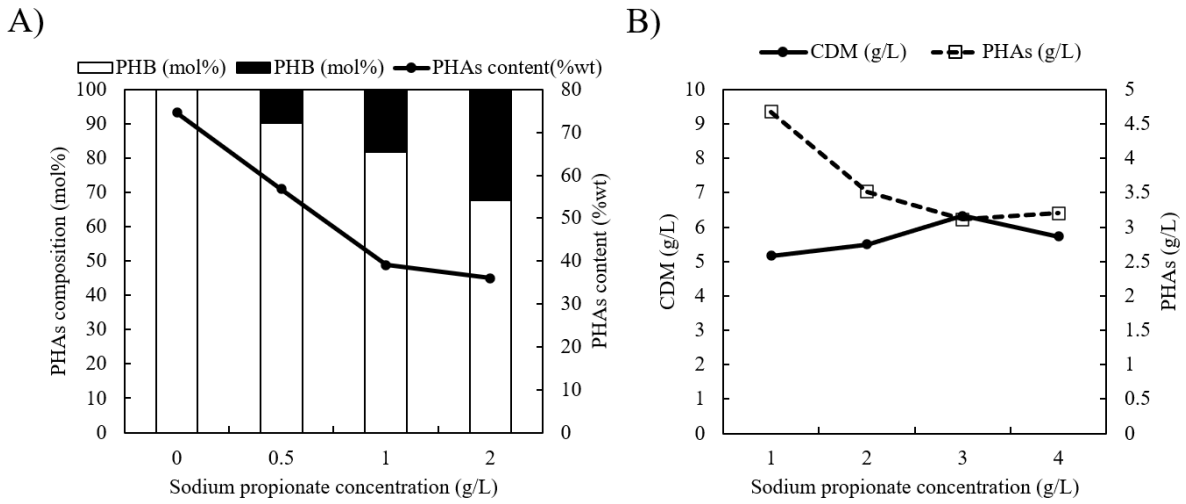

Figure 40 Effect of sodium propionate concentration on (A) P(3HB-*co*-3HV) compositions and PHAs content, (B) CDM (g/L) and PHAs concentration (g/L) accumulated by *E. coli* JW18401-pBSK*CAB*$_{A\text{-}04}$ cultivated at 30°C for 48 hours in LB medium supplemented with total carbon (glucose and sodium propionate) of 20 g/L

Table 21 Comparison of PHB production using glucose as carbon source by recombinant microorganisms

Strain	Strain characteristics	Carbon source	Condition	CDW (g/L)	PHB (%wt)	Reference
C. necator A-04	Native strain	Fructose	30ºC, 60 h	7.4 ± 1.5	78.4 ± 1.9	Napathorn, 2021
E. coli JM109	Harboring cold-shock inducible promoter of phaCAB from *C. necator* strain A-04	Glucose	37ºC, 18 h	7.9 ± 0.7	89.8 ± 2.3	Boontip et al., 2021
E. coli S17-1	Harboring cascaded P_{vgb} repeats and phaCAB from *C. necator*	Glucose	37ºC, 48 h	6.30	91	Wu et al., 2014
E. coli DH5α	Harboring pGETS109-*pha*	Glucose	30ºC, 72 h	11.2 ± 0.1	57 ± 1.6	Hiroe et al., 2012
E. coli JM109	Harboring pBAD/Thio-TOPO-phaCAB from *C. necator* strain A-04	Glucose	37ºC, 24 h	6.1 ± 1.1	93.3 ± 0.9	Napathorn et al., 2021
E. coli Δ*edd*	Harboring phaCAB from *C. necator* strain A-04	Glucose	30ºC, 24 h	7.5 ± 0.5	91.2 ± 5.2	This study
E. coli Δ*pgi*	Harboring phaCAB from *C. necator* strain A-04	Glucose	30ºC, 48 h	7.8 ± 0.5	72.4 ± 2.7	This study
E. coli BW25113	Harboring phaCAB from *C. necator* strain A-04	Glucose	30ºC, 24 h	6.9 ± 0.4	73.5 ± 2.8	This study

Table 21 Comparison of PHB production using crude glycerol as carbon source by recombinant microorganisms (*Cont.)*

Strain	Strain characteristics	Carbon source	Condition	CDW (g/L)	PHB (%wt)	Reference
Recombinant *R. glutinis*	Harboring codon-optimized towards phaCAB from *C. necator*	Crude glycerol	24ºC, 48 h	4.6	62	Aristya et al., 2022
E. coli JM109	Harboring pUC19-23119phaCAB$_{A-04}$	Crude glycerol	30ºC, 24 h	4.4 ± 0.3	7.4 ± 0.8	Photong et al., 2024
E. coli BL21 (DE3)	Harboring *phaA* and *phaB* from *C. necator* and *phaC* from *A. hydrophila*	Crude glycerol	37ºC, 24 h	4.0 ± 0.4	13.9 ± 2.5	Phithakrotchanakoon et al., 2014
E. coli Δ*edd*	Harboring phaCAB from *C. necator* strain A-04	Crude glycerol	30ºC, 24 h	3.7 ± 0.1	74.8 ± 1.4	This study
E. coli Δ*pgi*	Harboring phaCAB from *C. necator* strain A-04	Crude glycerol	30ºC, 48 h	5.5 ± 0.1	61.9 ± 1.9	This study
E. coli BW25113	Harboring phaCAB from *C. necator* strain A-04	Crude glycerol	30ºC, 48 h	3.4 ± 0.1	55.8 ± 0.9	This study

CHAPTER V
CONCLUSIONS AND RECOMMENDATIONS

i. Single gene deletion strain of *E. coli* JW18401 and JW39851 were obtained and studied. In the presence of glucose, both mutant strains exhibited significant decrease of cell growth resulted from metabolic perturbation of excess NADPH from pentose phosphate pathway.

ii. The PHB biosynthesis genes, $phaCAB_{A-04}$ from *C. necator* strain A-04 were successfully cloned into pBluescript SK II (native promoter) and transformed into *E. coli* strain JW18401, JW39851 and K12.

iii. Optimum temperature for PHB production by expression of $phaCAB_{A-04}$ from *C. necator* strain A-04 in recombinant *E. coli* was using 5%(v/v) inoculum concentration and 20 g/L glucose cultivating in LB medium at 30°C.

iv. Incorporation of PHB biosynthesis pathway and *pgi* deletion strain can only recover cell growth from the reducing power imbalance but not promote any extra PHB production from glucose. The maximum CDM obtained was 7.8±0.5 g/L with 72.4%wt PHB content in 48 hours of cultivation. On the contrary, by using crude glycerol as a sole carbon source, the *pgi* deletion strain can grow better reaching the maximum CDM of 5.5±0.1 g/L with 61.9%wt PHB content.

v. Introduction of PHB biosynthesis pathway to *edd* deletion strain greatly fastened the PHB accumulation process up to 24-30 hours with efficient amount of PHB production. The maximum CDM of *edd* deletion strain was 8.1±0.4 g/L with 93±2.3%wt PHB content in 30 hours of cultivation.

vi. Cultivation of *E. coli* strain JW18401 harboring pBSKCAB_{A-04} in a 10-L fermenter with fed-batch fermentation was observed. Due to the limitation of LB

medium, the scale-up of PHB production could be improved by using M9 medium for fed-batch cultivation.

vii. The *edd* deletion strain had its CDM of 4.9±0.1 g/L with 76.9%wt PHB in 48 hours feeding on crude glycerol waste from biodiesel industry.

viii. The total 9-32 mol% 3HV of P(3HB-co-3HV) with the PHAs content of 35.95-74.62 %wt was achieved from 0.5-2 g/L propionate salt by *edd* deletion strain.

ix. With the ability to accumulate PHB within a short cultivation and ability to utilize cheap carbon, *E. coli* strain JW18401 represented a promising candidate for PHAs production in future trend.

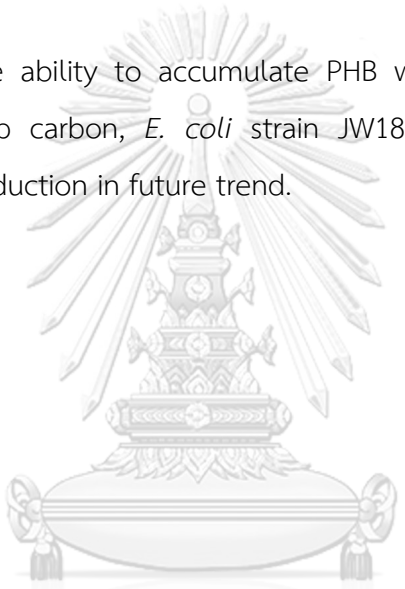

APPENDIX 1

Culture medium

Nutrient Broth (NB) medium

Peptone	5 g
Beef extract	3 g

Dissolve all components in ddH_2O to 1 L and adjust pH to 7.0 with NaOH or HCl. Sterile by autoclaving at 121°C, 15 lb/in^2 pressurized for 15 minutes. Add 15 g/L agar for NB agar medium.

Luria-Bertani (LB) medium

Sodium Chloride	10 g
Yeast extract	5 g
Tryptone Type-1 (Casitose Type-I)	10 g

Dissolve all components in ddH_2O to 1 L and adjust pH to 7.0 with NaOH or HCl. Sterile by autoclaving at 121°C, 15 lb/in^2 pressurized for 15 minutes. Add 15 g/L agar for LB agar medium.

APPENDIX 2

E. coli competent cell

TSS buffer

Polyethylene glycol (PEG) MW 3350	5 g
$MgCl_2 \cdot 6H_2O$	0.3 g
Dimethyl sulfoxide (DMSO)	2.5 mL

Dissolve polyethylene glycol MW 3350 and $MgCl_2 \cdot 6H_2O$ in 40 mL LB medium, add DMSO and adjust the final volume to 50 mL with LB medium. Sterile by 0.22 µm PTFE hydrophilic syringe filter.

SOC medium

Tryptone Type-1 (Casitose Type-I)	10 g
Yeast extract	5 g
Sodium Chloride	0.584 g
Potassium Chloride	0.186 g
Magnesium Sulfate	2.4 g

Dissolve all components in ddH_2O to 1 L and adjust pH to 7.0 with NaOH or HCl. Sterile by autoclaving at 121°C, 15 lb/in^2 pressurized for 15 minutes. Add filter sterilized glucose to final concentration 0.4% (w/v).

APPENDIX 3

Agarose gel electrophoresis

50X Tris-Acetate-EDTA (TAE) buffer

Tris base	242 g
EDTA	18.6 g
Gracial Acetic acid	57 mL

Dissolve all components in ddH_2O to 1 L and dilute the solution to 1X with ddH_2O prior use.

1.0% Agarose gel

Agarose	1 g
1X TAE buffer	100 ml

Dissolve agarose in 1X TAE buffer and heat until it becomes homogeneous prior use.

APPENDIX 4

Specific growth rate of *Escherichia coli* strain K12, JW18401 and JW39851

The specific growth rate is defined as the rate of increase of biomass of a cell population per unit of biomass concentration as mentioned in equation [1]. By plotting the natural logarithm of OD_{600} against time, specific growth rate is calculated with the slope of the graph.

Specific growth rate of *E. coli* K12 cultivated in LB medium supplemented with various concentration (0-20 g/L) of glucose at 37°C

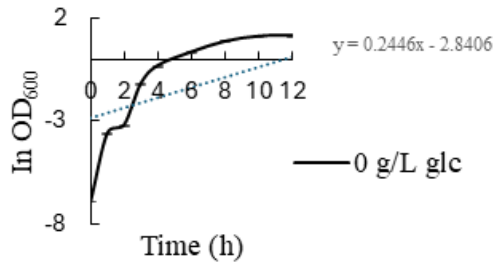

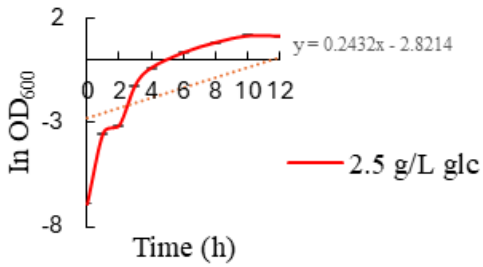

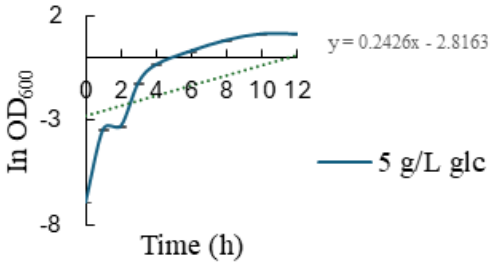

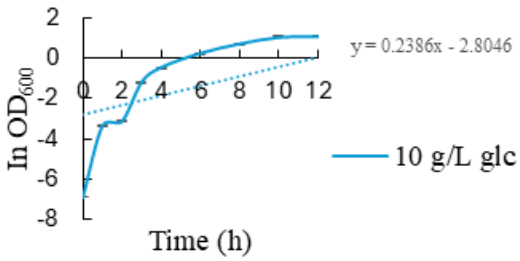

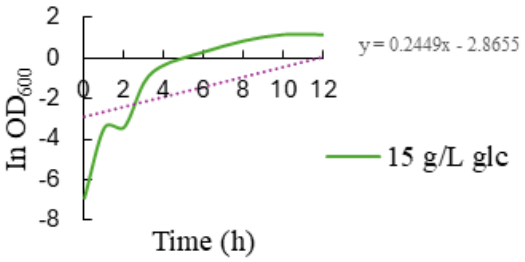

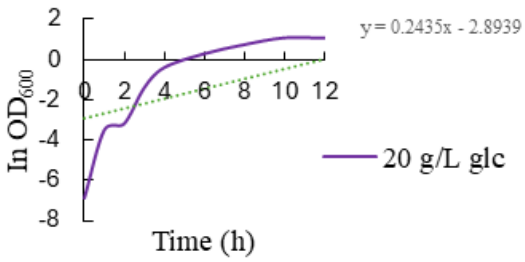

Specific growth rate of *E. coli* JW39851 cultivated in LB medium supplemented with various concentration (0-20 g/L) of glucose at 37°C

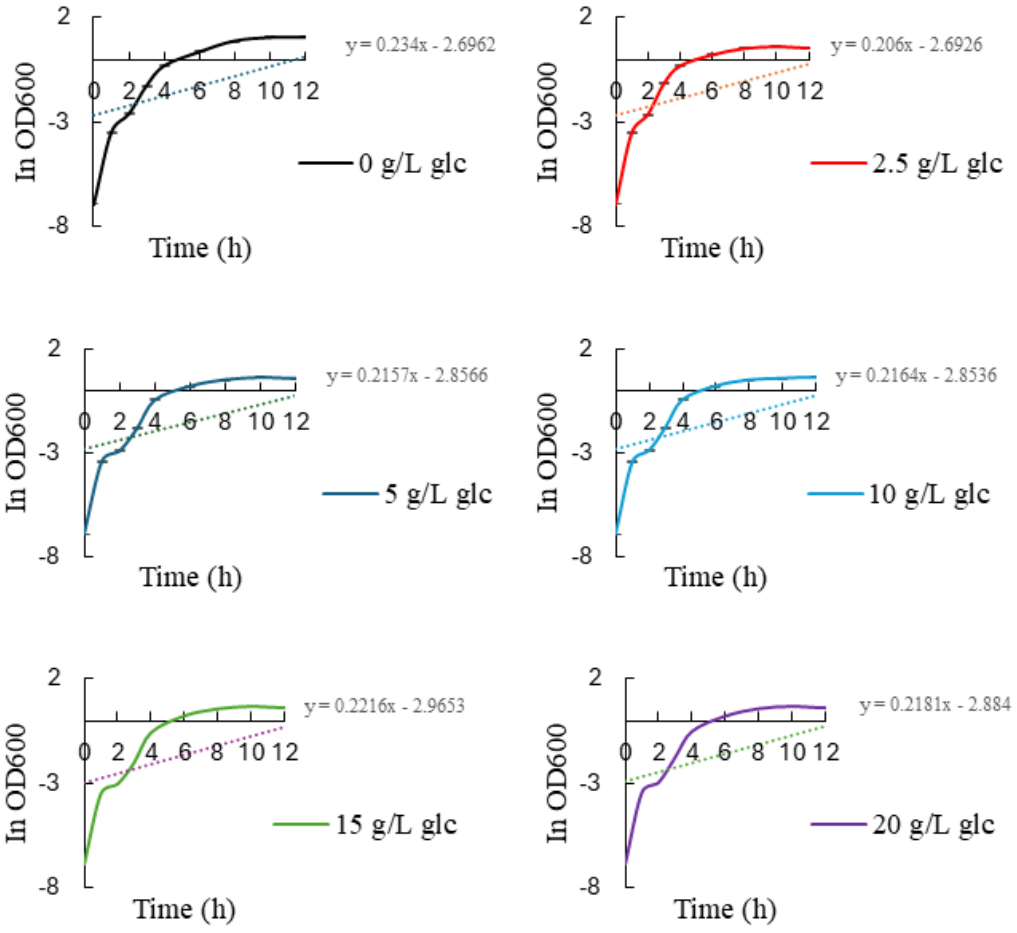

Specific growth rate of *E. coli* JW18401 cultivated in LB medium supplemented with various concentration (0-20 g/L) of glucose at 37°C

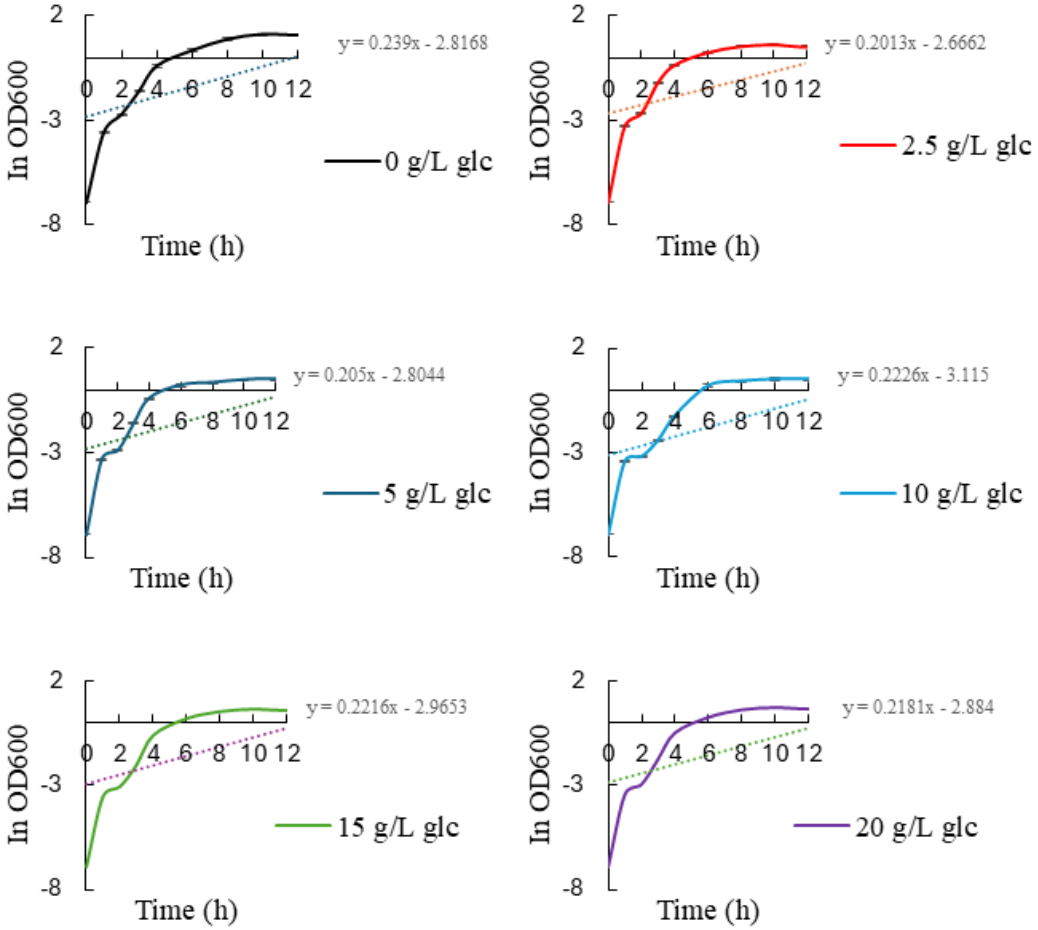

APPENDIX 5

Nucleotide sequence of *phaCAB* operon from *C. necator* A-04 in pBSKCAB$_{A-04}$ obtained from sequencing analysis (U2Bio., Co., Ltd., Bangkok, Thailand)

>pBSKCABA04

TGTGCTCGGTGATCGCCATCATCAGCGCCACGTAGAGCCAGCCAATGGCCACGATGTACATC
AAAAATTCATCCTTCTCGCCTATGCTCTGGGGCCTCGGCAGATGCGAGCGCTGCATACCGTC
CGGTAGGTCGGGAAGCGTGCAGTGCCGAGGCGGATTCCCGCATTGACAGCGCGTGCGTTGCA
AGGCAACAATGGACTCAAATGTCTCGGAATCGCTGACGATTCCCAGGTTTCTCCGGCAAGCA
TAGCGCATGGCGTCTCCATGCGAGAATGTCGCGCTTGCCGGATAAAAGGGGAGCCGCTATCG
GAATGGACGCAAGCCACGGCCGCAGCAGGTGCGGTCGAGGGCTTCCAGCCAGTTCCAGGGCA
GATGTGCCGGCAGACCCTCCCGCTTTGGGGGAGGCGCAAGCCGGGTCCATTCGGATAGCATC
TCCCCATGCAAAGTGCCGGCCAGGGCAATGCCCGGAGCCGGTTCGAATAGTGACGGCAGAGA
GACAATCAAATC**ATGGCGACCGGCAAAGGCGCGGCAGCTTCCACGCAGGAAGGCAAGTCCCA**
ACCATTCAAGGTCACGCCGGGGCCATTCGATCCAGCCACATGGCTGGAATGGTCCCGCCAGT
GGCAGGGCACTGAAGGCAACGGCCACGCGGCCGCGTCCGGCATTCCGGGCCTGGATGCGCTG
GCAGGCGTCAAGATCGCGCCGGCGCAGCTGGGTGATATCCAGCAGCGCTACATGAAGGACTT
CTCAGCGCTGTGGCAGGCCATGGCCGAGGGCAAGGCCGAGGCCACCGGTCCGCTGCACGACC
GGCGCTTCGCCGGCGACGCATGGCGCACCAACCTCCCATATCGCTTCGCTGCCGCGTTCTAC
CTGCCCAATGCGCGCGCCTTGACCGAGCTGGCCGATGCCGTCGAGGCCGATGCCAAGACCCG
CCAGCGCATCCGCTTCGCGATCTCGCAATGGGTCGATGCGATGTCGCCCGCCAACTTCCTTG
CCACCAATCCCGAGGCGCAGCGCCTGCTGATCGAGTCGGGCGGCGAATCGCTGCGTGCCGGC
GTGCGCAACATGATGGAAGACCTGACACGCGGCAAGATCTCGCAGACCGACGAGAGCGCGTT
TGAGGTCGGCCGCAATGTCGCGGTGACCGAAGGCGCCGTGGTCTTCGAGAACGAGTACTTCC
AGCTGTTGCAGTACAAGCCGCTGACCGACAAGGTGCACGCGCGCCCGCTGCTGATGGTGCCG
CCGTGCATCAACAAGTACTACATCCTGGACCTGCAGCCGGAGAGCTCGCTGGTGCGCCATGT
GGTGGAGCAGGGACATACGGTGTTTCTGGTGTCGTGGCGCAATCCGGACGCCAGCATGGCCG
GCAGCACCTGGGACGACTACATCGAGCACGCGGCCATCCGCGCCATCGAAGTCGCGCGCGAC
ATCAGCGGCCAGGACAAGATCAACGTGCTCGGCTTCTGCGTGGGCGGCACCATTGTCTCGAC
CGCGCTGGCGGTGCTGGCCGCGCGCGGCGAGCACCCGGCCGCCAGCGTCACGCTGCTGACCA
CGCTGCTGGACTTTGCCGACACGGGCATCCTCGACGTCTTTGTCGACGAGGGCCATGTGCAG
TTGCGCGAGGCCACGCTGGGCGGCGCCGGCGCGCCGTGCGCGCTGCTGCGCGGCCTTGA
GCTGGCCAATACCTTCTCGTTCTTGCGCCCGAACGACCTGGTGTGGAACTACGTGGTCGACA
ACTACCTGAAGGGCAACACGCCGGTGCCGTTCGACCTGCTGTTCTGGAACGGCGACGCCACC
AACCTGCCGGGGCCGTGGTACTGCTGGTACCTGCGCCACACCTACCTGCAGAACGAGCTCAA
GGTACCGGGCAAGCTGACCGTGTGCGGCGTGCCGGTGGACCTGGCCAGCATCGACGTGCCGA
CCTATATCTACGGCTCGCGCGAAGACCATATCGTGCCGTGGACCGCGGCCTATGCCTCGACC
GCGCTGCTGGCGAACAAGCTGCGCTTCGTGCTGGGTGCGTCGGGCCATATCGCCGGTGTGAT
CAACCCGCCGGCCAAGAACAAGCGCAGCCACTGGACTAACGATGCGCTGCCGGAGTCGCCGC
AGCAATGGCTGGCCGGCGCCATCGAGCATCACGGCAGCTGGTGGCCGGACTGGACCGCATGG
CTGGCCGGGCAGGCCGGCGCGAAACGCGCCGCGCCCGCCAACTATGGCAATGCGCGCTATCG
CGCAATCGAACCCGCGCCTGGGCGATACGTCAAAGCCAAGGCATGACGCTTGCATGAGTGCC
GGCGTGCGTCATGCACGGCGCCGGCAGGCCTGCAGGTTCCCTCCCGTTTCCATTGAAAGGAC
TACACA**ATGACTGACGTTGTCATCGTATCCGCCGCCCGCACCGCGGTCGGCAAGTTTGGCGG**
CTCGCTGGCCAAGATCCCGGCACCGGAACTGGGTGCCGTGGTCATCAAGGCCGCGCTGGAGC
GCGCCGGCGTCAAGCCGGAGCAGGTGAGCGAAGTCATCATGGGCCAGGTGCTGACCGCCGGT
TCGGGCCAGAACCCCGCACGCCAGGCCGCGATCAAGGCCGGCCTGCCGGCGATGGTGCCGGC
CATGACCATCAACAAGGTGTGCGGCTCGGGCCTGAAGGCCGTGATGCTGGCCGCCAACGCGA
TCATGGCGGGCGACGCCGAGATCGTGGTGGCCGGCGGCCAGGAAAACATGAGCGCCGCCCCG

CACGTGCTGCCGGGCTCGCGCGATGGTTTCCGCATGGGCGATGCCAAGCTGGTCGACACCAT
GATCGTCGACGGCCTGTGGGACGTGTACAACCAGTACCACATGGGCATCACCGCCGAGAACG
TGGCCAAGGAATACGGCATCACACGCGAGGCGCAGGATGAGTTCGCCGTCGGCTCGCAGAAC
AAGGCCGAAGCCGCGCAGAAGGCCGGCAAGTTTGACGAAGAGATCGTCCCGGTGCTGATCCC
GCAGCGCAAGGGCGACCCGGTGGCCTTCAAGACCGACGAGTTCGTGCGCCAGGGCGCCACGC
TGGACAGCATGTCCGGCCTCAAGCCCGCCTTCGACAAGGCCGGCACGGTGACCGCGGCCAAC
GCCTCGGGCCTGAACGACGGCGCCGCCGCGGTGGTGGTGATGTCGGCGGCCAAGGCCAAGGA
ACTGGGCCTGACCCCGCTGGCCACGATCAAGAGCTATGCCAACGCCGGTGTCGATCCCAAGG
TGATGGGCATGGGCCCGGTGCCGGCCTCCAAGCGCGCCCTGTCGCGCGCCGAGTGGACCCCG
CAAGACCTGGACCTGATGGAGATCAACGAGGCCTTTGCCGCGCAGGCGCTGGCGGTGCACCA
GCAGATGGGCTGGGACACCTCCAAGGTCAATGTGAACGGCGGCGCCATCGCCATCGGCCACC
CGATCGGCGCGTCGGGCTGCCGTATCCTGGTGACGCTGCTGCACGAGATGAAGCGCCGTGAC
GCGAAGAAGGGCCTGGCCTCGCTGTGCATCGGCGGCGGCATGGGCGTGGCGCTGGCAGTCGA
GCGCAAATAAGGAAGGGGTTTTCCGGGGCCGCGCGCGGTTGGCGCGGACCCGGCGACGATAA
CGAAGCCAATCAAGGAGTGGAC**ATG**ACTCAGCGCATTGCGTATGTGACCGGCGGCATGGGTG
GTATCGGAACCGCCATTTGCCAGCGGCTGGCCAAGGATGGCTTTCGTGTGGTGGCCGGTTGC
GGCCCCAACTCGCCGCGCCGCGAAAAGTGGCTGGAGCAGCAGAAGGCCCTGGGCTTCGATTT
CATTGCCTCGGAAGGCAATGTGGCTGACTGGGACTCGACCAAGACCGCATTCGACAAGGTCA
AGTCCGAGGTCGGCGAGGTTGATGTGCTGATCAACAACGCCGGTATCACCCGCGACGTGGTG
TTCCGCAAGATGACCCGCGCCGACTGGGATGCGGTGATCGACACCAACCTGACCTCGCTGTT
CAACGTCACCAAGCAGGTGATCGACGGCATGGCCGACCGTGGCTGGGGCCGCATCGTCAACA
TCTCGTCGGTGAACGGGCAGAAGGGCCAGTTCGGCCAGACCAACTACTCCACCGCCAAGGCC
GGCCTGCATGGCTTCACCATGGCACTGGCGCAGGAAGTGGCGACCAAGGGCGTGACCGTCAA
CACGGTCTCTCCGGGCTATATCGCCACCGACATGGTCAAGGCGATCCGCCAGGACGTGCTCG
ACAAGATCGTCGCGACGATCCCGGTCAAGCGCCTGGGCCTGCCGGAAGAGATCGCCTCGATC
TGCGCCTGGTTGTCGTCGGAGGAGTCCGGTTTCTCGACCGGCGCCGACTTCTCGCTCAACGG
CGGCCTGCATATGGGCTGACCTGCCGGCCTGGTTCAACCAGTCGGCAGCCGGCGCTGG

APPENDIX 6

Standard curve for PHAs quantification by gas-chromatography

Ratio area PHB to benzoic acid	Ratio area PHV to benzoic acid	Total PHAs (g/L)	PHB (g/L)	PHV (g/L)
0	0	0	0	0
0.46217	0.08171	2	1.92	0.08
0.79945	0.12999	4	3.84	0.16
1.24155	0.20314	6	5.76	0.24
1.60437	0.25812	8	7.68	0.32
1.8138	0.29263	10	9.6	0.4

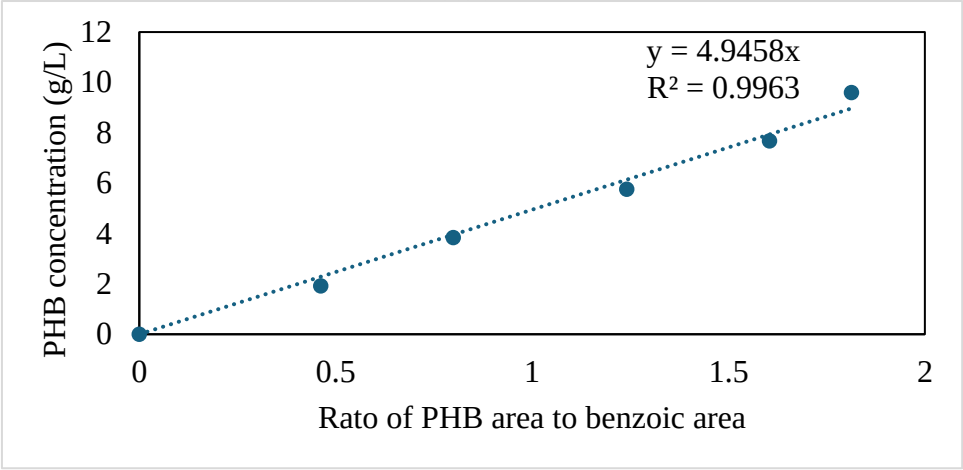

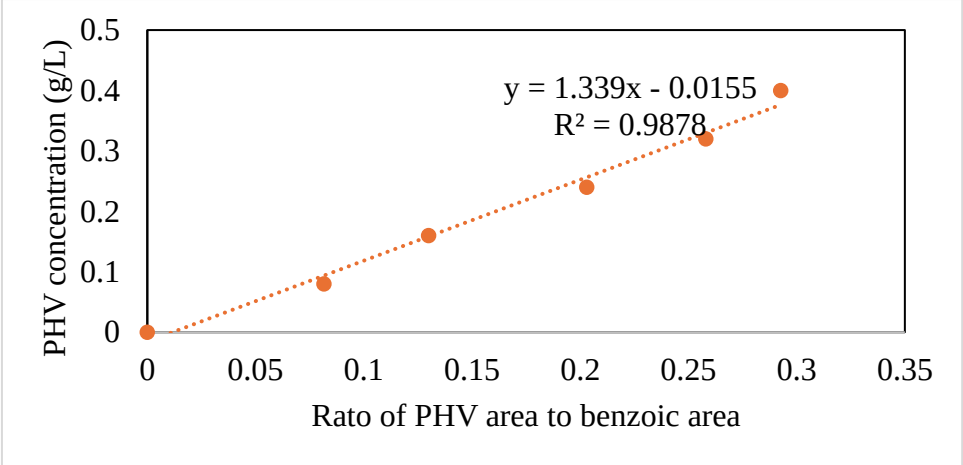

APPENDIX 7

Effect of temperature on PHB production in recombinant *E. coli* strain JW18401, JW39851 and K12 harboring pBSK*CAB*$_{A-04}$ cultivated in LB medium with and without 20 g/L glucose for 24 hours

E. coli strain	Initial glucose concentration (g/L)	Temp (°C)	CDM (g/L)	RCM (g/L)	Consumed glucose concentration (g/L)	PHB (g/L)	PHB content (%wt)
JW18401	20	30	3.97 ± 0.17	1.06 ± 0.33	5.32 ± 0.35	2.90 ± 0.18	73.2 ± 4.5
JW39851	20	30	3.20 ± 0.29	1.27 ± 0.38	4.11 ± 0.22	1.93 ± 0.15	60.2 ± 4.6
K12	20	30	3.30 ± 0.29	0.79 ± 0.35	5.40 ± 0.31	2.51 ± 0.13	76.0 ± 4.0
JW18401	0	30	0.77 ± 0.05	0.77 ± 0.05	0	0	0
JW39851	0	30	0.47 ± 0.05	0.47 ± 0.05	0	0	0
K12	0	30	0.93 ± 0.05	0.93 ± 0.05	0	0	0
JW18401	20	37	1.40 ± 0.22	0.77 ± 0.24	2.27 ± 0.80	0.62 ± 0.03	44.8 ± 2.2
JW39851	20	37	1.63 ± 0.13	0.77 ± 0.21	2.45 ± 0.7	0.86 ± 0.09	52.9 ± 5.3
K12	20	37	1.83 ± 0.21	0.93 ± 0.3	3.60 ± 0.34	0.90 ± 0.09	49.3 ± 4.9
JW18401	0	37	1.27 ± 0.05	1.27 ± 0.05	0	0	0
JW39851	0	37	1.03 ± 0.05	1.03 ± 0.05	0	0	0
K12	0	37	1.43 ± 0.09	1.43 ± 0.09	0	0	0

APPENDIX 8

Effect of inoculum concentration on PHB production in recombinant *E. coli* strain K12 harboring pBSK*CAB*$_{A-04}$ cultivated at 30°C in LB medium containing 20 g/L glucose for 24 hours

Cultivation time (h)	CDM (g/L)	RCM (g/L)	Consumed glucose concentration (g/L)	PHB (g/L)	PHB content (%wt)
1% inoculum					
6	1.07 ± 0.31	1.03 ± 0.31	n/a	0.04 ± 0.00	3.5 ± 0.2
24	2.60 ± 0.25	1.52 ± 0.25	9.73 ± 0.06	1.08 ± 0.02	41.5 ± 0.8
3% inoculum					
6	1.53 ± 0.17	1.37 ± 0.17	n/a	0.16 ± 0.00	10.5 ± 0.3
24	3.47 ± 0.17	1.54 ± 0.17	9.86 ± 0.05	1.93 ± 0.04	55.5 ± 1.2
5% inoculum					
6	1.43 ± 0.17	1.20 ± 0.17	n/a	0.23 ± 0.01	16.3 ± 0.5
24	3.53 ± 0.13	1.44 ± 0.12	10.27 ± 0.03	2.09 ± 0.03	59.2 ± 0.7
10% inoculum					
6	1.50 ± 0.08	1.09 ± 0.08	n/a	0.41 ± 0.02	27.1 ± 1.1
24	3.20 ± 0.08	1.40 ± 0.08	11.75 ± 0.32	1.80 ± 0.02	56.2 ± 0.6

APPENDIX 9

Effect of glucose concentration on PHB production in recombinant *E. coli* strain K12 harboring pBSK*CAB*$_{A-04}$ using 5%(v/v) inoculum concentration cultivated at 30°C in LB medium for 48 hour

Cultivation time (h)	CDM (g/L)	RCM (g/L)	Consumed glucose concentration (g/L)	PHB (g/L)	PHB content (%wt)
10 g/L glucose					
6	1.63 ± 0.09	1.58 ± 0.09	n/a	0.05 ± 0.01	3.3 ± 0.3
24	2.87 ± 0.05	2.11 ± 0.36	7.87 ± 0.02	0.76 ± 0.03	26.5 ± 0.9
48	2.70 ± 0.14	1.66 ± 0.14	7.95 ± 0.04	1.04 ± 0.02	38.7 ± 0.6
20 g/L glucose					
6	1.50 ± 0.08	1.41 ± 0.08	n/a	0.09 ± 0.00	6.0 ± 0.4
24	2.67 ± 0.19	1.47 ± 0.19	10.39 ± 0.08	1.20 ± 0.03	45.0 ± 2.7
48	2.83 ± 0.17	1.34 ± 0.17	13.78 ± 0.39	1.50 ± 0.17	48.9 ± 3.5
30 g/L glucose					
6	1.23 ± 0.17	1.14 ± 0.17	n/a	0.09 ± 0.01	7.6 ± 0.1
24	2.80 ± 0.14	1.47 ± 0.14	11.64 ± 0.20	1.33 ± 0.02	47.6 ± 1.2
48	2.70 ± 0.08	1.40 ± 0.08	12.30 ± 0.24	1.30 ± 0.03	48.2 ± 3.9
40 g/L glucose					
6	0.90 ± 0.16	0.87 ± 0.08	n/a	0.03 ± 0.01	2.1 ± 0.1
24	2.07 ± 0.13	1.62 ± 0.13	5.89 ± 0.45	0.44 ± 0.03	21.4 ± 1.7
48	2.23 ± 0.19	1.85 ± 0.17	7.09 ± 0.30	0.38 ± 0.29	23.3 ± 1.8

APPENDIX 10

PHB production by recombinant from recombinant *E. coli* strain JW18401, JW39851 and K12 harboring pBSK$CAB_{A\text{-}04}$ cultivated at 30°C for 48 hours supplemented with 20 g/L glucose as the sole carbon source in flask scale

Time courses of PHB production from recombinant *E. coli* strain JW18401, JW39851 and K12 harboring pBSK$CAB_{A\text{-}04}$ supplemented with 20 g/L glucose as the sole carbon source in flask scale

Time (h)	CDM (g/L)	PHB (g/L)	RCM (g/L)	PHB content (%wt)	Glucose (g/L)	Productivity (g/L.h)
JW18401						
6	0.70 ± 0.14	0.12 ± 0.03	0.59 ± 0.10	16.3 ± 1.9	20.0 ± 0.5	0.02
12	3.23 ± 0.23	2.47 ± 0.19	0.76 ± 0.19	76.5 ± 1.8	16.0 ± 0.6	0.21
24	7.50 ± 0.54	6.82 ± 0.23	0.68 ± 0.50	91.2 ± 5.2	6.6 ± 0.4	0.28
30	8.13 ± 0.37	7.55 ± 0.39	0.57 ± 0.33	93.0 ± 2.3	4.0 ± 0.5	0.25
36	8.34 ± 0.57	7.24 ± 0.65	1.00 ± 0.88	87.0 ± 3.5	0	0.20
48	9.33 ± 0.51	7.58 ± 0.52	1.75 ± 0.47	81.1 ± 0.5	0	0.16
JW39851						
6	0.46 ± 0.26	0.02 ± 0.00	0.44 ± 0.12	4.2 ± 1.3	20.0 ± 0.0	0.00
12	2.52 ± 0.51	0.64 ± 0.12	1.88 ± 0.46	25.6 ± 2.2	17.9 ± 0.6	0.05
24	5.06 ± 0.40	3.06 ± 0.24	2.00 ± 0.18	60.3 ± 3.2	7.5 ± 1.2	0.13
30	6.49 ± 0.49	4.50 ± 0.51	2.00 ± 0.42	69.2 ± 3.9	4.1 ± 0.1	0.15
36	7.63 ± 0.73	5.11 ± 0.55	2.53 ± 0.71	66.9 ± 3.4	0	0.14
48	7.83 ± 0.53	5.67 ± 0.46	2.16 ± 0.40	72.3 ± 2.7	0	0.12
K12						
6	1.84 ± 0.43	0.18 ± 0.06	1.67 ± 0.33	9.6 ± 2.0	20.0 ± 1.3	0.03
12	5.45 ± 0.23	3.54 ± 0.10	1.91 ± 0.15	65.0 ± 0.9	15.9 ± 0.6	0.30
24	6.85 ± 0.38	5.04 ± 0.42	1.81 ± 0.33	73.5 ± 2.8	10.5 ± 0.6	0.21
30	9.72 ± 0.52	7.10 ± 0.67	2.61 ± 0.31	73.1 ± 6.2	4.3 ± 0.2	0.24
36	9.63 ± 0.68	7.07 ± 1.06	2.56 ± 0.57	73.2 ± 8.6	4.1 ± 0.1	0.20
48	9.64 ± 0.83	7.34 ± 0.44	2.30 ± 0.80	76.5 ± 2.9	0	0.15

APPENDIX 11

P(3HB-*co*-3HV) production in recombinant recombinant *E. coli* strain JW18401 harboring pBSK$CAB_{A\text{-}04}$ cultivated at 30°C for 48 hours supplemented with 20 g/L total carbon of glucose and sodium propionate salt

Propionate salt concentration	CDM (g/L)	PHB (g/L)	PHV (g/L)	Total PHAs (g/L)	PHB (mol%)	PHV (mol%)	PHB (%wt)	PHV (%wt)	Total PHAs (%wt)	YPS
0	5.16	4.68	0	4.68	100	0	74.6	0	74.6	0.287
0.5	5.50	3.13	0.39	3.52	90.3	9.7	56.8	7.1	63.9	0.239
1	6.33	2.48	0.64	3.12	81.8	18.2	39.1	10.1	49.2	0.189
2	5.73	2.06	1.14	3.20	67.7	32.3	36.0	20.0	56.0	0.205

REFERENCES

A. L. Wong, P., Cheung, M. K., Lo, W.-H., Chua, H., & Yu, P. H. F. (2004). Investigation of the effects of the types of food waste utilized as carbon source on the molecular weight distributions and thermal properties of polyhydroxybutyrate produced by two strains of microorganisms. *4*(1). https://doi.org/doi:10.1515/epoly.2004.4.1.324 (e-Polymers)

Acuña, J., & Poblete-Castro, I. (2022). Rational engineering of natural polyhydroxyalkanoates producing microorganisms for improved synthesis and recovery. *Microbial biotechnology*, *16*. https://doi.org/10.1111/1751-7915.14109

Ahn, J., Chung, B. K., Lee, D. Y., Park, M., Karimi, I. A., Jung, J. K., & Lee, H. (2011). NADPH-dependent pgi-gene knockout Escherichia coli metabolism producing shikimate on different carbon sources. *FEMS Microbiol Lett*, *324*(1), 10-16. https://doi.org/10.1111/j.1574-6968.2011.02378.x

Alabi, O., Ologbonjaye, K., Awosolu, O., & Alalade, O. (2019). Public and Environmental Health Effects of Plastic Wastes Disposal: A Review. *Journal of Toxicology and Risk Assessment*, *5*. https://doi.org/10.23937/2572-4061.1510021

Aldor, I. S., Kim, S. W., Prather, K. L., & Keasling, J. D. (2002). Metabolic engineering of a novel propionate-independent pathway for the production of poly(3-hydroxybutyrate-co-3-hydroxyvalerate) in recombinant Salmonella enterica serovar typhimurium. *Appl Environ Microbiol*, *68*(8), 3848-3854. https://doi.org/10.1128/aem.68.8.3848-3854.2002

Alias, Z., & Tan, I. K. P. (2005). Isolation of palm oil-utilising, polyhydroxyalkanoate (PHA)-producing bacteria by an enrichment technique. *Bioresource Technology*, *96*(11), 1229-1234. https://doi.org/https://doi.org/10.1016/j.biortech.2004.10.012

Allen, J. R., Torres-Acosta, M. A., Mohan, N., Lye, G. J., & Ward, J. M. (2022). Segregationally stabilised plasmids improve production of commodity chemicals in glucose-limited continuous fermentation. *Microbial Cell Factories*, *21*(1), 229. https://doi.org/10.1186/s12934-022-01958-3

Alsiyabi, A., Brown, B., Immethun, C., Long, D., Wilkins, M., & Saha, R. (2021). Synergistic

experimental and computational approach identifies novel strategies for polyhydroxybutyrate overproduction. *Metab Eng*, *68*, 1-13. https://doi.org/10.1016/j.ymben.2021.08.008

Anbukarasu, P., Sauvageau, D., & Elias, A. (2015). Tuning the properties of polyhydroxybutyrate films using acetic acid via solvent casting. *Sci Rep*, *5*, 17884. https://doi.org/10.1038/srep17884

Anderson, A. J., & Dawes, E. A. (1990). Occurrence, metabolism, metabolic role, and industrial uses of bacterial polyhydroxyalkanoates. *Microbiol Rev*, *54*(4), 450-472. https://doi.org/10.1128/mr.54.4.450-472.1990

Arcos-Hernandez, M. V., Gurieff, N., Pratt, S., Magnusson, P., Werker, A., Vargas, A., & Lant, P. (2010). Rapid quantification of intracellular PHA using infrared spectroscopy: An application in mixed cultures. *Journal of Biotechnology*, *150*(3), 372-379. https://doi.org/https://doi.org/10.1016/j.jbiotec.2010.09.939

Arifin, Y., Sabri, S., Sugiarto, H., Krömer, J. O., Vickers, C. E., & Nielsen, L. K. (2011). Deletion of cscR in Escherichia coli W improves growth and poly-3-hydroxybutyrate (PHB) production from sucrose in fed batch culture. *J Biotechnol*, *156*(4), 275-278. https://doi.org/10.1016/j.jbiotec.2011.07.003

Aristya, G. R., Lin, Y.-J., Chang, J.-S., Chang, J.-J., & Yen, H.-W. (2022). Polyhydroxybutyrate (PHB) production from crude glycerol by genetic engineering of Rhodotorula glutinis. *Bioresource Technology Reports*, *18*, 101048. https://doi.org/https://doi.org/10.1016/j.biteb.2022.101048

Asgari, M., & Masoomi, M. (2013). Tensile and flexural properties of polypropylene/short poly(ethylene terephthalate) fibre composites compatibilized with glycidyl methacrylate and maleic anhydride. *Journal of Thermoplastic Composite Materials*, *28*(3), 357-371. https://doi.org/10.1177/0892705713484748

Assil-Companioni, L., Buchsenschutz, H. C., Solymosi, D., Dyczmons-Nowaczyk, N. G., Bauer, K. K. F., Wallner, S., Macheroux, P., Allahverdiyeva, Y., Nowaczyk, M. M., & Kourist, R. (2020). Engineering of NADPH Supply Boosts Photosynthesis-Driven Biotransformations. *ACS Catal*, *10*(20), 11864-11877. https://doi.org/10.1021/acscatal.0c02601

Assil-Companioni, L., Büchsenschütz, H. C., Solymosi, D., Dyczmons-Nowaczyk, N. G.,

Bauer, K. K. F., Wallner, S., Macheroux, P., Allahverdiyeva, Y., Nowaczyk, M. M., & Kourist, R. (2020). Engineering of NADPH Supply Boosts Photosynthesis-Driven Biotransformations. *ACS Catalysis*, *10*(20), 11864-11877. https://doi.org/10.1021/acscatal.0c02601

Augustine, R., Hasan, A., Patan, N. K., Dalvi, Y. B., Varghese, R., Antony, A., Unni, R. N., Sandhyarani, N., & Moustafa, A.-E. A. (2020). Cerium Oxide Nanoparticle Incorporated Electrospun Poly(3-hydroxybutyrate-co-3-hydroxyvalerate) Membranes for Diabetic Wound Healing Applications. *ACS Biomaterials Science & Engineering*, *6*(1), 58-70. https://doi.org/10.1021/acsbiomaterials.8b01352

Baba, T., Ara, T., Hasegawa, M., Takai, Y., Okumura, Y., Baba, M., Datsenko, K. A., Tomita, M., Wanner, B. L., & Mori, H. (2006). Construction of Escherichia coli K-12 in-frame, single-gene knockout mutants: the Keio collection. *Mol Syst Biol*, *2*, 2006.0008. https://doi.org/10.1038/msb4100050

Balaji, A. B., Pakalapati, H., Khalid, M., Walvekar, R., & Siddiqui, H. (2018). 1 - Natural and synthetic biocompatible and biodegradable polymers. In N. G. Shimpi (Ed.), *Biodegradable and Biocompatible Polymer Composites* (pp. 3-32). Woodhead Publishing. https://doi.org/https://doi.org/10.1016/B978-0-08-100970-3.00001-8

Barham, P. J., Keller, A., Otun, E. L., & Holmes, P. A. (1984). Crystallization and morphology of a bacterial thermoplastic: poly-3-hydroxybutyrate. *Journal of Materials Science*, *19*(9), 2781-2794. https://doi.org/10.1007/BF01026954

Berney, M., Greening, C., Conrad, R., Jacobs, W. R., & Cook, G. M. (2014). An obligately aerobic soil bacterium activates fermentative hydrogen production to survive reductive stress during hypoxia. *Proceedings of the National Academy of Sciences*, *111*(31), 11479-11484. https://doi.org/doi:10.1073/pnas.1407034111

Berridge, M. V., Herst, P. M., & Prata, C. (2023). Cellular reductive stress: Is plasma membrane electron transport an evolutionarily-conserved safety valve? *Redox Biochemistry and Chemistry*, *5-6*, 100016. https://doi.org/https://doi.org/10.1016/j.rbc.2023.100016

Bhattacharyya, A., Pramanik, A., Maji, S. K., Haldar, S., Mukhopadhyay, U. K., & Mukherjee, J. (2012). Utilization of vinasse for production of poly-3-(hydroxybutyrate-co-hydroxyvalerate) by Haloferax mediterranei. *AMB Express*,

2(1), 34. https://doi.org/10.1186/2191-0855-2-34

Bhuyan, S., Yadav, M., Giri, S. J., Begum, S., Das, S., Phukan, A., Priyadarshani, P., Sarkar, S., Jayswal, A., Kabyashree, K., Kumar, A., Mandal, M., & Ray, S. K. (2023). Microliter spotting and micro-colony observation: A rapid and simple approach for counting bacterial colony forming units. *Journal of Microbiological Methods*, *207*, 106707. https://doi.org/https://doi.org/10.1016/j.mimet.2023.106707

Bidlas, E., Du, T., & Lambert, R. J. (2008). An explanation for the effect of inoculum size on MIC and the growth/no growth interface. *Int J Food Microbiol*, *126*(1-2), 140-152. https://doi.org/10.1016/j.ijfoodmicro.2008.05.023

Blunt, W., Sparling, R., Gapes, D. J., Levin, D. B., & Cicek, N. (2018). The role of dissolved oxygen content as a modulator of microbial polyhydroxyalkanoate synthesis. *World J Microbiol Biotechnol*, *34*(8), 106. https://doi.org/10.1007/s11274-018-2488-6

Bombicz, P. (2022). Crystallization: from molecules to crystal structures. *Crystallography Reviews*, *28*(2-3), 67-69. https://doi.org/10.1080/0889311X.2022.2130587

Boontip, T., Waditee-Sirisattha, R., Honda, K., & Napathorn, S. (2020). *Enhanced functional expression of the polyhydroxyalkanoate synthase gene from Cupriavidus necator A-04 using a cold-shock promoter for efficient poly(3-hydroxybutyrate) production in Escherichia coli*. https://doi.org/10.21203/rs.3.rs-28241/v2

Boontip, T., Waditee-Sirisattha, R., Honda, K., & Napathorn, S. C. (2021). Strategies for Poly(3-hydroxybutyrate) Production Using a Cold-Shock Promoter in Escherichia coli. *Front Bioeng Biotechnol*, *9*, 666036. https://doi.org/10.3389/fbioe.2021.666036

Brämer, C. O., Vandamme, P., da Silva, L. F., Gomez, J. G., & Steinbüchel, A. (2001). Polyhydroxyalkanoate-accumulating bacterium isolated from soil of a sugar-cane plantation in Brazil. *International Journal of Systematic and Evolutionary Microbiology*, *51*(5), 1709-1713. https://doi.org/https://doi.org/10.1099/00207713-51-5-1709

Braunegg, G., Lefebvre, G., & Genser, K. F. (1998). Polyhydroxyalkanoates, biopolyesters from renewable resources: Physiological and engineering aspects. *Journal of*

Biotechnology, *65*(2), 127-161. https://doi.org/https://doi.org/10.1016/S0168-1656(98)00126-6

Braunegg, G., Sonnleitner, B., & Lafferty, R. M. (1978). A rapid gas chromatographic method for the determination of poly-β-hydroxybutyric acid in microbial biomass. *European journal of applied microbiology and biotechnology*, *6*(1), 29-37. https://doi.org/10.1007/BF00500854

Bresan, S., Sznajder, A., Hauf, W., Forchhammer, K., Pfeiffer, D., & Jendrossek, D. (2016). Polyhydroxyalkanoate (PHA) Granules Have no Phospholipids. *Scientific Reports*, *6*, 26612. https://doi.org/10.1038/srep26612

Brzostowicz, P., Blasko, M., & Rouvière, P. (2002). Identification of two gene clusters involved in cyclohexanone oxidation in Brevibacterium epidermidis strain HCU. *Applied Microbiology and Biotechnology*, *58*(6), 781-789. https://doi.org/10.1007/s00253-002-0968-x

Bugnicourt, E., Cinelli, P., Lazzeri, A., & Alvarez, V. (2015). Main Characteristics, Properties, Improvements, and Market Data of Polyhydroxyalkanoates. In (pp. 899-927). https://doi.org/10.1201/b19600-25

Bylund, J., Brown, K. L., Movitz, C., Dahlgren, C., & Karlsson, A. (2010). Intracellular generation of superoxide by the phagocyte NADPH oxidase: how, where, and what for? *Free Radic Biol Med*, *49*(12), 1834-1845. https://doi.org/10.1016/j.freeradbiomed.2010.09.016

Canonaco, F., Hess, T. A., Heri, S., Wang, T., Szyperski, T., & Sauer, U. (2001). Metabolic flux response to phosphoglucose isomerase knock-out in Escherichia coli and impact of overexpression of the soluble transhydrogenase UdhA. *FEMS Microbiology Letters*, *204*(2), 247-252. https://doi.org/10.1111/j.1574-6968.2001.tb10892.x

Cánovas, V., Garcia-Chumillas, S., Monzó, F., Simó-Cabrera, L., Fernández-Ayuso, C., Pire, C., & Martínez-Espinosa, R. M. (2021). Analysis of Polyhydroxyalkanoates Granules in Haloferax mediterranei by Double-Fluorescence Staining with Nile Red and SYBR Green by Confocal Fluorescence Microscopy. *Polymers*, *13*(10), 1582. https://www.mdpi.com/2073-4360/13/10/1582

Cao, J.-S., Xu, R.-Z., Luo, J.-Y., Feng, Q., & Fang, F. (2022). Rapid quantification of intracellular polyhydroxyalkanoates via fluorescence techniques: A critical review. *Bioresource Technology*, *350*, 126906. https://doi.org/https://doi.org/10.1016/j.biortech.2022.126906

Caputo, M. R., Shi, C., Tang, X., Sardon, H., Chen, E. Y. X., & Müller, A. J. (2023). Tailoring the Nucleation and Crystallization Rate of Polyhydroxybutyrate by Copolymerization. *Biomacromolecules*, *24*(11), 5328-5341. https://doi.org/10.1021/acs.biomac.3c00808

Chae, T. U., Kim, W. J., Choi, S., Park, S. J., & Lee, S. Y. (2015). Metabolic engineering of Escherichia coli for the production of 1,3-diaminopropane, a three carbon diamine. *Scientific Reports*, *5*(1), 13040. https://doi.org/10.1038/srep13040

Chandel, N. S. (2021). NADPH-The Forgotten Reducing Equivalent. *Cold Spring Harb Perspect Biol*, *13*(6). https://doi.org/10.1101/cshperspect.a040550

Chanprateep, S., Katakura, Y., Visetkoop, S., Shimizu, H., Kulpreecha, S., & Shioya, S. (2008). Characterization of new isolated Ralstonia eutropha strain A-04 and kinetic study of biodegradable copolyester poly(3-hydroxybutyrate-co-4-hydroxybutyrate) production. *J Ind Microbiol Biotechnol*, *35*(11), 1205-1215. https://doi.org/10.1007/s10295-008-0427-5

Chanprateep, S., & Kulpreecha, S. (2006). Production and characterization of biodegradable terpolymer poly(3-hydroxybutyrate-co-3-hydroxyvalerate-co-4-hydroxybutyrate) by Alcaligenes sp. A-04. *Journal of Bioscience and Bioengineering*, *101*(1), 51-56. https://doi.org/https://doi.org/10.1263/jbb.101.51

Charusanti, P., Conrad, T. M., Knight, E. M., Venkataraman, K., Fong, N. L., Xie, B., Gao, Y., & Palsson, B. O. (2010). Genetic basis of growth adaptation of Escherichia coli after deletion of pgi, a major metabolic gene. *PLoS Genet*, *6*(11), e1001186. https://doi.org/10.1371/journal.pgen.1001186

Chaukura, N., Gwenzi, W., Bunhu, T., Ruziwa, D. T., & Pumure, I. (2016). Potential uses and value-added products derived from waste polystyrene in developing countries: A review. *Resources, Conservation and Recycling*, *107*, 157-165. https://doi.org/https://doi.org/10.1016/j.resconrec.2015.10.031

Chemler, J. A., Fowler, Z. L., McHugh, K. P., & Koffas, M. A. G. (2010). Improving NADPH

availability for natural product biosynthesis in Escherichia coli by metabolic engineering. *Metabolic Engineering*, *12*(2), 96-104. https://doi.org/https://doi.org/10.1016/j.ymben.2009.07.003

Chen, G.-Q. (2009). Plastics Completely Synthesized by Bacteria: Polyhydroxyalkanoates. In (Vol. 14, pp. 17-37). https://doi.org/10.1007/978-3-642-03287-5_2

Chen, G. Q., & Patel, M. K. (2012). Plastics derived from biological sources: present and future: a technical and environmental review. *Chem Rev*, *112*(4), 2082-2099. https://doi.org/10.1021/cr200162d

Chen, Q., Wang, Q., Wei, G., Liang, Q., & Qi, Q. (2011). Production in Escherichia coli of Poly(3-Hydroxybutyrate-co-3-Hydroxyvalerate) with Differing Monomer Compositions from Unrelated Carbon Sources. *Applied and Environmental Microbiology*, *77*, 4886-4893. https://doi.org/10.1128/AEM.00091-11

Chia, K.-H., Ooi, T.-F., Saika, A., Tsuge, T., & Sudesh, K. (2010). Biosynthesis and characterization of novel polyhydroxyalkanoate polymers with high elastic property by Cupriavidus necator PHB−4 transformant. *Polymer Degradation and Stability*, *95*(12), 2226-2232. https://doi.org/https://doi.org/10.1016/j.polymdegradstab.2010.09.011

Chin, J. W., & Cirino, P. C. (2011). Improved NADPH supply for xylitol production by engineered Escherichia coli with glycolytic mutations. *Biotechnol Prog*, *27*(2), 333-341. https://doi.org/10.1002/btpr.559

Chohan, S. N., & Copeland, L. (1998). Acetoacetyl coenzyme A reductase and polyhydroxybutyrate synthesis in rhizobium (Cicer) sp. Strain CC 1192. *Appl Environ Microbiol*, *64*(8), 2859-2863. https://doi.org/10.1128/aem.64.8.2859-2863.1998

Chou, K.-S., Chang-Ho, H. W. R., & Goodrich, P. R. (1997). Poly(hydroxybutyrate-co-hydroxy-valerate) from swine waste liquor by Azotobacter vinelandii UWD. *Biotechnology Letters*, *19*(1), 7-10. https://doi.org/10.1023/A:1018342332141

Choy, M. (2012). Studies on the mechanism of polyhydroxybutyrate (PHB) granule formation in Ralstonia eutropha H16.

Chung, A.-L., Jin, H.-L., Huang, L.-J., Ye, H.-M., Chen, J.-C., Wu, Q., & Chen, G.-Q. (2011).

Biosynthesis and Characterization of Poly(3-hydroxydodecanoate) by β-Oxidation Inhibited Mutant of Pseudomonas entomophila L48. *Biomacromolecules*, *12*(10), 3559-3566. https://doi.org/10.1021/bm200770m

Chung, C. T., Niemela, S. L., & Miller, R. H. (1989). One-step preparation of competent Escherichia coli: transformation and storage of bacterial cells in the same solution. *Proc Natl Acad Sci U S A*, *86*(7), 2172-2175. https://doi.org/10.1073/pnas.86.7.2172

Cimmino, S., Pace, E. D., Martuscelli, E., & Silvestre, C. (1991). Syndiotactic polystyrene: crystallization and melting behaviour. *Polymer*, *32*(6), 1080-1083. https://doi.org/https://doi.org/10.1016/0032-3861(91)90595-A

Cori, C. F. (1983). Embden and the glycolytic pathway. *Trends in Biochemical Sciences*, *8*(7), 257-259. https://doi.org/https://doi.org/10.1016/0968-0004(83)90353-5

Costa, P., Basaglia, M., Casella, S., Kennes, C., Favaro, L., & Veiga, M. C. (2023). Autotrophic production of polyhydroxyalkanoates using acidogenic-derived H2 and CO2 from fruit waste. *Bioresource Technology*, *390*, 129880. https://doi.org/https://doi.org/10.1016/j.biortech.2023.129880

Datsenko, K. A., & Wanner, B. L. (2000). One-step inactivation of chromosomal genes in Escherichia coli K-12 using PCR products. *Proc Natl Acad Sci U S A*, *97*(12), 6640-6645. https://doi.org/10.1073/pnas.120163297

De, S., James, B., Ji, J., Wasti, S., Zhang, S., Kore, S., Tekinalp, H., Li, Y., Ureña-Benavides, E. E., Vaidya, U., Ragauskas, A. J., Webb, E., Ozcan, S., & Zhao, X. (2023). Biomass-derived composites for various applications. In (pp. 145-196). https://doi.org/10.1016/bs.aibe.2023.01.001

Delamarre, S. C., & Batt, C. A. (2006). Comparative study of promoters for the production of polyhydroxyalkanoates in recombinant strains of Wautersia eutropha. *Applied Microbiology and Biotechnology*, *71*(5), 668-679. https://doi.org/10.1007/s00253-005-0217-1

Demirel, B., Yaraş, A., & ElÇİÇEk, H. (2011). Crystallization Behavior of PET Materials. *Balıkesir Üniversitesi Fen Bilimleri Enstitü Dergisi*, *13*, 26-35.

Doi, Y., Kawaguchi, Y., Koyama, N., Nakamura, S., Hiramitsu, M., Yoshida, Y., & Kimura, H.

(1992). Synthesis and degradation of polyhydroxyalkanoates in Alcaligenes eutrophus. *FEMS Microbiology Letters*, *103*(2), 103-108. https://doi.org/https://doi.org/10.1016/0378-1097(92)90299-4

Doublet, B., Douard, G., Targant, H., Meunier, D., Madec, J.-Y., & Cloeckaert, A. (2008). Antibiotic marker modifications of λ Red and FLP helper plasmids, pKD46 and pCP20, for inactivation of chromosomal genes using PCR products in multidrug-resistant strains. *Journal of Microbiological Methods*, *75*(2), 359-361. https://doi.org/https://doi.org/10.1016/j.mimet.2008.06.010

Doyle, M. P., & Schoeni, J. L. (1984). Survival and growth characteristics of Escherichia coli associated with hemorrhagic colitis. *Appl Environ Microbiol*, *48*(4), 855-856. https://doi.org/10.1128/aem.48.4.855-856.1984

Duncan, E. M., Akbora, H. D., Baldi, P., Beton, D., Broderick, A. C., Cicek, B. A., Crowe-Harland, C., Davey, S., DeSerisy, T., Fuller, W. J., Haywood, J. C., Hsieh, Y. J., Kaya, E., Omeyer, L. C. M., Ozkan, M., Palmer, J. L., Roast, E., Santillo, D., Schneider, M. J.,...Godley, B. J. (2024). Marine turtles as bio-indicators of plastic pollution in the eastern Mediterranean. *Marine Pollution Bulletin*, *201*, 116141. https://doi.org/https://doi.org/10.1016/j.marpolbul.2024.116141

Durner, R., Witholt, B., & Egli, T. (2000). Accumulation of Poly[(R)-3-hydroxyalkanoates] in Pseudomonas oleovorans during growth with octanoate in continuous culture at different dilution rates. *Appl Environ Microbiol*, *66*(8), 3408-3414. https://doi.org/10.1128/aem.66.8.3408-3414.2000

Egan, S. E., Fliege, R., Tong, S., Shibata, A., Wolf, R. E., Jr., & Conway, T. (1992). Molecular characterization of the Entner-Doudoroff pathway in Escherichia coli: sequence analysis and localization of promoters for the edd-eda operon. *J Bacteriol*, *174*(14), 4638-4646. https://doi.org/10.1128/jb.174.14.4638-4646.1992

El-Nahrawy, S. (2009). *Study on poly-β-hydroxybutyrate in some bacteria*

Elhadi, D., Lv, L., Jiang, X.-R., Wu, H., & Chen, G.-Q. (2016). CRISPRi engineering E. coli for morphology diversification. *Metabolic Engineering*, *38*, 358-369. https://doi.org/https://doi.org/10.1016/j.ymben.2016.09.001

Erkske, D., Viskere, I., Dzene, A., Tupureina, V., & Savenkova, L. (2006). Biobased polymer

composites for films and coatings. Proceedings of the Estonian Academy of Sciences,

Faik, P., Kornberg, H. L., & McEvoy-Bowe, E. (1971). Isolation and properties of Escherichia coli mutants defective in 2-keto 3-deoxy 6-phosphogluconate aldolase activity. *FEBS Lett*, *19*(3), 225-228. https://doi.org/10.1016/0014-5793(71)80519-7

Favaro, L., Basaglia, M., & Casella, S. (2019). Improving polyhydroxyalkanoate production from inexpensive carbon sources by genetic approaches: a review. *Biofuels, Bioproducts and Biorefining*, *13*(1), 208-227. https://doi.org/https://doi.org/10.1002/bbb.1944

Fernández, C., & Puig, C. C. (2002). CHANGES IN MELTING BEHAVIOR AND MORPHOLOGY ON ANNEALING OF LINEAR AND BRANCHED POLYETHYLENE. *Journal of Macromolecular Science, Part B*, *41*(4-6), 991-1005. https://doi.org/10.1081/MB-120013078

Ferran, A., Dupouy, V., Toutain, P. L., & Bousquet-Mélou, A. (2007). Influence of inoculum size on the selection of resistant mutants of Escherichia coli in relation to mutant prevention concentrations of marbofloxacin. *Antimicrob Agents Chemother*, *51*(11), 4163-4166. https://doi.org/10.1128/aac.00156-07

Fidler, S., & Dennis, D. (1992). Polyhydroxyalkanoate production in recombinant Escherichia coli. *FEMS Microbiology Letters*, *103*(2), 231-235. https://doi.org/https://doi.org/10.1016/0378-1097(92)90314-E

Findrik Balogová, A., Hudák, R., Tóth, T., Schnitzer, M., Feranc, J., Bakoš, D., & Živčák, J. (2018). Determination of geometrical and viscoelastic properties of PLA/PHB samples made by additive manufacturing for urethral substitution. *J Biotechnol*, *284*, 123-130. https://doi.org/10.1016/j.jbiotec.2018.08.019

Fisk, H. L., West, A. L., Childs, C. E., Burdge, G. C., & Calder, P. C. (2014). The use of gas chromatography to analyze compositional changes of fatty acids in rat liver tissue during pregnancy. *J Vis Exp*(85). https://doi.org/10.3791/51445

Fliege, R., Tong, S., Shibata, A., Nickerson, K. W., & Conway, T. (1992). The Entner-Doudoroff pathway in Escherichia coli is induced for oxidative glucose metabolism via pyrroloquinoline quinone-dependent glucose dehydrogenase.

Appl Environ Microbiol, *58*(12), 3826-3829. https://doi.org/10.1128/aem.58.12.3826-3829.1992

Flores-Sanchez, A., López-Cuellar, M. D. R., Pérez-Guevara, F., López, U., Martín-Bufájer, J., & Vergara Porras, B. (2017). Synthesis of Poly-(R-hydroxyalkanoates) by Cupriavidus necator ATCC 17699 Using Mexican Avocado (Persea americana) Oil as a Carbon Source. *International Journal of Polymer Science*, *2017*, 1-10. https://doi.org/10.1155/2017/6942950

Foreman, J., Demidchik, V., Bothwell, J. H., Mylona, P., Miedema, H., Torres, M. A., Linstead, P., Costa, S., Brownlee, C., Jones, J. D., Davies, J. M., & Dolan, L. (2003). Reactive oxygen species produced by NADPH oxidase regulate plant cell growth. *Nature*, *422*(6930), 442-446. https://doi.org/10.1038/nature01485

Fradkin, J. E., & Fraenkel, D. G. (1971). 2-keto-3-deoxygluconate 6-phosphate aldolase mutants of Escherichia coli. *J Bacteriol*, *108*(3), 1277-1283. https://doi.org/10.1128/jb.108.3.1277-1283.1971

Fraenkel, D. G., & Levisohn, S. R. (1967). Glucose and gluconate metabolism in an Escherichia coli mutant lacking phosphoglucose isomerase. *J Bacteriol*, *93*(5), 1571-1578. https://doi.org/10.1128/jb.93.5.1571-1578.1967

French, C., & Ward, J. M. (1995). Improved production and stability ofE. coli recombinants expressing transketolase for large scale biotransformation. *Biotechnology Letters*, *17*(3), 247-252. https://doi.org/10.1007/BF01190631

Friehs, K. (2004). Plasmid copy number and plasmid stability. *Adv Biochem Eng Biotechnol*, *86*, 47-82. https://doi.org/10.1007/b12440

Fritzsche, K., Lenz, R. W., & Fuller, R. C. (1990). An unusual bacterial polyester with a phenyl pendant group. *Die Makromolekulare Chemie*, *191*(8), 1957-1965. https://doi.org/https://doi.org/10.1002/macp.1990.021910821

Fu, N., Meng, Z., Jiao, T., Luo, X., Tang, Z., Zhu, B., Sui, L., & Cai, X. (2019). P34HB electrospun fibres promote bone regeneration in vivo. *Cell Prolif*, *52*(3), e12601. https://doi.org/10.1111/cpr.12601

Fuhrman, L. K., Wanken, A., Nickerson, K. W., & Conway, T. (1998). Rapid accumulation of intracellular 2-keto-3-deoxy-6-phosphogluconate in an Entner-Doudoroff aldolase mutant results in bacteriostasis. *FEMS Microbiol Lett*, *159*(2), 261-266.

https://doi.org/10.1111/j.1574-6968.1998.tb12870.x

Fukui, T., Ito, M., Saito, T., & Tomita, K. (1987). Purification and characterization of NADP-linked acetoacetyl-CoA reductase from Zoogloea ramigera I-16-M. *Biochim Biophys Acta*, *917*(3), 365-371.

Furrer, P., Hany, R., Rentsch, D., Grubelnik, A., Ruth, K., Panke, S., & Zinn, M. (2007). Quantitative analysis of bacterial medium-chain-length poly([R]-3-hydroxyalkanoates) by gas chromatography. *Journal of Chromatography A*, *1143*(1), 199-206. https://doi.org/https://doi.org/10.1016/j.chroma.2007.01.002

Galán, B., Dinjaski, N., Maestro, B., de Eugenio, L. I., Escapa, I. F., Sanz, J. M., García, J. L., & Prieto, M. A. (2011). Nucleoid-associated PhaF phasin drives intracellular location and segregation of polyhydroxyalkanoate granules in Pseudomonas putida KT2442. *Mol Microbiol*, *79*(2), 402-418. https://doi.org/10.1111/j.1365-2958.2010.07450.x

Gao, Q., Yang, H., Wang, C., Xie, X.-Y., Liu, K.-X., Lin, Y., Han, S.-Y., Zhu, M., Neureiter, M., Lin, Y., & Ye, J.-W. (2022). Advances and trends in microbial production of polyhydroxyalkanoates and their building blocks [Mini Review]. *Frontiers in Bioengineering and Biotechnology*, *10*. https://doi.org/10.3389/fbioe.2022.966598

Gay, M., Cerf, O., & Davey, K. R. (1996). Significance of pre-incubation temperature and inoculum concentration on subsequent growth of Listeria monocytogenes at 14 degrees C. *J Appl Bacteriol*, *81*(4), 433-438. https://doi.org/10.1111/j.1365-2672.1996.tb03530.x

Ge, T., Yang, J., Zhou, S., Wang, Y., Li, Y., & Tong, X. (2020). The Role of the Pentose Phosphate Pathway in Diabetes and Cancer [Review]. *Frontiers in Endocrinology*, *11*. https://www.frontiersin.org/journals/endocrinology/articles/10.3389/fendo.2020.00365

Gebauer, B., & Jendrossek, D. (2006). Assay of poly(3-hydroxybutyrate) depolymerase activity and product determination. *Appl Environ Microbiol*, *72*(9), 6094-6100. https://doi.org/10.1128/aem.01184-06

Gerngross, T., & Martin, D. (1995). Enzyme-catalyzed synthesis of poly [(R)-(-)-3-hydroxybutyrate]: formation of macroscopic granules in vitro. *Proceedings of the*

National Academy of Sciences, *92*(14), 6279-6283.

Gonçalves, S. P. C., Martins-Franchetti, S. M., & Chinaglia, D. L. (2009). Biodegradation of the Films of PP, PHBV and Its Blend in Soil. *Journal of Polymers and the Environment*, *17*(4), 280-285. https://doi.org/10.1007/s10924-009-0150-y

Gorret, N., bin Rosli, S. K., Oppenheim, S. F., Willis, L. B., Lessard, P. A., Rha, C., & Sinskey, A. J. (2004). Bioreactor culture of oil palm (Elaeis guineensis) and effects of nitrogen source, inoculum size, and conditioned medium on biomass production. *J Biotechnol*, *108*(3), 253-263. https://doi.org/10.1016/j.jbiotec.2003.12.009

Grassie, N., Murray, E. J., & Holmes, P. A. (1984). The thermal degradation of poly(-(d)-β-hydroxybutyric acid): Part 2—Changes in molecular weight. *Polymer Degradation and Stability*, *6*(2), 95-103. https://doi.org/https://doi.org/10.1016/0141-3910(84)90075-2

Green, M. R., & Sambrook, J. (2016). Precipitation of DNA with Ethanol. *Cold Spring Harb Protoc*, *2016*(12). https://doi.org/10.1101/pdb.prot093377

Griebel, R., Smith, Z., & Merrick, J. (1968). Metabolism of poly (β-hydroxybutyrate). I. Purification, composition, and properties of native poly (β-hydroxybutyrate) granules from Bacillus megaterium. *Biochemistry*, *7*(10), 3676-3681.

Guitart Font, E., & Sprenger, G. A. (2020). Opening a Novel Biosynthetic Pathway to Dihydroxyacetone and Glycerol in Escherichia coli Mutants through Expression of a Gene Variant (fsaA(A129S)) for Fructose 6-Phosphate Aldolase. *Int J Mol Sci*, *21*(24). https://doi.org/10.3390/ijms21249625

Guo, D., Meng, Y., Jiang, X., & Lu, Z. (2023). Hexokinases in cancer and other pathologies. *Cell Insight*, *2*(1), 100077. https://doi.org/https://doi.org/10.1016/j.cellin.2023.100077

Guzik, M. W., Kenny, S. T., Duane, G. F., Casey, E., Woods, T., Babu, R. P., Nikodinovic-Runic, J., Murray, M., & O'Connor, K. E. (2014). Conversion of post consumer polyethylene to the biodegradable polymer polyhydroxyalkanoate. *Applied Microbiology and Biotechnology*, *98*(9), 4223-4232. https://doi.org/10.1007/s00253-013-5489-2

Hahladakis, J. N. (2024). A meta-research analysis on the biological impact of plastic litter in the marine biota. *Science of The Total Environment*, *928*, 172504. https://doi.org/https://doi.org/10.1016/j.scitotenv.2024.172504

Hamod, H. (2015). Suitability of recycled HDPE for 3D printing filament.

Hankermeyer, C. R., & Tjeerdema, R. S. (1999). Polyhydroxybutyrate: plastic made and degraded by microorganisms. *Rev Environ Contam Toxicol*, *159*, 1-24. https://doi.org/10.1007/978-1-4612-1496-0_1

Hany, R., Böhlen, C., Geiger, T., Schmid, M., & Zinn, M. (2004). Toward Non-Toxic Antifouling: Synthesis of Hydroxy-, Cinnamic Acid-, Sulfate-, and Zosteric Acid-Labeled Poly[3-hydroxyalkanoates]. *Biomacromolecules*, *5*(4), 1452-1456. https://doi.org/10.1021/bm049962e

Haywood, G. W., Anderson, A. J., Roger Williams, D., Dawes, E. A., & Ewing, D. F. (1991). Accumulation of a poly(hydroxyalkanoate) copolymer containing primarily 3-hydroxyvalerate from simple carbohydrate substrates by Rhodococcus sp. NCIMB 40126. *International Journal of Biological Macromolecules*, *13*(2), 83-88. https://doi.org/https://doi.org/10.1016/0141-8130(91)90053-W

Hein, S., Söhling, B., Gottschalk, G., & Steinbüchel, A. (1997). Biosynthesis of poly(4-hydroxybutyric acid) by recombinant strains of Escherichia coli. *FEMS Microbiol Lett*, *153*(2), 411-418. https://doi.org/10.1111/j.1574-6968.1997.tb12604.x

Hermann-Krauss, C., Koller, M., Muhr, A., Fasl, H., Stelzer, F., & Braunegg, G. (2013). Archaeal Production of Polyhydroxyalkanoate (PHA) Co- and Terpolyesters from Biodiesel Industry-Derived By-Products. *Archaea*, *2013*(1), 129268. https://doi.org/https://doi.org/10.1155/2013/129268

Hermawan, S., & Jendrossek, D. (2007). Microscopical investigation of poly (3-hydroxybutyrate) granule formation in Azotobacter vinelandii. *FEMS Microbiology Letters*, *266*(1), 60-64.

Higuchi-Takeuchi, M., & Numata, K. (2019). Acetate-Inducing Metabolic States Enhance Polyhydroxyalkanoate Production in Marine Purple Non-sulfur Bacteria Under Aerobic Conditions. *Front Bioeng Biotechnol*, *7*, 118. https://doi.org/10.3389/fbioe.2019.00118

Hill, G. (2006). Closure effects on oxygen transfer and aerobic growth in shake flasks. *Biotechnology and Bioengineering*, *95*, 15-21. https://doi.org/10.1002/bit.20930

Hiraishi, T., Kikkawa, Y., Fujita, M., Normi, Y. M., Kanesato, M., Tsuge, T., Sudesh, K., Maeda, M., & Doi, Y. (2005). Atomic force microscopic observation of in vitro polymerized poly [(R)-3-hydroxybutyrate]: insight into possible mechanism of granule formation. *Biomacromolecules*, *6*(5), 2671-2677.

Hiroe, A., Shiraishi, M., Mizuno, K., & Tsuge, T. (2015). Behavior of different polyhydroxyalkanoate synthases in response to the ethanol level in Escherichia coli cultures. *Polymer Journal*, *47*. https://doi.org/10.1038/pj.2015.53

Hiroe, A., Tsuge, K., Nomura, C. T., Itaya, M., & Tsuge, T. (2012). Rearrangement of gene order in the phaCAB operon leads to effective production of ultrahigh-molecular-weight poly[(R)-3-hydroxybutyrate] in genetically engineered Escherichia coli. *Appl Environ Microbiol*, *78*(9), 3177-3184. https://doi.org/10.1128/aem.07715-11

Hoffmann, N., & Rehm, B. H. A. (2004). Regulation of polyhydroxyalkanoate biosynthesis in Pseudomonas putida and Pseudomonas aeruginosa. *FEMS Microbiology Letters*, *237*(1), 1-7. https://doi.org/https://doi.org/10.1016/j.femsle.2004.06.029

Hollinshead, W. D., Rodriguez, S., Martin, H. G., Wang, G., Baidoo, E. E., Sale, K. L., Keasling, J. D., Mukhopadhyay, A., & Tang, Y. J. (2016). Examining Escherichia coli glycolytic pathways, catabolite repression, and metabolite channeling using Deltapfk mutants. *Biotechnol Biofuels*, *9*, 212. https://doi.org/10.1186/s13068-016-0630-y

Holms, H. (1996). Flux analysis and control of the central metabolic pathways in Escherichia coli. *FEMS Microbiol Rev*, *19*(2), 85-116. https://doi.org/10.1111/j.1574-6976.1996.tb00255.x

Hsieh, Y.-T., Nurkhamidah, S., & Woo, E. M. (2011). Lamellar orientation and interlamellar cracks in co-crystallized poly(ethylene oxide)/poly(L-lactic acid) blend. *Polymer Journal*, *43*(9), 762-769. https://doi.org/10.1038/pj.2011.63

Hsu, T.-M., & Chang, Y.-R. (2019). High-Copy-Number Plasmid Segregation—Single-Molecule Dynamics in Single Cells. *Biophysical Journal*, *116*(5), 772-780. https://doi.org/https://doi.org/10.1016/j.bpj.2019.01.019

Hua, Q., Yang, C., Baba, T., Mori, H., & Shimizu, K. (2003). Responses of the central metabolism in Escherichia coli to phosphoglucose isomerase and glucose-6-phosphate dehydrogenase knockouts. *J Bacteriol*, *185*(24), 7053-7067. https://doi.org/10.1128/jb.185.24.7053-7067.2003

Huang, G., & Hollingsworth, R. I. (1998). An efficient synthesis of (R)-3-hydroxytetradecanoic acid. *Tetrahedron: Asymmetry*, *9*(23), 4113-4115. https://doi.org/https://doi.org/10.1016/S0957-4166(98)00441-8

Huong, K. H., Sevakumaran, V., & Amirul, A. A. (2021). P(3HB-co-4HB) as high value polyhydroxyalkanoate: its development over recent decades and current advances. *Crit Rev Biotechnol*, *41*(4), 474-490. https://doi.org/10.1080/07388551.2020.1869685

Ichihara, K. i., & Fukubayashi, Y. (2010). Preparation of fatty acid methyl esters for gas-liquid chromatography[S]. *Journal of Lipid Research*, *51*(3), 635-640. https://doi.org/https://doi.org/10.1194/jlr.D001065

Ilhan, J., Kupczok, A., Woehle, C., Wein, T., Hülter, N. F., Rosenstiel, P., Landan, G., Mizrahi, I., & Dagan, T. (2018). Segregational Drift and the Interplay between Plasmid Copy Number and Evolvability. *Molecular Biology and Evolution*, *36*(3), 472-486. https://doi.org/10.1093/molbev/msy225

Iroegbu, A. O. C., Ray, S. S., Mbarane, V., Bordado, J. C., & Sardinha, J. P. (2021). Plastic Pollution: A Perspective on Matters Arising: Challenges and Opportunities. *ACS Omega*, *6*(30), 19343-19355. https://doi.org/10.1021/acsomega.1c02760

Janasch, M., Crang, N., Asplund-Samuelsson, J., Sporre, E., Bruch, M., Gynnå, A., Jahn, M., & Hudson, E. P. (2022). Thermodynamic limitations of PHB production from formate and fructose in Cupriavidus necator. *Metab Eng*, *73*, 256-269. https://doi.org/10.1016/j.ymben.2022.08.005

Jeff Sumardee, N. S., Mohd-Hairul, A. R., & Mortan, S. H. (2020). Effect of inoculum size and glucose concentration for bacterial cellulose production by Lactobacillus acidophilus. *IOP Conference Series: Materials Science and Engineering*, *991*(1), 012054. https://doi.org/10.1088/1757-899X/991/1/012054

Jendrossek, D. (2009). Polyhydroxyalkanoate granules are complex subcellular organelles (carbonosomes). *J Bacteriol*, *191*(10), 3195-3202.

https://doi.org/10.1128/jb.01723-08

Jendrossek, D., Selchow, O., & Hoppert, M. (2007). Poly (3-hydroxybutyrate) granules at the early stages of formation are localized close to the cytoplasmic membrane in Caryophanon latum. *Applied and Environmental Microbiology*, *73*(2), 586-593.

Jensen, S. I., Lennen, R. M., Herrgård, M. J., & Nielsen, A. T. (2015). Seven gene deletions in seven days: Fast generation of Escherichia coli strains tolerant to acetate and osmotic stress. *Scientific Reports*, *5*(1), 17874. https://doi.org/10.1038/srep17874

Jeong, E., Lee, J.-Y., & Redwan, M. (2024). Animal exposure to microplastics and health effects: A review. *Emerging Contaminants*, *10*(4), 100369. https://doi.org/https://doi.org/10.1016/j.emcon.2024.100369

Jiang, G., Hill, D. J., Kowalczuk, M., Johnston, B., Adamus, G., Irorere, V., & Radecka, I. (2016). Carbon Sources for Polyhydroxyalkanoates and an Integrated Biorefinery. *Int J Mol Sci*, *17*(7). https://doi.org/10.3390/ijms17071157

Jilani, S. B., Dev, C., Eqbal, D., Jawed, K., Prasad, R., & Yazdani, S. S. (2020). Deletion of pgi gene in E. coli increases tolerance to furfural and 5-hydroxymethyl furfural in media containing glucose-xylose mixture. *Microb Cell Fact*, *19*(1), 153. https://doi.org/10.1186/s12934-020-01414-0

Jilani, S. B., Dev, C., Eqbal, D., Jawed, K., Prasad, R., & Yazdani, S. S. (2020). Deletion of pgi gene in E. coli increases tolerance to furfural and 5-hydroxymethyl furfural in media containing glucose–xylose mixture. *Microbial Cell Factories*, *19*(1), 153. https://doi.org/10.1186/s12934-020-01414-0

Jirage, A., Baravkar, V., Kate, V., Payghan, S., & Disouza, J. (2013). Poly-β-Hydroxybutyrate: Intriguing Biopolymer in Biomedical Applications and Pharma Formulation Trends. *4*, 1107-1118.

Ju, H.-Q., Lin, J.-F., Tian, T., Xie, D., & Xu, R.-H. (2020). NADPH homeostasis in cancer: functions, mechanisms and therapeutic implications. *Signal Transduction and Targeted Therapy*, *5*(1), 231. https://doi.org/10.1038/s41392-020-00326-0

Jung, H.-R., Yang, S.-Y., Moon, Y.-M., Choi, T.-R., Song, H., Bhatia, S., Gurav, R., Kim, B.-G., & Yang, Y.-H. (2019). Construction of Efficient Platform Escherichia coli Strains for Polyhydroxyalkanoate Production by Engineering Branched Pathway. *Polymers*.

https://doi.org/10.3390/polym11030509

Jung, H. R., Yang, S. Y., Moon, Y. M., Choi, T. R., Song, H. S., Bhatia, S. K., Gurav, R., Kim, E. J., Kim, B. G., & Yang, Y. H. (2019). Construction of Efficient Platform Escherichia coli Strains for Polyhydroxyalkanoate Production by Engineering Branched Pathway. *Polymers (Basel)*, *11*(3). https://doi.org/10.3390/polym11030509

Kabir, M., & Shimizu, K. (2003). Fermentation characteristics and protein patterns in a recombinant Escherichia coli mutant lacking phosphoglucose isomerase for poly(3-hydroxybutyrate) production. *Applied Microbiology and Biotechnology*, *62*, 244-255. https://doi.org/10.1007/s00253-003-1257-z

Kabir, M. M., & Shimizu, K. (2003a). Fermentation characteristics and protein expression patterns in a recombinant Escherichia coli mutant lacking phosphoglucose isomerase for poly(3-hydroxybutyrate) production. *Appl Microbiol Biotechnol*, *62*(2-3), 244-255. https://doi.org/10.1007/s00253-003-1257-z

Kabir, M. M., & Shimizu, K. (2003b). Gene expression patterns for metabolic pathway in pgi knockout Escherichia coli with and without phb genes based on RT-PCR. *J Biotechnol*, *105*(1-2), 11-31. https://doi.org/10.1016/s0168-1656(03)00170-6

Kabir, M. M., & Shimizu, K. (2003). Gene expression patterns for metabolic pathway in pgi knockout Escherichia coli with and without phb genes based on RT-PCR. *Journal of Biotechnology*, *105*(1), 11-31. https://doi.org/https://doi.org/10.1016/S0168-1656(03)00170-6

Kahar, P., Agus, J., Kikkawa, Y., Taguchi, K., Doi, Y., & Tsuge, T. (2005). Effective production and kinetic characterization of ultra-high-molecular-weight poly[(R)-3-hydroxybutyrate] in recombinant Escherichia coli. *Polymer Degradation and Stability*, *87*(1), 161-169. https://doi.org/https://doi.org/10.1016/j.polymdegradstab.2004.08.002

Katrcolu, H., Aslm, B., Yüksekdao, Z. N., Mercan Dogan, N., & Beyatl, Y. (2003). Production of poly-β-hydroxybutyrate (PHB) and differentiation of putative Bacillus mutant strains by SDS-PAGE of total cell protein. *African Journal of Biotechnology*, *2*, 158-164.

Keenan, T. M., Tanenbaum, S. W., Stipanovic, A. J., & Nakas, J. P. (2004). Production and characterization of poly-beta-hydroxyalkanoate copolymers from Burkholderia cepacia utilizing xylose and levulinic acid. *Biotechnol Prog*, *20*(6), 1697-1704. https://doi.org/10.1021/bp049873d

Keller, P., Reiter, M. A., Kiefer, P., Gassler, T., Hemmerle, L., Christen, P., Noor, E., & Vorholt, J. A. (2022). Generation of an Escherichia coli strain growing on methanol via the ribulose monophosphate cycle. *Nature Communications*, *13*(1), 5243. https://doi.org/10.1038/s41467-022-32744-9

Kellerhals, M. B., Kessler, B., Witholt, B., Tchouboukov, A., & Brandl, H. (2000). Renewable Long-Chain Fatty Acids for Production of Biodegradable Medium-Chain-Length Polyhydroxyalkanoates (mcl-PHAs) at Laboratory and Pilot Plant Scales. *Macromolecules*, *33*(13), 4690-4698. https://doi.org/10.1021/ma000655k

Kichise, T., Fukui, T., Yoshida, Y., & Doi, Y. (1999). Biosynthesis of polyhydroxyalkanoates (PHA) by recombinant Ralstonia eutropha and effects of PHA synthase activity on in vivo PHA biosynthesis. *Int J Biol Macromol*, *25*(1-3), 69-77. https://doi.org/10.1016/s0141-8130(99)00017-3

Kim, B. S., Lee, S. C., Lee, S. Y., Chang, H. N., Chang, Y. K., & Woo, S. I. (1994). Production of poly(3-hydroxybutyric acid) by fed-batch culture of Alcaligenes eutrophus with glucose concentration control. *Biotechnol Bioeng*, *43*(9), 892-898. https://doi.org/10.1002/bit.260430908

Kim, B. S., Lee, S. C., Lee, S. Y., Chang, Y. K., & Chang, H. N. (2004). High cell density fed-batch cultivation of Escherichia coli using exponential feeding combined with pH-stat. *Bioprocess Biosyst Eng*, *26*(3), 147-150. https://doi.org/10.1007/s00449-003-0347-8

Kim, D. Y., Kim, H. W., Chung, M. G., & Rhee, Y. H. (2007). Biosynthesis, modification, and biodegradation of bacterial medium-chain-length polyhydroxyalkanoates. *J Microbiol*, *45*(2), 87-97.

Kim, H.-Y., & Shin, H.-D. (1995). Isolation of Glucose Utilizing Mutant of Alcaligenes eutrophus, its Substrate Selectivity, Accumulation of Poly b -hydroxybutyrate. *J. Microbiol.*, *33*.

Kim, Y. E., Cho, K. H., Bang, I., Kim, C. H., Ryu, Y. S., Kim, Y., Choi, E. M., Nong, L. K., Kim,

D., & Lee, S. K. (2022). Characterization of an Entner-Doudoroff pathway-activated Escherichia coli. *Biotechnol Biofuels Bioprod*, *15*(1), 120. https://doi.org/10.1186/s13068-022-02219-6

Klun, B., Rozman, U., Ogrizek, M., & Kalčíková, G. (2022). The first plastic produced, but the latest studied in microplastics research: The assessment of leaching, ecotoxicity and bioadhesion of Bakelite microplastics. *Environmental Pollution*, *307*, 119454. https://doi.org/https://doi.org/10.1016/j.envpol.2022.119454

Kocharin, K., Chen, Y., Siewers, V., & Nielsen, J. (2012). Engineering of acetyl-CoA metabolism for the improved production of polyhydroxybutyrate in Saccharomyces cerevisiae. *AMB Express*, *2*(1), 52. https://doi.org/10.1186/2191-0855-2-52

Koller, M., Atlic, A., De Sousa Dias, M., Reiterer, A., & Braunegg, G. (2009). Microbial PHA Production from Waste Raw Materials. In (Vol. 14, pp. 85-119). https://doi.org/10.1007/978-3-642-03287-5_5

Koller, M., Atlić, A., Gonzalez-Garcia, Y., Kutschera, C., & Braunegg, G. (2008). Polyhydroxyalkanoate (PHA) Biosynthesis from Whey Lactose. *Macromolecular Symposia*, *272*(1), 87-92. https://doi.org/https://doi.org/10.1002/masy.200851212

Koller, M., Vadlja, D., Braunegg, G., Atlić, A., & Horvat, P. (2017). Formal- and high-structured kinetic process modelling and footprint area analysis of binary imaged cells: Tools to understand and optimize multistage-continuous PHA biosynthesis. *The EuroBiotech Journal*, *1*(3), 203-211. https://doi.org/doi:10.24190/ISSN2564-615X/2017/03.01

Korotkova, N. A., Ashin, V. V., Doronina, N. V., & Trotsenko, Y. A. (1997). A new method for quantitative determination of poly-3-hydroxybutyrate and 3-hydroxybutyrate-3-hydroxyvalerate copolymer in microbial biomass by reversed-phase high-performance liquid chromatography [Article]. *Applied Biochemistry and Microbiology*, *33*(3), 302-305. https://www.scopus.com/inward/record.uri?eid=2-s2.0-0031526221&partnerID=40&md5=1cb16f2eb39e7bac3bc64c9102f4c726

Kotlarz, D., Garreau, H., & Buc, H. (1975). Regulation of the amount and of the activity of phosphofructokinases and pyruvate kinases in Escherichia coli. *Biochim Biophys*

Acta, *381*(2), 257-268. https://doi.org/10.1016/0304-4165(75)90232-9

Kourmentza, C., Plácido, J., Venetsaneas, N., Burniol-Figols, A., Varrone, C., Gavala, H. N., & Reis, M. A. M. (2017). Recent Advances and Challenges towards Sustainable Polyhydroxyalkanoate (PHA) Production. *Bioengineering*, *4*(2), 55. https://www.mdpi.com/2306-5354/4/2/55

Kshirsagar, P. (2013). Scale up production of polyhydroxyalkanoate (PHA) at different aeration, agitation and controlled dissolved oxygen levels in fermenter using Halomonas campisalis MCM B-1027. *Journal of biochemical technology*, *4*, 512-517.

Labuzek, S., & Radecka, I. (2001). Biosynthesis of PHB tercopolymer by Bacillus cereus UW85. *J Appl Microbiol*, *90*(3), 353-357. https://doi.org/10.1046/j.1365-2672.2001.01253.x

Lamba, P., Kaur, D. P., Raj, S., & Sorout, J. (2021). Recycling/reuse of plastic waste as construction material for sustainable development: a review. *Environmental Science and Pollution Research*, *29*. https://doi.org/10.1007/s11356-021-16980-y

Landau, B. R. (2004). Pentose Phosphate (Hexose Mono Phosphate) Pathway. In W. J. Lennarz & M. D. Lane (Eds.), *Encyclopedia of Biological Chemistry* (pp. 211-215). Elsevier. https://doi.org/https://doi.org/10.1016/B0-12-443710-9/00459-2

Langenbach, S., Rehm, B. H. A., & Steinbüchel, A. (1997). Functional expression of the PHA synthase gene phaC1 from Pseudomonas aeruginosa in Escherichia coli results in poly(3-hydroxyalkanoate) synthesis. *FEMS Microbiology Letters*, *150*(2), 303-309. https://doi.org/10.1111/j.1574-6968.1997.tb10385.x

Lee, E. Y., & Choi, C. Y. (1995). Gas chromatography-mass spectrometric analysis and its application to a screening procedure for novel bacterial polyhydroxyalkanoic acids containing long chain saturated and unsaturated monomers. *Journal of Fermentation and Bioengineering*, *80*(4), 408-414. https://doi.org/https://doi.org/10.1016/0922-338X(95)94214-C

Lee, H.-J., Jung, H. J., Kim, B., Cho, D.-H., Kim, S. H., Bhatia, S. K., Gurav, R., Kim, Y.-G., Jung, S.-W., Park, H. J., & Yang, Y.-H. (2023). Enhancement of polyhydroxybutyrate production by introduction of heterologous phasin combination in Escherichia coli. *International Journal of Biological*

Macromolecules, *225*, 757-766. https://doi.org/https://doi.org/10.1016/j.ijbiomac.2022.11.138

Lee, S., Jeon, E., Yun, H. S., & Lee, J. (2011). Improvement of fatty acid biosynthesis by engineered recombinant Escherichia coli. *Biotechnology and Bioprocess Engineering*, *16*(4), 706-713. https://doi.org/10.1007/s12257-011-0034-6

Lee, S. H., Oh, D. H., Ahn, W. S., Lee, Y., Choi, J., & Lee, S. Y. (2000). Production of poly(3-hydroxybutyrate-co-3-hydroxyhexanoate) by high-cell-density cultivation of Aeromonas hydrophila. *Biotechnol Bioeng*, *67*(2), 240-244. https://doi.org/10.1002/(sici)1097-0290(20000120)67:2<240::aid-bit14>3.0.co;2-f

Lee, S. Y., Hong, S., Park, S. J., Wegen, R., & Middelberg, A. (2005). Metabolic Flux Analysis on the Production of Poly(3-hydroxybutyrate). In. https://doi.org/10.1002/3527600035.bpol3a08

Lee, T. R., Lin, J. S., Wang, S. S., & Shaw, G. C. (2004). PhaQ, a new class of poly-beta-hydroxybutyrate (phb)-responsive repressor, regulates phaQ and phaP (phasin) expression in Bacillus megaterium through interaction with PHB. *J Bacteriol*, *186*(10), 3015-3021. https://doi.org/10.1128/jb.186.10.3015-3021.2004

Lemoigne, M. (1926). Products of dehydration and of polymerization of β-hydroxybutyric acid. *Bull Soc Chem Biol*, *8*, 770-782.

Leung, D. H. L., Lim, Y., Kasimayan, U., Pan, G.-T., Lin, J.-H., Chong, S., & Yang, T. C.-K. (2021). Engineering S. oneidensis for Performance Improvement of Microbial Fuel Cell—a Mini Review. *Applied Biochemistry and Biotechnology*, *193*, 1-17. https://doi.org/10.1007/s12010-020-03469-6

Lewis, C. A., Parker, S. J., Fiske, B. P., McCloskey, D., Gui, D. Y., Green, C. R., Vokes, N. I., Feist, A. M., Vander Heiden, M. G., & Metallo, C. M. (2014). Tracing compartmentalized NADPH metabolism in the cytosol and mitochondria of mammalian cells. *Mol Cell*, *55*(2), 253-263. https://doi.org/10.1016/j.molcel.2014.05.008

Li, D., Yin, F., & Ma, X. (2020). Towards biodegradable polyhydroxyalkanoate production from wood waste: Using volatile fatty acids as conversion medium. *Bioresource Technology*, *299*, 122629.

https://doi.org/https://doi.org/10.1016/j.biortech.2019.122629

Li, W., Wu, H., Li, M., & San, K.-Y. (2017). Effect of NADPH availability on free fatty acid production in E. coli. *Biotechnology and Bioengineering*, *115*. https://doi.org/10.1002/bit.26464

Li, Z.-J., Shi, Z.-Y., Jian, J., Guo, Y.-Y., Wu, Q., & Chen, G.-Q. (2010). Production of poly(3-hydroxybutyrate-co-4-hydroxybutyrate) from unrelated carbon sources by metabolically engineered Escherichia coli. *Metabolic Engineering*, *12*(4), 352-359. https://doi.org/https://doi.org/10.1016/j.ymben.2010.03.003

Liang, X., Cha, D. K., & Xie, Q. (2024). Properties, production, and modification of polyhydroxyalkanoates. *Resources, Conservation & Recycling Advances*, *21*, 200206. https://doi.org/https://doi.org/10.1016/j.rcradv.2024.200206

Lim, S.-J., Jung, Y.-M., Shin, H.-D., & Lee, Y.-H. (2002). Amplification of the NADPH-related genes zwf and gnd for the oddball biosynthesis of PHB in an E. coli transformant harboring a cloned phbCAB operon. *Journal of Bioscience and Bioengineering*, *93*(6), 543-549. https://doi.org/https://doi.org/10.1016/S1389-1723(02)80235-3

Lin, Z., Xu, Z., Li, Y., Wang, Z., Chen, T., & Zhao, X. (2014). Metabolic engineering of Escherichia coli for the production of riboflavin. *Microb Cell Fact*, *13*, 104. https://doi.org/10.1186/s12934-014-0104-5

Lin, Z., Zhang, Y., Yuan, Q., Liu, Q., Li, Y., Wang, Z., Ma, H., Chen, T., & Zhao, X. (2015). Metabolic engineering of Escherichia coli for poly(3-hydroxybutyrate) production viathreonine bypass. *Microbial Cell Factories*, *14*(1), 185. https://doi.org/10.1186/s12934-015-0369-3

Ling, C., Qiao, G. Q., Shuai, B. W., Olavarria, K., Yin, J., Xiang, R. J., Song, K. N., Shen, Y. H., Guo, Y., & Chen, G. Q. (2018). Engineering NADH/NAD(+) ratio in Halomonas bluephagenesis for enhanced production of polyhydroxyalkanoates (PHA). *Metab Eng*, *49*, 275-286. https://doi.org/10.1016/j.ymben.2018.09.007

Liu, A. W., Villar-Briones, A., Luscombe, N. M., & Plessy, C. (2022). Automated phenol-chloroform extraction of high molecular weight genomic DNA for use in long-read single-molecule sequencing. *F1000Res*, *11*, 240. https://doi.org/10.12688/f1000research.109251.1

Liu, Y., Lehnert, T., & Gijs, M. A. M. (2021). Effect of inoculum size and antibiotics on

bacterial traveling bands in a thin microchannel defined by optical adhesive. *Microsystems & Nanoengineering*, *7*(1), 86. https://doi.org/10.1038/s41378-021-00309-3

Liu, Y., Yang, S., Cao, L., Zhang, X., Wang, J., & Liu, C. (2020). Facilitated vascularization and enhanced bone regeneration by manipulation hierarchical pore structure of scaffolds. *Materials Science and Engineering: C*, *110*, 110622. https://doi.org/https://doi.org/10.1016/j.msec.2019.110622

Long, C. P., & Antoniewicz, M. R. (2019). Metabolic flux responses to deletion of 20 core enzymes reveal flexibility and limits of E. coli metabolism. *Metab Eng*, *55*, 249-257. https://doi.org/10.1016/j.ymben.2019.08.003

Loomis, W. F., Jr., & Magasanik, B. (1966). Nature of the effector of catabolite repression of beta-galactosidase in Escherichia coli. *J Bacteriol*, *92*(1), 170-177. https://doi.org/10.1128/jb.92.1.170-177.1966

López-Abelairas, M., García-Torreiro, M., Lú-Chau, T., Lema, J. M., & Steinbüchel, A. (2015). Comparison of several methods for the separation of poly(3-hydroxybutyrate) from Cupriavidus necator H16 cultures. *Biochemical Engineering Journal*, *93*, 250-259. https://doi.org/https://doi.org/10.1016/j.bej.2014.10.018

Lu, X., Zhang, W., Jian, J., Wu, Q., & Chen, G.-Q. (2005). Molecular cloning and functional analysis of two polyhydroxyalkanoate synthases from two strains of Aeromonas hydrophila spp. *FEMS Microbiology Letters*, *243*(1), 149-155. https://doi.org/10.1016/j.femsle.2004.11.051

Madorsky, S. L., & Straus, S. (1959). Thermal Degradation of Polymers at High Temperatures. *J Res Natl Bur Stand A Phys Chem*, *63a*(3), 261-268. https://doi.org/10.6028/jres.063A.020

Maehara, A., Taguchi, S., Nishiyama, T., Yamane, T., & Doi, Y. (2002). A repressor protein, PhaR, regulates polyhydroxyalkanoate (PHA) synthesis via its direct interaction with PHA. *J Bacteriol*, *184*(14), 3992-4002. https://doi.org/10.1128/jb.184.14.3992-4002.2002

Maestro, B., & Sanz, J. M. (2017). Polyhydroxyalkanoate-associated phasins as phylogenetically heterogeneous, multipurpose proteins. *Microb Biotechnol*,

10(6), 1323-1337. https://doi.org/10.1111/1751-7915.12718

Mahishi, L. H., Tripathi, G., & Rawal, S. K. (2003). Poly(3-hydroxybutyrate) (PHB) synthesis by recombinant Escherichia coli harbouring Streptomyces aureofaciens PHB biosynthesis genes: Effect of various carbon and nitrogen sources. *Microbiological Research*, *158*(1), 19-27. https://doi.org/https://doi.org/10.1078/0944-5013-00161

Martínez, M., Urzúa, L. S., Carrillo, Y. A., Ramírez, M. B., & Morales, L. J. M. (2023). Polyhydroxybutyrate Metabolism in Azospirillum brasilense and Its Applications, a Review. *Polymers (Basel)*, *15*(14). https://doi.org/10.3390/polym15143027

Martínez, M. E., Jorquera, L., Poirrier, P., Díaz, K., & Chamy, R. (2023). Effect of Inoculum Size and Age, and Sucrose Concentration on Cell Growth to Promote Metabolites Production in Cultured Taraxacum officinale (Weber) Cells. *Plants*, *12*(5), 1116. https://www.mdpi.com/2223-7747/12/5/1116

Matsumoto, K., Tanaka, Y., Watanabe, T., Motohashi, R., Ikeda, K., Tobitani, K., Yao, M., Tanaka, I., & Taguchi, S. (2013). Directed evolution and structural analysis of NADPH-dependent Acetoacetyl Coenzyme A (Acetoacetyl-CoA) reductase from Ralstonia eutropha reveals two mutations responsible for enhanced kinetics. *Appl Environ Microbiol*, *79*(19), 6134-6139. https://doi.org/10.1128/aem.01768-13

Matsumoto, K. i., Murata, T., Nagao, R., Nomura, C. T., Arai, S., Arai, Y., Takase, K., Nakashita, H., Taguchi, S., & Shimada, H. (2009). Production of Short-Chain-Length/Medium-Chain-Length Polyhydroxyalkanoate (PHA) Copolymer in the Plastid of Arabidopsis thaliana Using an Engineered 3-Ketoacyl-acyl Carrier Protein Synthase III. *Biomacromolecules*, *10*(4), 686-690. https://doi.org/10.1021/bm8013878

Mayer, M. P. (1995). A new set of useful cloning and expression vectors derived from pBlueScript. *Gene*, *163*(1), 41-46. https://doi.org/10.1016/0378-1119(95)00389-n

McKeen, L. W. (2023). Chapter 1 - Introduction to plastics, polymers, and their properties. In L. W. McKeen (Ed.), *The Effect of Temperature and Other Factors on Plastics and Elastomers (Fourth Edition)* (pp. 1-45). William Andrew Publishing. https://doi.org/https://doi.org/10.1016/B978-0-323-99555-9.00002-6

Meng, D.-C., Shen, R., Yao, H., Chen, J.-C., Wu, Q., & Chen, G.-Q. (2014). Engineering the

diversity of polyesters. *Current Opinion in Biotechnology*, *29*, 24-33. https://doi.org/https://doi.org/10.1016/j.copbio.2014.02.013

Meng, D.-C., Shi, Z.-Y., Wu, L.-P., Zhou, Q., Wu, Q., Chen, J.-C., & Chen, G.-Q. (2012). Production and characterization of poly(3-hydroxypropionate-co-4-hydroxybutyrate) with fully controllable structures by recombinant Escherichia coli containing an engineered pathway. *Metabolic Engineering*, *14*(4), 317-324. https://doi.org/https://doi.org/10.1016/j.ymben.2012.04.003

Meyer, F., Keller, P., Hartl, J., Gröninger, O. G., Kiefer, P., & Vorholt, J. A. (2018). Methanol-essential growth of Escherichia coli. *Nature Communications*, *9*(1), 1508. https://doi.org/10.1038/s41467-018-03937-y

Mezzolla, V., D'Urso, O. F., & Poltronieri, P. (2018). Role of PhaC Type I and Type II Enzymes during PHA Biosynthesis. *Polymers (Basel)*, *10*(8). https://doi.org/10.3390/polym10080910

Million-Weaver, S., & Camps, M. (2014). Mechanisms of plasmid segregation: Have multicopy plasmids been overlooked? *Plasmid*, *75*, 27-36. https://doi.org/https://doi.org/10.1016/j.plasmid.2014.07.002

Mitra, R., Xu, T., Chen, G. Q., Xiang, H., & Han, J. (2022). An updated overview on the regulatory circuits of polyhydroxyalkanoates synthesis. *Microb Biotechnol*, *15*(5), 1446-1470. https://doi.org/10.1111/1751-7915.13915

Mitra, R., Xu, T., Xiang, H., & Han, J. (2020). Current developments on polyhydroxyalkanoates synthesis by using halophiles as a promising cell factory. *Microbial Cell Factories*, *19*(1), 86. https://doi.org/10.1186/s12934-020-01342-z

Mittendorf, V., Robertson, E. J., Leech, R. M., Krüger, N., Steinbüchel, A., & Poirier, Y. (1998). Synthesis of medium-chain-length polyhydroxyalkanoates in arabidopsis thaliana using intermediates of peroxisomal fatty acid beta-oxidation. *Proc Natl Acad Sci U S A*, *95*(23), 13397-13402. https://doi.org/10.1073/pnas.95.23.13397

Morrissey, I., & George, J. T. (1999). The effect of the inoculum size on bactericidal activity. *Journal of Antimicrobial Chemotherapy*, *43*(3), 423-424. https://doi.org/10.1093/jac/43.3.423a

Mosberg, J. A., Lajoie, M. J., & Church, G. M. (2010). Lambda red recombineering in Escherichia coli occurs through a fully single-stranded intermediate. *Genetics*,

186(3), 791-799. https://doi.org/10.1534/genetics.110.120782

Mo**ż**ejko-Ciesielska, J., & Kiewisz, R. (2016). Bacterial polyhydroxyalkanoates: Still fabulous? *Microbiological Research*, *192*, 271-282. https://doi.org/https://doi.org/10.1016/j.micres.2016.07.010

Mozejko-Ciesielska, J., Szacherska, K., & Marciniak, P. (2019). Pseudomonas Species as Producers of Eco-friendly Polyhydroxyalkanoates. *Journal of Polymers and the Environment*, *27*. https://doi.org/10.1007/s10924-019-01422-1

Nair, A., & Sarma, S. J. (2021). The impact of carbon and nitrogen catabolite repression in microorganisms. *Microbiological Research*, *251*, 126831. https://doi.org/https://doi.org/10.1016/j.micres.2021.126831

Napathorn, S. C., Visetkoop, S., Pinyakong, O., Okano, K., & Honda, K. (2021). Polyhydroxybutyrate (PHB) Production Using an Arabinose-Inducible Expression System in Comparison With Cold Shock Inducible Expression System in Escherichia coli. *Front Bioeng Biotechnol*, *9*, 661096. https://doi.org/10.3389/fbioe.2021.661096

Nayanathara Thathsarani Pilapitiya, P. G. C., & Ratnayake, A. S. (2024). The world of plastic waste: A review. *Cleaner Materials*, *11*, 100220. https://doi.org/https://doi.org/10.1016/j.clema.2024.100220

Nitschke, M., Costa, S. G. V. A. O., & Contiero, J. (2011). Rhamnolipids and PHAs: Recent reports on Pseudomonas-derived molecules of increasing industrial interest. *Process Biochemistry*, *46*(3), 621-630. https://doi.org/https://doi.org/10.1016/j.procbio.2010.12.012

Nomura, C. T., Taguchi, K., Taguchi, S., & Doi, Y. (2004). Coexpression of genetically engineered 3-ketoacyl-ACP synthase III (fabH) and polyhydroxyalkanoate synthase (phaC) genes leads to short-chain-length-medium-chain-length polyhydroxyalkanoate copolymer production from glucose in Escherichia coli JM109. *Appl Environ Microbiol*, *70*(2), 999-1007. https://doi.org/10.1128/aem.70.2.999-1007.2004

Noor, R., Islam, Z., Munshi, S., & Rahman, F. (2013). Influence of Temperature on Escherichia coli Growth in Different Culture Media. *Journal of Pure and Applied*

Microbiology, *7*.

Obruca, S., Sedlacek, P., Slaninova, E., Fritz, I., Daffert, C., Meixner, K., Sedrlova, Z., & Koller, M. (2020). Novel unexpected functions of PHA granules. *Appl Microbiol Biotechnol*, *104*(11), 4795-4810. https://doi.org/10.1007/s00253-020-10568-1

Olavarria, K., Carnet, A., van Renselaar, J., Quakkelaar, C., Cabrera, R., Guedes da Silva, L., Smids, A. L., Villalobos, P. A., van Loosdrecht, M. C. M., & Wahl, S. A. (2021). An NADH preferring acetoacetyl-CoA reductase is engaged in poly-3-hydroxybutyrate accumulation in Escherichia coli. *J Biotechnol*, *325*, 207-216. https://doi.org/10.1016/j.jbiotec.2020.10.022

Olavarria, K., Pijman, Y. O., Cabrera, R., van Loosdrecht, M. C. M., & Wahl, S. A. (2022). Engineering an acetoacetyl-CoA reductase from Cupriavidus necator toward NADH preference under physiological conditions. *Scientific Reports*, *12*(1), 3757. https://doi.org/10.1038/s41598-022-07663-w

Ostle, A. G., & Holt, J. G. (1982). Nile blue A as a fluorescent stain for poly-beta-hydroxybutyrate. *Applied and Environmental Microbiology*, *44*(1), 238-241. https://doi.org/10.1128/aem.44.1.238-241.1982

Otsuka, M., Kato, F., & Matsuda, Y. (2000). Comparative evaluation of the degree of indomethacin crystallinity by chemoinfometrical Fourier-transformed near-infrared spectroscopy and conventional powder X-ray diffractometry. *AAPS pharmSci*, *2*, E9.

Ouyang, S.-P., Luo, R. C., Chen, S.-S., Liu, Q., Chung, A., Wu, Q., & Chen, G.-Q. (2007). Production of Polyhydroxyalkanoates with High 3-Hydroxydodecanoate Monomer Content by fadB and fadA Knockout Mutant of Pseudomonas putida KT2442. *Biomacromolecules*, *8*(8), 2504-2511. https://doi.org/10.1021/bm0702307

Pachence, J. M., Bohrer, M. P., & Kohn, J. (2007). Chapter Twenty-Three - Biodegradable Polymers. In R. Lanza, R. Langer, & J. Vacanti (Eds.), *Principles of Tissue Engineering (Third Edition)* (pp. 323-339). Academic Press. https://doi.org/https://doi.org/10.1016/B978-012370615-7/50027-5

Page, W. J. (1992). Production of polyhydroxyalkanoates by Azotobacter vinelandii UWD in beet molasses culture. *FEMS Microbiology Letters*, *103*(2), 149-157.

https://doi.org/https://doi.org/10.1016/0378-1097(92)90304-7

Pandey, R. P., Malla, S., Simkhada, D., Kim, B. G., & Sohng, J. K. (2013). Production of 3-O-xylosyl quercetin in Escherichia coli. *Appl Microbiol Biotechnol*, *97*(5), 1889-1901. https://doi.org/10.1007/s00253-012-4438-9

Pantazaki, A. A., Papaneophytou, C. P., Pritsa, A. G., Liakopoulou-Kyriakides, M., & Kyriakidis, D. A. (2009). Production of polyhydroxyalkanoates from whey by Thermus thermophilus HB8. *Process Biochemistry*, *44*(8), 847-853. https://doi.org/https://doi.org/10.1016/j.procbio.2009.04.002

Park, J.-K., Jeon, J.-M., Yang, Y.-H., Kim, S.-H., & Yoon, J.-J. (2024). Efficient polyhydroxybutyrate production using acetate by engineered Halomonas sp. JJY01 harboring acetyl-CoA acetyltransferase. *International Journal of Biological Macromolecules*, *254*, 127475. https://doi.org/https://doi.org/10.1016/j.ijbiomac.2023.127475

Park, S. J., Jang, Y.-A., Noh, W., Oh, Y. H., Lee, H., David, Y., Baylon, M. G., Shin, J., Yang, J. E., Choi, S. Y., Lee, S. H., & Lee, S. Y. (2015). Metabolic engineering of Ralstonia eutropha for the production of polyhydroxyalkanoates from sucrose. *Biotechnology and Bioengineering*, *112*(3), 638-643. https://doi.org/https://doi.org/10.1002/bit.25469

Pathak, G., Nichter, M., Hardon, A., Moyer, E., Latkar, A., Simbaya, J., Pakasi, D., Taqueban, E., & Love, J. (2023). Plastic pollution and the open burning of plastic wastes. *Global Environmental Change*, *80*, 102648. https://doi.org/https://doi.org/10.1016/j.gloenvcha.2023.102648

Peekhaus, N., & Conway, T. (1998). What's for dinner?: Entner-Doudoroff metabolism in Escherichia coli. *J Bacteriol*, *180*(14), 3495-3502. https://doi.org/10.1128/jb.180.14.3495-3502.1998

Peoples, O. P., & Sinskey, A. J. (1989). Poly-β-hydroxybutyrate (PHB) biosynthesis in Alcaligenes eutrophus H16: Identification and characterization of the PHB polymerase gene (phbC)*. *Journal of Biological Chemistry*, *264*(26), 15298-15303. https://doi.org/https://doi.org/10.1016/S0021-9258(19)84825-1

Peregrina Lavín, A., Martins-Lourenço, J., Freitas, F., Reis, M., & Arraiano, C. (2021). *Post-*

transcriptional control in the regulation of polyhydroxy- alkanoates synthesis.

Peters, V., Becher, D., & Rehm, B. H. (2007). The inherent property of polyhydroxyalkanoate synthase to form spherical PHA granules at the cell poles: the core region is required for polar localization. *Journal of Biotechnology*, *132*(3), 238-245.

Petpheng, B., Mudtaleb, B., Thongduang, S., Meekhai, T., Pechsiri, J., & Sangkharak, K. (2023). The production of medium-co-long chain length (mcl-co-lcl) polyhydroxyalkanoate from waste soybean oil by Enterobacter sp. and its application as an antibacterial agent. *Biomass Conversion and Biorefinery*. https://doi.org/10.1007/s13399-023-04454-9

Petrovova, E., Tomco, M., Holovska, K., Danko, J., Kresakova, L., Vdoviakova, K., Simaiova, V., Kolvek, F., Hornakova, P., Toth, T., Zivcak, J., Gal, P., Sedmera, D., Luptakova, L., & Medvecky, L. (2021). PHB/CHIT Scaffold as a Promising Biopolymer in the Treatment of Osteochondral Defects—An Experimental Animal Study. *Polymers*, *13*(8), 1232. https://www.mdpi.com/2073-4360/13/8/1232

Phothong, N., Boontip, T., Chouwatat, P., Aht-Ong, D., & Napathorn, S. C. (2024). Preparation and characterization of astaxanthin-loaded biodegradable polyhydroxybutyrate (PHB) microbeads for personal care and cosmetic applications. *International Journal of Biological Macromolecules*, *257*, 128709. https://doi.org/https://doi.org/10.1016/j.ijbiomac.2023.128709

Phothong, N., Pattarakankul, T., Morikane, S., Palaga, T., Aht-Ong, D., Honda, K., & Napathorn, S. C. (2024). Stability and release mechanism of double emulsification (W1/O/W2) for biodegradable pH-responsive polyhydroxybutyrate/cellulose acetate phthalate microbeads loaded with the water-soluble bioactive compound niacinamide. *Int J Biol Macromol*, *271*(Pt 2), 132680. https://doi.org/10.1016/j.ijbiomac.2024.132680

Pohlmann, A., Fricke, W. F., Reinecke, F., Kusian, B., Liesegang, H., Cramm, R., Eitinger, T., Ewering, C., Pötter, M., Schwartz, E., Strittmatter, A., Voß, I., Gottschalk, G., Steinbüchel, A., Friedrich, B., & Bowien, B. (2006). Genome sequence of the bioplastic-producing "Knallgas" bacterium Ralstonia eutropha H16. *Nature*

Biotechnology, *24*(10), 1257-1262. https://doi.org/10.1038/nbt1244

Poirier, Y., Erard, N., & Petétot, J. M.-C. (2001). Synthesis of polyhydroxyalkanoate in the peroxisome of Saccharomyces cerevisiae by using intermediates of fatty acid β-oxidation. *Applied and Environmental Microbiology*, *67*(11), 5254-5260.

Preusting, H., Kingma, J., Huisman, G., Steinbüchel, A., & Witholt, B. (1993). Formation of polyester blends by a recombinant strain ofPseudomonas oleovorans: Different poly(3-hydroxyalkanoates) are stored in separate granules. *Journal of environmental polymer degradation*, *1*(1), 11-21. https://doi.org/10.1007/BF01457649

Qi, Q., & Rehm, B. H. (2001). Polyhydroxybutyrate biosynthesis in Caulobacter crescentus: molecular characterization of the polyhydroxybutyrate synthase. *Microbiology (Reading)*, *147*(Pt 12), 3353-3358. https://doi.org/10.1099/00221287-147-12-3353

Quero-Jiménez, P., Felipe, L., Jorge Rodriguez, E., Molina-Ruiz, R., García, J., López, J. B., Norman, O., & Garrido, G. (2020). Development and validation of a gas chromatography with a flame ionization detector method for quantitative analysis of four major fatty acids extracted shark liver oil. *Journal of Pharmacy & Pharmacognosy Research*, *9*, 208-221. https://doi.org/10.56499/jppres20.936_9.2.208

Quillaguamán, J., Delgado, O., Mattiasson, B., & Hatti-Kaul, R. (2006). Poly(β-hydroxybutyrate) production by a moderate halophile, Halomonas boliviensis LC1. *Enzyme and Microbial Technology*, *38*(1), 148-154. https://doi.org/https://doi.org/10.1016/j.enzmictec.2005.05.013

Quillaguamán, J., Hashim, S., Bento, F., Mattiasson, B., & Hatti-Kaul, R. (2005). Poly(beta-hydroxybutyrate) production by a moderate halophile, Halomonas boliviensis LC1 using starch hydrolysate as substrate. *J Appl Microbiol*, *99*(1), 151-157. https://doi.org/10.1111/j.1365-2672.2005.02589.x

R., W., M., R., I., J., G., F., & E., C. (2015). Melting and crystallization of poly(3-hydroxybutyrate): effect of heating/cooling rates on phase transformation. *Polimeros*, *25*, 296-304.

Raberg, M., Bechmann, J., Brandt, U., Schlüter, J., Uischner, B., Voigt, B., Hecker, M., & Steinbüchel, A. (2011). Versatile metabolic adaptations of Ralstonia eutropha H16 to a loss of PdhL, the E3 component of the pyruvate dehydrogenase complex. *Appl Environ Microbiol*, *77*(7), 2254-2263. https://doi.org/10.1128/aem.02360-10

Rahman, A., Linton, E., Hatch, A. D., Sims, R. C., & Miller, C. D. (2013). Secretion of polyhydroxybutyrate in Escherichia coli using a synthetic biological engineering approach. *J Biol Eng*, *7*(1), 24. https://doi.org/10.1186/1754-1611-7-24

Rangel, C., Carvalho, G., Oehmen, A., Frison, N., Lourenço, N. D., & Reis, M. A. M. (2023). Polyhydroxyalkanoates production from ethanol- and lactate-rich fermentate of confectionary industry effluents. *Int J Biol Macromol*, *229*, 713-723. https://doi.org/10.1016/j.ijbiomac.2022.12.268

Rasmussen, S. C. (2021). From Parkesine to Celluloid: The Birth of Organic Plastics. *Angewandte Chemie International Edition*, *60*(15), 8012-8016. https://doi.org/https://doi.org/10.1002/anie.202015095

Ray, P. D., Huang, B. W., & Tsuji, Y. (2012). Reactive oxygen species (ROS) homeostasis and redox regulation in cellular signaling. *Cell Signal*, *24*(5), 981-990. https://doi.org/10.1016/j.cellsig.2012.01.008

Rehm, B. H. (2003). Polyester synthases: natural catalysts for plastics. *Biochem J*, *376*(Pt 1), 15-33. https://doi.org/10.1042/bj20031254

Rehm, B. H. A. (2007). Biogenesis of Microbial Polyhydroxyalkanoate Granules: A Platform Technology for the Production of Tailor-Made Bioparticles. *Current Issues in Molecular Biology*, *9*(1), 41-62.

Ren, Q., Sierro, N., Witholt, B., & Kessler, B. (2000). FabG, an NADPH-dependent 3-ketoacyl reductase of Pseudomonas aeruginosa, provides precursors for medium-chain-length poly-3-hydroxyalkanoate biosynthesis in Escherichia coli. *J Bacteriol*, *182*(10), 2978-2981. https://doi.org/10.1128/jb.182.10.2978-2981.2000

Ritchie, G. A., Senior, P. J., & Dawes, E. A. (1971). The purification and characterization of acetoacetyl-coenzyme A reductase from Azotobacter beijerinckii. *Biochem J*, *121*(2), 309-316. https://doi.org/10.1042/bj1210309

Robinson, T. P., Aboaba, O. O., Kaloti, A., Ocio, M. J., Baranyi, J., & Mackey, B. M. (2001).

The effect of inoculum size on the lag phase of Listeria monocytogenes. *International Journal of Food Microbiology*, *70*(1), 163-173. https://doi.org/https://doi.org/10.1016/S0168-1605(01)00541-4

Roman, L., Schuyler, Q., Wilcox, C., & Hardesty, B. (2020). Plastic pollution is killing marine megafauna, but how do we prioritize policies to reduce mortality? *Conservation Letters*, *14*. https://doi.org/10.1111/conl.12781

Rood, D. (1997). Gas Chromatography Problem Solving and Troubleshooting. *Journal of Chromatographic Science*, *35*(5), 239-240. https://doi.org/10.1093/chromsci/35.5.239

Saad, N., & Abd Karim, K. (2016). Factors affecting the establishment and growth of Pogostemon cablin cell suspension cultures.

Salamonsen, R. F., & Cole, W. J. (1977). Effect of polarity on the response of the flame ionization detector to halothane. *Br J Anaesth*, *49*(4), 387-390. https://doi.org/10.1093/bja/49.4.387

Salinas, A., McGregor, C., Irorere, V., Arenas-López, C., Bommareddy, R. R., Winzer, K., Minton, N. P., & Kovács, K. (2022). Metabolic engineering of Cupriavidus necator H16 for heterotrophic and autotrophic production of 3-hydroxypropionic acid. *Metabolic Engineering*, *74*, 178-190. https://doi.org/https://doi.org/10.1016/j.ymben.2022.10.014

Sánchez-Pascuala, A., de Lorenzo, V., & Nikel, P. I. (2017). Refactoring the Embden–Meyerhof–Parnas Pathway as a Whole of Portable GlucoBricks for Implantation of Glycolytic Modules in Gram-Negative Bacteria. *ACS Synthetic Biology*, *6*(5), 793-805. https://doi.org/10.1021/acssynbio.6b00230

Sarah Perreard, J. B., Martina Gallato, Melissa Gomis, Paolo Mazzatorta, Adrienne Gaboury and Noemie Voirin. (2024). *Plastic over shoot day*. https://plasticovershoot.earth/wp-content/uploads/2024/04/EA_POD_report_2024.pdf

Sato, S., Kanazawa, H., & Tsuge, T. (2011). Expression and characterization of (R)-specific enoyl coenzyme A hydratases making a channeling route to polyhydroxyalkanoate biosynthesis in Pseudomonas putida. *Appl Microbiol Biotechnol*, *90*(3), 951-959. https://doi.org/10.1007/s00253-011-3150-5

Satoh, H., Mino, T., & Matsuo, T. (1999). PHA production by activated sludge. *International Journal of Biological Macromolecules*, *25*(1), 105-109. https://doi.org/https://doi.org/10.1016/S0141-8130(99)00021-5

Sauer, U., Canonaco, F., Heri, S., Perrenoud, A., & Fischer, E. (2004). The Soluble and Membrane-bound Transhydrogenases UdhA and PntAB Have Divergent Functions in NADPH Metabolism of Escherichia coli*. *Journal of Biological Chemistry*, *279*(8), 6613-6619. https://doi.org/https://doi.org/10.1074/jbc.M311657200

Scheel, R. A., Ji, L., Lundgren, B. R., & Nomura, C. T. (2016). Enhancing poly(3-hydroxyalkanoate) production in Escherichia coli by the removal of the regulatory gene arcA. *AMB Express*, *6*(1), 120. https://doi.org/10.1186/s13568-016-0291-z

Seggiani, M., Cinelli, P., Verstichel, S., Puccini, M., Vitolo, S., Anguillesi, I., & Lazzeri, A. (2015). Development of Fibres-Reinforced Biodegradable Composites. *Chemical Engineering Transactions*, *43*, 1813-1818. https://doi.org/10.3303/CET1543303

Sengupta, J. (2024). Natural biodegradable polymers transforming lab on a chip technology: A mini review. *Green Analytical Chemistry*, *10*, 100119. https://doi.org/https://doi.org/10.1016/j.greeac.2024.100119

Seol, E., Ainala, S. K., Sekar, B. S., & Park, S. (2014). Metabolic engineering of Escherichia coli strains for co-production of hydrogen and ethanol from glucose. *International Journal of Hydrogen Energy*, *39*(33), 19323-19330. https://doi.org/https://doi.org/10.1016/j.ijhydene.2014.06.054

Sezonov, G., Joseleau-Petit, D., & D'Ari, R. (2007). Escherichia coli physiology in Luria-Bertani broth. *J Bacteriol*, *189*(23), 8746-8749. https://doi.org/10.1128/jb.01368-07

Shamala, T. R., Chandrashekar, A., Vijayendra, S. V., & Kshama, L. (2003). Identification of polyhydroxyalkanoate (PHA)-producing Bacillus spp. using the polymerase chain reaction (PCR). *J Appl Microbiol*, *94*(3), 369-374. https://doi.org/10.1046/j.1365-2672.2003.01838.x

Sheu, D.-S., Chen, W.-M., Lai, Y.-W., & Chang, R.-C. (2012). Mutations Derived from the Thermophilic Polyhydroxyalkanoate Synthase PhaC Enhance the

Thermostability and Activity of PhaC from Cupriavidus necator H16. *Journal of bacteriology*, *194*, 2620-2629. https://doi.org/10.1128/JB.06543-11

Shi, H., Nikawa, J., & Shimizu, K. (1999). Effect of modifying metabolic network on poly-3-hydroxybutyrate biosynthesis in recombinant Escherichia coli. *J Biosci Bioeng*, *87*(5), 666-677. https://doi.org/10.1016/s1389-1723(99)80132-7

Shimaoka, M., Kawasaki, H., Takenaka, Y., Kurahashi, O., & Matsui, H. (2005). Effects of edd and pgi disruptions on inosine accumulation in Escherichia coli. *Biosci Biotechnol Biochem*, *69*(7), 1248-1255. https://doi.org/10.1271/bbb.69.1248

Shiue, E., Brockman, I. M., & Prather, K. L. (2015). Improving product yields on D-glucose in Escherichia coli via knockout of pgi and zwf and feeding of supplemental carbon sources. *Biotechnol Bioeng*, *112*(3), 579-587. https://doi.org/10.1002/bit.25470

Shuto, H., Fukui, T., Saito, T., Shirakura, Y., & Tomita, K. (1981). An NAD-linked acetoacetyl-CoA reductase from Zoogloea ramigera I-16-M. *Eur J Biochem*, *118*(1), 53-59. https://doi.org/10.1111/j.1432-1033.1981.tb05485.x

Siedler, S., Bringer, S., Polen, T., & Bott, M. (2014). NADPH-dependent reductive biotransformation with Escherichia coli and its pfkA deletion mutant: influence on global gene expression and role of oxygen supply. *Biotechnol Bioeng*, *111*(10), 2067-2075. https://doi.org/10.1002/bit.25271

Silva, J. B., Pereira, J. R., Marreiros, B. C., Reis, M. A. M., & Freitas, F. (2021). Microbial production of medium-chain length polyhydroxyalkanoates. *Process Biochemistry*, *102*, 393-407. https://doi.org/https://doi.org/10.1016/j.procbio.2021.01.020

Sim, S., Snell, K., Kim, B., Rha, C., & Sinskey, A. (2001). Increased poly-β-hydroxybutyrate (PHB) chain length by the modulation of PHA synthase activity in recombinant Escherichia coli. *Biotechnology Letters*, *23*, 2057-2061. https://doi.org/10.1023/A:1013752000022

Sim, S. J., Snell, K. D., Hogan, S. A., Stubbe, J., Rha, C., & Sinskey, A. J. (1997). PHA synthase activity controls the molecular weight and polydispersity of polyhydroxybutyrate in vivo. *Nat Biotechnol*, *15*(1), 63-67.

https://doi.org/10.1038/nbt0197-63

Simkhada, D., Kim, E., Lee, H. C., & Sohng, J. K. (2009). Metabolic engineering of Escherichia coli for the biological synthesis of 7-O-xylosyl naringenin. *Mol Cells*, *28*(4), 397-401. https://doi.org/10.1007/s10059-009-0135-7

Simonzadeh, N., & Ronsen, B. (2012). An Isocratic HPLC Method for the Determination of Sorbitol and Glycerol in Pharmaceutical Formulations. *Journal of Chromatographic Science*, *50*(7), 644-647. https://doi.org/10.1093/chromsci/bms044

Sivashankari, R. M., Mierzati, M., Miyahara, Y., Mizuno, S., Nomura, C. T., Taguchi, S., Abe, H., & Tsuge, T. (2023). Exploring Class I polyhydroxyalkanoate synthases with broad substrate specificity for polymerization of structurally diverse monomer units. *Front Bioeng Biotechnol*, *11*, 1114946. https://doi.org/10.3389/fbioe.2023.1114946

Škulj, M., Okršlar, V., Jalen, Š., Jevševar, S., Slanc, P., Štrukelj, B., & Menart, V. (2008). Improved determination of plasmid copy number using quantitative real-time PCR for monitoring fermentation processes. *Microbial Cell Factories*, *7*(1), 6. https://doi.org/10.1186/1475-2859-7-6

Slater, S., Houmiel, K. L., Tran, M., Mitsky, T. A., Taylor, N. B., Padgette, S. R., & Gruys, K. J. (1998). Multiple beta-ketothiolases mediate poly(beta-hydroxyalkanoate) copolymer synthesis in Ralstonia eutropha. *J Bacteriol*, *180*(8), 1979-1987. https://doi.org/10.1128/jb.180.8.1979-1987.1998

Sodian, R., Sperling, J. S., Martin, D. P., Egozy, A., Stock, U., Mayer, J. E., Jr., & Vacanti, J. P. (2000). Fabrication of a trileaflet heart valve scaffold from a polyhydroxyalkanoate biopolyester for use in tissue engineering. *Tissue Eng*, *6*(2), 183-188. https://doi.org/10.1089/107632700320793

Söhling, B., & Gottschalk, G. (1996). Molecular analysis of the anaerobic succinate degradation pathway in Clostridium kluyveri. *J Bacteriol*, *178*(3), 871-880. https://doi.org/10.1128/jb.178.3.871-880.1996

Sokatch, J. R. (1969). 7 - AEROBIC METABOLISM OF CARBOHYDRATES. In J. R. Sokatch (Ed.), *Bacterial Physiology and Metabolism* (pp. 112-130). Academic Press. https://doi.org/https://doi.org/10.1016/B978-1-4832-3137-2.50011-6

Sood, S., Singhal, R., Bhat, S., & Kumar, A. (2011). 2.13 - Inoculum Preparation. In M. Moo-Young (Ed.), *Comprehensive Biotechnology (Second Edition)* (pp. 151-164). Academic Press. https://doi.org/https://doi.org/10.1016/B978-0-08-088504-9.00090-8

Spaans, S. K., Weusthuis, R. A., van der Oost, J., & Kengen, S. W. (2015). NADPH-generating systems in bacteria and archaea. *Front Microbiol*, *6*, 742. https://doi.org/10.3389/fmicb.2015.00742

Spector, M. P. (2009). Metabolism, Central (Intermediary). In M. Schaechter (Ed.), *Encyclopedia of Microbiology (Third Edition)* (pp. 242-264). Academic Press. https://doi.org/https://doi.org/10.1016/B978-012373944-5.00078-X

Steinbüchel, A., & Valentin, H. E. (1995). Diversity of bacterial polyhydroxyalkanoic acids. *FEMS Microbiology Letters*, *128*(3), 219-228. https://doi.org/https://doi.org/10.1016/0378-1097(95)00125-O

Stubbe, J., & Tian, J. (2003). Polyhydroxyalkanoate (PHA) hemeostasis: the role of PHA synthase. *Nat Prod Rep*, *20*(5), 445-457. https://doi.org/10.1039/b209687k

Stubbe, J., Tian, J., He, A., Sinskey, A. J., Lawrence, A. G., & Liu, P. (2005). Nontemplate-dependent polymerization processes: polyhydroxyalkanoate synthases as a paradigm. *Annu. Rev. Biochem.*, *74*(1), 433-480.

Sujatha, K., & Shenbagarathai, R. (2006). A study on medium chain length-polyhydroxyalkanoate accumulation in Escherichia coli harbouring phaC1 gene of indigenous Pseudomonas sp. LDC-5. *Lett Appl Microbiol*, *43*(6), 607-614. https://doi.org/10.1111/j.1472-765X.2006.02016.x

Sukruansuwan, V., & Napathorn, S. C. (2018). Use of agro-industrial residue from the canned pineapple industry for polyhydroxybutyrate production by Cupriavidus necator strain A-04. *Biotechnology for Biofuels*, *11*(1), 202. https://doi.org/10.1186/s13068-018-1207-8

Sumardee, N., Mohd-Hairul, A., & Mortan, S. (2020). Effect of inoculum size and glucose concentration for bacterial cellulose production by Lactobacillus acidophilus. *IOP Conference Series: Materials Science and Engineering*, *991*, 012054. https://doi.org/10.1088/1757-899X/991/1/012054

Summers, J. (2008). The melting temperature (or not melting) of poly(vinyl chloride).

Journal of Vinyl & Additive Technology - J VINYL ADDITIVE TECHNOL, *14*, 105-109. https://doi.org/10.1002/vnl.20151

Sundara Sekar, B., Seol, E., Mohan Raj, S., & Park, S. (2016). Co-production of hydrogen and ethanol by pfkA-deficient Escherichia coli with activated pentose-phosphate pathway: reduction of pyruvate accumulation. *Biotechnol Biofuels*, *9*, 95. https://doi.org/10.1186/s13068-016-0510-5

Suresh, S., Naik, A., & Premanath, R. (2023). Glucose-Induced Enhanced Virulence in Strains of Multidrug-Resistant Pseudomonas aeruginosa Isolated from Diabetic Patients. *Curr Microbiol*, *80*(3), 100. https://doi.org/10.1007/s00284-023-03200-8

Suzuki, T., Yamane, T., & Shimizu, S. (1990). Phenomenological Background and Some Preliminary Trials of Automated Substrate Supply in pH-Stat Modal Fed-Batch Culture Using a Setpoint of High Limit. *Journal of Fermentation and Bioengineering*, *69*(5), 292-297. https://doi.org/https://doi.org/10.1016/0922-338X(90)90108-9

Taguchi, S., Nakamura, H., Kichise, T., Tsuge, T., Yamato, I., & Doi, Y. (2003). Production of polyhydroxyalkanoate (PHA) from renewable carbon sources in recombinant Ralstonia eutropha using mutants of original PHA synthase. *Biochemical Engineering Journal*, *16*(2), 107-113. https://doi.org/https://doi.org/10.1016/S1369-703X(03)00027-5

Tajima, K., Satoh, Y., Satoh, T., Itoh, R., Han, X., Taguchi, S., Kakuchi, T., & Munekata, M. (2009). Chemo-Enzymatic Synthesis of Poly(lactate-co-(3-hydroxybutyrate)) by a Lactate-Polymerizing Enzyme. *Macromolecules*, *42*(6), 1985-1989. https://doi.org/10.1021/ma802579g

Tan, D., Wang, Y., Tong, Y., & Chen, G.-Q. (2021). Grand Challenges for Industrializing Polyhydroxyalkanoates (PHAs). *Trends in Biotechnology*, *39*(9), 953-963. https://doi.org/https://doi.org/10.1016/j.tibtech.2020.11.010

Tan, G.-Y., Chen, C.-L., Li, L., Ge, L., Wang, L., Razaad, I. M. N., Li, Y., Zhao, L., Mo, Y., & Wang, J.-Y. (2014). Start a Research on Biopolymer Polyhydroxyalkanoate (PHA): A Review. *Polymers*, *6*, 706-754. https://doi.org/10.3390/polym6030706

Tan, G.-Y. A., Chen, C.-L., Li, L., Ge, L., Wang, L., Razaad, I. M. N., Li, Y., Zhao, L., Mo, Y., & Wang, J.-Y. (2014). Start a Research on Biopolymer Polyhydroxyalkanoate (PHA):

A Review. *Polymers*, *6*(3), 706-754. https://www.mdpi.com/2073-4360/6/3/706

Tang, X., Thankappan, S. K., Lee, P., Fard, S. E., Harmon, M. D., Tran, K., & Yu, X. (2014). Chapter 21 - Polymeric Biomaterials in Tissue Engineering and Regenerative Medicine. In S. G. Kumbar, C. T. Laurencin, & M. Deng (Eds.), *Natural and Synthetic Biomedical Polymers* (pp. 351-371). Elsevier. https://doi.org/https://doi.org/10.1016/B978-0-12-396983-5.00022-3

Thompson, R. C., Moore, C. J., vom Saal, F. S., & Swan, S. H. (2009). Plastics, the environment and human health: current consensus and future trends. *Philos Trans R Soc Lond B Biol Sci*, *364*(1526), 2153-2166. https://doi.org/10.1098/rstb.2009.0053

Tripathi, L., Wu, L.-P., Dechuan, M., Chen, J., Wu, Q., & Chen, G.-Q. (2013). Pseudomonas putida KT2442 as a platform for the biosynthesis of polyhydroxyalkanoates with adjustable monomer contents and compositions. *Bioresource Technology*, *142*, 225-231. https://doi.org/https://doi.org/10.1016/j.biortech.2013.05.027

Tsang, Y. F., Kumar, V., Samadar, P., Yang, Y., Lee, J., Ok, Y. S., Song, H., Kim, K.-H., Kwon, E. E., & Jeon, Y. J. (2019). Production of bioplastic through food waste valorization. *Environment International*, *127*, 625-644. https://doi.org/https://doi.org/10.1016/j.envint.2019.03.076

Tsuge, T. (2016). Fundamental factors determining the molecular weight of polyhydroxyalkanoate during biosynthesis. *Polymer Journal*, *48*(11), 1051-1057. https://doi.org/10.1038/pj.2016.78

Tsuge, T., Fukui, T., Matsusaki, H., Taguchi, S., Kobayashi, G., Ishizaki, A., & Doi, Y. (2000). Molecular cloning of two (R)-specific enoyl-CoA hydratase genes from Pseudomonas aeruginosa and their use for polyhydroxyalkanoate synthesis. *FEMS Microbiol Lett*, *184*(2), 193-198. https://doi.org/10.1111/j.1574-6968.2000.tb09013.x

Unger, C., Lokmer, N., Lehmann, D., & Axmann, I. M. (2019). Detection of phenol contamination in RNA samples and its impact on qRT-PCR results. *Analytical Biochemistry*, *571*, 49-52. https://doi.org/https://doi.org/10.1016/j.ab.2019.02.002

Valentin, H. E., & Dennis, D. (1997). Production of poly(3-hydroxybutyrate-co-4-hydroxybutyrate) in recombinant Escherichia coli grown on glucose. *Journal of*

Biotechnology, *58*(1), 33-38. https://doi.org/https://doi.org/10.1016/S0168-1656(97)00127-2

Valentin, H. E., & Steinbüchel, A. (1995). Accumulation of poly(3-hydroxybutyric acid-co-3-hydroxyvaleric acid-co-4-hydroxyvaleric acid) by mutants and recombinant strains ofAlcaligenes eutrophus. *Journal of environmental polymer degradation*, *3*(3), 169-175. https://doi.org/10.1007/BF02068468

Valentin, H. F., & Dennis, D. (1996). Metabolic pathway for poly(3-hydroxybutyrate-co-3-hydroxyvalerate) formation in Nocardia corallina: inactivation of mutB by chromosomal integration of a kanamycin resistance gene. *Appl Environ Microbiol*, *62*(2), 372-379. https://doi.org/10.1128/aem.62.2.372-379.1996

van Wegen, R. J., Lee, S. Y., & Middelberg, A. P. (2001). Metabolic and kinetic analysis of poly(3-hydroxybutyrate) production by recombinant Escherichia coli. *Biotechnol Bioeng*, *74*(1), 70-80. https://doi.org/10.1002/bit.1096

Vasiljevs, S., Gupta, A., & Baines, D. (2023). Effect of glucose on growth and co-culture of Staphylococcus aureus and Pseudomonas aeruginosa in artificial sputum medium. *Heliyon*, *9*(11), e21469. https://doi.org/10.1016/j.heliyon.2023.e21469

Verma, R., Vinoda, K. S., Papireddy, M., & Gowda, A. N. S. (2016). Toxic Pollutants from Plastic Waste- A Review. *Procedia Environmental Sciences*, *35*, 701-708. https://doi.org/https://doi.org/10.1016/j.proenv.2016.07.069

Villar-Palasí, C., & Guinovart, J. J. (1997). The role of glucose 6-phosphate in the control of glycogen synthase. *Faseb j*, *11*(7), 544-558.

Visetkoop, S. (2009). *Cloning and expression of polyhydroxyalkanote biosynthesis genes from Ralstonia eutrophus strain A-04 in Escherichia coli* Chulalongkorn University]. Faculty of Science.

Volova, T. G., Boyandin, A. N., Vasiliev, A. D., Karpov, V. A., Prudnikova, S. V., Mishukova, O. V., Boyarskikh, U. A., Filipenko, M. L., Rudnev, V. P., Bá Xuân, B., Việt Dũng, V., & Gitelson, I. I. (2010). Biodegradation of polyhydroxyalkanoates (PHAs) in tropical coastal waters and identification of PHA-degrading bacteria. *Polymer Degradation and Stability*, *95*(12), 2350-2359. https://doi.org/https://doi.org/10.1016/j.polymdegradstab.2010.08.023

Volova, T. G., Prudnikova, S. V., Vinogradova, O. N., Syrvacheva, D. A., & Shishatskaya, E.

I. (2017). Microbial Degradation of Polyhydroxyalkanoates with Different Chemical Compositions and Their Biodegradability. *Microb Ecol*, *73*(2), 353-367. https://doi.org/10.1007/s00248-016-0852-3

Wang, C., Xin, F., Kong, X., Zhao, J., Weiliang, D., Zhang, W., Jiangfeng, m., Wu, H., & Jiang, M. (2018). Enhanced isopropanol–butanol–ethanol mixture production through manipulation of intracellular NAD(P)H level in the recombinant Clostridium acetobutylicum XY16. *Biotechnology for Biofuels*, *11*. https://doi.org/10.1186/s13068-018-1024-0

Wang, J.-Y., Mullin, N., & Hobbs, J. (2018). High-speed large area atomic force microscopy using a quartz resonator. *Nanotechnology*, *29*. https://doi.org/10.1088/1361-6528/aac7a3

Wang, L., Yang, Z., Fan, F., Sun, S., Wu, X., Lu, H., & Lu, X. (2019). PHBHHx Facilitated the Residence, Survival and Stemness Maintain of Transplanted Neural Stem Cells in Traumatic Brain Injury Rats. *Biomacromolecules*, *20*(9), 3294-3302. https://doi.org/10.1021/acs.biomac.9b00408

Wang, S., Ma, P., Wang, R., Wang, S., Zhang, Y., & Zhang, Y. (2008). Mechanical, thermal and degradation properties of poly(d,l-lactide)/poly(hydroxybutyrate-co-hydroxyvalerate)/poly(ethylene glycol) blend. *Polymer Degradation and Stability*, *93*(7), 1364-1369. https://doi.org/https://doi.org/10.1016/j.polymdegradstab.2008.03.026

Wang, X., Bengtsson, S., Oehmen, A., Carvalho, G., Werker, A., & Reis, M. A. M. (2019). Application of dissolved oxygen (DO) level control for polyhydroxyalkanoate (PHA) accumulation with concurrent nitrification in surplus municipal activated sludge. *New Biotechnology*, *50*, 37-43. https://doi.org/https://doi.org/10.1016/j.nbt.2019.01.003

Wang, Y., Chung, A., & Chen, G. Q. (2017). Synthesis of Medium-Chain-Length Polyhydroxyalkanoate Homopolymers, Random Copolymers, and Block Copolymers by an Engineered Strain of Pseudomonas entomophila. *Adv Healthc Mater*, *6*(7). https://doi.org/10.1002/adhm.201601017

Wang, Y., San, K. Y., & Bennett, G. N. (2013). Improvement of NADPH bioavailability in Escherichia coli through the use of phosphofructokinase deficient strains. *Appl*

Microbiol Biotechnol, *97*(15), 6883-6893. https://doi.org/10.1007/s00253-013-4859-0

Wang, Y., Wu, H., Jiang, X., & Chen, G.-Q. (2014). Engineering Escherichia coli for enhanced production of poly(3-hydroxybutyrate-co-4-hydroxybutyrate) in larger cellular space. *Metabolic Engineering*, *25*, 183-193. https://doi.org/https://doi.org/10.1016/j.ymben.2014.07.010

Wang, Y., Zhou, S., Li, R., Liu, Q., Shao, X., Zhu, L., Kang, M. K., Wei, G., Kim, S. W., & Wang, C. (2022). Reassessing acetyl-CoA supply and NADPH availability for mevalonate biosynthesis from glycerol in Escherichia coli. *Biotechnol Bioeng*, *119*(10), 2868-2877. https://doi.org/10.1002/bit.28167

Wang, Z., Liang, R., Cheng, X., Lan, Q., Xie, J., He, M., Pang, Y., Xiong, F., Lei, D., Zheng, L., & Zhao, J. (2019). Osteogenic Potential of Electrospun Poly(3-hydroxybutyrate-co-4-hydroxybutyrate)/ Poly(ethylene glycol) Nanofiber Membranes. *J Biomed Nanotechnol*, *15*(6), 1280-1289. https://doi.org/10.1166/jbn.2019.2757

Wei, Y.-H., Chen, W.-C., Huang, C.-K., Wu, H.-S., Sun, Y.-M., Lo, C.-W., & Janarthanan, O.-M. (2011). Screening and Evaluation of Polyhydroxybutyrate-Producing Strains from Indigenous Isolate Cupriavidus taiwanensis Strains. *International Journal of Molecular Sciences*, *12*(1), 252-265.

Wen, X., & Lu, X. (2012). Microbial Degradation of Poly(3-Hydroxybutyrate-co-4-Hydroxybutyrate) in Soil. *Journal of Polymers and the Environment*, *20*(2), 381-387. https://doi.org/10.1007/s10924-011-0387-0

Wendlandt, K. D., Geyer, W., Mirschel, G., & Hemidi, F. A.-H. (2005). Possibilities for controlling a PHB accumulation process using various analytical methods. *Journal of Biotechnology*, *117*(1), 119-129. https://doi.org/https://doi.org/10.1016/j.jbiotec.2005.01.007

White, J. L. (1999). Fifth of a Series: Pioneer of Polymer Processing John Wesley Hyatt (1837–1920). *14*(4), 314-314. https://doi.org/doi:10.3139/217.9904 (International Polymer Processing)

Wilson, J. E. (2003). Isozymes of mammalian hexokinase: structure, subcellular localization and metabolic function. *J Exp Biol*, *206*(Pt 12), 2049-2057.

https://doi.org/10.1242/jeb.00241

Wu, C.-S. (2014). Preparation and Characterization of Polyhydroxyalkanoate Bioplastic-Based Green Renewable Composites from Rice Husk. *Journal of Polymers and the Environment*, *22*(3), 384-392. https://doi.org/10.1007/s10924-014-0662-y

Wu, H.-A., Sheu, D.-S., & Lee, C.-Y. (2003). Rapid differentiation between short-chain-length and medium-chain-length polyhydroxyalkanoate-accumulating bacteria with spectrofluorometry. *Journal of Microbiological Methods*, *53*(1), 131-135. https://doi.org/https://doi.org/10.1016/S0167-7012(02)00232-4

Wu, H.-Y., Tomizawa, K., Matsushita, M., Lu, Y.-F., Li, S.-T., & Matsui, H. (2003). Poly-arginine-fused calpastatin peptide, a living cell membrane-permeable and specific inhibitor for calpain. *Neuroscience Research*, *47*(1), 131-135. https://doi.org/https://doi.org/10.1016/S0168-0102(03)00195-0

Wu, H., Chen, J., & Chen, G. Q. (2016). Engineering the growth pattern and cell morphology for enhanced PHB production by Escherichia coli. *Appl Microbiol Biotechnol*, *100*(23), 9907-9916. https://doi.org/10.1007/s00253-016-7715-1

Wu, H., Li, S., Ji, M., Chen, Q., Shi, J., Blamey, J. M., & Sun, J. (2020). Improvement of polyhydroxybutyrate production by deletion of csrA in Escherichia coli. *Electronic Journal of Biotechnology*, *46*, 8-13. https://doi.org/https://doi.org/10.1016/j.ejbt.2020.04.005

Xia, T., & Eiteman, M. A. (2017). Quercetin Glucoside Production by Engineered Escherichia coli. *Appl Biochem Biotechnol*, *182*(4), 1358-1370. https://doi.org/10.1007/s12010-017-2403-x

Xie, W., & Chen, G.-Q. (2008). Production and characterization of terpolyester poly(3-hydroxybutyrate-co-4-hydroxybutyrate-co-3-hydroxyhexanoate) by recombinant Aeromonas hydrophila 4AK4 harboring genes phaPCJ. *Biochemical Engineering Journal*, *38*, 384-389. https://doi.org/10.1016/j.bej.2007.08.002

Yabutani, T., Maehara, A., Ueda, S., & Yamane, T. (1995). Analysis of beta-ketothiolase and acetoacetyl-CoA reductase genes of a methylotrophic bacterium, Paracoccus denitrificans, and their expression in Escherichia coli. *FEMS Microbiol Lett*, *133*(1-2), 85-90. https://doi.org/10.1111/j.1574-6968.1995.tb07865.x

Yamane, T., Chen, X., & Ueda, S. (1996). Growth-Associated Production of Poly(3-

Hydroxyvalerate) from n-Pentanol by a Methylotrophic Bacterium, Paracoccus denitrificans. *Appl Environ Microbiol*, *62*(2), 380-384. https://doi.org/10.1128/aem.62.2.380-384.1996

Yamane, T., Fukunaga, M., & Lee, Y. W. (1996). Increased PHB productivity by high-cell-density fed-batch culture of Alcaligenes latus, a growth-associated PHB producer. *Biotechnol Bioeng*, *50*(2), 197-202. https://doi.org/10.1002/(sici)1097-0290(19960420)50:2<197::Aid-bit8>3.0.Co;2-h

Yang, J. E., Choi, S. Y., Shin, J., Park, S. J., & Lee, S. Y. (2013). Microbial production of lactate-containing polyesters. *Microbial biotechnology*, *6*. https://doi.org/10.1111/1751-7915.12066

Yuan, M. Q., Shi, Z. Y., Wei, X. X., Wu, Q., Chen, S. F., & Chen, G. Q. (2008). Microbial production of medium-chain-length 3-hydroxyalkanoic acids by recombinant Pseudomonas putida KT2442 harboring genes fadL, fadD and phaZ. *FEMS Microbiol Lett*, *283*(2), 167-175. https://doi.org/10.1111/j.1574-6968.2008.01164.x

Yuan, X., Mao, Y., Tu, S., Lin, J., Shen, H., Yang, L., & Wu, M. (2021). Increasing NADPH Availability for Xylitol Production via Pentose-Phosphate-Pathway Gene Overexpression and Embden–Meyerhof–Parnas-Pathway Gene Deletion in Escherichia coli. *Journal of Agricultural and Food Chemistry*, *69*(33), 9625-9631. https://doi.org/10.1021/acs.jafc.1c03283

Zhang, L., Jiang, Z., Tsui, T. H., Loh, K. C., Dai, Y., & Tong, Y. W. (2022). A Review on Enhancing Cupriavidus necator Fermentation for Poly(3-hydroxybutyrate) (PHB) Production From Low-Cost Carbon Sources. *Front Bioeng Biotechnol*, *10*, 946085. https://doi.org/10.3389/fbioe.2022.946085

Zhang, Z., Chen, L., Liu, L., Su, X., & Rabinowitz, J. D. (2017). Chemical Basis for Deuterium Labeling of Fat and NADPH. *J Am Chem Soc*, *139*(41), 14368-14371. https://doi.org/10.1021/jacs.7b08012

Zhang, Z., Gosset, G., Barabote, R., Gonzalez, C. S., Cuevas, W. A., & Saier, M. H., Jr. (2005). Functional interactions between the carbon and iron utilization regulators, Crp and Fur, in Escherichia coli. *J Bacteriol*, *187*(3), 980-990. https://doi.org/10.1128/jb.187.3.980-990.2005

Zheng, L. Z., Li, Z., Tian, H.-L., Li, M., & Chen, G.-Q. (2005). Molecular cloning and

functional analysis of (R)-3-hydroxyacyl-acyl carrier protein:coenzyme A transacylase from Pseudomonas mendocina LZ. *FEMS Microbiology Letters*, *252*(2), 299-307. https://doi.org/10.1016/j.femsle.2005.09.006

Zhuang, Q., Wang, Q., Liang, Q., & Qi, Q. (2014). Synthesis of polyhydroxyalkanoates from glucose that contain medium-chain-length monomers via the reversed fatty acid β-oxidation cycle in Escherichia coli [Article]. *Metabolic Engineering*, *24*, 78-86. https://doi.org/10.1016/j.ymben.2014.05.004

Zinn, M., & Hany, R. (2005). Tailored Material Properties of Polyhydroxyalkanoates through Biosynthesis and Chemical Modification. *Advanced Engineering Materials*, *7*(5), 408-411. https://doi.org/https://doi.org/10.1002/adem.200500053

Zou, H., Zhang, T., Li, L., Huang, J., Zhang, N., Shi, M., Hao, H., & Xian, M. (2018). Systematic Engineering for Improved Carbon Economy in the Biosynthesis of Polyhydroxyalkanoates and Isoprenoids. *Materials*, *11*, 1271. https://doi.org/10.3390/ma11081271

Zytner, P., Kumar, D., Elsayed, A., Mohanty, A., Ramarao, B. V., & Misra, M. (2023). A review on polyhydroxyalkanoate (PHA) production through the use of lignocellulosic biomass [10.1039/D3SU00126A]. *RSC Sustainability*, *1*(9), 2120-2134. https://doi.org/10.1039/D3SU00126A

VITA

NAME	Jittakan Pachimsawat
DATE OF BIRTH	12 May 1992
PLACE OF BIRTH	Bangkok, Thailand
INSTITUTIONS ATTENDED	B.Sc., Department of Biochemistry, Faculty of Science, Chulalongkorn University, Bangkok, Thailand
HOME ADDRESS	9/9 Ratcha 5, Bangyai, Nontaburi, 11140
PUBLICATION	1. Muangwong, A., Boontip, T., Pachimsawat, J and Napathorn, S. Chanprateep (2016) Medium chain length polyhydroxyalkanoates consisting primarily of unsaturated 3-hydroxy-5-cis-dodecanoate synthesized by newly isolated bacteria using crude glycerol, Microbial Cell Factories 15, 55.